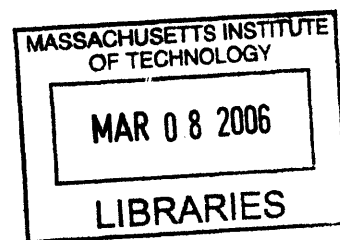


Glycosaminoglycan Regulation of Cell Function

by

David Berry

Submitted to the Biological Engineering Division
in Partial Fulfillment of the Requirements for the Degree of



Doctor of Philosophy

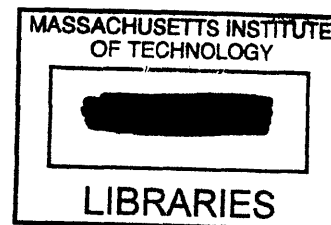
in

Molecular and Systems Toxicology and Pharmacology

at the

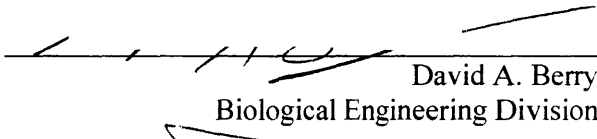
Massachusetts Institute of Technology

March, 2005



© 2005 Massachusetts Institute of Technology. All rights reserved

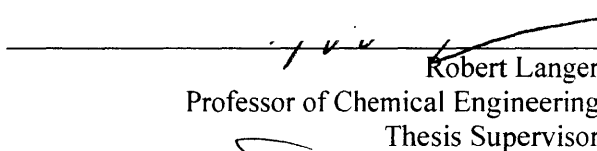
Author:


David A. Berry
Biological Engineering Division

Certified by:

Ram Sasisekharan
Professor of Biological Engineering
Thesis Supervisor

Certified by:

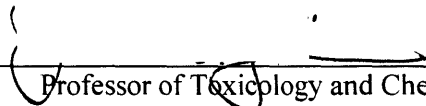

Robert Langer
Professor of Chemical Engineering
Thesis Supervisor

Accepted by:

Ram Sasisekharan
Chairman, Committee for Graduate Students

This thesis has been examined by a committee of the Biological Engineering Division as follows:


Professor John Essigmann



Professor of Toxicology and Chemistry
Thesis Committee Chairman

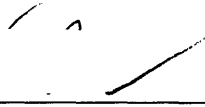


Professor Ram Sasisekharan




Professor of Biological Engineering
Thesis Co-Advisor

Professor Robert Langer



Germeshausen Professor of Chemical and
Biomedical Engineering
Thesis Co-Advisor

Professor Michael Rosenblatt



Professor of Physiology and Medicine
Tufts University School of Medicine

Glycosaminoglycan Regulation of Cell Function

by
David Berry

Submitted to the Biological Engineering Division
In Partial Fulfillment of the Requirements for the Degree of
Doctor of Philosophy in Molecular and Systems Toxicology and Pharmacology

Abstract

Glycosaminoglycans (GAGs) are complex polysaccharides that exist both on the cell surface and free within the extracellular matrix. The intrinsic sequence variety stemming from the large number of building blocks that compose this biopolymer leads to substantial information density as well as to the ability to regulate a wide variety of important biological processes. With the recent and progressive emergence of biochemical and analytical tools to probe GAG structure and function, efforts can be taken to understand the role of GAGs in cell biology and in disease in the various physiological locations where GAGs can exist.

As a first step to probe the functions of GAGs, the heparin/heparan sulfate-GAG (HSGAG)-fibroblast growth factor (FGF) system was examined. Understanding the role of HSGAGs in inducing FGF2 dimerization led to the development of a novel engineered protein that was found to be effective at promoting functional recovery in stroke. Subsequently, methods to isolate HSGAGs from the cell surface were optimized and the ability of HSGAGs to support FGF signaling was investigated. Cell surface HSGAGs can define the responsiveness of a given cell to FGF1 and FGF2 through multiple receptor isoforms. Stromal cell derived HSGAGs were also identified as critical regulators of tumor cell growth and metastasis, effecting not only FGF2, but also β_1 -integrin signaling. Other GAGs, including dermatan sulfates, were characterized as modulators of FGFs and vascular endothelial growth factors. Finally, FGFs and HSGAGs were found to have important roles in maintaining epithelial monolayer integrity, with syndecan-1 serving as a critical factor in inflammatory bowel disease.

In addition to understanding HSGAGs in their normal physiological settings, techniques to internalize them were developed. Poly(β -amino ester)s were found to condense heparin and enable its endocytosis into cells. Internalized heparin is preferentially taken up by cancer cells, which often have a faster endocytic rate than non-transformed cells, and promotes apoptotic cell death. Internalized heparin can also be used as a tool to probe cell function. In Burkitt's lymphoma, poly(β -amino ester)-heparin conjugates served to identify cell surface HSGAGs as an important modulator of cell growth that can be harnessed to inhibit growth.

Finally, studies that sought to broaden the scope of GAG biology were undertaken. Cell surface HSGAGs were identified as mediators of vascular permeability. Furthermore a novel technique to immobilize GAGs was employed. The interactions between GAG and substrate were via hydrogen bonding. Immobilization of GAGs alters their properties, such that they can affect cells in ways distinct from GAGs free in the ECM. Furthermore, immobilized GAGs can regulate cancer cell adhesion, growth and progression, and may offer a new way to regulate the activity of cancer cells. In addition to directly providing new potential therapeutics and drug targets, these studies represent a foundation to enable additional studies of GAG function. Future work harnessing the techniques presented may open new avenues of research and facilitate the development of novel GAG-based therapeutics.

Acknowledgements

First, I would like to thank my co-advisors, Ram Sasisekharan and Robert Langer. Ram provided me with outstanding encouragement and guidance. He has been inspirational in my development as a scientist and has provided me with unique insight into how to get “it” done. Bob has been an incredible visionary, helping me to see things for what they are and what they can be. He has been an exceptional motivator, demonstrating and making me believe in what is truly possible and truly meaningful. I would additionally like to thank the other members of my thesis committee: John Essigmann and Michael Rosenblatt. Your insight and constant support were essential to me to reach my ultimate goals. I am grateful for the financial support provided by the Howard Hughes Medical Institute predoctoral fellowship that subsidized me for the duration of my graduate studies.

I would also like to thank my fellow lab members, both past and present. Zachary Shriver and Barbara Natke taught me the essentials of laboratory work in the Sasisekharan lab. Robert Padera provided me fundamental insight as to how to balance medical and graduate educations. Thanks additionally to Nishla Keiser, Dr. Yiwei Qi, Kris Holley, Guido Jenniskens, and especially Chi-Pong Kwan and Kevin Pojasek for the help through the years. Eric Berry was and is a wonderful colleague, coworker, and brother. Daniel Anderson and Dave Lynn taught me the ins and outs of the Langer lab and were essential in designing and implementing the poly(β -amino ester) projects in the Langer lab. Ali Khademhosseini was a valuable colleague, providing a novel perspective on projects. For all of this help along the way, I am very grateful.

My friends in Boston and elsewhere have been an important and constant source of support. Scott Weiss, Christina Boulton, Zack Peacock, and Brad Williams have made the years dramatically more fun. Richard Resnick always provided the necessary focus: “why don’t you get your pipette and move some liquid.” Susan Inman has provided the perfect balance of real-world focus and support.

Finally, and most important, I am most thankful to my parents for their constant support and understanding.

Table of Contents

Abstract	3
Acknowledgements	4
Section 1: Introduction	6
Chapter 1. Introduction to glycosaminoglycans.....	6
Objectives.....	27
Section 2: Glycosaminoglycan-Growth Factor Interactions	29
Chapter 2. Dimeric fibroblast growth factor 2 in stroke*.....	30
Chapter 3. Cell derived HSGAGs differentially regulate FGF2*.....	38
Chapter 4. Quantitative assessment of FGF regulation by cell surface heparan sulfates.....	60
Chapter 5. Stromal cell surface HSGAGs regulate cancer growth and metastasis*.....	73
Chapter 6. Heparan sulfate and dermatan sulfate regulate FGF and VEGF activity*.....	92
Chapter 7. FGF1 is essential for FGF2 and FGF7 regulation of epithelial monolayer integrity.....	111
Chapter 8. Syndecan-1 is protective in inflammatory bowel disease.....	131
Section 3: Internalization of Heparin	148
Chapter 9. Poly(β -amino ester)s promote cellular uptake of heparin and cancer cell death.....	149
Chapter 10. HSGAGs as tools and targets for Burkitt's lymphoma	171
Chapter 11. Heparin and internalized heparin: dual mechanisms to inhibit prostate cancer growth.....	184
Section 4: Novel Roles for Glycosaminoglycans	199
Chapter 12. Heparan sulfates induce monolayer dysfunction*.....	200
Chapter 13. Characterization of chemisorbed hyaluronic acid directly immobilized on solid substrates.....	219
Chapter 14. Immobilized glycosaminoglycans regulate cancer cell activity.....	231
Section 5: Conclusions	247
Chapter 15. Conclusions and future work.....	247
Abbreviations	250
References	252

* Chapter headings are descriptive

Chapter 1. Introduction to glycosaminoglycans

1.1 The Extracellular Matrix

The extracellular matrix (ECM) has long been considered an inert scaffold that surrounds cells, providing them only with physical support. More recent evidence has revealed that the ECM plays essential roles in regulating cellular behavior [46, 200, 245, 435]. The contents of the ECM sequester water to provide the turgor of soft tissues, bind growth factors, serve as adhesion sites for cells, among other processes. Local cells secrete the components of the ECM, which self-assemble into a complex network within the extracellular space. The ECM is composed of three primary groups of macromolecules: structural proteins, adhesive glycoproteins, and glycosaminoglycans (GAGs) [491].

Structural proteins include collagens and elastins, the former of which is the most common protein in animals. Adhesive glycoproteins include fibronectin and laminin, which play an important role in assembling the signaling complexes at the intersection between cells and the ECM through integrins. GAGs and associated proteoglycans (PGs)

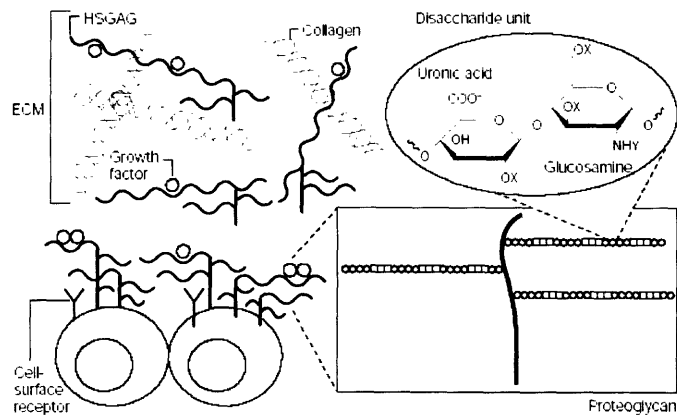


Figure 1.1. Physiological localization and structure of HSGAGs. HSGAGs (green lines) are bound to PGs (red lines) either free in the ECM or on the cell surface. The potential sites of acetylation or sulfation (X's) and sulfation, acetylation, or unsubstitution (Y's) influence the ability of HSGAGs to interact with growth factors and other proteins (orange circles) in the ECM. Figure from [427].

are the third general component of the ECM (**Figure 1.1**), and serve both to bind water, providing tissue turgor pressure, and to regulate a wide variety of essential cell processes [194]. GAGs additionally serve as an important extracellular reservoir for cytokines and chemokines.

1.2 Structure, Synthesis, and Biological Function of Glycosaminoglycans

GAGs are composed of disaccharide repeat units that broadly consist of an uronic acid (either α -L-iduronic acid or β -D-glucuronic acid) linked 1 \rightarrow 3 or 1 \rightarrow 4 to an amino sugar (either *N*-acetyl glucosamine or *N*-acetyl galactosamine). The specific monosaccharide constituents and bonds of the disaccharide repeat unit used throughout the GAG polymer define the category of the GAG. Four major categories of GAGs exist: heparin/heparan sulfate glycosaminoglycans (HSGAGs); chondroitin sulfate (CS)/dermatan sulfate (DS) GAGs; hyaluronic acid (HA); and keratan sulfate. Keratan sulfate is unique as it contains monosaccharides not seen in the other categories of GAGs [330, 338]. Additionally, keratan sulfate lacks uronic acid and contains branched regions [330, 338]. Unlike other GAGs, keratan sulfate has not been found to bind specifically to a protein of known function [330, 338, 483], and therefore, this GAG is not investigated in these studies.

The structures of HA, HSGAGs, CS, and DS, which are the subjects of this thesis, are provided in **Figure 1.2**.

HSGAGs, CS and DS are synthesized in the golgi apparatus with the GAG polymers attached to a PG core protein [426, 454] GAGs attach to PGs through the serine residue of consensus Ser-Gly/Ala-X-Gly motifs. All eukaryotic cells synthesize PGs, which are secreted into the ECM, stored in secretory granules, or attached to the cell membrane [427]. PGs can contain a single GAG type, as with HSGAG-

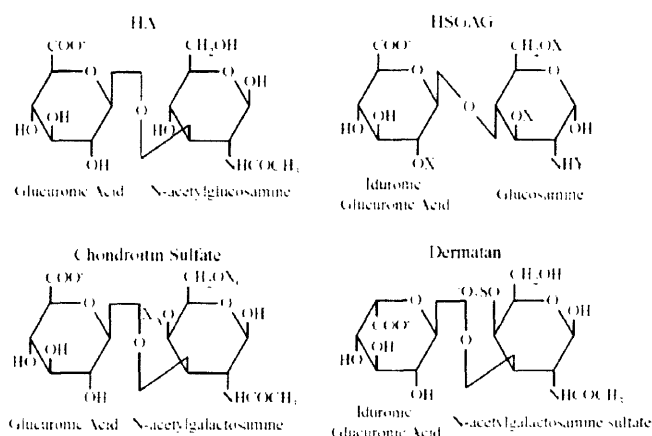


Figure 1.2. Structures of disaccharides composing the various GAGs used. The HSGAG disaccharide can be modified at five sites. Three sites (2-*O*, 3-*O*, and 6-*O*) indicated by "X" can be sulfated. The site denoted by "Y" can be unmodified, acetylated or sulfated. The epimerization state of C5 sugar of the uronic acid determines whether iduronic acid or glucuronic acid is present. Heparin is a highly sulfated HSGAG while HS is an undersulfated HSGAG. The CS disaccharide is sulfated specifically to determine its species. CS A is sulfated at X_A and unmodified at X_C, while CS C is sulfated at X_C and unmodified at X_A. The dermatan disaccharide can be sulfated in additional sites to those illustrated. The epimerization state of C5 site of the uronic acid determines whether iduronic acid or glucuronic acid is present.

specific glypicans or multiple types of GAGs, as with syndecans. HA, however, is not bound to a PG. Rather, HA is synthesized by an integral plasma membrane synthetase that releases the HA directly into the ECM [257].

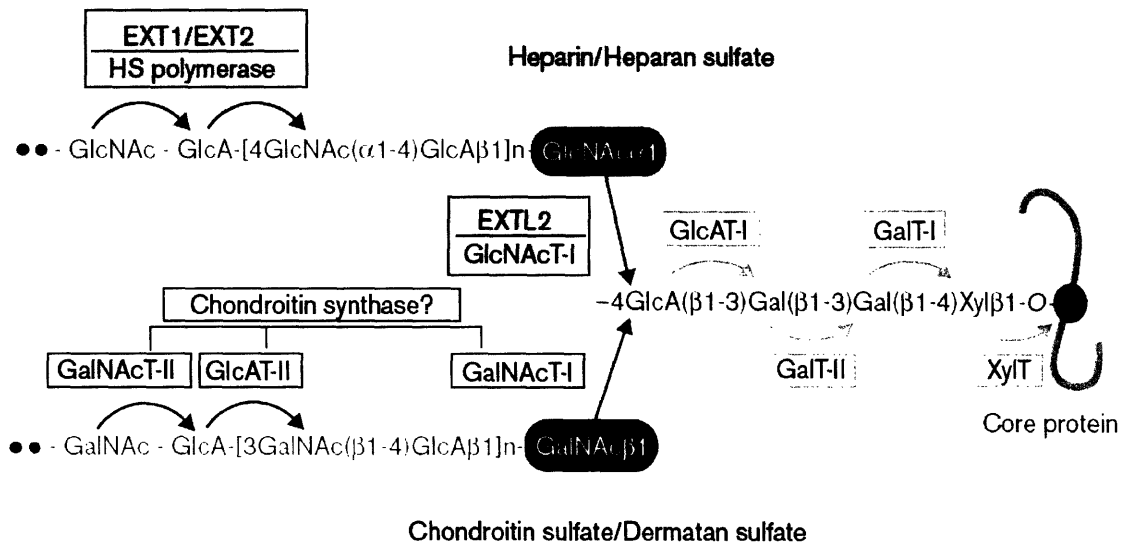


Figure 1.3. Current models of GAG biosynthesis. As described in the text, GAGs are synthesized linked to PGs by a GAG-protein linkage region of $\text{GlcA}(\beta 1-3)\text{Gal}(\beta 1-3)\text{Gal}(\beta 1-4)\text{Xyl}\beta 1-O$ -Ser, shared among HSGAGs, CS, and DS. After the formation of the linkage region by the action of specific glycosyltransferases, GAGs are elongated by the alternating addition of *N*-acetylhexosamine and GlcA residues. EXT denotes hereditary multiple exostoses gene, EXTL denotes EXT-like gene, Gal denotes galactose, GalNAc denotes *N*-acetylgalactosamine, GalT denotes galactosyltransferase, Glc denotes glucose, GlcA denotes glucuronic acid, GlcAT denotes glucuronyltransferase, GlcNAc denotes *N*-acetylglucosamine, and XylT denotes xylosyltransferase. Figure adapted from [454].

GAG biosynthesis is a highly complex process involving several groups of enzymes [426, 454]. In HSGAGs, CS, and DS, a tetrasaccharide linker ($\text{GlcA}\beta 1-3\text{Gal}\beta 1-3\text{Gal}\beta 1-4\text{Xyl}\beta 1$; **Figure 1.3**) is first assembled through the activity of four enzymes which connect the four monosaccharides. Chain elongation occurs subsequent to an essential phosphorylation of the 2-*O* position of the Xyl monosaccharide [363, 454]. The first step of chain elongation, transfer of either *N*-acetyl glucosamine (HSGAGs) or *N*-acetyl galactosamine (CS/DS) by one of two glycosyltransferases, determines the specific category that the particular GAG will become [454]. A multidomain glycosyltransferase then elongates the chain, adding β -D-glucuronic acid, *N*-acetyl glucosamine, or *N*-acetyl galactosamine, as appropriate, given the leader monosaccharide. Subsequently, the GAG polymer is modified by epimerization of some of the

β -D-glucuronic acid to α -L-iduronic acid, *O*-sulfation, *N*-sulfation, and *N*-deacetylation [269]. These modifications are not driven by a template, unlike other biopolymers such as DNA or proteins. The complexity intrinsic to GAG synthesis increases the information content of the polymer but also increases the difficulty associated with characterizing it [38, 488].

The sulfation pattern of the GAG polymer contributes to its biological functions. In HSGAGs, potential 2-*O* sulfation on the uronic acid, 6-*O* and 3-*O* sulfation of the glucosamine, and an unmodified, acetylated or sulfated amine, lead to 48 potential disaccharide units that compose the 10-100-mer HSGAG chain [370]. The four potential sites of sulfation make HSGAGs the most acidic biopolymers in nature. [138, 139]. HSGAGs are typically referred to as either heparin-like or heparan sulfate (HS)-like. Heparin is a highly sulfated HSGAG predominantly 2-*O*- 6-*O*- and *N*-sulfated, that is synthesized on the serglycin core protein and stored within mast cell granules, acting as a reservoir for proteases [189]. HS is ubiquitous on the cell surface with a more variable sulfation pattern which is lower than that of heparin, with a greater amount of unsulfated glucuronic acid [77, 106]. Commercially available HSGAGs typically have molecular weights ranging between 7 and 35 kDa [77].

DS contains regions of predominantly iduronic acid and those with mostly glucuronic acid. The galactosamine, though primarily 4-*O* sulfated, can be only 6-*O* sulfated or 4-*O*- and 6-*O* disulfated. 2-*O* sulfation of the uronic acid is additionally possible [330, 338]. In CS, the uronic acid is β -D-glucuronic acid, and can be sulfated at the 2-*O* and 3-*O* positions. On the galactosamine, CS can be sulfated at either the 4-*O* position (CS A) or at the 6-*O* position (CS C) [232, 508, 509]. CS is typically found in large, aggregating PGs with 20-100 chains, each with a molecular weight of 15-70 kDa. DS, however, is typically found in smaller PGs with only 2-8 chains of 15-55 kDa [104].

HA is distinct from both HSGAGs and CS/DS GAGs. The disaccharides are the same as in unmodified HSGAGs (β -D-glucuronic acid and *N*-acetyl glucosamine), but the glycosidic linkage reflects that observed in CS. HA is additionally unsulfated [13, 104, 257, 502]. HA polymers are much larger than those of other GAGs, with molecular weights of 100-1000 kDa, and up to 25,000 disaccharides in length [290, 324].

The combination of the specific modifications possible produces the set of disaccharides that serve as the building-block unit for GAGs, similar to nucleotides for DNA or amino acids for proteins. The great variety of disaccharide units that exist even within a single category of

GAGs leads to enormous potential primary sequence possibilities and greater information density than DNA or proteins.

Similar to protein structures, the GAG polymers can be described at multiple levels. In addition to the primary structure detailed above, which is defined by the composition of the specific disaccharide units and their order, the secondary structure of GAGs has been examined [13, 304, 307]. In general, the secondary structure of GAGs is repeated helical winding. A tertiary structure, similar to that of proteins, has not yet been described for GAGs.

1.3 GAG-degrading enzymes

While great steps have been made in understanding GAG biology, its study has lagged behind that of other biopolymers, namely nucleic acids and proteins. The increased number of building blocks (48 in HSGAGs) compared to nucleic acids (4) and proteins (20), leads to increased structural complexity, which, along with their highly charged nature, has hindered the development of necessary biochemical tools. Furthermore, unlike nucleic acids (polymerase chain reaction) and proteins (recombinant techniques), no amplification technique exists for GAGs.

HSGAG-degrading enzymes have served as the primary tool to dissect out structure-function relationships. Six HSGAG degrading enzymes have been isolated [104, 106, 270]. Of these, heparinase I (hepI), hepII, and hepIII have been well characterized [105, 154-156, 424, 425, 440-442, 488]. The heparinases digest different HSGAG sequences, each through a lytic enzymatic mechanism. In general, hepI cleaves highly sulfated domains, and hepIII cleaves undersulfated domains. HepII, however, does not have specific sulfation requirements, and cleaves regions that can be digested by each of hepI and hepIII.

The primary structures of these three enzymes show little homology and they are not well conserved with other proteins [422]. HepI and hepIII each have two HSGAG binding sequences, while hepII has three such sequences [58]. The HSGAG binding sequences are not required to the same extent in hepIII as they are in hepI, consistent with the specificity of hepIII for undersulfated HSGAGs. Additionally, hepI requires specific calcium binding for maximal activity, while hepII and hepIII are not calcium dependent [442].

These heparinases, derived from the ubiquitous soil bacteria *Flavobacterium heparinum*, are distinct from mammalian GAG-degrading enzymes [104]. The mammalian GAG-degrading enzymes have an exolytic mechanism compared to the hydrolytic and endolytic mechanism used by hepl, hepII, and hepIII [298, 478]. These enzymes would not make effective biochemical tools as they preferentially function at low pHs and are typically lysosomal membrane associated. A mammalian heparinase has been identified and characterized, however, that digests HS in the ECM through an endolytic mechanism, similar to the heparinases [19, 186, 494, 496]. While this enzyme has proven important in maintaining normal tissue architecture and cancer progression, its limited substrate specificity decreases its potential utility as a biochemical tool [496].

Understanding the biochemical basis by which HSGAG-degrading enzymes selectively depolymerize substrates has greatly increased their utility as tools in characterizing structure-function relationships. The use of heparinases coupled with mass spectrometry techniques has enabled the sequencing of HSGAG oligosaccharides [488]. Even without providing sequence information, heparinases have enabled critical insights into HSGAG-growth factor interactions [30] as well as the role of HSGAGs in cancer [274].

The HSGAG-degrading enzymes are the best characterized and most utilized of the GAG-degrading enzymes. Research has also focused on the isolation and characterization of enzymes that digest other categories of GAGs. *Flavobacterium heparinum* produces four chondroitin lyases, which digest CS and DS with known substrate specificities. Chondroitinase C cleaves CS C (6-O sulfated CS). Chondroitinase AC cleaves CS A (4-O sulfated CS) and CS C. Chondroitinase B specifically degrades DS (CS B), and is the only known enzyme to do so. Chondroitinase depolymerizes all of the CS and DS isomers [104, 204]. Chondroitinase AC and chondroitinase B have been cloned from *Flavobacterium heparinum*, but the genes for chondroitinase C and chondroitinase ABC have not yet been cloned. Rather, two isoforms of chondroitinase ABC from *Proteus vulgaris* have been cloned and characterized [302, 303, 428].

1.4 Cell surface HSGAGs

HSGAGs are found on the surface of every eukaryotic cell [427]. Cell surface HSGAGs are attached to the heparan sulfate PG (HSPG) families of syndecans and glypicans. Attachment

to other HSPG families, such as perlecan, predisposes HSGAGs to release into the ECM such that they are not directly cell-associated. The syndecan family consists of four gene products with a highly conserved, short, cytoplasmic domain, but distinct extracellular domains. The glypican family contains six gene products that are covalently linked to plasma membrane lipids via a glycosylphosphatidylinositol anchor [29, 529].

Cell surface HSGAGs are important in regulating the response of the cell to its microenvironment. Although the interactions between HSGAGs and proteins at the cell surface were once considered non-specific, recent research has demonstrated ligands, such as fibroblast growth factors (FGFs), which require HSGAG sequences of defined length and structure. In the ECM, HSGAGs may act as a “sink,” binding growth factors and cytokines, and protecting them from proteolysis. On the cell surface, HSGAGs localize proteins for receptor binding and signal transduction, as with growth factors, and for internalization and degradation, as with lipoprotein lipase and thrombospondin [29, 35, 320].

Cell surface HSGAGs act with the cell’s receptors to enable the cell to appropriately respond to its environment. HSGAG chains, however, are long enough to span the intracellular space, potentially enabling direct interaction between cells [46, 493]. HSGAGs and their associated HSPGs on the cell surface have been implicated in modulation of cellular response to mitogens, actin reorganization, adhesion, viral entry, membrane transcytosis, and other processes [89, 99, 456, 479]. The HSGAGs of a given cell type are unique, with specific compositions dependent on the quantities and isoforms of biosynthetic enzymes produced. The HSGAGs of a cell type, however, are by no means fixed, as extracellular and intracellular processes can have dynamic effects on the HSGAG composition [427]. Generating profiles of a cell’s surface HSGAG can offer insights into its function.

In addition to sequence, HSGAG location is also an important determinant of function. Only HSGAGs that are immobilized on the cell surface serve as FGF2 co-receptors [395, 511]. On the other hand, syndecan shedding is an important element in Wnt signaling [5]. Syndecan shedding occurs with proteolytic cleavage of the core protein within nine amino acids of the outer leaflet of the plasma membrane [29, 128]. Glypicans can also be shed via glycosylphosphatidylinositol-specific phospholipases [86]. After shedding, the HSPG ectodomains retain their ligand binding properties. Shed syndecans can, for example, *inhibit*

FGF2 activity [219]. HSPG shedding therefore represents another route by which HSGAGs can regulate cellular activities and enable communication between cells.

1.4.1 HSGAGs in Cancer

Not surprisingly, HSGAGs have been found to influence cancer in a multifaceted manner. Anticoagulation has long been known to have a protective effect in cancer [521, 522]. Heparin and low molecular weight heparins have been demonstrated to improve the mortality of cancer patients by preventing deep venous thrombosis and subsequent pulmonary embolism, one of the primary causes of death in cancer [79, 523]. Additionally, various cancers are growth factor dependent, enabling HSGAGs to regulate cell processes in these cancers. Changes in HSGAGs can influence autocrine and paracrine signaling loops potentially leading to unregulated tumor growth [472].

HSGAGs are also intimately involved in oncogenesis as well as tumor growth, progression, and metastasis. During tumor onset, cell surface HSGAGs are altered as the cell is transformed [38, 427]. This process may change cellular responses to extracellular mitogens and cytokines important to a tumor, potentially affecting growth [274]. Alternatively, changes in the cell surface HSGAG profile, including not only GAG fine structure, but also sequences in the core protein, may play a more fundamental role [427]. Syndecan-1 expression is downregulated in several cancers including uterine carcinoma, with progressively decreasing levels as the tumor becomes invasive [417]. Glypican-1 also acts as a negative regulator of growth for some cancers [123]. The cell surface HSGAGs additionally contain cryptic regions that can promote or inhibit proliferation and metastasis [274].

In addition to cell surface HSGAGs, those in the ECM also play important roles in cancer. HSGAGs are a major component of the basement membrane, which acts as a barrier to tumor invasion and metastasis. Breakdown of the basement membrane and other ECM components by enzymes including heparanase, is an important step in cancer metastasis [186, 495, 496]. Exogenous highly sulfated HSGAGs inhibit tumor cell adhesion, an essential step in metastasis [44]. Endostatin, a collagen XVIII-derived fragment that prevents tumor growth, is additionally inhibited by specific HSGAG fine structures [40, 247, 345, 421, 503]. HSGAGs also indirectly affect cancer viability by regulating angiogenesis, a process that is essential for cancers to grow beyond 1-2 mm [133, 196]. The multitude of angiogenic factors regulated by

HSGAGs, including FGFs and vascular endothelial growth factors (VEGFs) enable changes in HSGAGs to promote or inhibit angiogenesis [423].

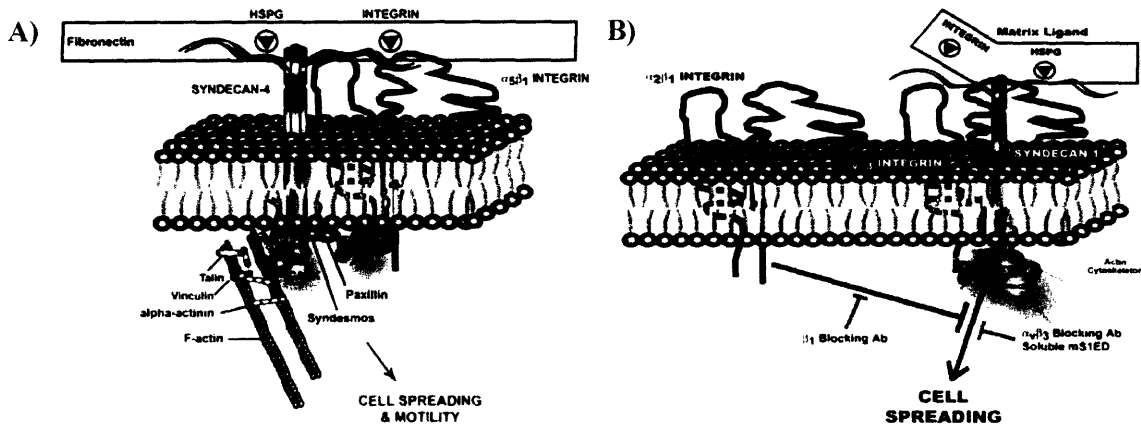


Figure 1.4. Syndecan-integrin interactions. Various mechanisms by which syndecans and integrins can interact to influence cell spreading. Figure adapted from [24].

1.4.2 HSGAGs and integrin signaling

Cell adhesion is a critical aspect of proliferation migration and differentiation. Cell surface adhesion receptors bind directly to ECM components, serving as a link between the ECM and cell signaling pathways [306, 408]. Several ECM ligands contain closely spaced binding domains to integrins and to PGs, suggesting the possibility of signaling complexes concurrently involving both components. Nonetheless, only the role of the integrin component of this putative complex has been established [23]. The GAG component of syndecans is well characterized in its ability to bind several ECM components including collagens, fibronectin, and laminin [29]. The syndecan core protein has also been implicated in adhesion-mediated signaling. Focal adhesions and stress fiber formation, for example, require both syndecan-4 and integrins (**Figure 1.4A**) [199, 505]. Syndecan-1 expression can also promote cell spreading, focal adhesion formation and stress fiber formation [59, 173]. Syndecan-1 has been implicated in acting in concert with β_1 integrin (**Figure 1.4B**). Syndecans are thought to trigger cell spreading associated signaling cascades either by exposing a cryptic binding site or by directly modulating their activation state [23, 190]. Recent evidence has demonstrated that, syndecan-1 can form a signaling complex with $\alpha_v\beta_3$ integrins, which promotes cell signaling [24]. Furthermore, syndecan-4 has been postulated to provide a mechanical link between $\alpha_v\beta_1$ integrins and F-actin

[24]. Syndecans and associated HSGAGs may therefore serve as a potent mediator of integrin signaling and cell spreading.

1.4.3 Cell surface HSGAGs and monolayer integrity

Tissue injury due to infection or physical damage promotes an inflammatory response that is essential to regaining normal homeostasis. An important component of this process is the translocation of various white blood cells from the vascular system through the endothelial lining and the ECM to the injured tissue [3]. Acute inflammation is also associated with an increase in vascular permeability that has pathological consequences including tissue edema, inappropriate tissue oxygenation

leading to organ failure, and potential multiorgan failure subsequent to trauma and sepsis [259, 284, 297].

Vascular permeability is increased by a complex four-step

process (Figure 1.5) involving back-and-forth cell-cell crosstalk [3]. The

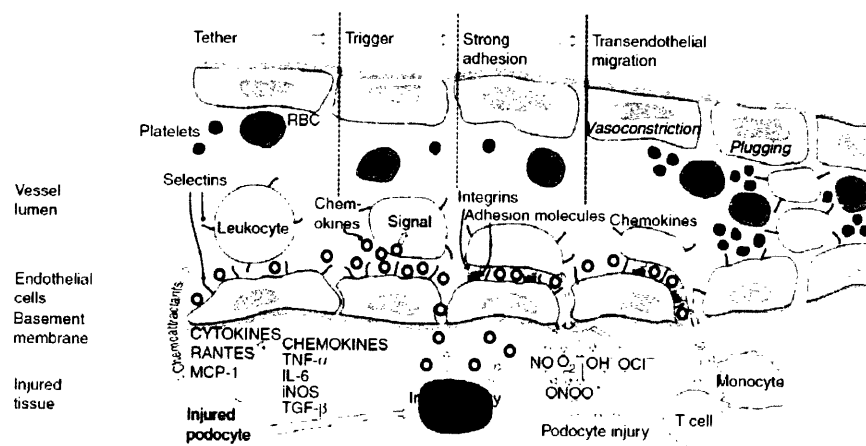


Figure 1.5. Steps by which injury and inflammation promote leukocyte diapedesis and homing. Tissue injury causes leukocytes to roll along the endothelial lining via reversible binding through L- and P-selectins, expressed on the leukocytes and endothelial cells respectively. The cell-cell contact facilitates crosstalk by chemokines which causes leukocyte flattening and subsequent diapedesis through the endothelial lining. Figure from [406].

critical first step involves the elaboration of chemoattractants, cytokines, and complement components from the site of injury, which activate the endothelium as well as leukocytes [406]. Neutrophils release inflammatory peptides from azurophilic granules, which contain cationic peptides including heparin-binding protein(HBP)/azurocidin which, along with elastase and cathepsin G, has been implicated in vascular permeability changes [43]. The method by which HBP induces vascular permeability, however, remains unknown. The highly cationic nature of these proteins supports possible HSGAG binding. Furthermore, anticoagulant therapy in acute

lung injury has been demonstrated to increase pulmonary vascular permeability [256]. HSGAGs may therefore be essential mediators of monolayer integrity.

1.5 GAG-Protein Interactions

GAG-protein interactions play important roles in a wide variety of physiological and pathological processes (see [61, 77, 476]). Ligand-GAG binding has a wide variety of functional consequences including: ligand immobilization increasing the local concentration; induction of conformation changes in the ligand or the GAG chain enabling presentation to receptors; oligomerization of growth factors or chemokines; and protection of growth factors and chemokines from proteolysis and denaturation [60, 86, 109, 140, 202]. Interactions between HSGAGs and other ECM components regulate development, angiogenesis, wound healing, and tumor progression [77, 167, 207, 268, 370]. HSGAGs, CS, and DS can also serve as cofactors, regulators of enzymatic activity, signaling molecules, and bacterial virulence factors [90, 411, 432, 474]. By regulating the coagulation cascade as well as a plethora of morphogens, cytokines, and chemokines, GAGs play a critical role throughout biology (**Table 1.1**).

FGF-1 ^c	Penta to heptasaccharide containing IdoA(2-OSO ₃), GlcNS, GlcNS(6-OSO ₃) Decasaccharide required for activity (63)
FGF-2	Tetradecasaccharide containing [IdoA(2-OSO ₃)-GlcNS] ₅ Pentasaccharide Hex-A-GlcNS-Hex-A-GlcNS-IdoA.(2-OSO ₃) Decasaccharide with 6-O sulfate required for activity (3, 60)#32]
HGF/SF (HS site)	[IdoA-GlcNS(6-OSO ₃)] ₃ ; Octasaccharide required for activity (81)
HGF/SF (DS site)	[IdoA-GalNac(4-OSO ₃)] ₃ (80)
TGFβ-1	Long S-domain or two short ones separated by a heptasaccharide (91, 92)
PDGF	Hex/octasaccharide containing IdoA(2-OSO ₃)-GlcNS(6-OSO ₃) (98)
HARP/HB-GAM	HS, DS, S-domains (84)
Wnt family	?
EGF family members	S-domains
VEGF	?
Collagens	S-domains (110)
Fibronectin Hep II	Octasaccharide containing IdoA(2S)-GlcNS, 6-O-sulfate increases affinity (3, 117)
Laminin	Dodecasaccharide [IdoA(2-OSO ₃)-GlcNS(6-OSO ₃)] ₆ (129)
IGFBP ₃ and IGFBP ₅	S-domain containing O-sulfate (102)

Table 1.1 HS and DS structures specific to GAG-binding proteins. Table adapted from [90].

1.5.1 The coagulation cascade

One of the primary reasons HSGAGs are the most studied among the GAGs is heparin's role in anticoagulation and thromboembolic disorders. Hemostasis is carefully maintained by a complex system involving protein coagulation factors and platelets. The activation of this system promotes the sequential cleavage of a cascade of zymogens (**Figure 1.6**), ultimately forming a fibrin clot. The coagulation cascade contains a series of intrinsic feedback mechanisms by which the resultant activity can be altered after the cascade is initiated. These include antithrombin III (AT-III), heparin cofactor II, tissue factor pathway inhibitor, protein C, protein S, and fibrinolysis [293]. This regulation is essential to limit coagulation to the site of local injury and prevent potentially lethal conditions including disseminated intravascular coagulation [48].

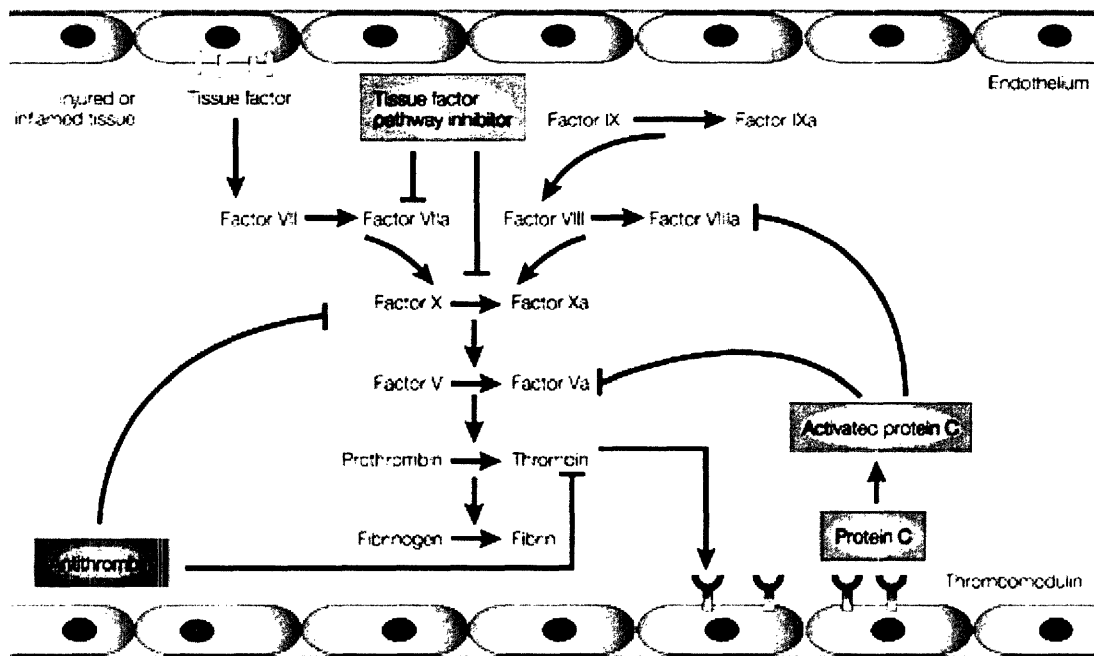


Figure 1.6. The coagulation cascade and its inhibitors. Coagulation is initiated by either tissue factor interacting with Factor VII to produce activated Factor VII (Factor VIIa), or the activation of Factor IX via activated Factor XII activating Factor XI (not shown). These pathways converge on Factor X, and ultimately lead to fibrin clot formation. Antithrombin blocks the activation of Factors XII, XI, IX, X and II. Figure from [293].

Heparin's ability to inhibit coagulation through AT-III is essential to its therapeutic use. Heparin binds thrombin (Factor IIa) and AT-III forming a ternary complex that increases the

ability of AT-III to inhibit thrombin by over 2000-fold, thereby preventing progression of the cascade [372]. AT-III binds heparin through a specific pentasaccharide [443], present in only 3% of commercially available heparin, forming a 1:1 complex that inhibits Factor Xa. Since heparin is mostly non-AT-III binding and its sequence heterogeneity allows for a wide range of functions, a number of side effects, including heparin-induced thrombocytopenia, are associated with heparin therapy. Furthermore, the low level of active sequences leads to relatively unpredictable anticoagulant activity [499]. The pentasaccharide specifically activates AT-III for rapid inhibition of Factor Xa, but the actual inhibition of thrombin requires a chain of 16-18 monosaccharides that has not yet been defined [372]. The sequence and chain length of heparin are therefore critical determinants of anticoagulant activity.

Heparin plays a range of additional roles in coagulation. These include regulating the release of tissue factor pathway inhibitor, modulating heparin cofactor II activity and regulating von Willebrand Factor activity [11, 212, 418, 444]. DS has also been demonstrated to affect the coagulation cascade. A specific DS hexasaccharide binds with high affinity to heparin cofactor II and inhibits thrombin [291]. This hexasaccharide, three 2-*O* sulfated iduronic acid moieties and three 4-*O* sulfated galactosamines, constitutes only 2% of hexasaccharides in DS. Binding of the hexasaccharide to heparin cofactor II inhibits the thrombin-fibrin complex [263]. Additionally, a cell surface CS PG, modulates thrombin activity through a specific terminal CS trisaccharide, although this is not sufficient for thrombin inhibition [47, 48].

1.5.2 Fibroblast growth factor and cell signaling

The role of HSGAGs in modulating cell signaling has been best studied in the FGF family of proteins [164, 166, 397, 449]. FGFs interact with both cell surface tyrosine kinase FGF receptors (FGFRs) and the HSGAG component of HSPGs [153, 178, 348, 396]. Currently 23 members of the FGF family have been identified, all of which contain an identifiable, albeit varying, HSGAG binding sites [349]. There are five FGFRs which possess different isoforms due to alternative splicing [119, 445]. The ectodomain of the FGFR contains three immunoglobulin (Ig)-like domains (IgD1-IgD3). IgD2 and IgD3 mediate FGF binding. The alternative splicing, primarily within IgD3, influences FGF binding specificity [191, 348, 379, 514].

The interactions of HSGAGs with both FGF and FGFR provide receptor selectivity and modulate the downstream response [6, 163, 213, 354, 389]. HSGAGs fractions that promote only FGF1 signaling, only FGF2 signaling, or both, have been identified, suggesting that different oligosaccharide structures are responsible for the activation of different ligands [246, 383, 388, 389]. The distinct HSGAG moieties have important physiological roles. For example, within the neuroepithelium, there is a developmental switch in mRNA production of FGF2 (also bFGF) to FGF1 (also aFGF) that is reflected by structural changes within cell surface HSPGs [335]. Although FGF1 and FGF2 are the best studied members of the FGF family, these phenomena are likely extendable to the other FGFs. The HSGAG binding sites in FGF1 and FGF2 are more basic than the HSGAG binding site of FGF7 (also keratinocyte growth factor or KGF) [512]. Furthermore, FGF2 and FGF4 recognize distinct HSGAG structures [6].

Because of the importance of HSGAGs in defining FGF activity, extensive research has focused on how HSGAGs modulate FGF signaling. HSGAGs are thought to facilitate and stabilize self oligomerization of FGFs [87]. The interaction of HSGAGs with FGF2 may increase affinity for the receptor [331, 402] as well as promote dimerization [250, 449]. Furthermore, HSGAG-FGFR interactions regulate the kinetics of ternary complex formation [383]. Oligomeric FGF binding to FGFR facilitates receptor oligomerization, leading to tyrosine kinase phosphorylation and subsequent signal transduction [511].

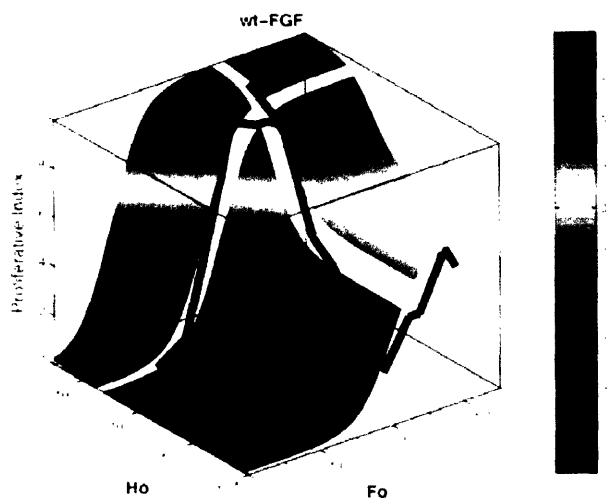
Various mechanisms by which HSGAGs mediate FGF oligomerization have been proposed and investigated [87, 178, 250, 486, 487]. Crystal structures have provided insight into how FGF family members interact with HSGAGs and with FGFRs. Co-crystals of FGF1-HSGAG [92], FGF2-HSGAG [111], FGF1-FGFR1 [379], FGF2-FGFR1 [378], FGF1-FGFR2 [451], FGF2-FGFR2 [379], have been obtained along with ternary complex crystal structures of FGF1-HSGAG-FGFR2 [365] and FGF2-HSGAG-FGFR1 [431]. High and low affinity binding domains within FGF1 define its interactions with HSGAGs [504]. FGF1 interacts with FGFR2 forming two 1:1 complexes that, based on heparin induced rotation, produce an asymmetric ternary complex with heparin interacting with both ligands but only one receptor [365]. Specifically, the two FGF1 ligands are linked by heparin [92]. FGF2 dimers, however, assume a distinct structure. Dimerized FGF2 forms a stable complex with FGFR in the absence of heparin, but leaves a canyon in which heparin likely interacts with both FGFs in *cis* as well as with the FGFR [378]. Correspondingly, heparin has been found to interact with FGF2 and

FGFR1, promoting dimerization and stabilizing the ternary complex [431]. Heparin binds FGF2 without altering the protein conformation, though the heparin chain itself undergoes changes in backbone torsion angles upon ligand binding [111, 392].

The combination of these structural studies as well as other biochemical studies has identified critical sequences that bind to FGFs and modulate signaling. The predominant oligosaccharides in FGF-HSGAG and FGF-HSGAG-FGFR co-crystal structures are a repeat sequence composed of a 2-*O* sulfated iduronic acid linked to a 6-*O*- and *N*-sulfated glucosamine. FGF2-HSGAG interactions are defined by the degrees of *N*- and 2-*O*-sulfation [289, 477, 501]. In fact, both FGF1 and FGF2 require *N*- and 2-*O*-sulfation for signaling [162]. The 6-*O* sulfate group promotes FGFR1 activation [111, 197, 280], and is thought to be critical for FGF1, but not FGF2, activity [365, 431]. Of note, pentasulfated trisaccharides consisting of a 2-*O* sulfated iduronic acid flanked on either side by *N*- and 6-*O* sulfated glucosamines bind FGF2, but prevent formation of the ternary complex [62]. The HSGAG chain length necessary for activation has also been studied. Typically, tetrasaccharides and hexasaccharides can bind FGF1 or FGF2, but octasaccharides and longer are necessary to bridge a dimerized FGF2 to form a ternary signaling complex with the receptor [178, 365, 431]. Nonetheless, HSGAG polymers as small as disaccharides and trisaccharides have been found to support FGF signaling [347].

1.5.2.1 The compensation model

Even with the multitude of co-crystal structures that have been solved, the specific role of HSGAGs in modulating FGF activity has not been fully understood. HSGAGs are not required for FGF2 to induce a cellular



$$y = \frac{0.60 + 0.25H_o}{0.93 + 0.25H_o + \frac{1}{F_o}}$$

Figure 1.7. Heparin enhances the strength of FGF2 cellular mediated responses. Using the compensation model for FGF2-heparin interactions, the concentrations of the two components (F_o and H_o) can be used to predict the level of cellular mediated response as described mathematically by the equation, which dictates the 3-dimensional surface observed. The equation is specific for wildtype FGF2 and heparin. Figure adapted from [358].

mediated response through FGFR1 [114, 358, 402]. The ability of HSGAGs to facilitate FGF self-association has suggested that HSGAGs serve to enhance signaling by facilitating a cellular response at lower ligand concentrations and/or with more rapid kinetics [87, 383]. Producing a unified mathematical model that accounts for HSGAG-dependent and HSGAG-independent signaling by FGF2 can serve to characterize how optimal cellular mediated responses can be achieved by a FGF2-HSGAG-FGFR ternary interaction. Correspondingly, a single equation that can predict the normalized cellular response as a function of heparin and FGF2 concentration (**Figure 1.7**) reveals that a given output can be achieved by appropriately adjusting the concentrations of FGF2 and HSGAG [358]. Furthermore, several FGF2-HSGAG combinations can yield the same level of signaling, suggesting that as with other equilibrium reactions, reductions in the binding interactions between any two components, either by decreased concentration or by mutation, can be compensated for by increasing the effective concentration of the other components [358]. This finding is of significance as it demonstrates that HSGAGs are an important component of the FGF signaling complex that serve to facilitate cellular responses as well as to fine tune the specific cellular response to make it appropriate for extracellular cues. Physiologically, upregulation and downregulation of cell surface or extracellular HSGAGs, therefore, serve as an important mechanism by which cells define the nature and strength of FGF2-mediated signaling [255].

1.5.2.2 Dimeric FGF2

Multiple models of FGF2 oligomerization in the presence of HSGAGs have been suggested. FGF2-HSGAG co-crystal structures [111] as well as several biochemical studies [87, 178, 486] reveal a *cis* conformation where FGF2 molecules have substantial protein-protein interactions. NMR studies, however, suggest a symmetrical FGF2 dimer with possible disulfated bond formation [317]. Notably, FGF1 dimerization occurs in a *trans* confirmation, without protein-protein contacts [92]. An effort to understand how FGF2 dimerizes, led to the development of a novel engineered protein, dimeric FGF2 (dFGF2),

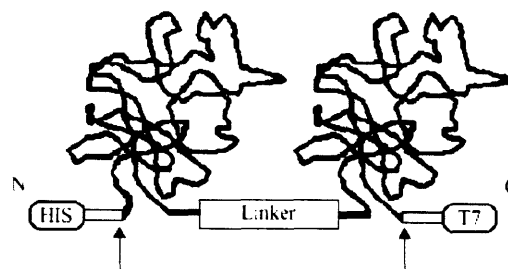


Figure 1.8. Diagram of dFGF2. Figure adapted from [250].

which has the activity of heparin-bound FGF2 in a heparin-free environment, by directly linking two FGF2 molecules together (**Figure 1.8**) [250]. This novel protein provided evidence that the functional FGF2 dimer involves substantial non-covalent protein-protein interactions with the two FGFs in the *cis* conformation. One could predict, based on the compensation model, pre-dimerizing FGF2 would increase the cellular response. As such, using dFGF2 eliminates the requirement of heparin for a maximally FGF2-mediated response [18, 250, 358]. Depending of the specific assay, dFGF2 requires a lower concentration to achieve the same output (increased potency) and/or elicits a higher absolute cellular response (increased efficacy; **Figure 1.9**).

The ability of dFGF2 to produce equally or more efficacious biological effects at doses 8-10 fold less than FGF2 suggests that the administration of the engineered growth factor may offer substantial therapeutic potential. Members of the FGF family are in clinical trials for several important indications including dermal wounds, peripheral vascular disease, and coronary artery disease. FGF2 had been previously investigated for its efficacy in the treatment of acute ischemic stroke, but both the American and European trials were discontinued before

completion. Clinical trials of intravenous FGF2 initiated for acute stroke failed to show efficacy, but suggest a potential benefit of FGF2 treatment in the subacute, recovery phase following stroke [41]. Given its: known neuroprotective and vasoactive capacities; its success in both

Response	FGF2 1.5 pmole	FGF2 6.0 pmole	dFGF2 0.7 pmole
Linear length (mm)	0.24 ± 0.05*	1.56 ± 0.04	1.84 ± 0.05
Clock hours	0.38 ± 0.07	1.50 ± 0.07	2.06 ± 0.16

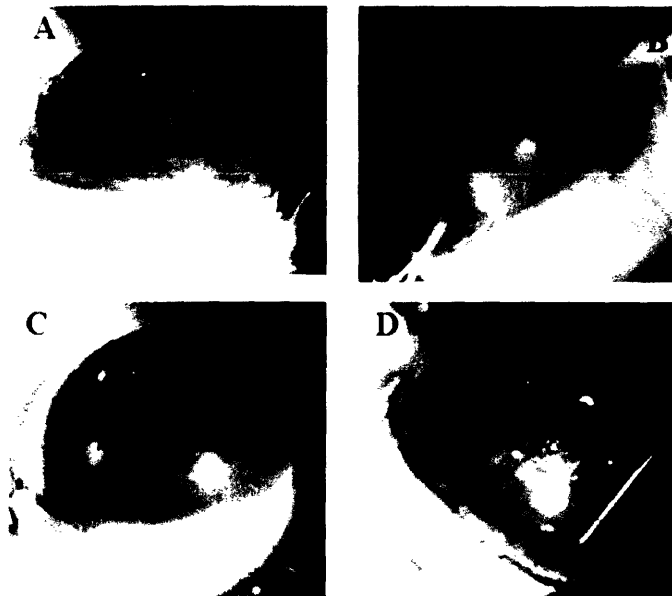
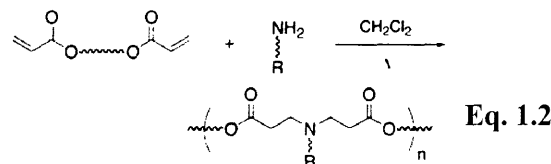
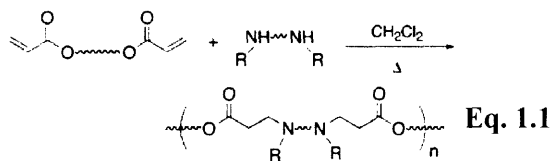


Figure 1.9. dFGF2 has increased potency and efficacy compared to FGF2 *in vivo*. Slit lamp photographs of rat corneas six days after implantation of Hydron pellets containing A) No FGF2 B) 6.0 pmol FGF2 C) 1.5 pmol FGF2 or D) 0.7 pmol dFGF2. Arrows denote location of pellet implantation. The control pellet did not stimulate angiogenesis while those with FGF2 and dFGF2 did. The angiogenic response elicited with dFGF2 was greater than that elicited by FGF2 at ~ten-fold greater concentration. Figure adapted from [250].

treating acute cerebral ischemia and in enabling functional recovery after stroke; the short plasma half-life of 85 ± 11 minutes; and its well characterized metabolism yielding no truncated metabolites, FGF2 remains an important growth factor for investigation in the setting of stroke [16, 222, 224, 233, 288, 480, 517]. The failure of FGF2 in clinical trials underscores the need to develop more efficient approaches to achieve the therapeutic effect in order to minimize serious potential adverse reactions. The physiological role of FGF2 in stroke, wherein FGF2 is elaborated into the cerebral ECM by movement through the damaged blood-brain barrier [127] suggests that appropriate dosing with increased efficacy, as can be achieved with dFGF2, may offer a potential method to treat stroke.

1.6 Intracellular delivery of large, anionic biopolymers using poly (β -amino ester)s

The ability to deliver DNA and nucleotide-based drugs has long offered the potential for therapeutics that could reshape the medical landscape [10, 83, 318]. Although viral techniques have led to the greatest clinical success to date, issues regarding the safety of such vectors have given rise to efforts to develop alternative strategies, including polymer delivery vehicles [281-283]. One area that has been extensively investigated is that of cationic polymers. The negatively charged strands of DNA allow for conjugation with cationic polymers, which leads to condensation into nanometer-scale complexes that can enter cells via endocytosis [282]. The use of cationic polymers, such as poly(ethylene imine) (PEI) and polylysine, has been associated with drawbacks including substantial cytotoxicity [387, 524]. Safer alternatives to these polymers were developed by producing degradable polyesters with cationic side chains, which condense DNA, mediate gene transfer, and exhibit low cytotoxicity [264-266, 387]. Poly(β -amino ester)s (PAEs) were developed in attempting to maintain functionality associated with the cationic side chain polyesters while reducing the need for



Equations adapted from [7].

expensive coupling reagents or specialized monomers [285]. These polymers are synthesized by the conjugate addition of primary or secondary amines to diacrylates (**Equations 1.1 and 1.2**) [285, 286].

PAEs, as a class of polymers, degrade hydrolytically and condense plasmid DNA. PAEs additionally offer the advantages of having inexpensive monomers and simple, one step polymerization without requiring purification. The simplicity of synthesis allows for a large variety of possible polymers to be produced [286]. Nonetheless, structural variations can have a significant impact on DNA binding and transfection efficacies [285]. A first generation library of 140 PAEs was produced by the combinatorial addition of 7 diacrylates (**A-G**) to 20 amines (**1-20**). Within the first library, 70 polymers were water soluble, and 56 condensed DNA (**Figure 1.10A**) at a 1:20 DNA:polymer (w/w) ratio. Notably, two polymers, **B14** and **G5**, were 4-8 times more effective at internalizing DNA than PEI (**Figure 1.10B**), but exhibited notably less cytotoxicity. Additionally, studies of this library revealed that PAEs best promote transfection with a diameter less than 250 nm, a positive zeta potential, and a near neutral pH [4].

While PAEs offer potential advantages including simplicity of production, low toxicity, and reduced vector size limitations, their viral transfection efficiency in the first library, with 140 members, was much lower

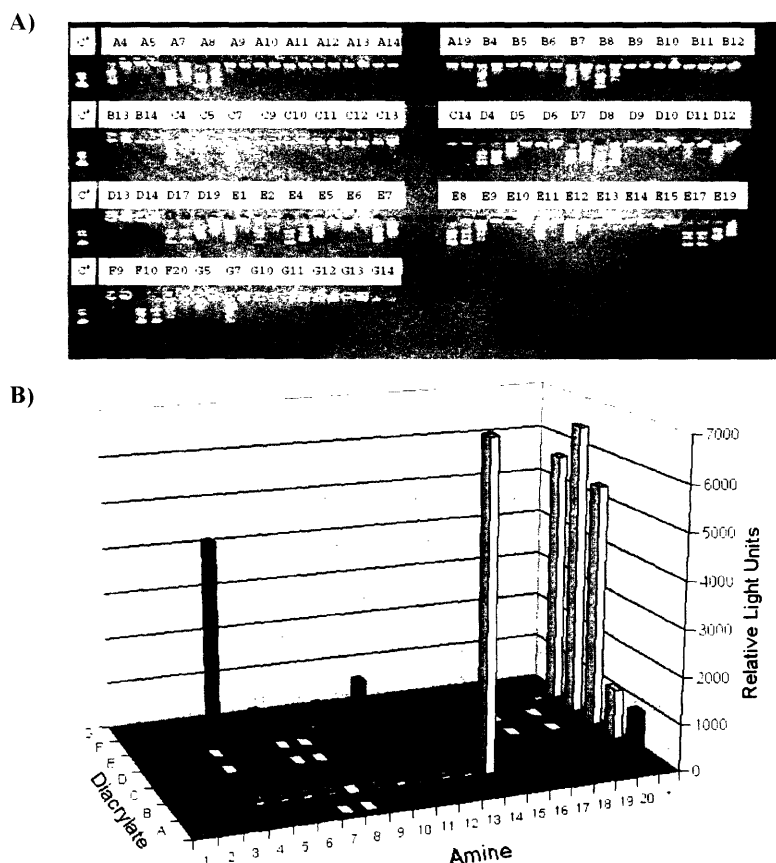


Figure 1.10. PAEs condense and internalize DNA. A) Gel shift assay to explore binding of PAEs to DNA. B) Transfection capacity of DNA-polymer conjugates. Figure adapted from [286].

than that of viral vehicles [258, 286]. In an attempt to overcome the efficacy limitations of PAEs, a high-throughput, semi-automated technique was employed, yielding 2350 structurally unique polymers (produced from 94 amines and 25 diacrylates), 46 of which had a higher transfection efficiency than PEI [7]. Furthermore, 26 of these polymers had greater transfection rates than the best conventional reagent, lipofectamine 2000. PAEs have additionally been demonstrated to have *in vivo* efficacy [8, 273].

The anionic nature of DNA is essential for effective binding and internalization by PAEs. HSGAGs, however, are more anionic than DNA, raising the question as to whether HSGAGs could be condensed and brought into cells by PAEs. HSGAGs are normally brought into the cell in a controlled fashion. Heparin binds to FGF2 and FGFR1, for example, forming a ternary complex that is internalized [365, 448]. Furthermore, a subset of PGs exist and function within intracellular compartments [243]. This is of potential importance because the relative biological location of HSGAGs and HSPGs influences function: the tumorigenicity of an HSGAG chain is distinct whether it is free in the ECM or attached to an HSPG on the cell surface [274]. The role of diffuse heparin within the cell, however, has not yet been established.

1.7 Immobilized GAGs

GAGs have long been used to coat medical surfaces, beginning with the coating of medical implants with heparin to reduce thrombogenicity [179, 248, 401]. When heparin is used to coat stents, it stimulates neo-intima formation, potentially by interacting with growth factors [278, 328, 460]. Fucosylated CS, however, inhibits smooth muscle cell (SMC) proliferation [461]. Interestingly, CS C, which is typically devoid of anticoagulant activity, prevents thrombin formation when immobilized on a surface [228], demonstrating that immobilization can change the functionality of some GAGs. The ability to augment GAG behavior with immobilization can potentially elicit novel and enhanced therapeutic functionality.

Immobilized GAGs have been demonstrated to have a wide range of other medically important roles. HS, CS, and HA have been extensively studied for the prevention of urologic stone formation [179, 230]. Immobilized HA is also notable for its ability to greatly reduce bacterial cell adhesion and to inhibit mammalian cell binding [311]. The heterogeneity of GAGs would suggest that a wide variety of functions in addition to those presented here are possible.

The formation of GAG-coated surfaces has been demonstrated by a wide range of techniques, including covalent attachment, photoimmobilization, layer-by-layer deposition, and binding via natural ligands [67, 294, 311, 374, 437, 466]. Chemisorbed techniques, with lower costs and fewer required reagents, also enable immobilization, although the mechanism is unclear. Charge interactions, GAG conformation and dehydration through interactions with water, and hydrogen bonding have each been proposed [312]. Given the potential therapeutic importance of immobilized GAGs, understanding the mechanisms by which adherence occurs using less expensive techniques is of importance.

Objectives

The overall aim of this thesis is to understand the mechanisms by which GAGs modulate cell function, and how the activities of GAGs in various settings can be harnessed to gain insight into and to develop potential treatments for diseases. This thesis focuses on three areas: (a) GAG-growth factor interactions, (b) intracellular GAGs, and (c) new role for GAGs.

GAG-growth factor interactions

GAGs have been well characterized in their ability to regulate cellular behavior by modulating the activity of growth factors. In order to understand the ability of GAGs to influence signals from the ECM, the effects on the FGF family will be examined as a model system, and used to also enable study of other growth factor families. The primary goals of this section are as follows:

- Explore the effects of a novel engineered growth factor in stroke
- Examine the effects of cell derived HSGAGs on FGF activity
- Determine the mechanisms by which cell derived HSGAGs influence cell behavior
- Understand how GAGs influence cell behavior in the presence of multiple growth factor families
- Define mechanisms by which FGFs can induce cellular responses in the absence of cell surface receptors

Intracellular GAGs

The majority of studies focus on the roles of GAGs in the ECM. Nonetheless, GAGs are brought into the cytoplasm in various physiological and pathological processes. This section will focus on the development of a novel system to promote the internalization of GAGs and to explore how intracellular GAGs can influence cell function. The primary goals of this section are as follows:

- Create a method to internalized GAGs
- Explore the effects of internalized GAGs on cells
- Define the potential utility of this technique

New roles for GAGs

The regulatory potential of GAGs has not yet been fully elucidated. In this section, previously unexplored functions of GAGs will be defined and investigated:

- The role of GAGs in vascular permeability.
- Develop GAG surfaces
- Explore the effects of GAG surfaces on cells

The multifaceted approach employed allows for a more thorough understanding of the role of GAGs in modulating cell function. The results of these studies will not only reveal important features of how GAGs regulate cellular activity, but also develop a more complete understanding of various important diseases, leading to potential new therapeutic targets and treatments.

Section 2. Glycosaminoglycan-Growth Factor Interactions

Overview

Section 2 examines how glycosaminoglycans interact and modulate the activity of growth factors. Exploring how HSGAGs interact with FGF2 reveals how they dimerize, from which a novel, engineered growth factor, dFGF2, can be produced. This growth factor was found to enable functional recovery after stroke. Cell surface HSGAGs can also regulate FGF2 activity, though the ability of a given cell to elicit an effect is based on the fine structure intrinsic to that cell type. HSGAG modulation of FGF activity also extends to FGF1 as well to various FGFR isoforms. Cell surface HSGAGs can also regulate tumor cell activity. HSGAGs with distinct fine structures, however, regulate different cell processes, such that a given cell surface HSGAG can inhibit tumor growth while another can inhibit metastasis. GAGs beyond HSGAGs can also regulate the activity of various FGFs, as well as of VEGFs. Different GAGs, however, elicit different cellular effects for specific ligands, and can be used to select for desired cellular responses in a pool of growth factors. The ability of HSGAGs to influence FGF activity also has important implications in inflammatory bowel disease. In a specific *in vitro* model, FGF2 and FGF7 could induce cellular effects in the absence of corresponding FGFRs. This effect was dependent on FGF1. Specifically, FGF1 enabled syndecan-1 to shuttle FGF2 and FGF7 to the nucleus, where they could affect cellular responses. Syndecan-1 was additionally identified as a protective factor in inflammatory bowel disease.

Chapter 2. Enhanced functional recovery after focal cerebral ischemia with dimeric fibroblast growth factor-2, a novel engineered growth factor

2.0 Summary

Dimerized fibroblast growth factor FGF2, dFGF2, is a protein consisting of two monomers of FGF2, joined by a tripeptide linker, putting the monomers in optimal conformation to interact with high-affinity FGF receptors and to promote a cellular response. This engineered growth factor is stable in the active form and is less dependent than FGF2 on extracellular heparan sulfate moieties for its maximal biological effects. In previous studies, we showed that the intracisternal administration of FGF2 enhanced sensorimotor recovery in a model of focal cerebral infarction (stroke) in rats. In the current study, we show that the intracisternal administration of dFGF2 at one and three days after stroke also enhances sensorimotor and vestibulomotor recovery following focal cerebral infarction in rats. dFGF2 represents a potential treatment that enhances functional recovery after stroke and offers several advantages over FGF2, including stability and independence from extracellular heparin sulfates.

2.1 Introduction

Previous preclinical studies have demonstrated the potential usefulness of FGF2 in animal models of acute stroke and stroke recovery. If FGF2 is given intracerebroventricularly or intravenously within four hours after the onset of permanent or temporary focal ischemia in rats, infarct size is reduced, likely due, in part, to reduction of apoptotic cell death at the borders of focal infarcts [15, 241, 398]. If, on the other hand, FGF2 is given intracisternally starting at one day after permanent focal ischemia in rats, infarct size is not reduced, but recovery of neurological function is enhanced [223-225]. Mechanisms of this recovery-promoting effect likely include: (1) stimulation of new axonal sprouting and new synapse formation in

undamaged regions of brain in both the ipsilateral and contralateral hemispheres [224, 225], and (2) stimulation of proliferation, migration, and differentiation of progenitor cell populations in brain [497]. Clinical trials of intravenous FGF2 initiated for acute stroke failed to show efficacy, but suggest a potential benefit of FGF2 treatment in the subacute, recovery phase following stroke [41].

In the process of FGF2 signaling, two FGF2 monomers come together to promote dimerization of high-affinity FGF cell surface receptors, thus initiating the signal transduction cascade [234, 250]. Covalent bonding of two FGF2 monomers with a tripeptide linker puts the monomers in an optimal conformation for this process [250]. The resulting molecule, dFGF2 is stable and more potent on a molar basis than monomeric FGF2 in several *in vitro* and *in vivo* assays, including endothelial cell proliferation and angiogenesis [250]. dFGF2 is also less dependent than FGF2 on binding to extracellular heparin sulfate moieties to achieve a maximal biological effect [250]. In the current study, we examined the effects of dFGF2 in promoting neurological recovery in a model of focal cerebral ischemia in rats.

2.2 Results

Occlusion of the right proximal middle cerebral artery (MCA) produced infarction in the dorsolateral cerebral cortex and underlying striatum, as described previously [223-225, 497]. At 30 days after MCA occlusion, total, cortical, or striatal infarct volume were not different between vehicle- or dFGF2-treated animals (**Table 2.1**).

Treatment	N	Total (%)	Cortex (%)	Striatum (%)
Vehicle	10	30.07 ± 2.53	39.43 ± 3.43	55.01 ± 5.50
dFGF2	10	31.15 ± 3.39	41.81 ± 4.66	47.31 ± 5.73

Table 2.1. Measurements of infarct volume. There were no differences in infarct volume between vehicle- and dFGF2-treated animals. Data are expressed as percent of intact hemispheric volume (all p values not significant.).

No hemorrhage, tumor formation, excessive inflammation, or other histological changes, other than infarction, were seen in post-stroke brains. Body weight after surgery was not different between vehicle- and dFGF2-treated animals (**Figure 2.1**).

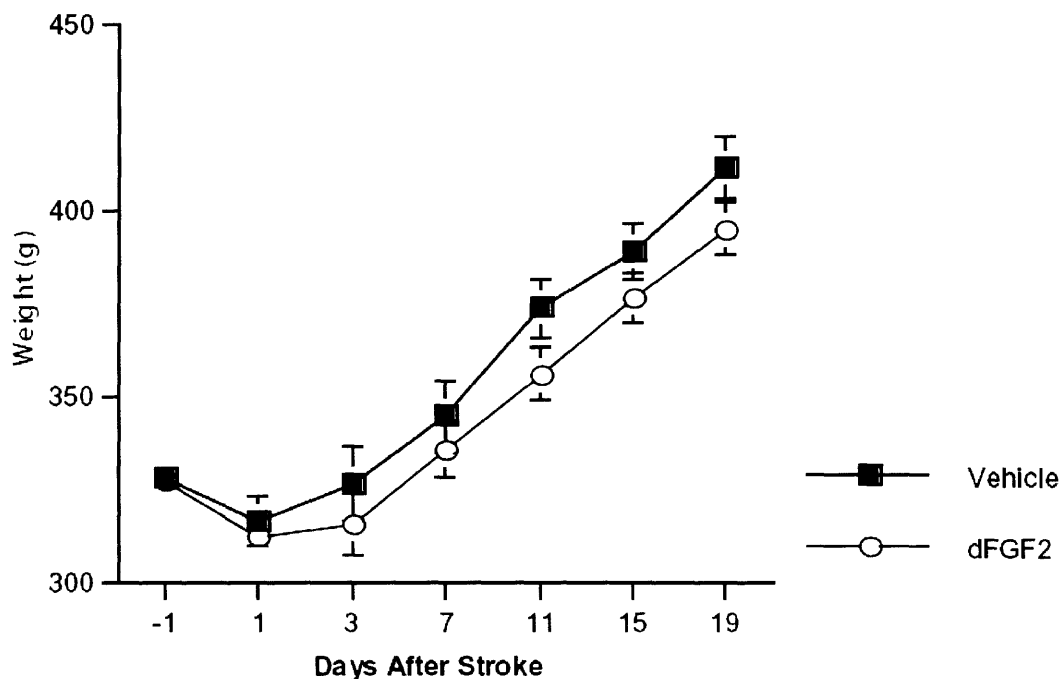


Figure 2.1. Body weight measurements. There was no difference in body weight after surgery between vehicle- and dFGF2-treated animals (N = 10 vs. 10, all p values not significant).

Treatment with intracisternal dFGF2 produced marked enhancements of functional recovery in three of four behavioral tests performed, namely the forelimb and hindlimb placing tests and the body swing test (**Figure 2.2**). No enhancement of function was seen on the spontaneous limb use (cylinder) test.

2.3 Discussion

In summary, we found that intracisternal dFGF2 enhanced recovery of sensorimotor and vestibulomotor function following unilateral cerebral infarction in rats. These results were most pronounced on forelimb and hindlimb placing tests and the body swing test and not evident on

the spontaneous limb use test. These results parallel those that we have obtained using other growth factors, in which we have found that limb placing and body swing tests appear to be more sensitive to treatment effects than the spontaneous limb use test (unpublished data).

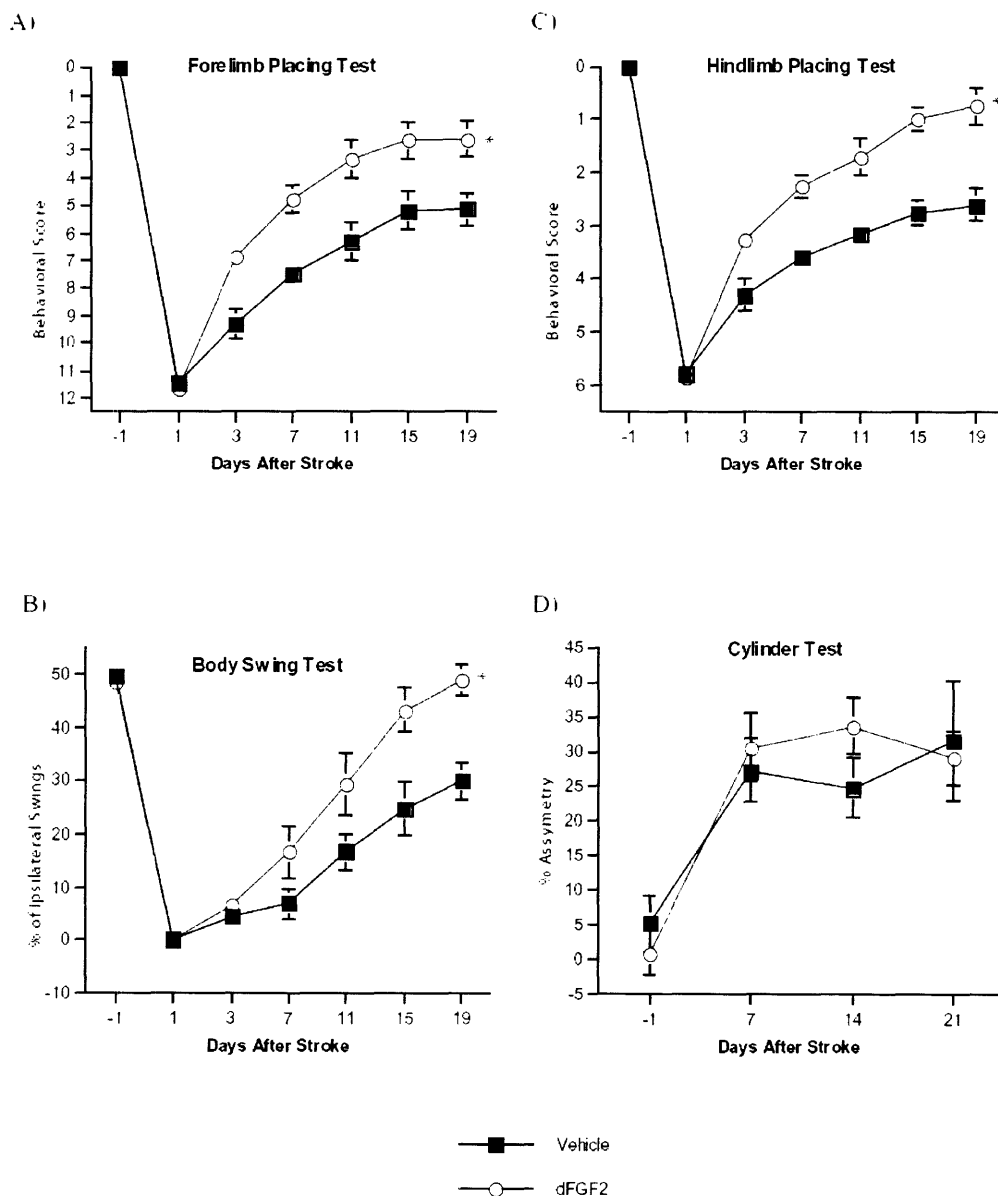


Figure 2.2. Behavioral outcome of dFGF2 treatment. Significant enhancement in behavioral recovery was seen in dFGF2-treated (N = 10) vs. vehicle-treated animals (N = 10) in the: A) forelimb placing test ($p < 0.002$), B) hindlimb placing test ($p < 0.0001$), and C) body swing test ($p < 0.005$), but not the D) spontaneous limb use (cylinder) test (all p values not significant).

In particular, current results obtained with intracisternal dFGF2 are similar to those obtained in previous studies using equivalent doses and dosing schedules of FGF2 [223-225]. Possible mechanisms by which FGF2 may enhance neurological recovery after stroke include: (1) enhancement of neural sprouting and new synapse formation in uninjured parts of brain, and (2) stimulation of progenitor cell proliferation, migration, and differentiation in the post-stroke brain. Indeed, in previous studies [224, 225], we showed that intracisternal FGF2 upregulates the expression of a molecular marker of new axonal sprouting, GAP-43, in cerebral cortex surrounding focal infarcts and in the contralateral homologous cortex. Moreover, inhibition of GAP-43 upregulation by intracisternal co-administration of GAP-43 antisense oligonucleotide with FGF2 blocks enhancement of sensorimotor recovery [225]. Intracisternal FGF2 also promotes progenitor cell proliferation in the subventricular zone (SVZ) and dentate gyrus of the hippocampus (DG) following focal infarction [497]. Some of these proliferating cells in the SVZ subsequently acquire an immature neuronal phenotype and appear to migrate out of the SVZ, whereas those in the DG remain *in situ*, acquiring a mature neuronal phenotype [497]. Changes in progenitor cell proliferation, migration, and differentiation following FGF2 treatment after stroke may contribute to enhancement of functional recovery [497]. Because dFGF2 represents a dimeric form of FGF2 that is optimized for binding to high-affinity FGF2 receptors, the mechanisms of action of dFGF2 in promoting recovery after stroke are likely to be the same as FGF2.

Both intracisternal FGF2 and dFGF2 may prove useful as treatments to enhance neurological recovery after stroke. Indeed, dFGF2 may prove superior to FGF2 in several respects. First, dFGF2 is a stable molecule in its active form, as opposed to FGF2, which must interact with a second monomer in an appropriate manner to exert its biological effects. Second, dFGF2 is not dependent on extracellular concentrations of heparin/heparan-like glycosaminoglycans for its effects [250]. Third, dFGF2 may prove to be a more potent molecule than FGF2. Indeed, dFGF2 is more potent than FGF2 in *in vitro* assays of smooth muscle cell proliferation and endothelial cell survival, as well as in *in vivo* assays of angiogenesis [250]. Although the effect of intracisternal dFGF2 in promoting neurological recovery in a rat model of stroke was similar to that previously-reported for equivalent doses of FGF2, this does not exclude the possibility that dFGF2 is more potent at other doses. Further studies are required to resolve this issue.

2.4 Significance

The results of this study demonstrate that dFGF2, a dimeric form of FGF2, shows promise as a potential treatment to enhance neurological recovery following stroke. Further study of dFGF2 is warranted to explore its full therapeutic potential.

2.5 Experimental Procedures

Construction of dFGF2. dFGF2 was cloned and purified as previously described [250]. Briefly, a template of wild-type FGF2 was used and modified by incorporation of DNA sequences corresponding to a his tag, a T7 tag, a tripeptide linker, and a thrombin cleavage site through PCR. Introduction of the restriction sites *NdeI*, *SacI*, and *SpeI* to the 5' and 3' of two FGF2 genes enabled controlled subcloning of two differentially modified FGF2 genes into the pET14b variant expression vector (gift of Dr. David Ornitz, Washington University, Saint Louis, MO). The vector was transfected into the *E. Coli* strain BL21, enabling expression of the protein. The protein was then purified by Ni²⁺ chromatography [106, 358], and subsequent T7-affinity chromatography, as described by the manufacturer (Novagen, Madison, WI). The concentration of the expressed and purified protein was determined by enzyme-linked immunosorbent assay. dFGF2 was stored in PBS containing imidazole (1.2 mM) and Tris HCl (48 M), pH 7.4, at -85°C until use. After production, and again before use, the activity of dFGF2 was validated using a BaF3 proliferation assay as described [30, 358] with slight modification. Briefly, BaF3 cells previously transfected with FGFR1c were plated and treated with PBS, 50 ng/ml dFGF2 alone, 50 ng/ml FGF2, or 50 ng/ml FGF2 supplemented with 500 ng/ml heparin. Cell proliferation was determined after three days by whole cell count. dFGF2 was considered active if the proliferative capacity of dFGF2 was the same as FGF2 with heparin, and significantly greater than FGF2 alone.

MCA occlusion. Proximal MCA occlusion was employed to induce focal infarcts of the right dorsolateral cerebral cortex and underlying striatum [223-225, 497]. Male Sprague-Dawley rats

(Charles River Breeding Laboratories), 300-350 g, were handled daily for one week before surgery. One day prior to surgery, animals were injected intraperitoneally with 40 mg/kg cefazolin sodium. Rats were anesthetized with 2% isoflurane in a nitrous oxide/oxygen mixture (2:1). Core body temperature was thermostatically maintained at 37°C during the procedure. The proximal right MCA was electrocoagulated from just proximal to the olfactory tract to the inferior cerebral vein, and subsequently transected. The surgery was performed sparing the facial nerve and without removing the zygomatic arch. Following surgery, animals were again injected intraperitoneally with 40 mg/kg cefazolin sodium and were placed into individual cages. All rats were weighed the day prior to surgery and on days of behavioral assessment thereafter.

dFGF2 administration. Recombinant dFGF2 was diluted to a concentration of 10 µg/ml in PBS supplemented with 100 µg/ml BSA (Boehringer Mannheim, Cat. #711454). The vehicle solution contained the same constituents without dFGF2. Prior to intracisternal injections, rats were re-anesthetized with 2% isoflurane in nitrous oxide/oxygen (2:1) and placed into a stereotaxic frame. Rats received either 50 µl of dFGF2 in vehicle (0.5 µg) or vehicle alone by percutaneous injection into the cisterna magna, as described previously [224, 225, 497]. Intracisternal injections of dFGF2 or vehicle were administered at 24 and 72 hours after MCA occlusion (total dose of dFGF2 administered = 1 µg).

Behavioral testing. Rats were examined for behavioral function by employing standardized tests to assess sensorimotor function in the limbs as well as vestibulomotor function. Limb placing tests and body swing tests were performed one day prior to surgery, one day after surgery but prior to injection, day 3, and then every fourth day through day 19 after intracisternal treatment. Limb placing tests were performed as described previously [224, 225]. The forelimb placing test determined sensorimotor function in response to whisker tactile, visual, tactile, and proprioceptive stimuli with scoring between 0 and 12, where 12 indicates maximal impairment. Hindlimb placing tests measured sensorimotor function of the hindlimb in response to tactile and proprioceptive stimuli, and scored between 0 and 6, where 6 represents maximal impairment. The body swing test provides a measure of vestibulomotor function. Function was measured as a percentage of the number of body swings towards the side ipsilateral to the MCA occlusion, where 50% is normal, and 0% is maximal impairment. Sensorimotor function of the forelimbs

was additionally tested by the cylinder (spontaneous limb use) test [208, 224]. In this test, animals are videotaped as they rear up in a narrow glass cylinder. The number of spontaneous movements made by each forelimb to initiate rearing, to land on or to move laterally along the wall of the cylinder, or to land on the floor after rearing are counted, and expressed as an asymmetry score $[(\text{total contralateral forelimb use} - \text{total ipsilateral forelimb use}) / \text{total forelimb use}] \times 100$. Normally, there is no asymmetry between sides on the test. but, after stroke, the affected (contralateral) side is used less (asymmetry score is > 0). This test was done on the day before and weekly after stroke.

Infarct volume determination. After the completion of behavioral testing, animals were euthanized by deep anesthesia with chloral hydrate and transcardially perfused with 10% formalin in saline. The brains were subsequently removed, fixed in formalin, dehydrated, and embedded in paraffin. A microtome was used to cut 5 μm coronal sections, which were mounted onto glass slides and stained with hematoxylin/eosin (H&E). Six slices (+4.7, +2.7, +0.7, -1.3, -3.3, -5.3 mm compared with bregma) were used to determine the area of cerebral infarcts via a computer-interfaced imaging system (Bioquant, Nashville, TN), through the “indirect method” (intact contralateral hemispheric area – intact ipsilateral hemisphere area), to correct for brain shrinkage during preparation and processing [458]. Infarct volume was calculated as the sum of infarct areas per brain multiplied by slice thickness and expressed as a percentage of the intact contralateral hemispheric volume. Infarct volumes in the cortex and striatum were also separately determined using the same method. H&E staining also allowed for the examination of gross histological changes.

Data analysis. Experimenters performing the behavioral assessments and infarct volume determinations were blinded to treatment assignment. Behavioral and weight data were analyzed by repeated measures two-factor ANOVAs (treatment by time), and infarct volume data were analyzed by two-tailed t-tests.

Chapter 3. Heparan sulfate glycosaminoglycans derived from endothelial cells and smooth muscle cells differentially modulate fibroblast growth factor-2 biological activity through fibroblast growth factor receptor-1

This report was previously published in *Biochemical Journal* in 2003. See reference [31] for details. All figures in this chapter were adapted from the original publication.

3.0 Summary

FGF signaling is involved in a wide range of important biological activities with differential effects in various cell types. The activity of FGF is modulated by HSGAGs, found both in the extracellular matrix and on the cell surface. HSGAGs affect FGF signaling by interacting with both the growth factor and the FGFR. In this study we sought to investigate whether HSGAGs at the cell surface of bovine aortic endothelial cells (BAEC) and SMCs can differentially modulate FGF signaling in these cell types and modulate their differential response to FGF. We find that SMC and BAEC express the same FGFR isoforms and bind FGF2 with equal affinity at the cell surface, yet FGF has a markedly higher proliferative effect on SMC than on BAEC. Isolated HSGAGs from these two cell types were found to elicit distinct patterns of proliferation in chlorate-treated cells. Furthermore, examination of focal sequences reveals that HSGAGs from SMC, but not those from BAEC, retain the sulfation pattern necessary to induce FGF2 activity. As such, the differences in FGF2-mediated proliferation can be explained by the distinct cell surface HSGAGs of the two cell types. We conclude that the focal sequences of cell surface HSGAGs from SMC and BAEC govern, at least in part, the differential activity of FGF2 on these two cell types.

3.1 Introduction

SMC and endothelial cells (EC) have been implicated in the pathophysiology of many disease states, including atherosclerosis. Key events in the induction of atherosclerosis include migration of SMC to the intima and subsequent proliferation [409]. Basic fibroblast growth factor (FGF2) is one of a spectrum of potent stimulatory molecules that act on SMC. FGF2 is typically stored extracellularly, bound to HSGAGs. HSGAGs, the polymeric carbohydrate moiety of proteoglycans, are ubiquitous in the ECM and on the cell surface [77]. HSGAGs in the ECM store FGF2 and prevent its degradation by proteolytic enzymes [414]. Alterations to the vascular endothelium are thought to induce the onset of pathological states such as atherosclerosis [149] through the release of mitogenic molecules, such as FGF2, from their ECM storage sites. Once released from the ECM, FGF2 is incorporated into a ternary complex by binding to its high affinity protein kinase receptor and low affinity HSGAGs found on membrane associated HSPGs. Formation of a proper complex leads to activation of intracellular signaling pathways [511]. In this manner, HSGAGs, depending on their location and sequence context, can serve to either store FGF in an inactive form or promote FGF signaling through protein tyrosine kinase cell surface receptors.

All HSGAGs are characterized by repeating disaccharide building blocks, each of which consists of an uronic acid linked 1→4 to a glucosamine. These carbohydrate polymers are structurally and chemically diverse, varying both in terms of the number of disaccharide units as well as in the sulfation pattern present on each disaccharide. The glucosamine subcomponent of the disaccharide can be sulfated at the N, 3-O, and 6-O positions. Additionally, the uronic acid exists as one of two isomers (α -L-iduronic or β -D-glucuronic acid). The 2-O position of the uronic acid can also be either sulfated or unsulfated. These five potential binary modifications lead to an extraordinary level of sequence diversity in the nascent chain that together define the interactions between HSGAGs and various growth factors, morphogens, and cytokines, including FGF2 [370]. As a result, HSGAG patterns and sequences have been implicated as important modulators in a wide range of normal and pathological biological processes [167, 268]. Furthermore, HSGAG sequences expressed on the surface of cells and in the ECM are not static, but are rather dynamic, enabling a carefully controlled regulation of mitogenic signaling pathways [370].

Recent studies have elucidated some of the roles for HSGAGs in modulating FGF2-induced SMC and BAEC proliferation. Addition of exogenous highly sulfated HSGAGs, such as heparin [292], as well as lower sulfated HSGAGs derived from BAEC [101, 134, 170], such as perlecan, the major HSPG secreted by EC, have been found to inhibit FGF2-mediated proliferation of SMC [333]. The latter effect can be systematically mitigated via treatment of the conditioned media with specific HSGAG degrading enzymes [170, 332]. Furthermore, HSGAGs at the SMC surface can serve dual functions, either inducing or inhibiting proliferation, depending on the biological context [115]. Exogenous heparin has also been reported to inhibit FGF2-mediated proliferation of EC [150]. Additionally, inhibition of HSGAG synthesis in BAEC abrogates the ability of FGF2 to induce a mitogenic response in this cell type [136]. Therefore, cell surface HSGAGs play an important role in regulating the responses of SMC and BAEC to FGF2 as well as mediating the interaction between the two cell types.

Previous work from our laboratory has demonstrated that SMC-derived HSGAGs modulate FGF2-HSGAG interactions through specific FGFR isoforms in a sequence dependent manner [30]. This study serves to extend these findings by determining how specific HSGAG structures on the cell surface of SMC, as opposed to those found on EC, influence FGF-induced proliferation. We find, consistent with previous findings, that SMC-derived HSGAGs promote FGF-induced proliferation to a greater extent than EC-derived HSGAGs. Furthermore, we find that these activities are dependent on specific HSGAG structural motifs. Furthermore, we find that these two cell types possess HSGAG structural differences that are substantially more pronounced within specific sequence contexts than in global composition. Furthermore, the ability of specific HSGAG fragments to support FGF2 signaling was found to be dependant on specific structural motifs released upon enzymatic treatment. These findings provide insight into the ability for HSGAG to greatly influence cell function through regulation of the activity of HSGAG-binding growth factors like FGF2. Finally, these experiments demonstrate that HSGAGs derived from distinct cell types, even those physiologically adjacent *in vivo*, elicit distinct proliferative responses.

3.2 Results

3.2.1 FGF2 induces a significant mitogenic response in both SMC and BAEC.

Previous studies have identified that FGF2 is a potent mitogen for both SMC and EC. To confirm this observation and provide a basis for additional studies, we determined the proliferative effect of FGF2 on SMC and BAEC. Each cell type was incubated with 5 ng/mL of FGF2, and the extent of tritium incorporation over 3 hr was measured. Consistent with previous reports [332, 507], FGF2 promoted a significant mitogenic response in both SMC and BAEC (Table 3.1). While the background tritium incorporation for BAEC cells is higher, the relative increase in ^3H counts upon FGF2 stimulation is much greater (roughly six times) for SMC than for BAEC. Dose response studies, varying by tenfold the amount of exogenous FGF2 added to the culture, demonstrate that approximately the same amount of FGF2 is required to induce a maximal proliferative response in SMC and BAEC. Thus, in terms of an FGF-inducible proliferative response, SMC appear more responsive to FGF2 stimulation than do BAEC as determined by tritium incorporation.

	SMC	BAEC
- FGF	2780	14,000
+ FGF (5 ng/mL)	11,400 (310)	20,700 (48)
+ FGF (50 ng/mL)	12,400 (350)	21,100 (51)

Table 3.1. ^3H -incorporation into SMC and BAEC. SMC or BAEC were treated with 0–50 ng/ml FGF2, and proliferation was determined by thymidine incorporation. The effect of the various treatments was measured in counts per minute (c.p.m.). The percent increase is shown in parentheses.

The above results were extended to include an analysis of intracellular signaling pathways induced by FGF2 stimulation of either SMC or BAEC. Both cell types were treated for 20 minutes with either FGF2 or PBS, and after treatment activation of intracellular signaling pathways was assessed by Western blot. As shown in **Figure 3.1**, phospho Erk1 and Erk2, known markers of proliferation [267], were upregulated in both SMC and BAEC, but the effect was more pronounced in SMC, consistent with the more dramatic effect of FGF2 on SMC proliferation. Examination of other signaling pathways revealed a similar finding. Taken

together, these results demonstrate that the administration of FGF2 induces a downstream activation of intracellular signaling pathways to an extent consistent with the observed proliferative response (*i.e.*, tritium incorporation). These results point to the fact that while SMC respond more readily to exogenous FGF2 administration than do BAEC, the difference is in the *extent* of activation, rather than the *kind* of activation.

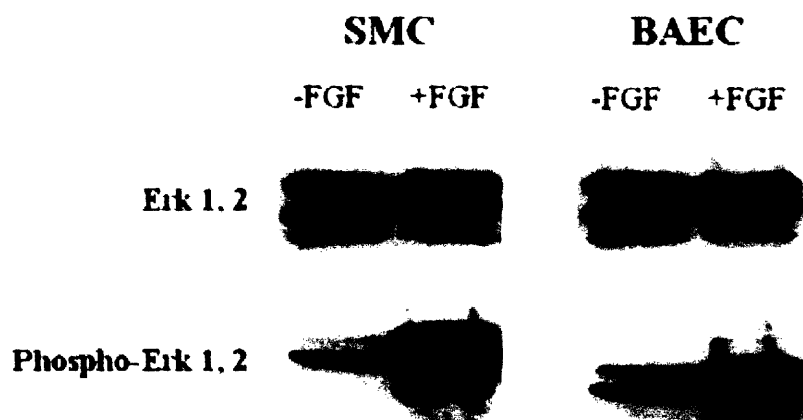


Figure 3.1. Western blot of SMC and BAEC after FGF2 stimulation. SMC and BAEC were treated with 5 ng/ml FGF2 or an equivalent volume of PBS for 10 min. after which the cells were lysed, and a Western blot was performed utilizing antibodies specific to Erk1 and Erk2, known markers of proliferation.

There are several possible explanations for this observed difference in the proliferative response of SMC vs. BAEC. One possible explanation is that SMC and BAEC express distinct patterns of FGFR isoforms on their cell surface, and accordingly, the distinct receptor isoform repertoire modulates the extent of signaling induced by FGF2. Previous studies have identified that several FGFR isoforms, including FGFR1c, FGFR3c, and FGFR4, efficiently mediate FGF2 binding to the cell surface and activation of intracellular signaling pathways leading to cell proliferation [351]. To test whether SMC and BAEC express different FGFRs, Reverse transcriptase (RT)-PCR was performed on both SMC and BAEC to determine their receptor expression profile. Both cell types were tested with specific probes to FGFR1c, FGFR2b, FGFR2c, and FGFR3c. Since existing evidence indicates that FGFR4 is primarily present at sites other than the cell surface [74], it was not included in this study. As seen in **Figure 3.2**, both SMC and BAEC primarily express FGFR1c, with very little, if any, evidence of expression of other receptor isoforms. Therefore, it seems unlikely that the observed differences in

mitogenic response observed upon FGF2 stimulation of SMC and BAEC can be attributed to differences in isoforms of FGFR that are expressed at the cell surface of the two cell types.

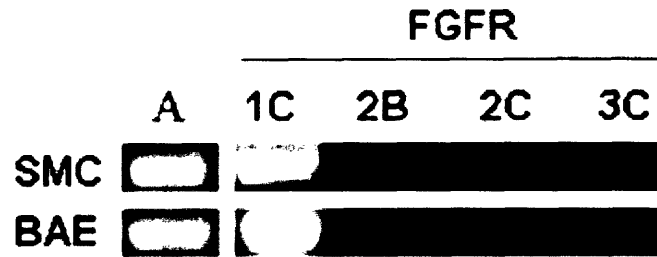


Figure 3.2. RT-PCR of FGFRs expressed by SMC and BAEC. RT-PCR was performed using primers specific to four FGFR isoforms to determine the expression pattern of FGFRs by SMC and BAEC. Expression levels were controlled for total cell protein based on RT-PCR of β -actin. A, actin; 1C, 2B, 2C and 3C refer to the various FGFR isoforms.

While the expression of FGFR isoforms is the same between SMC and BAEC, it is possible that SMC and EC express different quantities of FGFR1c on their respective cell surfaces. However, the signal intensity derived from RT-PCR of FGFR1c is similar in EC and SMC, especially when referenced to an actin control. To address this issue further and confirm this conclusion, FGF2 binding to low- and high-affinity receptors on SMC and BAEC was determined using a ^{125}I -FGF2 binding assay. We find that FGF2 binding to both high- and low-affinity receptors is similar for both SMC and BAEC (**Figure 3.3**). Given that these cells primarily express only one receptor isoform, the similarity in binding affinity suggests that both cell types display a similar quantity of receptors on their surface. Taken together, these results point to the fact that the difference in the proliferative response between SMC and EC does not seem to be primarily related to differential FGFR expression. As such, we sought to determine whether differences in cell surface HSGAGs, important for formation of an active signaling complex, could account for the marked differences in FGF-mediated signaling between SMC and BAEC.

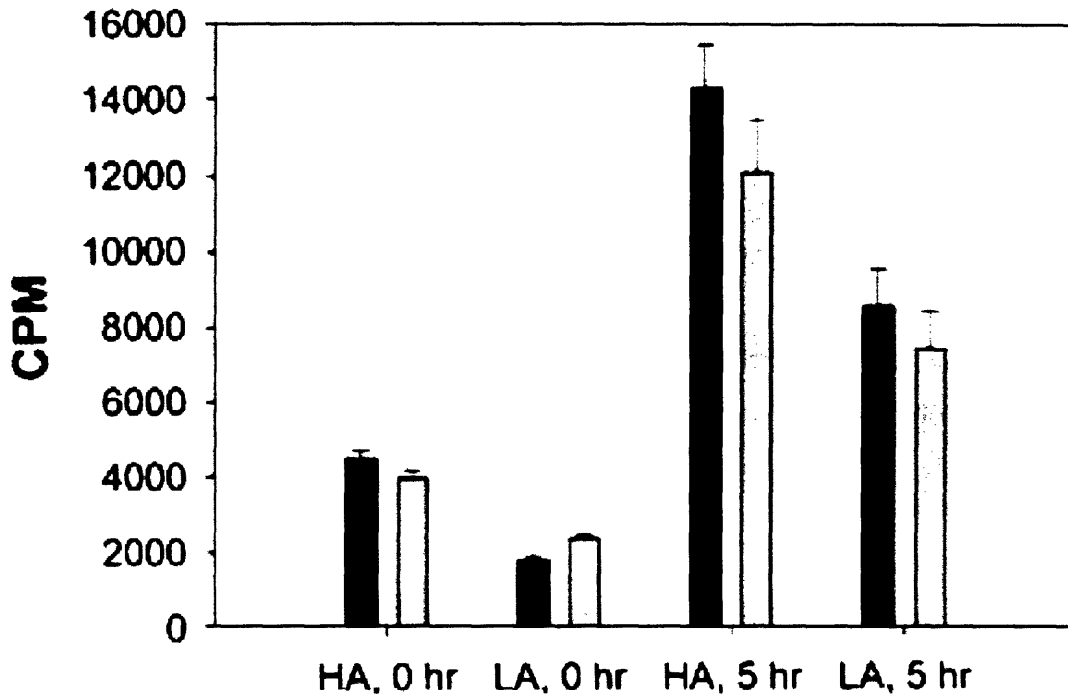


Figure 3.3. FGF2 binding to SMC and BAEC-expressed FGFR. SMC (black bars) and BAEC (grey bars) were incubated with 2 ng 125I-FGF2 for 2 h at 4°C. Bound 125I-FGF2 was released from separately from low affinity (LA) receptors and high affinity (HA) receptors. The amount of ligand bound was determined at 0 h and 5 h after incubation with 125I-FGF2. CPM, counts per minute.

3.2.2. Cell surface HSGAG can be efficiently harvested

HSGAGs were harvested from SMC and BAEC by two methods. The first method employed trypsin digestion of the cell surface to cleave the proteoglycan core of membrane-bound HSGAGs, liberating intact HSGAG chains coupled to parts of the proteoglycan protein core. After boiling to inactivate the trypsin and other potential contaminating proteins, the suspensions were concentrated using a 3,000 Da molecular weight cut-off filter. The solutions were then purified by anion-exchange chromatography and reconcentrated. Yields were determined by Alcian blue and carbazole assays as described in the *Experimental* section. Given the nature of this isolation procedure, other polysaccharides, such as chondroitin sulfate and dermatan sulfate, could be isolated, especially considering that perlecan, found prominently on vascular basement membranes, contains both heparan sulfate as well as chondroitin sulfate [195]. In order to confirm and extend our results using trypsin-derived material, a second harvesting

method was employed wherein SMC and BAEC were treated with heparinase I, II, or III (hepI, II, III) or PBS. Since hepI-III have unique substrate specificity and are anticipated to release structurally distinct HSGAG fragments, this methodology also provides some information about the influence of HSGAG fine structure on FGF-mediated proliferation of BAEC and SMC. With each enzyme application, treatment times were set to liberate an identical amount of HSGAGs from each cell type. Cell-free HSGAG solutions were collected and boiled to eliminate residual enzyme activity as well as the activity of any proteins potentially secreted during enzymatic treatment. Subsequently, the solutions were filtered through 0.45 μm syringe filters. The method employed preferentially releases HSGAGs over other glycosaminoglycan polysaccharides because the activity of heparinases (heps) are specific to this type of glycosaminoglycan [104]. Solutions containing hep-derived HSGAG fragments were purified and concentrated by anion-exchange chromatography followed by dialysis in a similar manner to trypsin-derived HSGAG material.

To confirm the absence of contaminating activities in the various HSGAG preps that might compromise further analysis, all material was tested for its mitogenic potential in the absence of exogenous ligand using a BaF3 cell line. Based on previous observations [30], we anticipated that HSGAG material of sufficient purity would not induce a significant proliferative (or inhibitory) response. BaF3 cells transfected with FGFR1c were washed three times in media lacking IL-3 and plated at a density of 1×10^5 cells/ml. Cells were then treated with either porcine mucosa heparin or cell-derived HSGAGs at a final concentration of 500 ng/ml. After incubating for 72 hours, proliferation was measured by whole cell counts as determined by an electronic cell counter. We find that none of the cell surface HSGAG fractions significantly induced a proliferative or inhibitory response (data not shown). These findings suggest that the cell-derived HSGAG fractions do not produce a proliferative response in the absence of exogenous ligand, and are therefore sufficiently free of contaminating activities that would potentially complicate analysis.

3.2.3 SMC proteoglycans promote FGF-induced signaling

To further test whether observed differences in FGF-mediated cellular proliferation between SMC and BAEC could be due, at least in part, to differences in their respective HSGAG composition [63], the effect of trypsin-harvested SMC and BAEC HSGAG on cell mitogenesis

was examined. In this case, recipient SMC or BAEC were *first* treated with chlorate to suppress endogenous HSGAG production. Then, exogenous FGF2, in combination with either SMC or BAEC-derived HSGAGs, was added to chlorate-treated cells. In a prior experiment, SMC and BAEC were treated with varying amounts of chlorate to determine the chlorate level that was effective at abrogating HSGAG production without being cytotoxic. We find that cellular responses to the addition of exogenous FGF2, as well as sulfation of HSGAGs at the cell surface, were maximally reduced in media supplemented with 50 mM sodium chlorate. Furthermore, both SMC and BAEC that were chlorate treated possessed a similar cell morphology to untreated controls and maintained a parallel proliferative capacity in the absence of exogenously-added ligand. Together, these results suggest that 50 mM chlorate has very few, if any, nonspecific cytotoxic effects on the cells. Notably, however, in both cell types tritium incorporation upon addition of 5 ng/ml FGF2 was dramatically suppressed such that it was statistically indistinguishable from negative controls, indicating the effective suppression of functional HSGAGs on the cell surface.

Having confirmed that chlorate-treated SMC and BAEC lack fully sulfated (and functional) HSGAGs at their cell surface, we examined the effect of the addition of trypsin-derived SMC or BAEC HSGAGs on FGF-induced proliferation. To test this, chlorate-treated SMC and BAEC were supplemented with FGF2 as well as with isolated HSGAGs from either SMC or BAEC. We find that when chlorate treated SMC cells were treated with HSGAGs derived from SMC in addition to FGF2, a significant increase in tritium incorporation was observed above the negative control (**Figure 3.4**). In fact, the observed increase rivaled the response observed when FGF and exogenous heparin were added to chlorate-treated SMC. Conversely, when chlorate-treated BAEC cells were treated with exogenous BAEC HSGAGs and FGF2, no significant tritium incorporation was observed beyond the negative control. Importantly, SMC HSGAGs added to chlorate treated BAEC yielded a response that was significantly above the negative control, indicating that SMC proteoglycans can support FGF2-induced proliferation even when added to BAEC. Together, these results suggest that HSGAG proteoglycans from the cell surface of SMC cells facilitate FGF2-mediated signaling to a greater extent than BAEC-derived HSGAGs. We examined whether the observed functional differences could be correlated with differences in HSGAG fine structure.

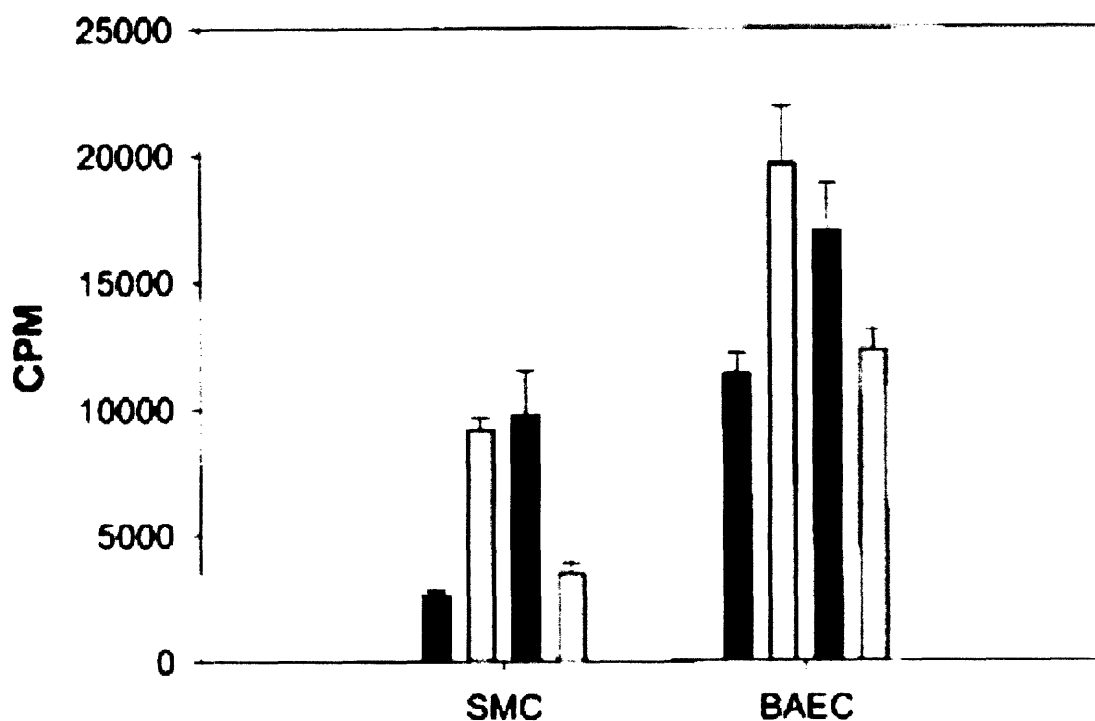


Figure 3.4. Effect of cell-derived HSGAG on FGF2-mediated SMC and BAEC Mitogenicity. SMC and BAEC were incubated with 50 mM sodium chlorate to inhibit endogenous HSGAG production. Cells were supplemented with (from left to right) PBS, 5 ng/ml FGF2 and 500 ng/ml heparin, 5 ng/ml FGF2 and 500 ng/ml SMC-derived HSGAG, or 5 ng/ml FGF2 and 500 ng/ml BAEC-derived HSGAG. The mitogenic response was determined by ^3H -thymidine incorporation. CPM, counts per minute.

3.2.4 Determination of HSGAG proteoglycan fine structure that promotes FGF2 signaling

The composition of the HSGAG component of the cell surface HSGAGs from SMC and BAEC was assessed using enzymatic treatment and capillary electrophoresis according to a previously defined methodology [227]. We find that the cell surface HSGAGs of SMC and BAEC, isolated by trypsin treatment, while similar in structure, display subtle differences in the relative amounts of disaccharide building blocks (**Figure 3.5**). For example, though the HSGAGs of BAEC and SMC both contain the trisulfated disaccharide $\Delta\text{U}_{2\text{S}}\text{H}_{\text{NS},6\text{S}}$, it is present in higher amounts in SMC HSGAGs. Similar trends are observed for several of the other disaccharide constituents, *viz.*, $\Delta\text{UH}_{\text{NS},6\text{S}}$ and $\Delta\text{UH}_{\text{NAC},6\text{S}}$. Taken together, these results suggest that functional differences in SMC *vs.* BAEC HSGAGs can, at least partially, stem from the fine structure of the HSGAGs at their respective cell surface.

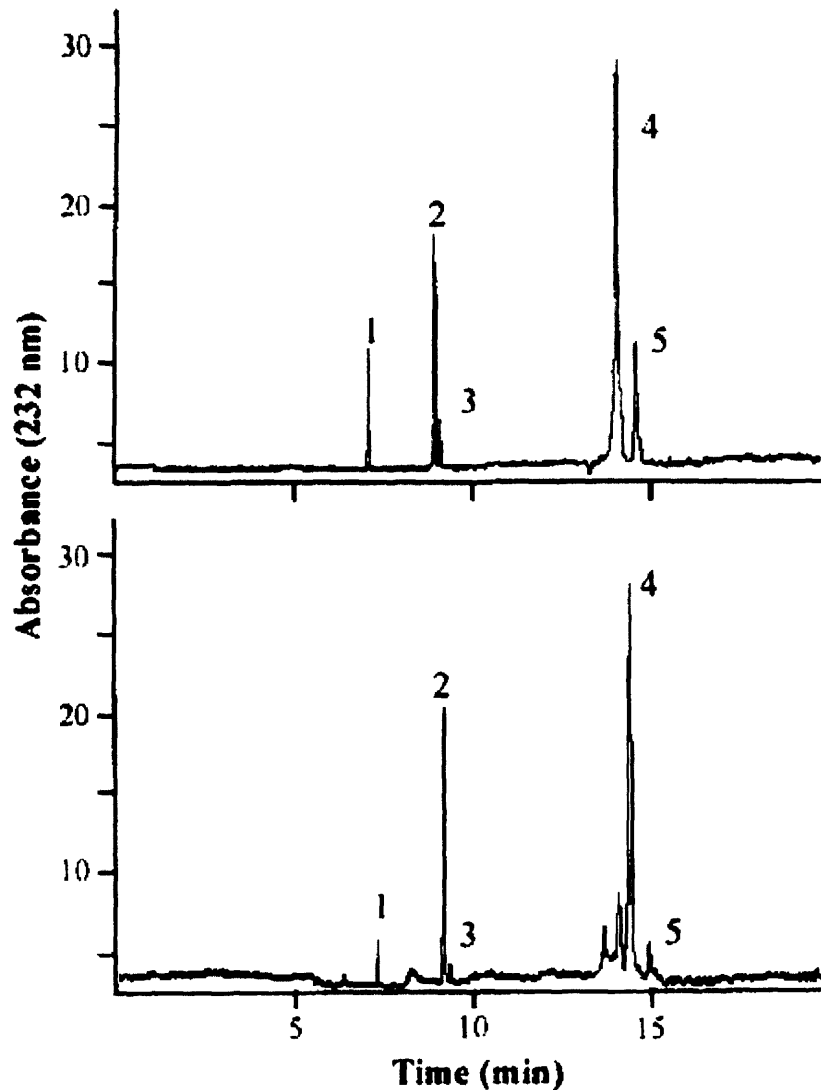


Figure 3.5. Compositional analysis of SMC (upper) and BAEC (lower) as determined by exhaustive digestion of the sample with a heparinase cocktail and separation of the resulting disaccharides by capillary electrophoresis. The observed disaccharides were identified by co-migration with known standards: (1) $\Delta U_{2S}H_{NS,6S}$; (2) $\Delta U_{2S}H_{NS}$; (3) $\Delta UH_{NS,6S}$; (4) ΔUH_{NS} ; (5) $\Delta UH_{NAc,6S}$.

To extend the above findings to include an examination of the fine structure of HSGAGs at the cell surface of BAEC and SMC, we determined whether fragments of specific structure, released from the cell surface, would promote or inhibit FGF2-induced proliferation. To this end we utilized the heps from *Flavobacterium heparinum*, a family of three enzymes that depolymerize HSGAGs with defined substrate specificities. Heps I cleaves highly-sulfated, or

heparin-like, domains leaving intact undersulfated, or heparan-like, regions. Conversely, hepIII digests regions of low sulfation, and hepII cleaves both heparin- and heparan-like domains [104]. SMC treated with hepIII prior to introduction of FGF, incorporated significantly more tritium than those untreated with hepIII prior to addition of FGF (data not shown). A similar effect was not observed with hepI treatment, suggesting that the observed effect was due to the unique substrate specificity of hepIII. Indeed, compositional analysis of hepI-, hepII-, and hepIII-released fragments indicated that hepIII-derived fragments were higher in 2-O sulfation than those derived from hepII and especially hepI (**Table 3.2**), consistent with the published substrate specificity of the heps. Previous studies have implicated 2-O sulfation in high affinity FGF binding [477, 501]. Notably, SMC HSGAGs had a higher degree of 6-O sulfation when isolated by hepII or hepIII treatment than those isolated via hepI treatment. This sulfate group has also been associated with FGF2 activity through FGFR1 [280].

Disaccharide	SMOOTH MUSCLE CELLS			ENDOTHELIAL CELLS		
	HepI	HepII	HepIII	HepI	HepII	HepIII
$\Delta U_{2S}H_{NS,6S}$	5	4	16	2	3	8
$\Delta U_{2S}H_{NS}$	22	24	30	22	34	33
$\Delta UH_{NS,6S}$	6	8	8	6	3	5
$\Delta U_{2S}H_{NAc,6S}$	0	0	0	0	0	0
ΔUH_{NS}	31	18	20	33	29	30
$\Delta U_{2S}H_{NAc}$	0	0	0	0	0	0
$\Delta UH_{NAc,6S}$	8	12	7	6	4	2
ΔUH_{NAc}	28	34	19	31	27	22

Table 3.2. Compositional analysis of HSGAG fragments from SMC or BAEC after heparinase I, II or III treatment. The composition of the various pools was determined by capillary electrophoresis after full digestion by heparinase I, II and III (hepI, II and III respectively).

Further confirmation that cell surface HSGAGs from SMC and BAEC are distinct arises from the fact that hepIII treatment of BAEC cannot recapitulate the effect observed with SMC HSGAGs, *viz.*, the promotion of tritium incorporation by hepIII treatment of cell surface HSGAG. Compositional analysis of BAEC HSGAG fragments released after hepI, II, or III treatment, wherein differential cleavage of HSGAGs enables the examination of the fine

structure of the building block sequences, confirmed that these fragments are structurally distinct from SMC-derived HSGAG oligosaccharides (**Table 3.2**).

3.2.5 BaF3 cells provide an appropriate model to analyze the effect of cell derived HSGAG on FGF2-mediated mitogenic activity via different FGFR.

The ability of hep treatment to markedly influence cell proliferation differently in SMC and BAEC suggested that the fine structure of the cell surface HSGAGs may influence FGF2-mediated responses. To examine this possibility we employed a simplified system to more accurately assess the ability of subsets of the HSGAG pool to induce an FGF2 response. To this end, activity was tested with proliferation assays using BaF3 cells engineered to express FGFR1c [351]. The use of BaF3 cells enabled the introduction of a simple, clean, and biologically relevant system, as these cells lack cell surface HSGAGs and express only the transfected FGFR. The proliferative potential of these cells was characterized by culturing them in the presence or absence of FGF2, with or without HSGAGs. In this case, porcine intestinal mucosa heparin was used as a positive control [358].

The biological activity of the cell derived HSGAGs was measured by whole-cell proliferation over a three-day period when transfected BaF3 cells were cultured with cell surface HSGAGs and FGF2. The cell counts were converted to a proliferation index (PI). All values are expressed as PI, where a value of 1 indicates the “maximal” proliferative response, as induced by FGF2 and heparin, and a PI of 0 indicates a negligible response, equivalent to that of untreated cells. The formula for the PI has been previously described [358]. The reference point of PI = 1 was from BaF3 cells stimulated with 50 ng/ml FGF2 and 500 ng/ml heparin. This reference point allows for the proliferative response to be standardized, enabling comparisons between HSGAG preparations.

SMC HSGAG fragments derived by treatment with either hepII or hepIII consistently elicited a significantly higher PI than the PBS control in BaF3 transfected with FGFR1c in the presence of FGF2 (**Figure 3.6**). The proliferative response induced by these fragments was similar to that of exogenous heparin. HepI-derived HSGAG fragments, however, did not yield a response greater than that of the PBS control. Conversely, BAEC HSGAGs derived by hepIII treatment (as well as HSGAGs obtained from hepI treatment) did not elicit a response

significantly greater than that of the PBS control, confirming our findings that highly sulfated HSGAGs from the cell surface of SMC were most efficient at promoting FGF2-induced cellular proliferation. The reproducibility of this *in vitro* data suggests that similar HSGAG fractions are obtained with different isolations.

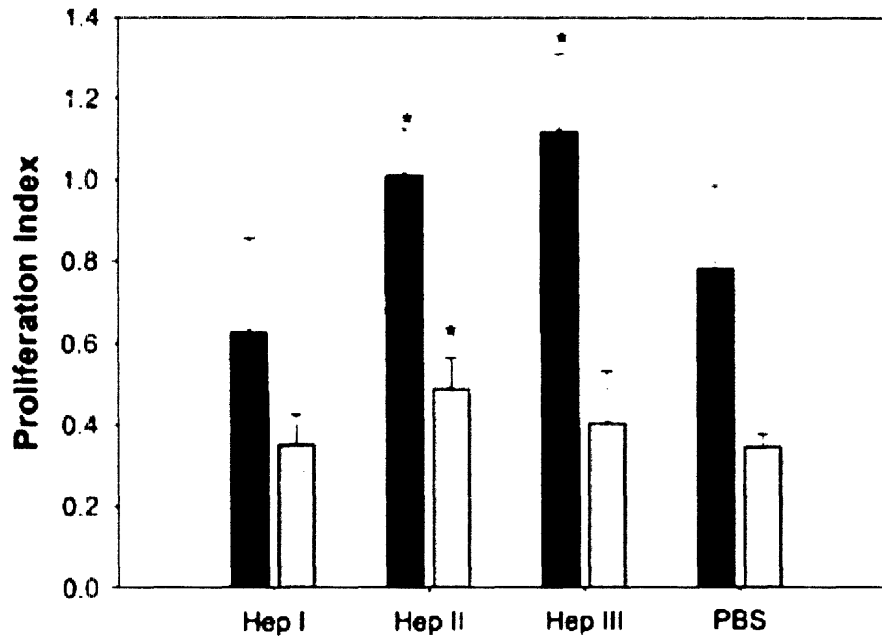


Figure 3.6. FGF2-mediated proliferation of BaF3 cells expressing FGFR1c. Transfected BaF3 cells were incubated in the presence of 50 ng/ml FGF-2 and cell derived HSGAG fragments from SMC (black bars) or BAEC (grey bars). Fragments were isolated by treatment with 10 mM HepI, HepII or HepIII, or an equivalent volume of PBS. Proliferation is represented by PI, as described in the Experimental Procedures section. * denotes $P < 0.05$.

3.3 Discussion

The HSGAGs in the ECM and at the cell surface have been shown to act as co-receptors in FGF signaling by binding to both FGF and FGFR [112, 214, 350] and forming a ternary complex at the cell surface. Through the use of cells deficient in aspects of HSGAG biosynthesis, it has been demonstrated that growth factors, including FGF2, depend on cell surface HSGAGs for their mitogenic activity [197, 395, 511]. Furthermore, HSGAGs serving the co-receptor function have been suggested to influence the strength and type of cellular response induced by FGF. The ability of the HSGAG co-receptor to mediate FGF binding and

activity is dependent on both the location and composition of the HSGAG in question. Not only do cell surface and soluble, ECM-derived HSGAGs appear to function differently [115], but studies have demonstrated that subtle modifications in HSGAG structure can alter their ability to induce a cellular response [336, 388]. Therefore, alterations in composition and sequence within a given HSGAG subset (ECM as opposed to cell surface), may alter the capacity of the HSGAG to alter function as appropriate to its location.

Using a variety of cell types as well as *in vitro* binding assays, previous studies have addressed the structural requirements for HSGAG binding to FGF2. In general, these studies have found that HSGAG-FGF2 interactions are thought to be determined by the N- and 2-O-sulfate content of the saccharide chain [477, 501]. In addition, others have indicated that activation of FGFR1 by FGF2 can be prevented by selective elimination of 6-O sulfate groups [280]. These studies have determined the structural requirements for high affinity FGF binding and provided some context to fragments that promote FGF activity. However, many of these studies utilized fully sulfated heparin as a surrogate for cell surface heparan sulfate, or they added exogenous heparan sulfate to cells that already expressed a repertoire of HSGAGs at their cell surface, thus failing to address FGF activity within the context of these cell surface HSGAGs. Significantly, the membrane association of HSPGs has been suggested to determine the capacity of a given HSGAG to promote an FGF2 response [526]. The previously reported inhibitory effects of FGF2 are associated with soluble HSPGs, including constitutively shed syndecans and glypicans [129, 299], while HSPGs that promote the response, even with the same protein core, are typically cell surface in nature [42, 75]. As such, these studies provided an important foundation for additional work that probes fine structure of HSGAGs at the cell surface. In this study, we sought to extend previous results by directly probing whether HSGAG fine structure *at the cell surface* modulates FGF-mediated cell proliferation and whether the structural rules developed using exogenous heparin fragments are consistent with reference to HSGAGs at the cell surface.

Thus, there are three major findings of this paper. First, we find that HSGAGs at the surface of SMC and BAEC are one of the primary regulators of FGF-mediated signaling and, as such, they regulate the “output” of FGF binding to its cell surface receptor. Second, we find that this differential regulation is due to differences in the fine structure of HSGAGs. We find that the global composition of BAEC and SMC is fairly similar, yet we show here that HSGAGs

isolated from each have a profoundly different effect on FGF-mediated proliferation. Using the heps, we map the fine structure of both and confirm the suggestion that it is not simply composition but structural elements that dictate HSGAGs' ability to promote FGF signaling. Finally, this study represents a confirmation and extension of several previous findings that a HSGAG fragment's ability to mediate FGF binding and activity is correlated with 2-O and, to a lesser extent, 6-O sulfation of the polysaccharide chain. Given that structural studies have shown that promitogenic sequences of HSGAGs bind to both FGF2 and FGFR1 at distinct sites on the carbohydrate chain, the possibility existed that HSGAGs with similar or even identical compositions can, through the presence or absence of distinct sequences, have different capacities to induce a cellular response. Using SMC and BAEC, we confirm that this is possible in that the global composition of the HSGAGs of these cell types is similar, yet, due to differences in fine structure, possess a markedly different ability to promote FGF-induced proliferation.

In the context of the structural formation of a ternary complex, the differential effect exhibited between the cell types, given the gross similarities in HSGAG composition but differences in fine structure, suggests that the sequence of BAEC HSGAGs is one in which disaccharides with sulfate groups necessary for ligand binding and those required for receptor activation are sufficiently far apart to prevent activation while enabling binding. These results, therefore, imply that either ligand-receptor interactions are highly sensitive to specific compositional patterns, or specific HSGAG sequences are required to optimally bind FGF2 and/or induce a response through FGFR1c [355], supporting the notion that a proper spatial display of sulfated groups promotes optimal ligand-receptor interactions [30].

As shown in this study, the ability of bovine aortic SMC and BAEC to respond differently to FGF2, as mediated by their cell surface HSGAGs, has potential implications in pathological settings. In the normal aorta, EC and SMC share the same physiological microenvironment. Extrapolating the results of this study suggest that theoretically, in a setting conducive to hyperplasia, the enhanced response to FGF2 imparted by SMC HSGAGs, as opposed to those from BAEC, suggests that SMC would undergo proliferation much more readily. Under normal conditions, EC HSPGs are necessary for the inhibition of SMC [110]. Importantly, this supports the notion that the differential response of SMC and EC *in vivo* could be a function of their distinct HSGAG compositions. Given the capacity for variable HSGAG

compositions to affect both FGF2/FGFR1 binding and therefore, the ability of FGF2 to induce a biological response, a further understanding of the specific nature of HSGAG fragments defining given levels of response will provide further insight into the nature of the induction of FGF2 signaling through the ternary complex, as well as the pathogenesis of proliferative vascular disorders such as atherosclerosis.

3.4 Significance

HSGAGs are important regulators of FGF signaling. The interactions of HSGAGs with both the FGF and the cell surface FGFR are important in defining the cellular response. N- and 2-O sulfates are thought to mediate HSGAG-FGF2 interactions, while 6-O sulfates are important for HSGAG regulation of activity through FGFR1. Previous work demonstrated that cell surface HSGAGs could be effectively harvested from SMCs by heparinase digestion, and that the information content of these distinct HSGAGs could differentially regulate FGF2 activity through various FGFRs. This report details a novel way to isolate a more complete HSGAG set from cells by trypsin digestion and subsequent purification with anion-exchange chromatography. When this technique was applied to SMCs and BAECs, HSGAGs with similar disaccharide compositions were obtained. The two sets of HSGAGs, however, had distinct abilities to support and regulate FGF2 activity. The fine structure of the HSGAGs, rather than just the quantities of specific sulfate groups, is important in determining the regulatory capacity of cell derived HSGAGs. This result explains the finding that SMCs are more responsive to FGF2 than are BAECs, even though both cell types have the same FGFR expression profile and the same concentration of receptors. Furthermore, this finding has implications regarding the physiological responses of aortic SMCs with the loss of endothelial cells, as well as the basis for SMC proliferation in restenosis.

3.5 Experimental Procedures

Proteins and reagents. Recombinant human FGF2 was a gift from Scios, Inc. (Mountainview, CA). Recombinant heparinases were expressed as previously described. [326]. Fetal bovine serum (FBS) was from Hyclone (Logan, UT). L-glutamine, penicillin, and streptomycin were obtained from GibcoBRL (Gaithersburg, MD). Mouse recombinant IL-3 was from R & D Systems (Minneapolis, MN). DMEM, RPMI-1640, and phosphate buffered saline (PBS) were from BioWhittaker (Walkerville, MD). ³H-thymidine and ¹²⁵I-Bolton-Hunter reagent were from New England Nuclear (Boston, MA). Porcine intestinal mucosa heparin was purchased from Celsus Laboratories (Columbus, Ohio). BaF3 cells transfected with FGFR1c were generously provided by Dr. David Ornitz (Washington University, St. Louis, MO). BAEC were generously provided by Dr. Elezar Edelman (MIT, Cambridge, MA).

Cell culture. Bovine aortic SMC were isolated from fresh calf aortas as previously described [331]. SMC were maintained in DMEM supplemented with 10% FBS, 100 µg/ml penicillin, 100 U/ml streptomycin, and 500 µg/ml L-glutamine. SMC were grown in 75 cm² flasks at 37°C in a 5% CO₂ humidified incubator, and were passaged 2-3 times a week, when cells reached confluence. SMC cultures were discarded after passage 8. BAEC were maintained in DMEM (low glucose), supplemented with (100 units/ml), streptomycin (100 µg/ml), glutamine (2 mM), and 10% FBS (HyClone), as described [333]. BAEC were employed so long as they retained a cobblestone appearance at confluence [14] and elicited a robust response to FGF2.

BaF3 cells transfected with various FGFR isoforms were maintained as independent suspension cultures in propagation media composed of RPMI-1640 supplemented with 10% FBS, 100 µg/ml penicillin, 100 U/ml streptomycin, 500 µg/ml L-glutamine, and 500 ng mouse recombinant IL-3. Cultures were grown in 75 cm² flasks at 37°C in a 5% CO₂ humidified incubator, and were passaged 1:10 by dilution three times a week.

RT-PCR. 5 µg of total RNA was isolated from SMC as well as from BAEC using Trizol reagent (Life Tech, Rockville, MD) followed by reverse transcription with random hexamers. Specific oligomers were designed based on the published sequences of FGFR1c (accession number:

X51803), FGFR2b (M97193), FGFR2c (X52832), and FGFR3c (M61881) in order to detect the expression of specific FGFR isoforms. Sequences of primer pairs corresponding to distinct FGFR isoforms were as follows: FGFR1c: 5'-TGG AGC TGG AAG TGC CTC CTC-3' and 5'-GTG ATG GGA GAG TCC GAT AGA-3'; FGFR2b 5'-GTC AGC TGG GGT CGT TTC ATC-3' and 5'-CTG GTT GGC CTG CCC TAT ATA-3'; FGFR2c: 5'-GTC AGC TGG GGT CGT TTC ATC-3' and 5'-GTG AAA GGA TAT CCC AAT AGA-3' and FGFR3c: 5'-GTA GTC CCG GCC TGC GTG CTA-3' and 5'-TCC TTG CAC AAT GTC ACC TTT-3'. To control for total cell protein, RT-PCR was also performed on β -actin using the primers 5'-GCC AGC TCA CCA TGG ATG ATG ATA T-3' and 5'-GCT TGC TGA TCC ACA TCT GCT GGA A-3'. PCR was performed using the Advantage-GC cDNA kit from Clontech as per manufacturer's instructions (Palo Alto, CA).

FGF-2 binding assay. 125 I-Hunter-Bolton Reagent was used to radiolabel FGF-2 as previously described [331]. A sephadex G-10 column was used to separate labeled protein from unconjugated reagent. Protein fractions were pooled, the activity therein was measured, and subsequently, the concentration was determined using an enzyme-linked immunoabsorbant assay. Preparations were tested in a mitogenic assay to ensure biological activity and protein viability. Binding assays were performed as previously described for SMC [332], with an identical method used herein for BAEC. Briefly, SMC (or BAEC) were seeded in 24-well tissue culture plates and incubated for 72 h at 37°C until near confluence. Cells were washed once in DMEM-supplemented media lacking FBS, treated with 0.1 – 100 nM hepI, hepII, or hepIII in DMEM supplemented media with 0.1% FBS, and incubated for 30 min at 37°C, then placed at 4°C for 15 minutes. As previously described [326], experimental and control wells were treated with 2 ng and 2 μ g 125 I-FGF-2 respectively. The cells were incubated for 2 h at 4°C and subsequently washed 3 times with cold PBS (pH 7.4) to remove unbound ligand. The cells were then washed quickly with 0.5 ml HEPES (pH 7.0, 2 M NaCl) per well to remove FGF-2 bound to the low affinity receptors. Each well was washed twice with 0.5 ml sodium acetate buffer (pH 4.0, 2 M NaCl) to remove FGF-2 bound to high affinity receptors. Each wash was collected and counted on a Wallace 1270 Gamma Counter. Procedures were repeated three times for each condition and each cell type.

Isolation of HSGAGs from SMC and BAEC. Cell surface HSGAG fragments were collected from SMC and BAEC using one of two methods. In the first procedure fully confluent SMC were treated with 2 ml trypsin-EDTA (GibcoBRL) per 75 cm² tissue culture flask for 2 minutes, collected with 13 ml media, centrifuged at 195 x g for 3 minutes, and diluted 1:20 with supplemented DMEM-based media after the supernatant was discarded. One hundred twenty ml of suspension culture were added to each of four 500 cm² tissue culture plates, which were incubated for 72 h at 37°C in a 5% CO₂ humidified incubator. Each plate was washed twice with 60 ml PBS and subsequently treated with 12 ml trypsin-EDTA. The plates were incubated at 37°C for 25 minutes to harvest cell surface proteoglycans. The resulting cell/trypsin solution was collected and boiled for 10 minutes to deactivate the trypsin and other proteins in the solution. Subsequently, the solution was centrifuged at 4500 x g for 5 minutes. The supernatant was collected, and the pellet was discarded. Samples were concentrated by centrifuging at 2800 x g in a Centriprep 3 (Amicon, Beverly, MA) for 6 hr.

The purification of harvested proteoglycans was completed by anion-exchange chromatography. Briefly, 1 ml of DEAE Sephacel (Pharmacia Biotech, Uppsala, Sweden) was added to a polypropylene pipette tip plugged with glass wool. The column was equilibrated with 5 column volumes of DEAE wash buffer (200 mM NaCl). The collected supernatant was added to the column. Non-specific binders were eluted with 20 column volumes of DEAE wash buffer. HSGAGs and associated proteoglycans were eluted with 5 column volumes of DEAE elution buffer (1 M NaCl). The collected samples were buffer exchanged in distilled water using a Centriprep 3. Samples were stored at -20°C until use.

To eliminate potentially confounding effects of the remnant proteoglycan protein core and other co-isolates, cell surface HSGAGs were isolated via a second procedure. Confluent SMC and BAEC were trypsinized and diluted 1:10 with supplemented DMEM media into twelve 75 cm² tissue culture flasks per cell type. Cells were incubated until they reached full confluence, at which point each flask was washed twice with 20 ml PBS, and the medium was replaced with 2 ml PBS. HepI, hepII, or hepIII was added to three flasks each for both SMC and BAEC, sufficient to yield final concentrations of 10 nM. An equivalent volume, 10 µl, of PBS was added to the three remaining flasks for each cell type. SMC and BAEC were then incubated for 30 min and 9 h, respectively, at 37°C, sufficient time to yield the same concentration of HSGAG from each cell type. The preparations were collected and centrifuged at 4500 x g for 10

min at 4°C. The pellet was discarded, and the samples were boiled for 30 minutes to eliminate residual enzymatic activity and inactivate proteins ordinarily in SMC or BAEC conditioned media. The HSGAG samples were filtered using a 0.45 µm syringe filter and subsequently purified by anion-exchange chromatography as outlined above.

Quantification of isolated HSGAGs. Saccharide amounts of SMC- and BAEC-derived HSGAGs were quantified by Alcian blue with slight modifications from a previously described method [37] and by the carbazole assay. Undiluted HSGAG samples as well as those diluted 1:10 were used for the carbazole assay. Two hundred µl of each sample was supplemented with 20 µl of 4 M ammonium sulfamate as well as 1 ml of 25 mM sodium tetraborate in H₂SO₄ in screw-cap vials. The solutions were boiled for 5 minutes and allowed to cool to room temperature. Forty µl of 7.5% (w/v) carbazole in 95% ethanol was added to each solution. The mixtures were then boiled for 15 minutes and allowed to cool to room temperature. Absorbance was measured at 520 nm. Uronic acid concentrations were obtained by normalizing absorbance readings to a heparin standard curve produced during the analysis of cell surface HSGAG samples.

Compositional analysis. Cell surface HSGAG samples were treated with 200 nM hepl, hepII, and hepIII in a buffer composed of 25 mM sodium acetate, 100 mM NaCl, and 5 mM calcium acetate, pH 7.0. Fragments were incubated with the various heps overnight at 30°C to ensure complete digestion and analyzed by capillary electrophoresis in reverse polarity using a running buffer composed of 50 mM tris/phosphate and 10 µM dextran sulfate, pH 2.5. Identities of the resultant saccharides were determined based on comigration with known standards.

SMC and BAEC proliferation assays. Confluent SMC and BAEC were treated with 2 ml trypsin-EDTA (GibcoBRL) per 75 cm² tissue culture flask for 2 minutes and centrifuged at 195 x g for 3 minutes, after which the supernatant was discarded. Cells were resuspended in the appropriate proliferation media, and plated at a 1:10 dilution, 1 ml/well in 24 well plates. The cells were then incubated for 24 hours at 37°C, 5% CO₂, after which they were treated with 500 ng/ml HSGAG or 10 µl PBS and 5 ng/ml FGF2 or 10 µl PBS and incubated at 37°C, 5% CO₂ for 21 hrs. The concentrations added had been previously determined to induce a maximal response

in these cell types. After the incubation, each well was treated with ^3H -thymidine sufficient to yield a final concentration of $1\ \mu\text{Ci}$. The cells were incubated for 3 hrs. Each well was washed three times with PBS and treated with $500\ \mu\text{l}$ of a 1M NaOH solution until the cells lysed. The contents of each well were mixed with $5\ \text{ml}$ scintillation fluid and the mitogenic response was measured in counts per minute (CPM) as determined by a scintillation counter.

BaF3 proliferation assay with SMC and BAEC HSGAGs. BaF3 expressing FGFR1c were washed and resuspended to a density of 1×10^5 cells/ml in supplemented DMEM. The cell suspension was divided into 24 samples, $6\ \text{ml}$ each. Cell samples were centrifuged at $195 \times g$ for $3\ \text{min}$ at room temperature and resuspended in $3\ \text{ml}$ of the cell derived HSGAG preparations (from hep treatments) such that two sets of cells in each condition were produced, yielding a total of 6 distinct samples in duplicate for each cell type. One of each set of two was supplemented with $50\ \text{ng/ml}$ FGF2 and the other was supplemented with an equivalent volume, $10\ \mu\text{l}$, of PBS. A volume of $1\ \text{ml}$ from each condition was added to each of three wells on 24-well tissue culture plates. After incubating for $72\ \text{h}$ at 37°C , the whole cell number was determined by Coulter counter, and data from each of three experiments were normalized using a proliferative index, as previously described [358]. The index is defined as the increase in cell number for the experimental case divided by the increase in cell number for the positive control. The PI was calculated independently for each experiment.

Chapter 4. Quantitative assessment of FGF regulation by cell surface heparan sulfates

This report was previously published in *Biochemical and Biophysical Research Communications* in 2004. See reference [33] for details. All figures in this chapter were adapted from the original publication.

4.0 Summary

Heparin/heparan sulfate-like glycosaminoglycans HSGAGs modulate the activity of the FGF family of proteins. Through interactions with both FGFs and FGFRs, HSGAGs mediate FGF-FGFR binding and oligomerization leading to FGFR phosphorylation and initiation of intracellular signaling cascades. We describe a methodology to examine the impact of heparan sulfate fine structure and source on FGF-mediated signaling. Mitogenic assays using BaF3 cells transfected with specific FGFR isoforms allow for the quantification of FGF1 and FGF2 induced responses independent of conflicting influences. As such, this system enables a systematic investigation into the role of cell surface HSGAGs on FGF signaling. We demonstrate this approach using cell surface-derived HSGAGs and find that distinct HSGAGs elicit differential FGF response patterns through FGFR1c and FGFR3c. We conclude that this assay system can be used to probe the ability of distinct HSGAG species to regulate the activity of specific FGF-FGFR pairs.

4.1 Introduction

FGF family members interact with both cell surface tyrosine kinase FGFRs [119, 445] and the HSGAG component of HSPGs [153, 178, 348, 396]. HSGAGs are linear polysaccharides characterized by repeating disaccharide units, each of which may have any arrangement of five sets of binary modifications [77]. Of the currently identified 23 FGF family members, all bind to HSGAGs, albeit with potentially different domains defining the type and strength of the interaction [349]. The specificity of FGF-FGFR interactions is also governed by protein

structure and by interactions of both ligand and receptor with cell surface HSGAGs [191, 348, 514]. Together, these interactions provide receptor selectivity and modulate downstream signaling responses [6, 163, 213, 354, 389]. In addition, even though they may bind to the same receptor, different FGFs can activate distinct intracellular signaling pathways through specific interactions with both FGFRs and cell surface HSGAGs [65].

Crystal structure analysis and modeling studies have provided a wealth of insight into how FGF family members interact with heparin (as a model HSGAG) and FGFRs. Modeling FGF1–FGFR4 after IL-1 β -IL1R reveals an electrostatic sandwich with heparin between the ligand and receptor [185]. Crystal structure analysis reveals that FGF1 dimerizes such that the two FGF1 molecules are linked by heparin [92]. In this case, the interactions between heparin and FGF1 are defined by regions of high and low affinities within the protein [504]. FGF1 binds to FGFR2 forming two 1:1 complexes that produce an asymmetric ternary complex with heparin, wherein heparin makes contact with both ligands but with only one receptor [365]. Heparin additionally binds FGF2 without altering the protein conformation, though the heparin chain does undergo changes in the backbone torsion angles upon ligand binding [111, 392]. Dimerized FGF2 can form a stable complex with FGFR in the absence of heparin, leaving a canyon in which heparin likely interacts with both FGFs as well as the FGFR [378]. FGF2 and FGFR1 form 1:1 assemblages that dimerize [451]. Heparin itself binds both FGF2 and FGFR1, stabilizing FGF–FGFR interactions as well as promoting dimerization [431]. However, despite the wealth of structural information outlined here, which has served to elucidate the specifics of FGF–HSGAG, FGFR–HSGAG, and FGF–FGFR interactions, understanding how HSGAGs mediate FGF-promoted cellular activity remains elusive.

Various attempts have been made to define how FGFs, FGFRs, and HSGAGs interact to promote cellular activity. These studies have invariably pointed to the fact that the FGF system is a complex one, with few observations being readily extendable to all members of the FGF family. For example, previous studies have demonstrated that HSGAGs are required for efficient FGF1-mediated cellular responses [449]. Unlike with FGF1, however, FGF2 induces a proliferative response through the same receptor in the absence of HSGAGs, albeit to a lower degree [346, 358, 511]. Thus, with FGF2, it appears that HSGAGs may be playing distinct or additional roles in regulating activity compared to FGF1 [115]. Similar comparisons appear to be true for other members of the FGF family. As such, research into an all-encompassing

mechanism by which FGFs, FGFRs, and HSGAGs interact to promote a cellular-mediated response has led to apparently conflicting results. What is required to address apparent contradictions and confusion are defined cell-based methodologies that can study the interactions of cell–surface HSGAGs with different members of the FGF family, either alone or in combination, free of potential complications.

Herein, we define a system to examine the relative effect of various HSGAGs including those derived from cell surfaces on FGF-mediated cellular responses. The capacity of heparin, SMC-, and EC-derived HSGAGs to modulate FGF1 and FGF2 signaling through FGFR1 and FGFR3 was examined to demonstrate the feasibility and rigor of this system. We find that heparin, as well as HSGAGs from SMCs and those from ECs, differentially regulates FGF1 and FGF2 activation of intracellular signaling pathways through FGFR1c and FGFR3c. Taken together, these results demonstrate that such a cell-based system can be used to tease apart the differential effects of HSGAGs on the activation of distinct FGFRs by FGF family members.

4.2 Results and discussion

4.2.1 Mitogenic assays can quantify FGF1 and FGF2 biological responses

HSGAGs interact both with members of the FGF family and with the ectodomain of FGFRs [365, 431]. The use of complex cell-based systems to assess the biological response of FGFs can lead to conflicting results due to variable receptor and/or HSGAG expression patterns [115, 346, 358, 511]. A simpler biological system, with a defined receptor expression pattern as well as defined HSGAG structural motifs, is required to understand how distinct HSGAGs influence the binding to and activation of an FGFR isoform by a given member of the FGF family. The BaF3 cell system, which can be transfected with various FGFRs, but lacks cell surface HSGAGs, serves as an ideal starting point for such studies [347, 348].

The capacity of FGF1 and FGF2 to induce a cellular-mediated response in FGFR1c-transfected BaF3 cells was measured by both whole cell proliferation and thymidine incorporation assays. FGF1 promoted heparin-dependent mitogenesis as measured by thymidine incorporation, but could not elicit whole cell proliferation even in the presence of heparin (**Figures 4.1A and 4.1B**). FGF2, however, induced heparin-independent proliferation and

mitogenesis. Heparin was required to reach the maximal proliferative potential, but it only increased the potency of FGF2 when cellular response was measured by mitogenesis (**Figures 4.1C and 4.1D**). Cellular-mediated responses from FGF1 and FGF2 were uniformly evident through dose-dependent increases in mitogenesis. The heparin dependence of FGF1 and FGF2 cellular-mediated responses is therefore specific to the method by which the response is measured. In order to use a unified system to examine the contribution of specific HSGAG structural motifs on FGF1 and FGF2 activity, thymidine incorporation was used as a measure of mitogenesis to enable comparisons between the ligands. Additionally, since both FGFR1c and FGFR3c support each of FGF1- and FGF2-mediated mitogenic responses to a similar level [348], separate BaF3 cell lines expressing either FGFR1c or FGFR3c were used to demonstrate that this system can potentially be expanded to explore multiple FGFRs.

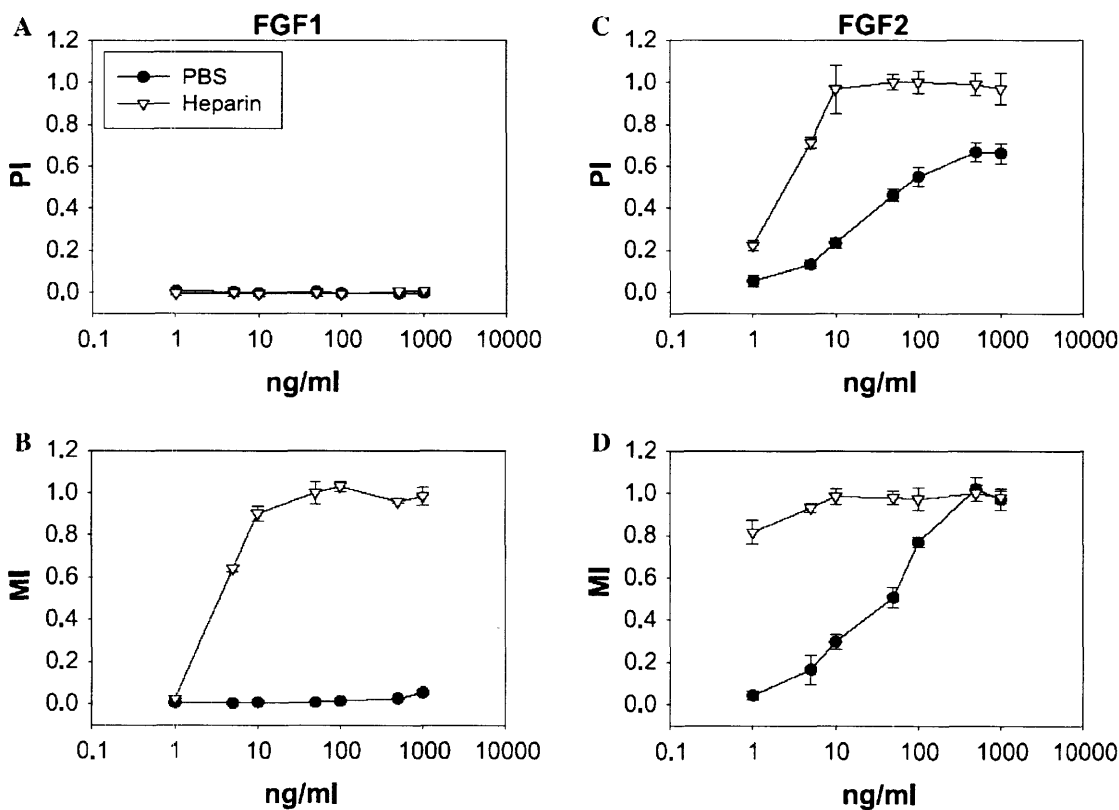


Figure 4.1. Heparin differentially modulates FGF1 and FGF2 based on the method of analysis. BaF3 cells transfected with FGFR1 were treated with varying amounts of FGF1 (A,B) or FGF2 (C,D) in the presence of PBS or 500 ng/ml heparin. The cellular-mediated response was measured by proliferation (A,C) or mitogenesis (B,D) and converted to PI or MI, respectively.

4.2.2 Digestion of heparin differentially modulates FGF1 and FGF2 through both FGFR1c and FGFR3c

We examined whether this system could be used to distinguish the effects of distinct HSGAGs on modulating FGF–FGFR interactions to produce cellular responses. Initial studies were performed with heparin as a model HSGAG, since several studies use heparin as a surrogate HSGAG. Heparin was differentially digested with hepI, hepII, or hepIII to generate three distinct HSGAG pools (**Table 4.1**), which were added exogenously to an FGF–FGFR pair (either FGF1–FGFR1c, FGF1–FGFR3c, FGF2–FGFR1c, or FGF2–FGFR3c). After ligand and HSGAG addition to the appropriate transfected BaF3 culture, the mitogenic response was measured and converted to percent of positive control for the specific ligand and receptor, defined by the FGF in the presence of undigested heparin.

Disaccharide	Heparin	SMCs	BAECs
$\Delta U_{2S} H_{NS,6S}$	61.5	13.2	7.9
$\Delta U_{2S} H_{NS}$	4.0	24.8	29.9
$\Delta U H_{NS,6S}$	12.9	6.6	5.1
$\Delta U_{2S} H_{NAc,6S}$	1.7	0	0
$\Delta U H_{NS}$	3.8	25.6	22.4
$\Delta U_{2S} H_{NAc}$	0.2	0	0
$\Delta U H_{NAc,6S}$	8.6	6.6	5.6
$\Delta U H_{NAc}$	4.7	23.1	29.0

Table 4.1. Compositional analysis of heparin and HSGAGs derived from SMCs and from BAECs. Numbers represent a percentage of total disaccharide within the given condition. Each disaccharide is composed of an unsaturated uronic acid (ΔU) with or without 2-O sulfation (2S), as well as a glucosamine (H), with or without each of N-sulfation (NS), N-acetylation (NAc) or 6-O sulfation (6S).

We find that hepI-digested heparin was unable to support FGF1-induced mitogenesis through FGFR1c as efficaciously as undigested heparin (**Figure 4.2A**). However, digestion of heparin with either hepII or hepIII did not influence heparin’s ability to support mitogenesis. Conversely, hepI, hepII, or hepIII treatment of heparin reduced the mitogenic response induced by FGF2 through FGFR1c. In the case of BaF3 cells transfected with FGFR3c, hepI and hepII digestion of heparin led to a reduced ability of FGF1 to promote a mitogenic response compared

to undigested heparin (**Figure 4.2B**), while heparin fragments generated by hepIII digestion were functionally equivalent to undigested heparin. Conversely, with FGF2, only hepI-digested material produced an effect that was statistically different from undigested heparin. These findings reveal that mitogenic assays for FGF activity in the BaF3 cell system can be used to detect differential effects of distinct HSGAG pools on influencing FGF-mediated mitogenesis. We find that specific heparin structures mediate FGF1 or FGF2-induced mitogenesis and that the structural requirements of FGF1 and FGF2 are distinct, consistent with previous investigations [389, 392].

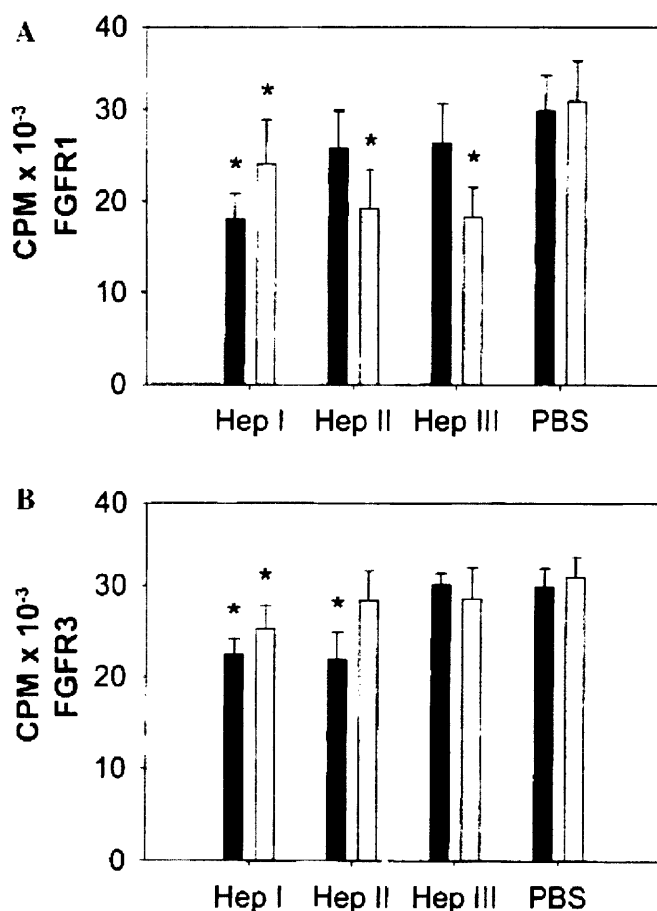


Figure 4.2. Heparinase digested heparin differentially affects FGF1- and FGF2-mediated mitogenesis. BaF3 cells expressing either (A) FGFR1 or (B) FGFR3 were incubated with 5 ng/ml FGF1 (■) or FGF2 (□) and 500 ng/ml heparin pretreated with hepI, hepII, hepIII or PBS. Cellular-mediated response is represented as the percent of the response induced by undigested heparin. * denotes $p < 0.05$ for heparinase digested heparin compared to undigested heparin.

4.2.3 SMC- and BAEC-derived HSGAGs differentially regulate FGF1 and FGF2

To further examine the validity of the FGFR-transfected BaF3 cell system, cell surface derived HSGAGs were used. HSGAGs were isolated from SMCs and BAECs by trypsin digestion. Typical yields from four 500 cm² plates were ~200 and ~170 µg for SMCs and BAECs, respectively. Compositional analysis was performed on SMC-derived HSGAGs as well as BAEC-derived HSGAGs and compared to the composition of heparin (**Table 4.1**). Heparin is predominantly composed of trisulfated disaccharides. Cell surface HSGAGs from SMCs and BAECs, however, had higher levels of di-, mono-, and unsulfated disaccharides.

SMC- and BAEC-derived HSGAGs were pretreated with heparinases or PBS, and their effects on FGF1- or FGF2-induced mitogenesis through FGFR1c or FGFR3c were determined. Undigested cell surface HSGAGs (PBS treated) did not elicit FGF1 or FGF2 responses through either FGFR1c or FGFR3c as efficiently as heparin. Similarly, HSGAGs from Balb/c3T3 cells and human umbilical vein endothelial cells support lower degrees of mitogenesis than heparin [527]. Our findings can be rationalized based on the compositional analysis. Heparin averages 2.40 sulfate groups per disaccharide, while SMC and BAEC average 1.35 and 1.20 sulfate groups per disaccharide, respectively. Interestingly, the mitogenic response elicited in the presence of undigested BAEC-derived HSGAGs is only slightly higher than that of FGF1 or FGF2 alone, suggesting that BAEC HSGAGs do not efficiently support FGF-mediated activity. This finding confirms that the model system described is sensitive to the differential capacity of distinct HSGAG pools to promote FGF1- and FGF2-induced responses.

SMC-derived HSGAGs were then systematically digested with heparinases to allow for a more thorough examination of the ability of the BaF3 system to reveal differential cellular responses to distinct HSGAG pools. In contrast to digestion of heparin, hepIII digestion of SMC-derived HSGAGs (as opposed to hepI for heparin) inhibited FGF1 activity through FGFR1c while digestion of SMC HSGAGs with hepII or hepI (as opposed to hepIII for heparin) had no effect (**Figure 4.3A**). For FGF2, HSGAGs isolated from SMC behaved similarly to heparin in that hepI, II, or III treatment reduced FGF2s mitogenic activity. In the case of FGFR3c, heparinase treatment of SMC-derived HSGAGs enhanced the FGF1-mediated response, with the response most pronounced after hepI digestion (**Figure 4.3B**). Similarly, digestion of SMC

HSGAGs with either hepl or hepII enhanced FGF2-induced mitogenesis through FGFR3c relative to undigested HSGAGs.

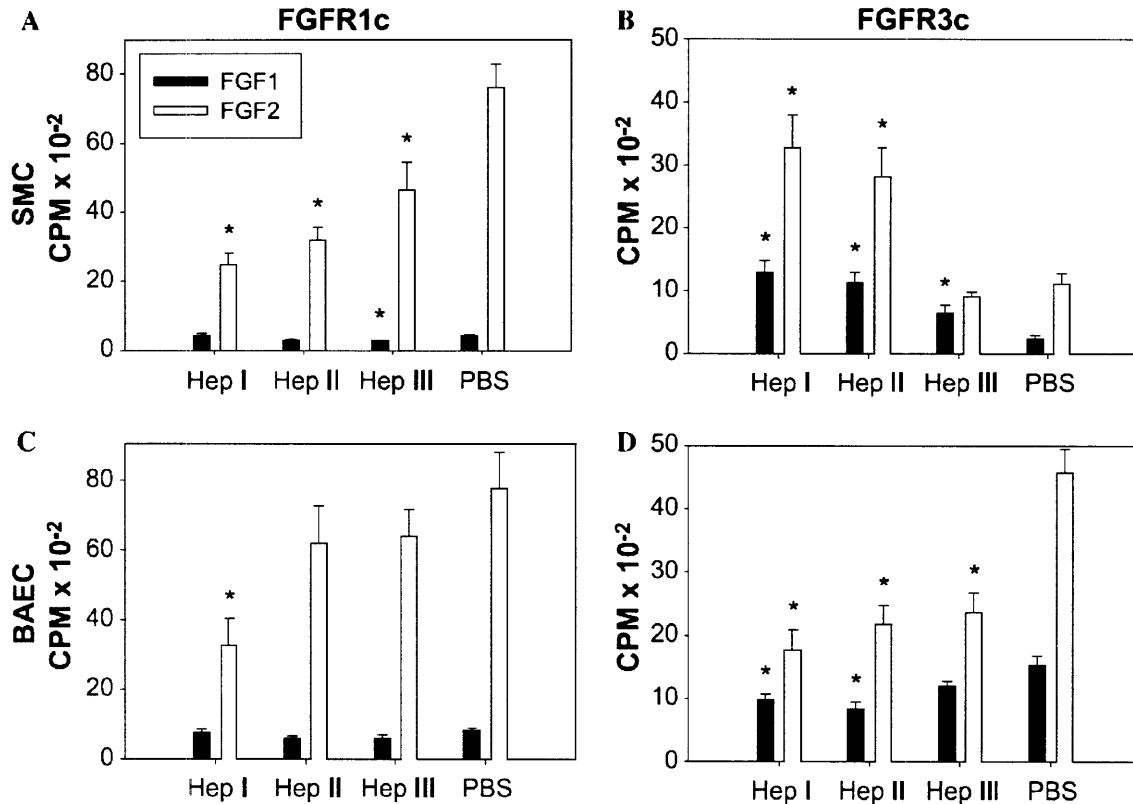


Figure 4.3. Cell surface HSGAGs promote FGF-induced mitogenesis. BaF3 cells expressing either FGFR1 (A,C) or FGFR3 (B,D) were incubated with 5 ng/ml FGF1 (■) or FGF2 (□) and 500 ng/ml HSGAG derived from either SMC (A,B) or BAEC (C,D) with trypsin, and pretreated with hepI, hepII, hepIII or PBS. Cellular-mediated response is represented as CPM incorporated $\times 10^{-2}$. * denotes $p < 0.05$ for heparinase digested HSGAGs compared to undigested HSGAGs.

Previous studies have demonstrated that HSGAGs from BAECs have a similar composition to those from SMCs, but promote distinct patterns of biological responses due to alterations in fine structure [34]. Therefore, we sought to examine whether the BaF3 model system presented herein can distinguish any functional differences between BAEC- and SMC-derived material. To test this, HSGAGs from BAECs were treated with heparinases in a similar manner to SMC-derived material (and heparin). With BAEC-derived HSGAGs, we find that heparinase digestion does not alter FGF1-mediated mitogenesis through FGFR1c (**Figure 4.3C**). Conversely, with FGF2, hepI digestion of BAEC-derived HSGAGs inhibits a mitogenic

response; hepII or hepIII treatment does not alter the response. Thus, these findings confirm and extend the notion that BAEC HSGAG fragments are functionally distinct from SMC HSGAGs.

Differences between FGF1 and FGF2 are also observed upon moving from BaF3 cells expressing FGFR1c to those expressing FGFR3c. In this case, hepI or hepII treatment of BAEC HSGAGs lowered FGF1-mediated mitogenic responses compared to undigested BAEC HSGAGs (**Figure 4.3D**), whereas digestion with any of the heparinases reduced the ability of BAEC HSGAGs to induce mitogenesis through FGFR3c.

4.2.4 The use of a consistent system allows for insights into HSGAG modulation of FGF–FGFR interactions

The data presented herein demonstrate that a simple mitogenic assay utilizing FGFR-transfected BaF3 cells can be used to analyze the differential effects of HSGAGs, including those from the cell surface, on FGF-mediated cellular response. In every FGF–FGFR pair examined, digestion of HSGAG material to produce oligosaccharides of distinct composition and fine structure [34] induced distinct patterns of biological response. Given that each FGF–FGFR pair elicited a similar "baseline" positive control in the presence of undigested heparin, the specific contribution of HSGAGs on several FGF–FGFR sets can be assessed and compared. Taken together, the data presented here outline a rigorous methodology that can be used to profile cell surface HSGAG fragments in terms of their functional ability to promote FGF-mediated activity through defined FGFR isoforms. As such, we anticipate that this system will prove valuable in future examinations of the role of HSGAG fine structure in FGF and growth factor-mediated activation of intracellular signaling pathways.

4.3 Significance

The interactions between HSGAGs and FGF family members have been extensively studied. HSGAGs, which bind all FGFs known to date, mediate the binding of FGF to FGFRs, and facilitate oligomerization, which in turn, promotes receptor phosphorylation, activation of intracellular signaling cascades, and subsequent cellular response. Previous work demonstrated that cell surface HSGAGs can regulate cellular proliferation in response to FGF2 signaling

through FGFR1c. The fine structure intrinsic to the HSGAGs derived from a specific cell type, however, defines the effect that the specific HSGAGs has on the growth factor. This study served to extend previous analyses by examining the effects of full length heparin, SMC-derived HSGAGs, and BAEC-derived HSGAGs on FGF1 and FGF2 signaling through FGFR1c and FGFR3c. Mitogenic assays, but not proliferative assays, could detect cellular responses to FGF1 and FGF2. Consistent with previous studies, heparinase treatment of heparin did alter the mitogenic response. HSGAGs from SMCs and BAECs, digested with heparinases, also elicited differential FGF responses patterns, for both FGF1 and FGF2, through FGFR1c and FGFR3c. Fine structure in cell surface HSGAGs can therefore modulate the cellular response of various FGF-FGFR pairs. The cellular response is defined not only by the FGF-FGFR pair, but also by the HSGAG component. Importantly, the ability for a single system to demonstrate HSGAG modulation of multiple FGFs through FGFRs, suggests that this assay system can be extended to probe the ability of distinct HSGAG species to define the cellular response in specific FGF-FGFR pairs beyond those described.

4.4 Experimental Procedures

Proteins and reagents. Recombinant human FGF1 was from Amgen (Thousand Oaks, CA). Recombinant human FGF2 was a gift from Scios (Mountain View, CA). Recombinant heparinases were expressed as previously described [326]. FBS was from Hyclone (Logan, UT). DMEM, RPMI-1640, PBS, L-glutamine, and penicillin/streptomycin were obtained from Gibco-BRL (Gaithersburg, MD). Mouse recombinant IL-3 was from R&D Systems (Minneapolis, MN). Porcine intestinal mucosa heparin was purchased from Celsus Laboratories (Columbus, OH). BaF3 cells transfected with FGFR1c or FGFR3c were generously provided by Dr. David Ornitz (Washington University, St. Louis, MO). BAECs were generously provided by Dr. Elezar Edelman (MIT, Cambridge, MA).

Cell culture. Bovine aortic SMCs were isolated from calf aortas as previously described [331]. SMCs were maintained in DMEM supplemented with 10% FBS, 100 µg/ml penicillin, 100 U/ml streptomycin, and 500 µg/ml L-glutamine. BAECs were maintained in DMEM (low glucose),

supplemented with 10% FBS, 100 µg/ml penicillin, 100 U/ml streptomycin, and 500 µg/ml L-glutamine, as described [115]. SMCs and BAECs were propagated in 75 cm² flasks at 37°C in a 5% CO₂ humidified incubator and passaged 2–3 times a week, when cells reached confluence. BaF3 cells transfected with various FGFR isoforms were maintained as independent suspension cultures in propagation media composed of RPMI-1640 supplemented with 10% FBS, 100 µg/ml penicillin, 100 U/ml streptomycin, 500 µg/ml L-glutamine, and 1 ng/ml mouse recombinant IL-3. Cultures were grown in 75 cm² flasks at 37 °C in a 5% CO₂ humidified incubator and passaged 1:10 by dilution three times a week.

HSGAG isolation and purification. Cell surface HSGAG fragments were collected from SMCs and BAECs and purified as described with slight modifications. Confluent SMCs or BAECs were treated with 3 ml trypsin–EDTA per 75 cm² tissue culture plate for 3–5 min, centrifuged at 195g for 3 min, and resuspended in DMEM supplemented with 10% FBS. One hundred and twenty milliliters of suspension culture was added to each of four 500 cm² tissue culture plates and incubated at 37 °C in a 5% CO₂ humidified incubator until confluent. Each plate was washed twice with 60 ml PBS. Plates were treated with 5 ml trypsin–EDTA and incubated at 37 °C for 25 min to cleave cell surface proteoglycans. The resulting cell/trypsin solution was boiled for 10 min to deactivate the trypsin. The solution was centrifuged at 4500g for 7 min, the supernatant was collected, and the pellet was discarded. Samples were concentrated by centrifuging in a Centriprep 3 (Amicon, Beverly, MA) overnight at 4 °C at 2500g.

PGs were isolated by anion-exchange chromatography. One milliliter of DEAE Sephacel (Pharmacia Biotech, Uppsala, Sweden) was added to a polypropylene pipette tip plugged with glass wool. The column was equilibrated with 5 column volumes of DEAE wash buffer containing 200 mM NaCl. The supernatant was added to the column. Contaminants were eluted with 15 column volumes of DEAE wash buffer. Proteoglycans and associated HSGAGs were eluted with 5 column volumes of DEAE elution buffer containing 1 M NaCl. The collected samples were buffer exchanged in PBS using a Centriprep 3. Samples were stored at –20 °C until use.

HSGAG quantification and compositional analysis. Amounts of SMC- and BAEC-derived HSGAGs were quantified by Alcian blue with slight modifications from a previously described

method [37] and by carbazole assay [34], with slight modification. HSGAG samples, undiluted and diluted 1:10 in a final volume of 20 μ l, were supplemented with 2 μ l of 4 M ammonium sulfamate and 100 μ l of 25 mM sodium tetraborate in H₂SO₄. The solutions were boiled for 5 min and allowed to cool to room temperature. Four microliters of 7.5% (w/v) carbazole in 95% ethanol was added to each solution. The mixtures were boiled for 15 min and allowed to cool to room temperature. Absorbance was measured at 520 nm. Uronic acid concentrations were obtained by normalizing absorbance readings to a heparin standard curve.

For compositional analysis, samples were treated with 200 nM hepl, hepII, and hepIII in a buffer composed of 25 mM sodium acetate, 100 mM NaCl, and 5 mM calcium acetate, pH 7.0. HSGAGs were incubated with the heparinases overnight at 30 °C to ensure complete digestion, and subsequently analyzed by capillary electrophoresis in reverse polarity, using a running buffer composed of 50 mM Tris/phosphate and 10 μ M dextran sulfate, pH 2.5. Identities of the disaccharides were determined based on comigration with known standards [100, 361, 399, 488].

BaF3 proliferation assay. BaF3 cells transfected with FGFR1c, previously verified by RT-PCR [34], were employed to measure the heparin dependence of FGF1 and FGF2 cellular-mediated responses as described [34] with slight modifications. FGFR1c-transfected BaF3 cells were seeded at a density of 1×10^5 cells/ml in IL-3 deficient RPMI-1640 after washing three times. Cell suspension was added to each well of 24-well plates, 1 ml/well. Cells were supplemented with FGF1 or FGF2 as well as PBS or 500 ng/ml heparin. After incubating for 72 h, whole cell number was determined using an electronic cell counter, and data from each of three experiments were normalized using a PI, as described [358]. The index is defined as the increase in cell number for the experimental case divided by the increase in cell number for the positive control. A value of 0 is defined by cells treated with PBS only, while a value of 1 is defined by the positive control, produced by 50 ng/ml FGF2 and 500 ng/ml heparin.

BaF3 mitogenic assay. BaF3 cells expressing FGFR1c and FGFR3c isoforms [34] were washed three times to remove IL-3 and resuspended to a density of 1×10^5 cells/ml in IL-3 deficient media. Cells were added to 96-well tissue culture plates with a volume of 100 μ l/well. In the first set of experiments, cells were supplemented with FGF1 and FGF2 over a range of concentrations in the presence or absence of heparin. For the second set of experiments, heparin was treated

with 10 nM of hepI, II, III or PBS for 30 min and digestion was verified by UV spectroscopy at 232 nm. Samples were boiled for 30 min and filtered using a 0.45 μ m syringe filter. The resulting fragments were added to cells at a final concentration of 500 ng/ml. FGF1 or FGF2 was added to each well sufficient yield a final ligand concentration of 5 ng/ml. Cells in media without heparin or ligand served as the negative control. The positive controls were cells supplemented with 5 ng/ml ligand and 500 ng/ml PBS-treated heparin. Cells were incubated at 37°C for 21 hours, treated with 1 μ Ci [³H]thymidine in a volume of 10 μ l, and incubated at 37 °C for 3 h. Subsequently, cells were harvested onto glass filter paper using a cell harvester. Each filter sheet was coated with 4 ml scintillation fluid and counts per minute (CPM) were determined by scintillation counter. These experiments were also performed using HSGAGs derived from SMCs and from BAECs. Data were normalized using a mitogenic index (MI), which is calculated similar to the PI, with the negative control defined as zero, and the heparin-FGF2 combination inducing the maximum proliferation defined as 1.

Chapter 5. Stromal cell surface heparin/heparan sulfate-like glycosaminoglycans regulate tumor cell proliferative and metastatic potentials

5.0 Summary

HSGAGs are linear polysaccharides found at the cell surface and in the ECM. HSGAGs have emerged as important modulators of several biological processes notably including cancer growth and progression. Given the importance of the interplay between tumor cells and stromal cells in regulating various important phases of cancer; including proliferation, neovascularization, ECM breakdown, and metabolism; we investigated whether stromal derived HSGAGs could modulate tumor cell properties. HSGAGs from BAECs potently inhibited B16-F10 cell proliferation and increased adhesion. Smooth muscle cell HSGAGs, however, only moderately inhibited tumor cell growth. The cell-derived HSGAGs have similar HSGAG disaccharide compositions by distinct elements of fine structure. Correspondingly, BAEC HSGAGs were found to elicit their affects through β_1 -integrin while SMC HSGAGs modulated FGF2 signaling. The *in vitro* finding that the two HSGAG sets regulated cancer growth and progression was reiterated *in vivo*. HSGAGs from BAECs additionally inhibited primary tumor growth more than SMC HSGAGs *in vivo*, while SMC HSGAGs, but not BAEC HSGAGs, inhibited metastasis. Stromal cell HSGAGs can therefore serve as important regulators of tumor cell growth and progression. Furthermore, the specific affects of stromal cell derived HSGAGs are likely defined by elements of HSGAG fine structure. The specific fine structure of stromal cell derived HSGAGs may therefore play an important role in determining the ability of tumor cells to thrive in a specific region.

5.1 Introduction

The interplay between tumor cells and the surrounding microenvironment is important in determining the growth and progression of tumors [272]. Several of the events involved in tumor growth and metastasis are influenced by interactions between the cancerous cells and the surrounding ECM. Signals from the ECM can confer metastatic fitness, a factor associated with tumor cells that comprise metastatic foci [122, 382, 393]. HSGAGs are key components of the cell-ECM interface, and correspondingly, have been implicated in modulating tumor growth and metastasis [5, 44, 274].

HSGAGs are complex biological polymers attached to HSPG core proteins, found ubiquitously on the cell surface and free in the ECM. Various modifications to the disaccharide repeat unit yield 48 distinct possible structures [77]. The individual disaccharides combine to produce a variety of sequences that enable the regulation and modulation of several important biological processes, including tumor growth and metastasis [426]. Cellular expression of various HSGAG modifying enzymes serves to regulate the relative quantities of specific disaccharides as well as the fine structure of the HSGAGs produced by that cell type [269].

Cancer cells undergo changes in HSPG expression, HSGAG composition and HSGAG fine structure [38]. The alterations of cell surface HSGAGs additionally correlate with cancer progression [446]. These changes in HSGAGs can serve to differentially regulate cellular activities and responses to extracellular cues. Altering the HSGAG profile, for example, can promote or inhibit FGF2 activity, an important factor in melanoma growth [158, 161, 274]. The HSGAG pool in the cancer cell microenvironment is composed of HSGAGs from the cancer cells themselves as well as stromal cells.

Stromal cell HSGAGs could be expected to influence tumor cell growth and metastasis in a similar way to cancer cell HSGAGs, and are therefore an important, yet unexamined component of the tumor cell microenvironment. With potentially distinct HSGAG compositions and fine structures, HSGAGs from stromal cells may make important contributions to the growth potential and metastatic fitness of the cancer cells themselves. In this study, we investigated whether stromal cells could impact tumor cells through their HSGAGs. Using BAECs and SMCs as stromal cells, we found that HSGAGs from stromal cells can inhibit B16-F10 murine

melanoma cell growth. The HSGAGs from these two cell types have similar disaccharide compositions, but BAEC HSGAGs potently inhibit proliferation and also promote cell adhesion, while SMC HSGAGs only modestly inhibit proliferation and do not modulate cell adhesion. The HSGAGs from the two cell types also regulate distinct cellular pathways. BAEC HSGAGs influence B16-F10 cells through β_1 -integrins while SMC HSGAGs alter FGF2 signaling. Additionally, BAEC HSGAGs inhibited primary tumor growth *in vivo* to a greater extent than SMC HSGAGs. SMC HSGAGs, but not BAEC HSGAGs, however, inhibited metastasis *in vivo*. Stromal cell derived HSGAGs can therefore modulate tumor cell processes. Further, fine structure of the stromal cell HSGAG influences the mechanism and magnitude of effect on the cancer cells.

5.2 Results and Discussion

5.2.1 The proliferative and metastatic potentials of cancer cells can be regulated by HSGAGs

HSGAGs are important regulators of tumor growth and metastasis, interacting directly and indirectly with cancer cells. The direct interactions between HSGAGs and cancer cells are complex, with several mechanisms identified to date [44, 271, 274, 523]. Angiogenic and coagulation factors, which are strongly regulated by HSGAGs, for example, play important roles in defining cancer growth and metastasis of various cancers without acting on the cancer cells themselves [196, 427]. In the tumor microenvironment, HSGAGs are contributed by tumor cells and by stromal cells. Cancer cell derived HSGAGs are important regulators of cancer growth and progression by directly altering cell processes [274]. As interactions between stromal and tumor cells provide important influence over features of cancer growth and progression [172], we investigated whether stromal cell-derived HSGAGs could also influence tumor growth and progression.

5.2.2 Stromal cells differentially affect B16-F10 melanoma cells in co-culture

To probe the interaction between cancer and stromal cells, BAECs and SMCs were each co-cultured with B16-F10 murine melanoma cells at various cell:cell ratios and the resulting whole cell number was determined. The co-culture system was used to observe if these cell lines could impact B16-F10 cells through either cell-cell interactions or secreted factors, both potentially important for stromal cell regulation of tumor cells [484, 492]. After three days, co-culture whole cell number was compared to the sum of the whole cell numbers of the two cell lines grown independently with the same initial cell numbers. Co-cultures with BAEC:B16-F10 ratios of 1:1 ($p < 0.003$), 4:1 ($p < 0.0002$), 10:1 ($p < 5 \times 10^{-9}$), and 100:1 ($p < 0.0003$) had significantly fewer cells than the corresponding independent cultures (Figure 5.1). Co-cultures of SMCs and B16-F10 cells, however, were not significantly different from the sum of independent cultures at any SMC:B16-F10 ratio examined (data not shown). Stromal cells can therefore differentially effect cancer cell growth, but the effect varies between stromal cell types.

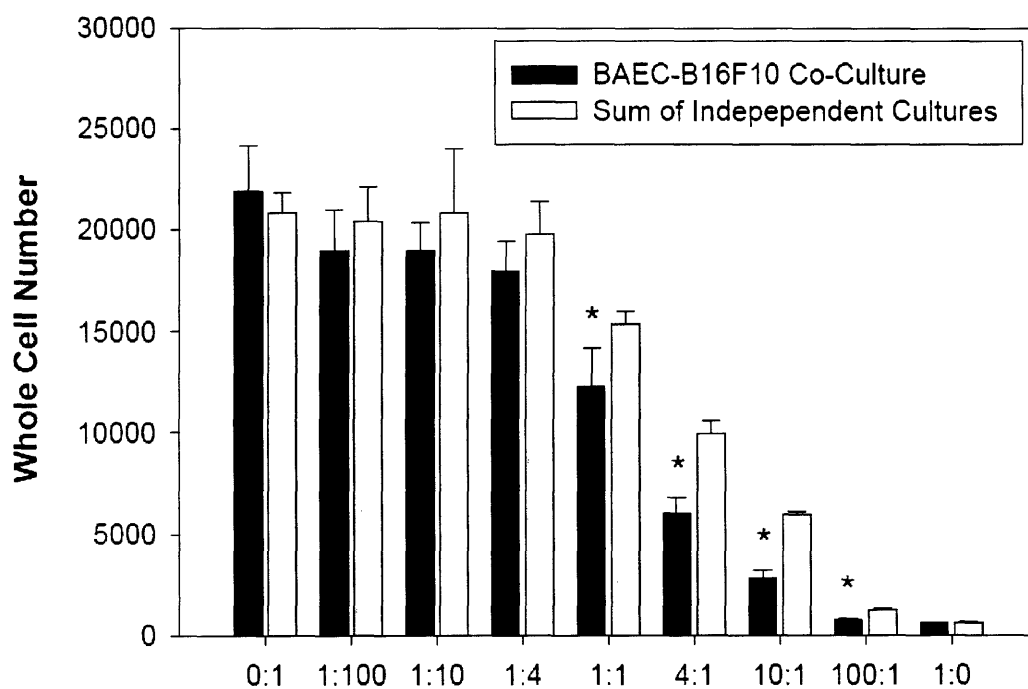


Figure 5.1. BAECs inhibit B16-F10 proliferation. BAECs and B16-F10 cells were co-cultured at various ratios with a total cell number of 5×10^4 cells/ml, or grown independently with identical initial cell numbers. The total cell number was determined after three days, and the total cell number from the co-culture was compared to the sum of that from the independent cultures. * denotes $p < 0.05$ for the co-culture value versus the independent sum value at a given ratio.

5.2.3 BAEC HSGAGs confer growth inhibition

We next sought to define the factors by which BAECs inhibited B16-F10 cells. Both secreted and stromal cell surface factors were investigated. Conditioned media was collected from BAECs and from SMCs, and added to B16-F10 cells to identify any critical secreted factors. SMC-derived conditioned media was used as a control as no growth inhibitory effect was observed in SMC-B16-F10 co-cultures. Conditioned media from BAECs supported less B16-F10 proliferation than conditioned media from SMCs (**Figure 5.2A**), consistent with secreted factors influencing B16-F10 cell growth. To dissect out the factors in conditioned media that enabled BAECs to inhibit B16-F10 proliferation, the conditioned media was boiled prior to addition to B16-F10 cells. Boiled conditioned media from BAECs still supported less B16-F10 cell growth than boiled conditioned media from SMCs (**Figure 5.2B**). Finally, conditioned media was treated with both hepl and hepIII, and subsequently boiled. Heparinase treatment of conditioned media abrogated the proliferative differences between BAEC- and SMC-derived conditioned media (**Figure 5.2C**), suggesting that HSGAGs are the critical secreted factor conferring the BAEC-mediated growth inhibition, given the specificity of the heparinases for HSGAGs [104].

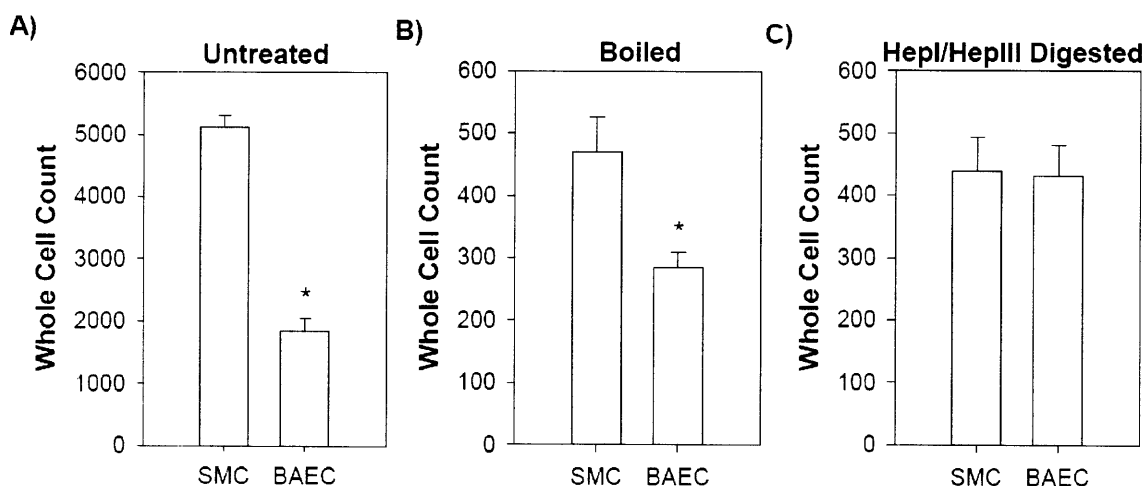


Figure 5.2. The HSGAG component of BAEC conditioned media reduces B16-F10 whole cell number. BAECs and SMCs were grown in serum deficient media for 24 hours, after which the media was transferred to B16-F10 cultures. The affect on whole cell number was determined for A) untreated media, B) boiled media, and C) boiled then hepl and hepIII treated media. * denotes $p < 0.05$ for proliferation in BAEC conditioned media compared to that in SMC conditioned media.

To examine whether cell surface HSGAGs could also contribute to the observed B16-F10 inhibition in co-culture, HSGAGs were isolated from BAECs and SMCs, purified, and added to

B16-F10 cells. Purification was performed through anion exchange chromatography and buffer exchange against water. Other GAGs were removed prior to administration of B16-F10 cells by complete digestion with chondroitinase ABC and subsequent buffer exchange. Cell derived HSGAGs reduced B16-F10 whole cell number after a 72 hour incubation. HSGAGs from BAECs reduced B16-F10 whole cell number $88.1 \pm 2.3\%$ ($p < 3 \times 10^{-10}$) while those from SMCs reduced it by only $53.7 \pm 4.5\%$ ($p < 7 \times 10^{-10}$). Cell surface HSGAGs therefore also inhibit tumor cell growth.

5.2.4 The fine structure of cell derived HSGAGs define their growth inhibitory activity

After defining that cell derived HSGAGs were sufficient to inhibit B16-F10 growth, we sought to further probe the structural components responsible for this phenotype. HSGAGs from BAECs and SMCs have similar disaccharide compositions [31], suggesting that the ability of cell derived HSGAGs to inhibit B16-F10 cell growth is therefore not defined by composition. To examine the importance of HSGAG fine structure and to confirm that composition alone is not a defining factor, stromal cell derived HSGAGs, as well as heparin and HS were pretreated with PBS, hepI, or hepIII. Enzymatic treatments were controlled to only partially digest HSGAGs. Digestion was verified and the degree thereof measured by UV spectroscopy at 232 nm. Control PBS treatments enabled assessment of the undigested HSGAGs, and heparinase digestions were used to probe the fine structure of these HSGAGs by comparing the biological response induced by the digested HSGAGs to that of heparinase treated HSGAGs [31].

Neither the highly sulfated heparin nor the undersulfated HS inhibited B16-F10 proliferation (**Figure 5.3**). The similarity between heparin and HS is consistent with composition alone not being sufficient to define B16-F10 cell growth. When heparin was pretreated with hepIII, but not hepI, B16-F10 whole cell number was reduced ($p < 1 \times 10^{-5}$). Heparinase treatment did not significantly alter HS-mediated proliferative effects. Heparinase digestions, however, did alter the growth inhibitory effects of cell derived HSGAGs. Each of hepI and hepIII digestion increased the magnitude of the inhibitory effect of BAEC HSGAGs ($p < 0.02$), but decreased it for SMC HSGAGs ($p < 0.002$), relative to the corresponding PBS treated HSGAG. These results are consistent with the presence of distinct fine structures in BAEC- and SMC-derived HSGAGs. Heparinases have been proposed to or inhibit the ability of

HSGAGs to impact tumor cell growth by releasing or digesting “cryptic” regions, elements of the fine structure, that are important in regulating cell processes [274, 443]. The differences in fine structure and the unique fragments released by heparinase digestion in BAEC and SMC HSGAGs may account for the distinct B16-F10 cellular responses elicited in co-cultures and by conditioned media.

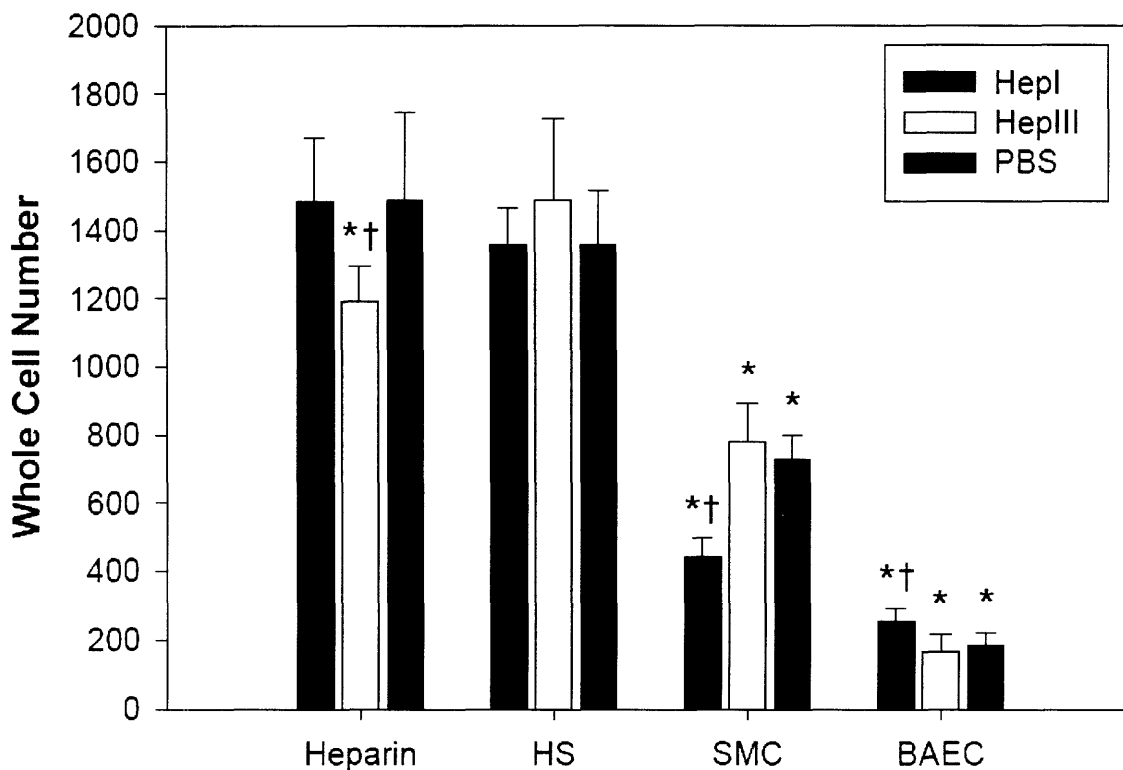


Figure 5.3. BAEC cell surface HSGAGs inhibit B16-F10 proliferation. B16-F10 cells were treated with 500 ng/ml of HSGAGs pretreated with hepI, hepIII, or PBS, and B16-F10 whole cell count was determined after 72 hours. * denotes $p < 0.05$ for the experimental condition compared to the PBS only control. † denotes $p < 0.05$ for digested HSGAGs compared to the same HSGAG treated with PBS.

5.2.5 BAEC- derived HSGAGs promote cell adhesion

In addition to influencing tumor cell growth, HSGAGs, specifically those attached to syndecan core proteins, interact with integrins and modulate processes including cell adhesion and spreading [24]. We therefore examined whether HSGAGs harvested from BAECs and from SMCs could also modulate B16-F10 cell adhesion. B16-F10 cell suspensions were treated with

cell derived HSGAGs, and the number of unattached cells was determined over two hours. HSGAGs from BAECs showed significantly fewer unattached cells, or more attached cells, at times of 30 ($p < 0.004$), 60 ($p < 0.04$), 90 ($p < 0.006$), and 120 ($p < 0.05$) minutes (**Figure 5.4**). SMC HSGAGs, however, did not alter cell adhesion. Cell derived HSGAGs therefore differentially regulate cell adhesion.

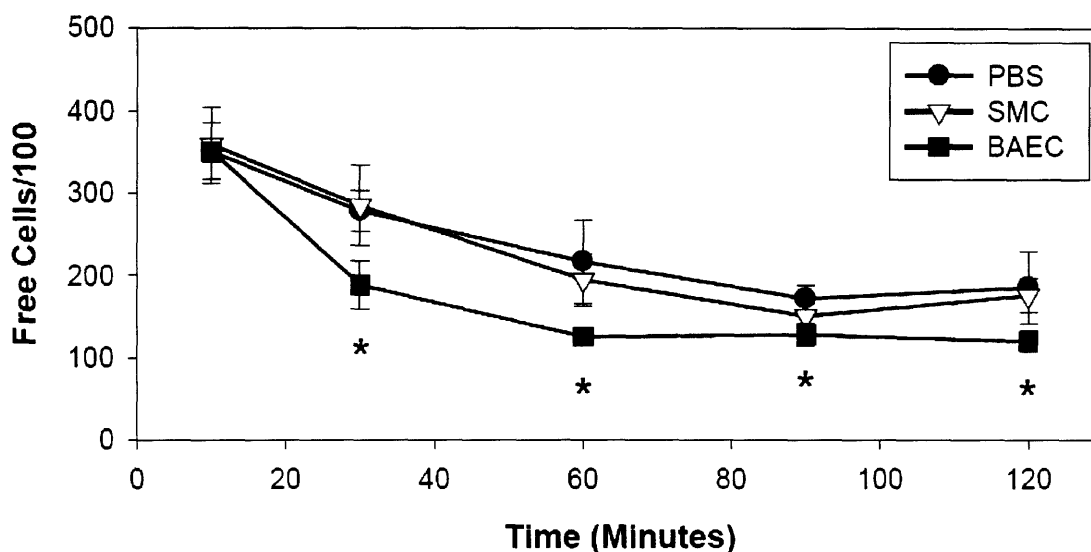


Figure 5.4. Cell surface HSGAGs from BAECs promote B16-F10 adhesion. B16-F10 cells were added to wells containing PBS or either SMC- or BAEC-derived HSGAGs sufficient to yield a final concentration of 500 ng/ml. The number of unbound cells was determined at 10, 30, 60, 90, and 120 minutes. * denotes $p < 0.05$ compared to PBS treatment.

5.2.6 SMC HSGAGs inhibit B16-F10 cell growth by enhancing FGF2 activity

HSGAGs from BAECs and SMCs have distinct fine structures that can differentially regulate important cellular processes [30, 31, 33], likely affecting B16-F10 cells. We next explored whether these distinct elements in fine structure exerted their influence over common or distinct cell processes in B16-F10 cells. HSGAGs from SMCs more efficiently regulate cellular response to FGF2 than HSGAGs from BAECs [31]. Furthermore, FGF2 has an essential autocrine role in some melanomas [158, 161]. To probe whether differential regulation of FGF2 was a critical factor involved in the distinct behaviors of SMC- and BAEC-derived HSGAGs, the affect of FGF2 on B16-F10 cells was first explored. FGF2 maximally reduced whole cell

number at 50 ng/ml FGF2, with a magnitude of $34.6 \pm 3.5\%$ (**Figure 5.5A**). FGF2 at 10 ng/ml reduced whole cell number by $26.0 \pm 2.6\%$. This concentration was used for further experiments in order to enable detection of either inhibition or enhancement of FGF2 activity.

We next examined how cell derived HSGAGs effected B16-F10 proliferation in the presence of FGF2. Independent addition of FGF2 ($22.1 \pm 7.5\%$; $p < 0.001$) and SMC-derived HSGAGs ($24.0 \pm 9.4\%$; $p < 0.002$) inhibited B16-F10 proliferation after 48 hours (**Figure 5.5B**). The combination of both also inhibited proliferation ($37.3 \pm 7.9\%$; $p < 6 \times 10^{-6}$), significantly more than either FGF2 ($p < 0.01$) or SMC HSGAGs ($p < 0.04$) independently, demonstrating that SMC HSGAGs increase the magnitude of the FGF2 induced cellular mediated response, previously demonstrated with HSGAGs free in the ECM [115]. The affect of BAEC HSGAGs on B16-F10 cell growth was not altered by FGF2 ($p > 0.36$).

Treatment of B16-F10 cells with antibodies specific to FGFR1 abrogated the growth inhibition induced by FGF2 ($p > 0.34$), SMC HSGAGs ($p > 0.79$), as well as the combination of both ($p > 0.06$). B16-F10 cells have been previously demonstrated to express FGFR1, a receptor through which FGF2 induces cellular mediated responses [254, 348]. Similarly, antibodies specific to FGF2 prevented reductions in whole cell number after treatment with FGF2 ($p > 0.86$), SMC HSGAGs ($p > 0.12$), or both together ($p > 0.42$). These results suggest that SMC HSGAGs inhibit B16-F10 proliferation through an FGF2 mediated mechanism.

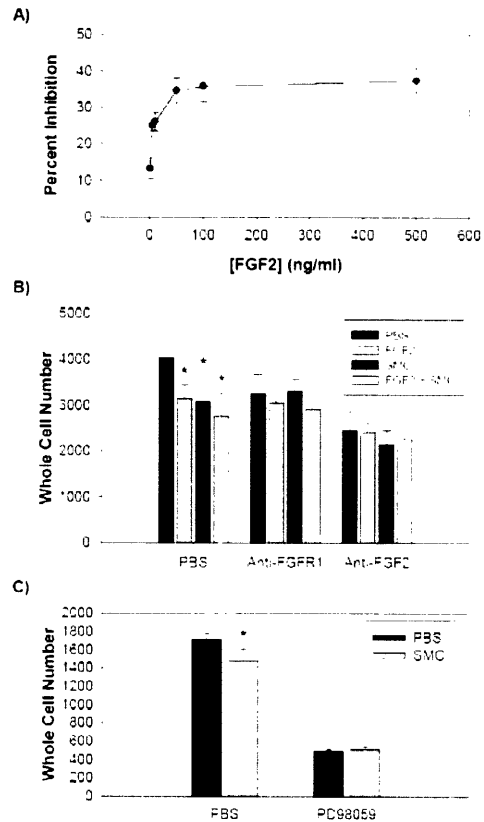


Figure 5.5. SMC-derived HSGAGs inhibit B16-F10 proliferation by promoting FGF2 activity. A) B16-F10 cells were treated with various concentrations of FGF2. Whole cell number was determined after 48 hours and converted to a percent reduction in whole cell number compared to PBS treated cells. B) B16-F10 cells were treated with PBS, 10 ng/ml FGF2, 500 ng/ml SMC HSGAG or both FGF2 and SMC HSGAG in the presence of PBS, anti-FGFR1 antibody (1:100) or anti-FGF2 antibody (1:100). Data is presented as whole cell number, determined after 48 hours. * denotes $p < 0.05$ compared to the corresponding PBS treatment. C) B16-F10 cells were treated with PBS or 500 ng/ml SMC HSGAG, in the presence of either PBS or 20 μ M PD98059. Data is presented as whole cell number, determined after 48 hours. * denotes $p < 0.05$ for SMC HSGAGs compared to PBS treatment.

To further confirm that the FGF2 pathway is used by SMC HSGAGs, we examined whether PD98059, which inhibits Erk, could also prevent the observed growth inhibition with HSGAGs from SMCs. Pretreatment with PD98059 did prevent the reduction in whole cell number induced by SMC HSGAGs ($p > 0.26$; **Figure 5.5C**). SMC HSGAGs induce the observed inhibition of B16-F10 cells through the FGF2 pathway. Antibody treatment did not, however, prevent BAEC HSHAG-mediated growth inhibition. Additionally, BAEC HSGAGs were also still able to inhibit B16-F10 proliferation in the presence of PD98059 ($p < 0.002$). These findings suggest that BAEC HSGAG mediated inhibition of B16-F10 cell proliferation occurred through a different mechanism than by that which SMC HSGAGs inhibited cell growth.

5.2.7 BAEC HSGAGs affect B16-F10 cells through β_1 -integrin

We next sought to understand how BAEC HSGAGs inhibit B16-F10 proliferation. Treating B16-F10 cells with 100 ng/ml BAEC HSGAGs reduced whole cell number by $42.0 \pm 10.6\%$ after a 48 hour incubation. The shorter incubation period and lower dose were used as the smaller magnitude of effect allowed for treatments that either increased or decreased the BAEC HSGAG mediated inhibition to be assessed. Pretreating B16-F10 cells with phorbol 12-myristate 13-acetate (PMA) increased the magnitude of the BAEC HSGAG mediated growth inhibition (**Figure 5.6A**), yielding a $65.2 \pm 5.2\%$ reduction in whole cell number, significantly greater than BAEC HSGAGs alone ($p < 0.05$). PMA activates protein kinase C (PKC), which

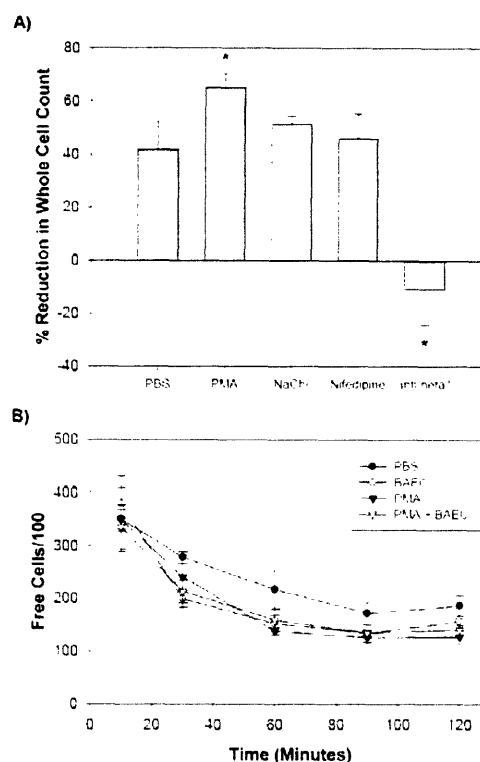


Figure 5.6. BAEC-derived HSGAGs reduce B16-F10 whole cell number through β_1 integrins. A) B16-F10 cells were treated with PBS or BAEC-derived HSGAGs as well as PBS, PMA, sodium chlorate, nifedipine or anti- β_1 integrin antibodies (1:50). Whole cell number was determined after 48 hours. The percent reduction in whole cell number with BAEC-derived HSGAGs normalized to PBS treatment with the same media supplement was determined. Data is presented as the percent reduction in whole cell number induced by BAEC HSGAGs. * denotes $p < 0.05$ for the percent reduction in whole cell number induced by BAEC HSGAGs for a given media treatment compared to unsupplemented cells. B) B16-F10 cells were added to wells containing PBS or BAEC-derived HSGAGs as well as PBS or PMA. The number of unbound cells was determined at 10, 30, 60, 90, and 120 minutes.

accelerates syndecan shedding [129]. Neither sodium chlorate ($51.3 \pm 3.1\%$; $p > 0.26$) nor nifedipine ($46.0 \pm 9.4\%$; $p > 0.63$) significantly altered the growth inhibitory effect of BAEC HSGAGs, suggesting that B16-F10 cell surface HSGAGs and L-type calcium channels were not necessary for the BAEC HSGAG-mediated effects. Antibodies to β_1 -integrin, however, abrogated the growth inhibitory effect. The resultant $10.7 \pm 13.5\%$ increase in whole cell number with β_1 integrin antibodies was not significantly different from untreated cells ($p > 0.25$), and was significantly different than BAEC HSGAGs alone ($p < 0.003$).

The increased growth inhibitory potential of BAEC HSGAGs with PMA suggests that syndecans on the B16-F10 cells themselves may play an important role in the pathway targeted by BAEC HSGAGs. Both syndecan-1 and syndecan-4 cluster with integrins [24]. PKC activation, which induces syndecan shedding, occurs downstream of β_1 -integrins. These results are consistent with BAEC HSGAGs inducing a cellular response through β_1 integrins. HSGAGs do otherwise regulate β_1 -integrin activity [229], and the interaction between syndecans and β_3 -integrin is sufficient to generate a cellular response influenced by β_1 -integrin [23]. The increase in response seen with PMA would therefore be due to enhanced PKC activity, mimicking the β_1 -integrin pathway, but with a greater downstream response.

In addition to inhibiting proliferation, BAEC HSGAGs also promoted B16-F10 cell adhesion. When B16-F10 cells were pretreated with PMA, the BAEC HSGAGs did not alter cell adhesion relative to PBS (**Figure 5.6B**). PMA, BAEC HSGAGs, and PMA + BAEC HSGAGs all promoted increased cell adhesion relative to untreated cells, with no difference between any of the three groups. The influence of β_1 -integrin was not examined by antibody, as control antibodies had non-specific effects that altered the ability to cells to adhere to tissue culture plates. PKC activation, induced by PMA, is necessary for cell spreading [467]. Similar to that found with B16-F10 proliferation, PMA induced the affects of BAEC HSGAGs for B16-F10 adhesion. The mechanism by which BAEC HSGAGs influence cell adhesion is therefore likely the same by which they inhibited proliferation.

To further confirm that BAEC HSGAGs elicit cellular effects through β_1 -integrin, immunohistochemistry was performed on B16-F10 cells for nuclei (4'-6-Diamidino-2-phenylindole; DAPI), F-actin (phalloidin) and β_1 integrin. The distribution of F-actin (red) and β_1 -integrin (green) both changed after the administration of BAEC HSGAGs (**Figure 5.7**). F-

actin was examined because syndecan-4, associated with β_1 integrin, may serve as a link between the ECM as well as β_1 -integrin and the actin cytoskeleton. The change in F-actin and β_1 -integrin distribution observed after BAEC HSGAG treatment is consistent with the effects mediated through β_1 -integrin and syndecans to the actin cytoskeleton. Modulation of β_1 -integrin, syndecans, and the actin cytoskeleton are associated with proliferation and adhesion [24, 519].

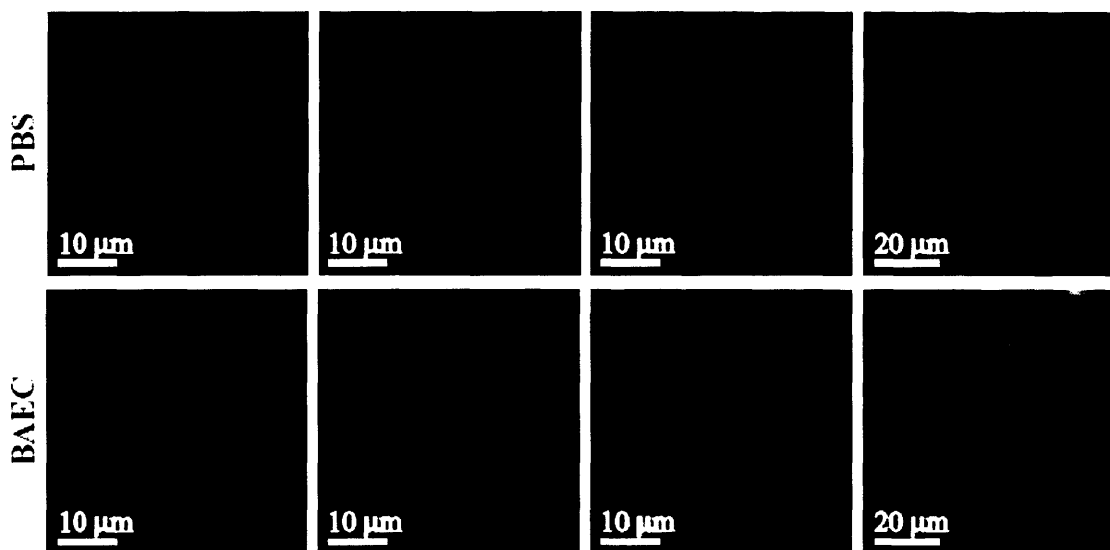


Figure 5.7. BAEC-derived HSGAGs alter β_1 integrin distribution. B16-F10 cells treated with PBS or BAEC HSGAGs were stained for F-actin (red), β_1 integrin (green) and nuclei using DAPI (blue). The three leftmost images for each condition are of the same cells.

5.2.8 Cell derived HSGAGs differentially affect B16-F10 tumor growth and metastasis

BAEC- and SMC-derived HSGAGs utilized distinct cellular pathways to inhibit cell growth and promote adhesion in B16-F10 cells *in vitro*. We next sought to determine if the differential effects of BAEC and SMC HSGAGs were present *in vivo*. The ability of intact HSGAGs to influence B16-F10 primary tumor growth was therefore investigated. Mice were treated with 2 $\mu\text{g}/\text{kg}/\text{day}$ of cell derived HSGAGs. HSGAGs from both BAECs and SMCs inhibited primary tumor growth (**Figure 5.8A**). BAEC HSGAGs inhibited tumor growth $55.3 \pm 13.4\%$ after 14 days, while those from SMCs inhibited growth $29.5 \pm 8.8\%$ over the same time

period. HSGAGs from BAECs and SMCs recapitulated the tumor growth inhibition observed *in vitro*, with BAEC HSGAGs inhibiting primary tumor growth more than SMC HSGAGs.

The anti-tumor effects of HSGAGs have been associated with anticoagulant activities as well as by directly affecting tumor cell processes [29, 417, 523]. Anti-IIa and anti-Xa activities were measured to determine if the relative *in vivo* primary tumor growth activities could be attributed to the anticoagulant behavior of the cell-derived HSGAGs. SMC HSGAGs had anti-Xa activity of 83.9 IU/mg and anti-IIa activity of 69.93 IU/mg, yielding a Xa/IIa ratio of 1.2, similar to unfractionated heparin [314]. The ability of SMC HSGAGs to influence primary tumor growth could be attributed to its ability to specifically inhibit B16-F10 growth *in vitro* through FGF2, its anti-coagulant activity, or a combination of both factors. BAEC HSGAGs, however, had no detectable anti-Xa or anti-IIa activity. HSGAGs from BAECs therefore impact primary tumor growth by directly influencing cell function, potentially through the β_1 -integrin-syndecan pathway identified *in vitro*.

To investigate the role of cell derived HSGAGs on metastasis, B16-F10 cells were suspended in solutions containing 2 $\mu\text{g}/\text{ml}$ BAEC- or SMC-derived HSGAGs and injected into the tail vein of mice. While BAEC HSGAGs did not alter the number of lung nodes after 15 days compared to untreated B16-F10 cells (**Figure 5.8B**), SMC HSGAGs reduced the number of nodes > 50% ($p < 0.0007$). SMC HSGAGs may therefore be potent inhibitors of metastasis.

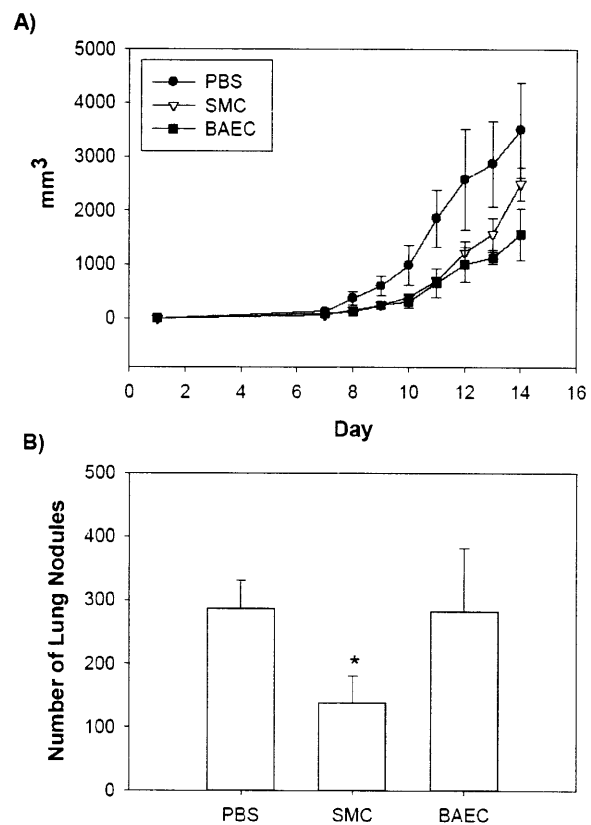


Figure 5.8. Stromal cell derived HSGAGs regulate tumor proliferation and metastasis. A) Mice were treated with cell surface HSGAGs from SMCs or BAECs (2 $\mu\text{g}/\text{kg}/\text{day}$) or a PBS control ($n = 5$). Measurement of lung colonization by B16-F10 cells subsequent to treatment with HSGAGs. B16-F10 cells were resuspended in PBS or HSGAGs from either BAECs or SMCs, and injected into the tail veins ($n = 8$). * denotes $p < 0.05$.

The results herein demonstrate that HSGAGs derived from non-cancerous cells influence the growth and metastatic potential of tumor cells. The fine structure of the HSGAGs, different based on cell type of origin, defines the mechanism by which the HSGAG can impact tumor cells. The HSGAGs examined herein specifically affected B16-F10 cells through the FGF2 signaling pathway and through β_1 -integrin interactions with syndecans and the actin cytoskeleton. This study demonstrates that the HSGAG fine structure of specific stromal cells can differentially impact tumor growth and metastasis in specific and distinct manners.

Stromal cells have important interactions with cancer cells throughout tumor growth and progression [200]. The normal cellular environment exerts homeostatic control to resist the development and growth of tumors [386]. The two sets of non-cancerous cell derived HSGAGs examined in this study inhibited tumor growth. Tumors that survive would therefore be expected to change the stroma. Cancer cells, for example, change the ECM to promote survival by releasing the glycoprotein galectin-1 to induce T-cell apoptosis [176]. HSGAGs may normally maintain a cancer resistant microenvironment until the HSGAG fine structure is altered via tumor-derived signals to one that allows or even promotes tumor growth. Cell derived HSGAGs also affected tumor cell adhesion and metastasis. The cell surface HSGAGs of stromal cells may therefore help to define when a primary tumor becomes metastatic or where metastatic cells in the blood stream adhere and survive.

Stromal cell HSGAGs are therefore important modulators of tumor cell growth and progression. The results presented demonstrate that fine structure governs the ability of HSGAGs from a given stromal cell to impact the tumor cell by defining the cellular mechanisms that can be modulated. Specific stromal cells may be more permissive or more inhibitory to primary tumor cell growth, cancer progression, and metastasis. HSGAGs from specific stromal cells may prove useful as therapies to prevent the growth, progression, and metastasis of tumors with the potential to develop cancer type- and stage-specific therapies. Future work is necessary to understand whether tumors change the HSGAG profile of stromal cells to facilitate their development as well as to appreciate the full therapeutic potential of stromal cell HSGAG.

5.3 Significance

Several studies have focused on understanding the ability of HSGAGs to influence cancer growth and progression. The majority of studies have focused on the highly sulfated heparin, typically used as an anticoagulant. Only recently has evidence emerged that cancer cell surface HSGAGs may be important in influencing its growth and progression. The importance of stromal cells surrounding tumors in defining various elements of the lifecycle of a cancer led us to explore the potential contribution of stromal HSGAGs in regulating cancer. HSGAGs from BAECs and SMCs, which have been demonstrated to have similar compositions but unique elements of fine structure, were employed. HSGAGs from BAECs, whether secreted from cells or derived from the cell surface, potently inhibited murine melanoma B16-F10 cell growth, and promoted cell adhesion. HSGAGs specifically derived from the surface of SMCs, however, only moderately inhibited B16-F10 proliferation. These findings demonstrated that stromal cell HSGAGs can influence the activities of cancer cells. As the activities were distinct, subsequent studies explored the mechanism by which these HSGAGs affected cancer cells. SMC HSGAGs inhibited FGF2 activity, while BAEC HSGAGs acted through β_1 -integrin, PKC, and F-actin. The different fine structures of the two sets of HSGAGs therefore enabled regulation of distinct cellular pathways. Finally, the ability of these HSGAGs to influence cancer cells was examined *in vivo*. BAEC HSGAGs inhibited primary tumor growth but had no effect on metastasis. SMC HSGAGs only minimally inhibited primary tumor growth and strongly inhibited metastasis. Stromal HSGAGs can therefore serve as important regulators of cancer growth and progression. This study provides the first evidence that cell derived HSGAGs from non-cancer cells can play an important role in defining the cancer phenotype, and demonstrates that these HSGAGs may have important therapeutic potential.

5.4 Experimental Procedures

Proteins and reagents. FBS was from Hyclone (Logan, UT). L-glutamine, penicillin, and streptomycin were obtained from GibcoBRL (Gaithersburg, MD). Minimum essential medium alpha (MEM), DMEM, RPMI-1640, and PBS were from BioWhittaker (Walkersville, MD). Recombinant heparinases were expressed as described [30]. Non-transformed BAECs previously isolated from calf aortas were generously provided by Dr. Elezar Edelman (MIT, Cambridge, MA).

Cell culture. SMCs were isolated from fresh calf aortas [331] and maintained in DMEM supplemented with 10% FBS. Cells were used for experiments between passage 2 and passage 6. BAECs were maintained under identical conditions as SMCs except that BAECs were used between passage 3 and passage 7. B16-F10 cells were maintained in MEM supplemented with 10% FBS, and used for *in vivo* studies only prior to passage 5. All cells were passaged 2-3 times a week at confluence. All cells were supplemented with 100 µg/ml penicillin, 100 U/ml streptomycin, and 500 µg/ml L-glutamine. Cultures were grown in 75 cm² flasks at 37°C in a 5% CO₂ humidified incubator, and passaged 1:10 by dilution three times a week.

Co-culture analysis. SMC, BAEC and B16-F10 cultures were grown until confluent, treated with 3 ml trypsin-EDTA per 75 cm² flask for 3-5 minutes until cells detached, pelleted, resuspended in FBS supplemented MEM, and diluted to 5×10^4 cells/ml based on the reading on an electronic cell counter. BAECs or SMCs were added with B16-F10 cells to 24-well plates in a total volume of 1 ml/well such that the BAEC:B16-F10 or SMC:B16-F10 ratio was initially 0:1, 1:100, 1:10, 1:4, 1:1, 4:1, 10:1, 100:1 and 1:0. For example, 1:4 is formed by 200 µl BAEC suspension and 800 µl B16-F10 suspension. Equivalent quantities of each cell type were plated alone, with the remaining volume replaced with media. The plates were incubated for 72 hours at 37°C in a 5% CO₂ humidified incubator. Subsequently, wells were washed with PBS, treated with 400 µl trypsin-EDTA per well, incubated for 5 minutes, and whole cell number was determined using an electronic cell counter.

Conditioned media treatments. SMC and BAEC cultures were grown until confluent, split 1:10 in MEM supplemented with 10% FBS in 75 cm² flasks, and incubated for 24 hours. Cells were washed and treated with MEM containing 0.1% FBS. The conditioned media was removed after 24 hours. The media was left untreated, boiled for 30 minutes, or digested with hepl and hepIII overnight and subsequently boiled for 30 minutes. Conditioned media was stored at 4°C until use.

B16-F10 cultures were grown until confluent, trypsin treated, pelleted, resuspended in 10 ml MEM with 10% FBS, and diluted to 5×10^4 cells/ml. Each well of 24-well plates was treated with 1 ml of cell suspension and incubated for 24 hours, washed, serum-starved for 24 hours, and supplemented with 1 ml/well SMC- or BAEC-derived conditioned media. B16-F10 cells were incubated for 72 hours, treated with 400 μ l trypsin, and whole cell count was determined with an electronic cell counter.

Isolation and analysis of cell surface HSGAGs. Intact cell surface glycosaminoglycans (GAGs) were collected from SMCs and BAECs independently, boiled, and purified by anion-exchange chromatography and subsequent buffer exchange to water [31]. Samples were digested overnight with chondroitinase ABC, and buffer exchanged using a 3 kDa molecular weight cut-off filter to eliminate chondroitin sulfate and dermatan sulfate GAGs. Quantities of total cell-derived HSGAGs were quantified by Alcian blue assay as described [37] with slight modifications, and by carbazole assay [31], both after removal of chondroitin sulfate and dermatan sulfate. Relative composite disaccharide amounts isolated from cell surface HSGAGs were determined by capillary electrophoresis [30, 33]. Samples were stored at -20°C until use.

B16-F10 proliferation assay. Heparin, HS, SMC HSGAGs, and BAEC HSGAGs at 50 μ g/ml in PBS, were treated with hepl, hepIII or PBS for 30 minutes and boiled for 30 minutes [30]. Partial digestion was confirmed by UV spectroscopy at 232 nm [31]. B16-F10 cultures were grown until confluent, trypsin treated, pelleted, resuspended in MEM, and diluted to 5×10^4 cells/ml. Cell suspension was added to 24-well plates, 1 ml/well, incubated 24 hours, serum-starved for 24 hours, and treated with HSGAGs to yield a final concentration of 500 ng/ml. Whole cell number was measured as previously described using an electronic cell counter after

72 hours for initial experiments with cell derived HSGAGs, and 48 hours for subsequent experiments to determine the mechanism by which HSGAGs impacted cells.

To further probe the affect of cell derived HSGAGs, cells treated with undigested HSGAGs and untreated controls were supplemented with FGF2 (10 ng/ml), PMA (100 ng/ml; Sigma, St. Louis, MO), sodium chlorate (50 mM), nifedipine (50 μ M), or anti- β_1 -integrin antibodies (1:100; Santa Cruz Biotechnology, Santa Cruz, CA). Cells treated with FGF2 were additionally supplemented with anti-FGFR1 antibodies (1:100; Santa Cruz Biotechnology, Santa Cruz, CA), anti-FGF2 antibody (1:100; Santa Cruz Biotechnology), PD98059 (20 μ M; Promega, Madison, WI) or an equivalent volume of PBS. Whole cell number of HSGAG treated cells was normalized to cells with the equivalent media supplement.

B16-F10 adhesion assay. Wells of 24-well plates were treated with 500 μ l MEM supplemented with 0.1% FBS. HSGAGs derived from either SMCs or BAECs were added at 1 μ g/ml. FGF2 (20 ng/ml), PD98059 (40 μ M), PMA (200 ng/ml), sodium chlorate (100 mM), and nifedipine (100 μ M) were added as appropriate. B16-F10 cultures were grown until confluent, trypsin treated, pelleted, resuspended in MEM, and diluted to 1×10^5 cells/ml. Cell suspension was added to 24-well plates 500 μ l/well. After 10, 30, 60, 90 or 120 minutes, 400 μ l was removed from wells, and used to determine whole cell number by electronic cell counter.

Immunohistochemistry. B16-F10 cultures were grown until confluent, trypsin treated, pelleted, resuspended in MEM supplemented with 10% FBS, and diluted to 1×10^5 cells/ml. Cell suspension was added to collagen coated glass cover slips in 12 well plates, 1 ml/well. Plates were incubated for 24 hours, serum starved for 24 hours, and treated with PBS or HSGAGs from either SMCs or BAECs at 500 ng/ml. After 6 hours, cells were washed with PBS and fixed for 10 minutes in 3.7% formalin. Cells were treated with 0.1% triton X-100 for 5 minutes and preincubated in 1% bovine serum albumin in PBS for 30 minutes. Goat polyclonal antibodies to β_1 -integrin (Santa Cruz Biotechnology) were added at a 1:100 dilution and incubated 4 hours. FITC-labeled chicken α -goat secondary antibody (Molecular Probes, Eugene, OR) and Texas-red labeled phalloidin (Molecular Probes) were added and incubated 1 hour. DAPI was then added for 5 minutes at room temperature. Fluorescent optical images were obtained using an

inverted microscope (Axiovert 200, Zeiss) and acquired with Openlab 3.1.5 software. Images were processed using Adobe Illustrator 10.0.

Tumor implantation and lung metastasis. Primary tumor implantation and lung metastasis analysis were performed as described [274]. Briefly, 4×10^5 B16-F10 cells in log growth-phase were injected subcutaneously in a volume of 100 μ l PBS into the right flank of C57BL/6 mice on day 1. Osmotic pumps (Alza, Mountain View, CA) were implanted on day 2, and delivered 0.5 μ l/hr of cell surface HSGAGs from SMCs or BAECs for 14 days. Additional daily injections of fragment solutions began on day 5 and continued for the remainder of the experiment. Tumor volume (mm^3) was measured daily starting on day 7 using calipers.

For lung metastasis analysis, 200 μ l cell surface HSGAG suspensions containing 2×10^5 tumor cells were injected via tail vein on day 1. Suspensions were produced immediately prior to injection. Mice were sacrificed on day 14, and the lungs were harvested. The number of lung nodules on the surface was determined using a dissection microscope.

Chapter 6. Heparan sulfate and dermatan sulfate glycosaminoglycans regulate fibroblast growth factor and vascular endothelial growth factor activity

6.0 Summary

Heparin/heparan sulfate-like glycosaminoglycans have been well characterized in their ability to regulate the activities of the FGF and vascular endothelial growth factor (VEGF) families. DS also supports the activities of FGF2 and FGF7. We investigated the capacity of various GAGs to regulate FGF and VEGF family proteins in rat bladder cancer cells. Heparin, the highly sulfated DS fraction DT (DS DT), and chondroitin-6-sulfate, promoted FGF7 activity. FGF1, FGF2 and VEGF activities were affected with similar magnitude and effect by both heparin and DS DT. Heparin and DS DT, however, differentially regulated FGF7 and VEGF in the same cellular environment. The differential cellular response was found to stem from ligand-induced upregulation of VEGF-D and subsequent GAG-mediated modulation of VEGF-D-mediated cellular response through VEGF receptor (VEGFR) isoform 3. Chemically oversulfated GAGs can also increase the FGF7-mediated response. These findings demonstrate that fractions of various GAG families can regulate the activities of several FGF and VEGF family members, both independently and in a common environment. Selectively developed GAGs offer a novel approach to select for the activity of growth factor subsets even in a complex pool, as exists in healing wounds and in the tumor microenvironment.

6.1 Introduction

GAGs are important regulators of biological functions. All GAGs are linear polysaccharides composed a disaccharide repeat unit that contains uronic acid and a hexosamine, where the specific nature of each defines the class of GAG [427]. The HSGAGs are the best studied of the glycosaminoglycans. The five sites of variation in the HSGAG disaccharide allow

for enormous structural heterogeneity that enables them to modulate a wide range of important biological processes including development and tumor progression [38, 427]. HSGAGs interact with all known members of the FGF family [392]. Other GAGs, such as DS and CS have also emerged as important regulators of biological processes including FGF-mediated activity [474].

The FGF protein family consists of 23 members. Each FGF interacts with at least one of five high affinity cell surface tyrosine kinase receptors [119, 445], and with the GAG component of proteoglycans [153, 178, 396]. While HSGAGs interact with all known FGFs, the structural requirement of a HSGAG to promote a cellular response differs based on the FGF [213, 392, 512]. FGFR isoforms support cellular activity downstream only of specific FGF family members [348]. HSGAGs interact with both the FGF and the FGFR to provide receptor selectivity and to regulate the cellular response [6, 213, 354]. FGF7 induces a downstream response through FGFR2b [124, 348]. The magnitude of cellular response to FGF7 can be regulated by HSGAGs as well as DS [475, 512]. HSGAGs and DS regulate FGF2-mediated activity through FGFR1c, while only HSGAGs have been shown to regulate that of FGF1 [366, 475].

VEGF is a major regulator of angiogenesis and cell growth [485]. VEGF isoforms show variable interactions with HSGAGs [400]. VEGF signals through the tyrosine kinases VEGFR1 and VEGFR2, which are predominantly, but not exclusively, found on endothelial cells [201, 400]. VEGF-C and VEGF-D signal through VEGFR2 and VEGFR3 [2, 209]. VEGFR3 activity is associated with lymphangiogenesis [249]. VEGF-D, but not VEGF, promotes the lymphatic spread of tumors [450]. While the dependence of VEGF on HSGAGs has been established [196], the interactions of VEGF-C and VEGF-D with HSGAGs and other GAGs have not been determined.

The ability of HSGAGs, DS, and other GAGs to modulate FGFs and VEGFs is important in several physiological and pathological settings. FGF7 signaling through FGFR2b is important in wound healing, for example [203]. DS derived from wound fluid promotes FGF7 activity through its receptor [475]. VEGFR3 is also upregulated during wound healing, where it promotes angiogenesis downstream of VEGF-C and VEGF-D [357]. FGF, VEGF and various GAGs have also been implicated in cancer growth and progression [196, 427], promoting not only angiogenesis, but also primary tumor growth directly, such as in prostate cancer [201, 356]. FGF and VEGF can activate similar pathways to produce a common biological outcome, though

the activity of one ligand may be dependent on the activity of the other [249, 390]. Understanding the ability of GAGs to differentially interact with various FGFs and VEGFs, both individually and in the same cellular environment, can shed insight into the role of each of these components in biologically important settings.

In this study, the regulatory potential of GAGs on FGF- and VEGF-mediated cellular responses. Using FGF7 as a model growth factor due to its specificity for a single FGFR isoform, we first examined how various GAGs altered its proliferative effects. We then extended this analysis to FGF1, FGF2, and VEGF. GAGs induced growth factor-specific proliferative effects, which led us next to examine if GAGs could regulate or even define the biological effect with multiple growth factors in the same cellular environment. Heparin and highly sulfated DS differentially regulated the combination of FGF7 and VEGF. We find that this response stems primarily from the upregulation of VEGF-D, which itself, is differentially regulated by heparin and DS DT. These findings demonstrate that GAGs can selectively regulate growth factor activity and define the net biological response in a pool of growth factors.

6.2 Results

6.2.1 Heparin and DS DT support FGF7-mediated responses

Studies exploring the interactions between GAGs and FGF family members are typically confined to the binding of heparin and other HSGAGs to FGF, and subsequent downstream responses. Recent findings have demonstrated, however, that DS can also bind to and modulate the activities of both FGF2 and FGF7 [366, 475]. We sought to understand the differential effects of various GAGs on growth factor signaling. The Nara bladder tumor No. 2 (NBT-II) cell line, previously demonstrated to respond to various FGFs and to express FGFR2b, necessary for FGF7-mediated proliferation [36, 348, 354], was used. Dose response curves revealed that FGF7 elicits its maximal effect on cell growth in NBT-II cells at 5 ng/ml. The magnitude of this effect remains constant through 100 ng/ml. The maximal proliferative effect, however, was not achieved until 10 ng/ml in the presence of 50 mM sodium chlorate.

Each of heparin, HS, CS A, CS C, unfractionated DS (UDS), and DS DT were added at various concentrations to NBT-II cells, along with 10 ng/ml FGF7. The addition of GAG alone had no effect on whole cell proliferation. In the presence of FGF7, GAGs showed differential capacities to modulate the FGF7-mediated response (**Figure 6.1**), both in the presence and absence of sodium chloride. Heparin and DS DT were the most potent and efficacious of the GAGs, promoting $51.2 \pm 3.0\%$ and $40.2 \pm 4.5\%$ reductions in whole cell number respectively, and $165.6 \pm 21.6\%$ and $145.8 \pm 14.9\%$ increases in whole cell number respectively in the presence of chlorate. FGF7 alone induced a $14.1 \pm 2.5\%$ reduction and $28.4 \pm 11.8\%$ increase in whole cell number untreated with and treated with sodium chloride respectively.

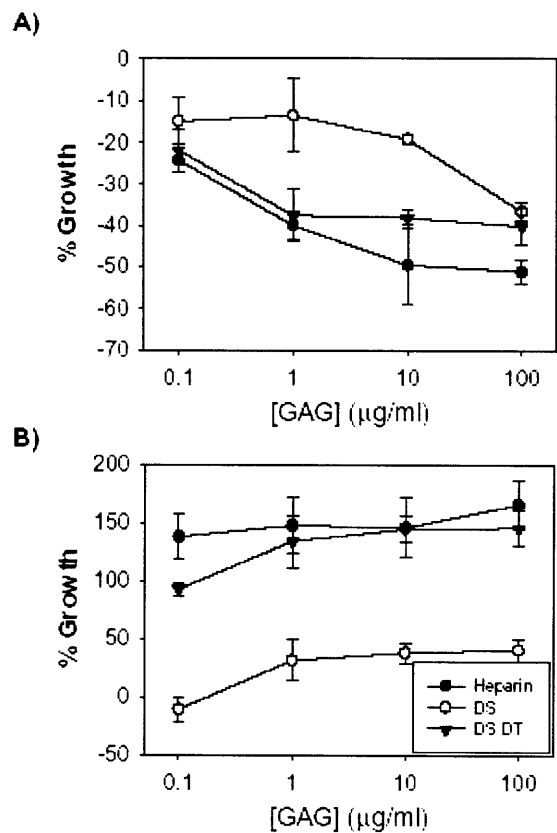


Figure 6.1. GAGs differentially promote FGF7-mediated effects. NBT-II cells were treated with FGF7 supplemented with GAGs. A) The inhibitory effect was measured by reduction in whole cell number relative to untreated cells. B) Cells were treated with sodium chlorate. The proliferative effect was measured by increase in whole cell number compared to cells treated with sodium chloride only.

6.2.2 Heparin and DS DT modulate FGF1-, FGF2-, and VEGF-mediated effects

We next examined the modulatory capacity of GAGs on other growth factors. NBT-II cells have been previously demonstrated to support FGF1, FGF2, and VEGF signaling [36]. RT-PCR was performed to verify that NBT-II cells expressed receptors to support the responses of these ligands. Cells clearly expressed FGFR2b, FGFR3b, FGFR4, and VEGFR3 (**Figure 6.2A**). Lower levels of VEGFR2 were observed. FGF2 and VEGF reduced whole cell number (**Table 6.1**), while FGF1 did not induce significant proliferative effects in the absence of GAGs.

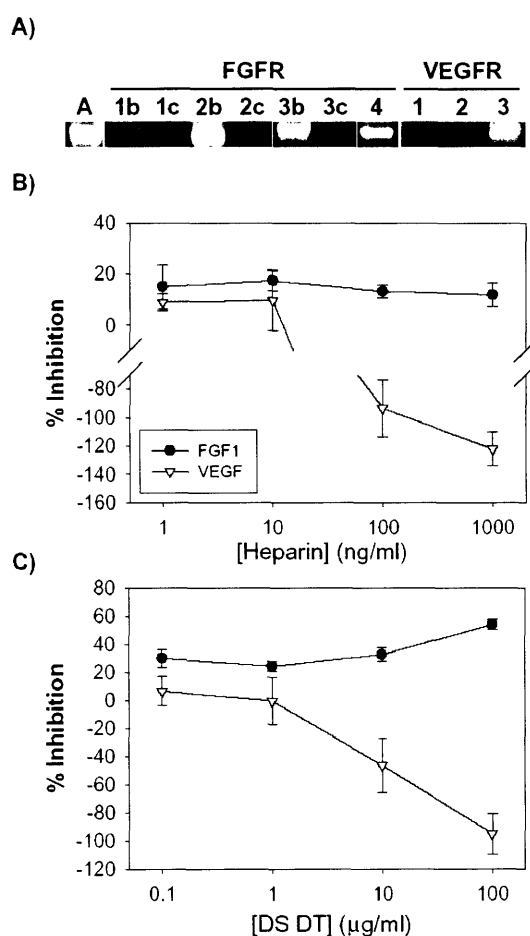


Figure 6.2. GAGs modulate FGFs and VEGFs. A) RT-PCR of NBT-II cells for Act (A), FGFR isoforms 1b, 1c, 2b, 2c, 3b, 3c, and 4, and VEGFR isoforms 1, 2, and 3. B) NBT-II cells were treated with 10 ng/ml FGF1 or VEGF with varying concentrations of heparin. Data is presented as percent inhibition of cell growth compared to ligand alone. C) NBT-II cells were treated with 10 ng/ml FGF1 or VEGF with varying concentrations of DS DT. Data is presented as percent inhibition of cell growth compared to ligand alone.

GAGs modulated the effects of each of the ligands examined. Heparin (**Figure 6.2B**) and DS DT (**Figure 6.2C**), however, had the most striking effects. Heparin only slightly augmented FGF1- and FGF2-mediated responses, leading to $11.9 \pm 4.7\%$ and $7.1 \pm 4.9\%$ reductions in whole cell number at the highest concentration examined relative to FGF1 and FGF2 respectively. The addition of DS DT, however, additionally reduced whole cell number $54.0 \pm 11.7\%$ relative to FGF1, but only $12.2 \pm 6.0\%$ relative to FGF2. While VEGF alone lead to a reduction in whole cell number, the addition of either heparin or DS DT yielded substantial *increases* in whole cell number of $122.3 \pm 12.1\%$ and $95.1 \pm 14.1\%$ respectively. Since VEGF induces responses through VEGFR1 and VEGFR2, but not VEGFR3 [120, 249], and the cells expressed VEGFR2 and VEGFR3, we next confirmed that the VEGF mediated effects observed were dependent on VEGFR2. Co-administration of neutralizing anti-VEGFR2 antibodies prevents both the inhibitory effect of VEGF alone and the proliferative capacity of VEGF supplemented by heparin or DS DT ($p > 0.05$).

	PBS	FGF7
PBS	0.0 ± 5.6	14.1 ± 2.5
FGF1	5.4 ± 8.3	18.0 ± 2.6
FGF2	18.3 ± 5.0	30.4 ± 8.7
VEGF	19.8 ± 4.5	30.1 ± 7.0

Table 6.1. Inhibitory effects of growth factors. Column and row heading represent the addition of ligand (at 10 ng/ml) or PBS. Numbers represent percent reduction in whole cell number \pm standard deviation.

6.2.3 Heparin and DS DT differentially regulate growth factor function

The most pronounced growth modulatory effects induced by GAGs were exhibited with FGF7 and VEGF. We next explored the cellular response with the co-administration of multiple ligands. The addition of FGF7 with FGF1, FGF2, or VEGF reduced whole cell number in an additive manner (**Table 6.1**). The addition of GAGs, however, substantially changed the observed response. Heparin with FGF1+FGF7 reduced whole cell number by $25.9 \pm 0.6\%$ compared to the ligands only (**Figure 6.3A**). Heparin did not alter the effects of FGF2+FGF7. Heparin with VEGF+FGF7 increased whole cell number $29.5 \pm 7.1\%$ compared to only ligands. The addition of UDS (**Figure 6.3B**) led to a greater reduction in whole cell number for FGF1+FGF7, but did not have effects distinct from heparin, for either FGF2+FGF7 or VEGF+FGF7. DS DT (**Figure 6.3C**) had a similar effect as UDS on FGF1+FGF7, reducing

whole cell number $57.2 \pm 3.0\%$ relative to the ligand combination, but showed a unique response with VEGF+FGF7, reducing whole cell number $26.5 \pm 10.0\%$ compared to the ligand combination. Heparin and DS DT at $1 \mu\text{g/ml}$ therefore show unique capacities to regulate VEGF+FGF7 (**Figure 6.3D**), with heparin promoting proliferation and DS DT inhibiting it.

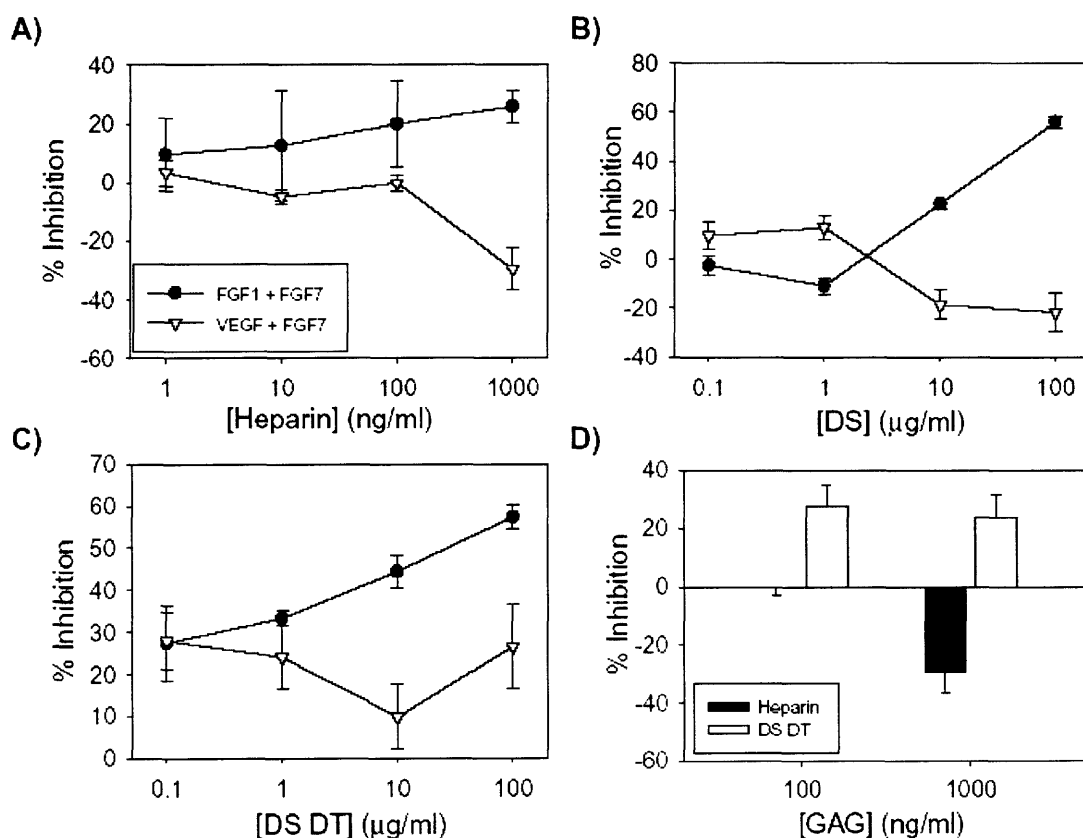


Figure 6.3. Heparin and DS DT differentially impact the co-administration of FGF7 and VEGF. NBT-II cells were treated with 10 ng/ml of one of FGF1 or VEGF, as well as 10 ng/ml FGF7. Cells were additionally treated with A) heparin, B) UDS, or C) DS DT over a range of concentrations. The effect of GAG addition was normalized to the effect of the ligand pair alone. The legend in A applies to A-C. D) Cells were treated with VEGF and FGF7 and supplemented with either heparin or DS DT. The proliferative effect was normalized to the effect of VEGF and FGF7 unsupplemented by GAGs.

6.2.4 FGF7 and VEGF utilize different signaling cascades

Heparin and DS DT both inhibit proliferation in the presence of FGF7, and support proliferation in the presence of VEGF. In the presence of both ligands, the two GAGs unveil distinct effects. We therefore examined the signal cascades activated by the ligands supplemented with PBS, heparin, and DS DT. VEGF increased phosphorylated Erk1/2 and

Mek1/2 when treated with heparin or DS DT (**Figure 6.4**). No changes in Erk1, Erk2, Mek1, or Mek2 levels were observed for with any ligand-GAG combination tested. Erk1/2 phosphorylation was increased 1.65 ± 0.02 -fold with heparin ($p < 0.0004$) and 2.01 ± 0.36 -fold with DS DT ($p < 0.02$). Mek1/2 phosphorylation was increased 1.92 ± 0.21 -fold with heparin ($p < 0.002$) and 2.47 ± 0.25 -fold with DS DT ($p < 0.0004$). When FGF7 was present along with VEGF and heparin or DS DT, however, the increase in Erk1/2 and Mek1/2 phosphorylation was abrogated.

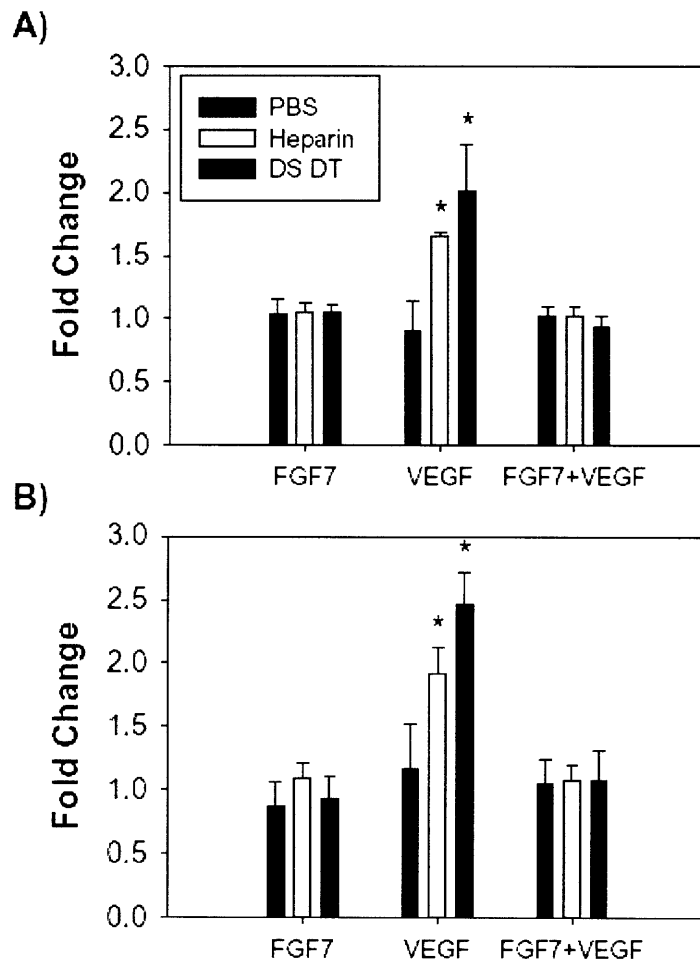


Figure 6.4. VEGF induces proliferation through Erk and Mek. NBT-II cells were treated with FGF7, VEGF, or FGF7 and VEGF in the presence of PBS, heparin or DS DT. ELISAs were performed for A) phospho-Erk1/2, and B) phospho-Mek1/2. The change in response was determined in terms of its relative level compared to untreated cells. * denotes $p < 0.05$ compared to untreated cells.

While changes in Erk1/2 and Mek1/2 phosphorylation were consistent with cellular responses to VEGF in the presence of heparin or DS DT, they did not reflect the changes induced by FGF7, unsupplemented VEGF, or by VEGF+FGF7. To this end, induction of Akt1/2/3 phosphorylation was examined. Levels of Akt1/2 were not affected by any ligand-GAG combination. FGF7 in the presence of either heparin ($27.8 \pm 3.8\%$; $p < 0.005$) or DS DT ($27.4 \pm 4.6\%$; $p < 0.004$) reduced phosphorylation of Akt1/2/3 (Ser 473; **Figure 6.5A**). FGF7 and VEGF+FGF7 also reduced phosphorylation of Akt1/2/3 (Thr 308; **Figure 6.5B**) ~20% in the presence of PBS, heparin or DS DT.

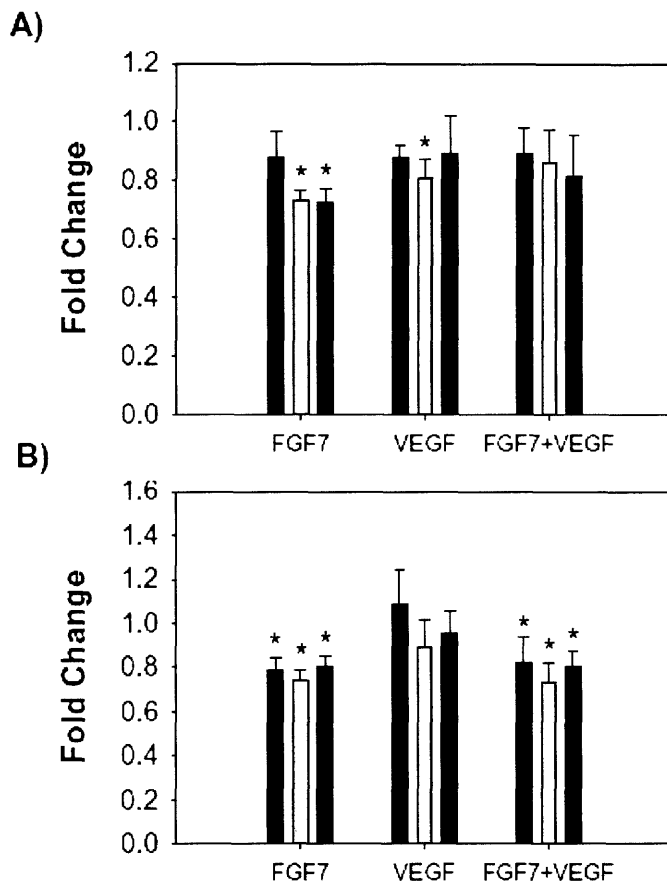


Figure 6.5. FGF7 affects proliferation through Akt. NBT-II cells were treated with FGF7, VEGF, or FGF7 and VEGF in the presence of PBS, heparin or DS DT. ELISAs were performed for A) phospho-Akt1/2/3 (Ser 473), or B) phospho-Akt1/2/3 (Thr 308). The change in response was determined in terms of its relative level compared to untreated cells. * denotes $p < 0.05$ compared to untreated cells.

6.2.5 Upregulated VEGF-D is responsible for the distinct modulatory capacities of heparin and DS DT

The changes in Erk1/2, Mek1/2, and Akt1/2/3 phosphorylation were consistent with the effects of FGF7 or VEGF in the presence of PBS, heparin, or DS DT as observed by whole cell counts. The results, however, were not sufficient to explain the effects observed with FGF7 and VEGF together. We next sought to define which receptors were responsible for the differential effects of heparin and DS DT on FGF7+VEGF. Blocking VEGFR2 with a neutralizing antibody produced a VEGF+FGF7 response similar to FGF7, consistent with the VEGF response being dependent on VEGFR2. Correspondingly, blocking FGFR2, through which FGF7 signals [348], produced a VEGF+FGF7 response similar to VEGF alone. Blocking VEGFR3 did not alter either FGF7- or VEGF-mediated responses, but surprisingly eliminated the capacity of heparin and DS DT to modulate the effects of the ligands when co-administered.

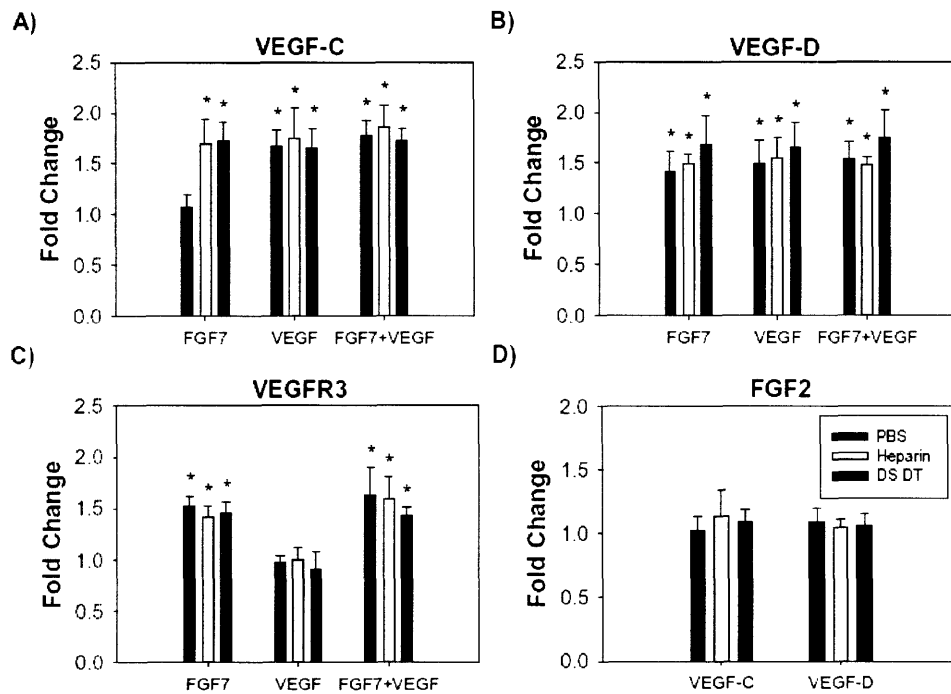


Figure 6.6. FGF7 and VEGF upregulate VEGF-C and VEGF-D. NBT-II cells were treated with (A-C) FGF7, VEGF, FGF7 and VEGF or D) FGF2 in the presence of PBS, heparin or DS DT. ELISAs were performed after 24 hours for A) VEGF-C, B) VEGF-D, or C) VEGFR3, or D) both VEGF-C and VEGF-D. The change in response was determined in terms of its relative level compared to untreated cells. * denotes $p < 0.05$ compared to untreated cells.

VEGFR3 supports signaling from VEGF-C and VEGF-D [249]. Therefore, we next investigated the potential source of VEGF-C and/or VEGF-D. The ability of FGF7 and VEGF in the presence of GAGs to increase levels of VEGF-C and VEGF-D was examined over 24-hours. VEGF-C levels were increased by VEGF regardless of GAG used, FGF7 in the presence of heparin or DS DT, and VEGF+FGF7 regardless of the GAG used (**Figure 6.6A**). VEGF-D levels were elevated by all combinations of FGF7, VEGF, and GAG (**Figure 6.6B**). Interestingly, addition of FGF7, but not VEGF, caused an increase in VEGFR3 production (**Figure 6.6C**). FGF2 did not alter the production of VEGF-C or VEGF-D (**Figure 6.6D**), suggesting that the effect is ligand specific.

The capacity of VEGF-C and VEGF-D to promote NBT-II proliferation was subsequently investigated. VEGF alone reduced cell number $19.8 \pm 4.5\%$, and $30.1 \pm 7.0\%$ in the presence of FGF7. VEGF-C alone similarly reduced cell number $13.4 \pm 8.7\%$ ($p < 0.05$ compared to untreated cells), but only $5.9 \pm 5.0\%$ in the presence of FGF7 ($p > 0.18$ compared to untreated cells). VEGF-D alone reduced cell number $16.2 \pm 10.8\%$ ($p < 0.05$ compared to untreated cells), and $34.5 \pm 1.5\%$ in the presence of FGF7 ($p < 0.0004$ compared to untreated cells). We then explored whether heparin and DS DT could modulate VEGF-C and VEGF-D signaling alone and in the presence of FGF7. The addition of heparin and DS DT with VEGF-C or VEGF-D reduced whole cell number more than either ligand alone (**Figure 6.7A**). The capacity of heparin and DS DT to modulate VEGFs+FGF7 was subsequently examined. Heparin promoted a similar

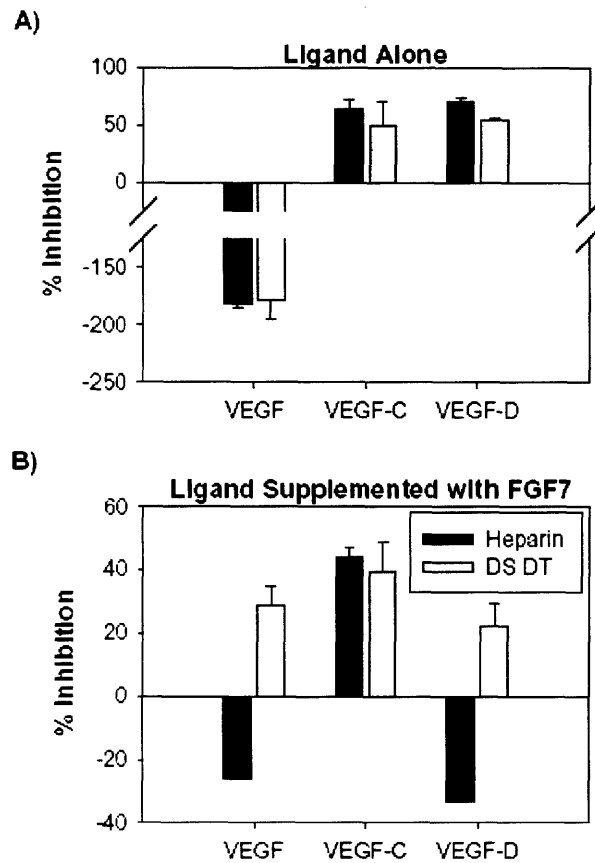


Figure 6.7. Heparin and UDS differentially regulate VEGF-D. NBT-II cells were treated with VEGF, VEGF-C, and VEGF-D either A) alone or B) with FGF7. Ligands were supplemented with heparin or DS DT. The proliferative effect was determined by whole cell count. Data was converted to the percent inhibition in total cell number compared to untreated cells.

increase in whole cell number for VEGF+FGF7 and VEGF-D+FGF7 relative to ligands only (**Figure 6.7B**). DS DT also promoted a similar reduction in whole cell number for both VEGF+FGF7 and VEGF-D+FGF7 relative to ligands only.

6.2.6 Oversulfated DS species promote greater cellular mediated responses

The ability of the oversulfated DS DT to selectively induce an FGF7-like response when mixed with other growth factors led us to examine the effects of chemically oversulfated GAGs on FGF7 activity. CS D, CS E, chemically oversulfated DS DT (diDS), and doubly chemically oversulfated DS DT (ddDS), are CS and DS species with increased degrees of sulfation compared to other similar GAGs examined [45, 226]. The ability of these species to alter FGF7 cellular mediated responses was examined in comparison to DS DT. When normalized to the effects of FGF7, 100 µg/ml DS DT reduced whole cell number $22.7 \pm 3.6\%$ (**Figure 6.8**). CS D elicited a smaller magnitude of response at 100 µg/ml ($15.0 \pm 5.4\%$ $p < 0.03$), but showed no difference at any other concentration examined. The effects of CS E were not significantly different than DS DT at any concentration. The similarities between the effects induced by oversulfated CS species and DS DT are notable as while CS A and CS C

did not support FGF7-mediated effects as efficaciously as DS DT, the CS species with increased sulfated induced a greater magnitude of response. Similarly, in the presence of FGF7, diDS reduced whole cell number greater than DS DT at 100 ng/ml ($p < 0.03$), 1 µg/ml ($p < 0.008$),

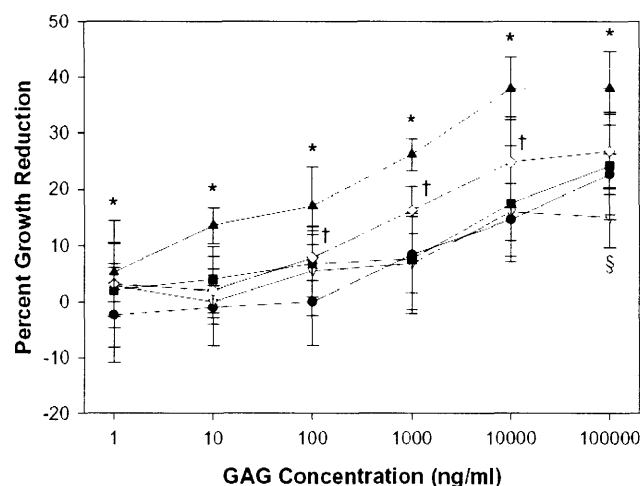


Figure 6.8. Chemical oversulfation of DS DT increases FGF7 activity. NBT-II cells were treated with 10 ng/ml FGF7 supplemented with PBS or GAGs at concentrations ranging between 1 and 100,000 ng/ml. The reduction in whole cell number observed in the presence of GAGs and FGF7 was normalized to that observed with FGF7 alone. * denotes $p < 0.05$ for ddDS compared to DS DT at the same concentration. † denotes $p < 0.05$ for diDS compared to DS DT at the same concentration. § denotes $p < 0.05$ for CS D compared to DS DT at the same concentration. GAGs did not otherwise elicit a significantly different effect than DS DT at the same concentration.

and 10 $\mu\text{g/ml}$ ($p < 0.03$), but the difference was absent at 100 $\mu\text{g/ml}$. 10 $\mu\text{g/ml}$ diDS had a similar effect ($24.8 \pm 8.0\%$), however, to 100 $\mu\text{g/ml}$ DS DT, demonstrating an increase in potency. The addition of a DS species with even higher sulfation, ddDS produced a response that was significantly greater than the elicited with DS DT at each and every concentration examined ($p < 0.03$).

6.3 Discussion

DS and heparin, but not CS, have been previously demonstrated to modulate FGF7 signaling in cells lacking surface GAGs as well as normal keratinocytes [475]. Herein, we first extended this analysis to pathological cells. NBT-II cells express FGFR2b, the receptor for FGF7 [348], and have cell surface GAGs, as evidenced by the change in cellular response to FGF7 and various GAGs after sodium chlorate treatment, which abrogates cell surface HSPGs [448]. While heparin and DS DT promoted maximal cellular mediated responses, species from each of HSGAGs, CS GAGs, and DS notably regulated FGF7 activity in cancer cells. CS C importantly and specifically supported substantial FGF7-induced responses, albeit to a lower degree than either heparin or DS DT. These results demonstrate that specific CS fractions can therefore support FGF7 activity. The specific role of CS C in promoting FGF7 mediated cell proliferation, however, is not clear. CS has been demonstrated to upregulate FGF7 production [419], which could account for the increased cellular-mediated response observed, although sufficient FGF7 to induce the maximal response in the absence of exogenous GAG was added at the outset of the experiment. As such, this report provides the first evidence of CS C modulating FGF7-mediated responses.

Given that specific fractions of all GAG families examined could promote FGF7 activity, this analysis was extended to other FGFs and the VEGF family. FGF1 and FGF2 were chosen based on the FGFR isoform expression profile of NBT-II cells, as well as their previously demonstrated role in defining NBT-II growth and progression [36]. VEGF was used given its important role in bladder cancer growth [506]. Heparin and DS DT, which promoted equivalent FGF7-mediated activities that were greater than all other GAGs examined, modulated each of FGF1, FGF2, FGF7, and VEGF cellular mediated responses. The strong regulatory capacity

observed with DS DT demonstrates that DS species can in fact impact members of the FGF family, such as FGF1. Additionally, DS can regulate the activity of VEGF, whose interactions with DS had previously not been examined. DS may also regulate FGF2 activity through FGFR3c and/or FGFR4, in addition to FGFR1c, the isoform previously associated with DS-FGF2 interactions [366] given the observed response in cells lacking FGFR1c.

Heparin and DS DT modulated VEGF-induced responses to promote substantial proliferation while VEGF alone led to growth inhibition. This finding was unique to VEGF, as the addition of exogenous GAGs enhanced the inhibitory capacity of the FGFs examined. VEGF in the presence of GAGs promoted Erk1/2 and Mek1/2 phosphorylation, unlike VEGF alone or FGF7, consistent with the observed proliferative effects [453]. Heparin is essential for the activity of certain VEGF isoforms to promote cellular responses [113]. The growth inhibitory effects of FGF7 and VEGF, however, appear to be Akt-mediated. In addition to merely modulating ligand activity, heparin and DS DT elicit distinct patterns of cellular response from multiple ligands. Heparin with VEGF+FGF7 had a proliferative response while DS DT with VEGF+FGF7 had an inhibitory one. The unique patterns of response suggest that these two GAGs can be used to initiate specific cellular responses in a complex mix of growth factors, such as that which exists in the ECM. Altering the GAG composition of the ECM may therefore be a mechanism that cells use to change biological activities in response to various environmental cues.

The cellular pathways by which heparin and DS DT elicit distinct cellular responses are important in order to understand their effects. The cellular activities of VEGF are altered in the presence of FGF7. Unlike VEGF supplemented with GAG, Erk1/2 and Mek1/2 were not phosphorylated in response to VEGF+FGF7. Further, VEGF signaled through VEGFR2, with neutralizing antibodies eliminating its effect. Though the combined VEGF+FGF7 response was dependent on VEGFR3, suggesting the involvement of VEGF-C and/or VEGF-D [249]. Each of FGF7, VEGF, and VEGF+FGF7 promoted VEGF-C and VEGF-D activity in the presence of GAGs. The cellular response to VEGF-D was additionally modulated by heparin and DS DT in the same manner as VEGF+FGF7. Therefore, the differential regulation of VEGF+FGF7 by heparin and DS DT is based on the upregulation of VEGF-D production and subsequent modulation of its activity, mediated by VEGFR3.

The distinct cellular responses obtained with heparin and DS DT stem primarily from differential regulation of VEGF-D. Heparin and DS DT affect VEGF-mediated cellular activity in a similar manner. Their relative regulatory capacities are, however, distinct between various VEGFs. Various GAGs may therefore be important physiological and pathological regulators of VEGF.

The results presented herein demonstrate that specific GAG fractions beyond heparin can serve a regulatory role for several growth factors. The highly sulfated heparin modulated the response to all growth factors examined. The highly sulfated dermatan sulfate fraction DS DT elicited a similar yet novel ability to affect the growth factors examined with comparable magnitudes but a distinct net effect from heparin. CS additionally promoted FGF7 activity. Interestingly, increasing the sulfation of CS and DS species supported higher levels of FGF7 activity than corresponding GAGs with lower degrees of sulfation. These findings demonstrate that the ability of GAGs to regulate FGFs, VEGFs, and mixtures of growth factors, extend well beyond those of HSGAGs. As heparin and DS can promote selective cellular activities in a mixture of growth factors, the development of chemically oversulfated species such as ddDS may further enable controlled growth factor activity and specification of cellular behavior. The selectivity of highly sulfated DS species for FGF7 activity and the increased magnitude of response elicited by ddDS suggests that it may be an important new therapeutic for wound healing especially in the complex environment created by the physiological response to insult. Identification of highly active GAG fractions for specific growth factors as well as further understanding the specific interactions of GAG-growth factor sets may prove highly informative in understanding and developing methods to regulate processes such as wound healing and cancer growth.

6.4 Significance

The ability of HSGAGs to regulate cellular response to FGFs and VEGFs has been extensively studied. Recent evidence, however, has demonstrated that other GAGs may also bind to specific FGFs and influence the downstream response. Specifically, UDS has been found to modulate FGF2 and FGF7 activity. This study set out to explore the ability of various GAGs to influence

the cellular response to FGFs and VEGFs. DS DT and heparin supported FGF7 activity more than other GAGs. DS DT and heparin were subsequently found to influence the cellular response to each of FGF1, FGF2, and VEGF, demonstrating that UDS species can regulate each of these ligands. After demonstrating that DS DT and heparin could regulate the activities of several growth factors, the ability of these GAGs to affect multiple growth factors in the same environment was explored. Although DS DT and heparin similarly influence cellular response to FGF7 and to VEGF, these two GAGs differentially define the cellular response to a combination of FGF7 and VEGF. The mechanism by which this effect occurred was next explored, and found to stem from a uniform upregulation of VEGF-D, whose activity through VEGFR3 was itself differentially regulated by heparin and DS DT. Furthermore, chemically oversulfated GAGs can increase the FGF7-mediated response. These results demonstrate that the presence of specific GAGs can define the net cellular outcome in a pool of growth factors. GAGs can be additionally developed to favor specific responses, which may be of importance in physiological and pathological settings with an abundance of growth factor families, including wound healing and cancer progression.

6.5 Experimental Procedures

Proteins and reagents. FBS was from Hyclone (Logan, UT). L-glutamine, penicillin/streptomycin, PBS, and Trizol reagent were from GibcoBRL (Gaithersburg, MD). Unfractionated heparin, HS, UDS, and DS DT were from Celsus Laboratories (Cincinnati, OH). diDS, and ddDS were produced as described [45, 226]. CS A and CS C were from Sigma (St. Louis, MO). CS D and CS E were from Celsus laboratories. Recombinant FGF1 was a gift from Amgen (Thousand Oaks, CA). Recombinant human FGF2 was a gift from Scios (Mountainview, CA). Recombinant FGF7 and VEGF₁₆₄ were from Sigma. Rabbit α -Akt1/2, rabbit α -phospho-Akt1/2/3 (Ser 473), rabbit α -phospho-Akt1/2/3 (Thr 308), rabbit α -VEGF, rabbit α -VEGF-C, rabbit α -VEGF-D, goat α -VEGFR2/Flk-1, rabbit α -VEGFR3/Flt-4, rabbit α -Erk1, rabbit α -Erk2, goat α -phospho-Erk1/2 (Thr 202/Tyr 204), rabbit α -Mek1, rabbit α -Mek2, goat α -phospho-Mek1/2 (Ser 218/Ser 222), rabbit α -goat conjugated to horseradish peroxidase

(HRP), and goat α -rabbit conjugated to HRP were from Santa Cruz Biotechnology (Santa Cruz, CA).

Cell culture. NBT-II cells (American Type Culture Collection, Manassas, VA) were maintained in minimum essential medium (American Type Culture Collection) supplemented with 1.5 mg/mL sodium bicarbonate, 0.1 mM non-essential amino acids, 1.0 mM sodium pyruvate, 100 μ g/ml penicillin, 100 U/ml streptomycin, 500 μ g/ml L-glutamine and 10% FBS. Cells were grown in 75 cm² flasks at 37°C in a 5% CO₂ humidified incubator. Confluent cultures were split 1:5 to 1:10, two times per week.

Proliferation assays. NBT-II cells were grown until confluence in 75 cm² flasks. Each flask was washed with 20 ml PBS and treated with 3 ml trypsin-EDTA at 37°C for ~15 minutes until cells completely detached. Cells were centrifuged for 3 minutes at 195 x g. The supernatant was aspirated and the cells were resuspended in 10 ml media. Cell density was measured using an electronic cell counter, and the suspension was diluted to 50,000 cells/ml. The suspension was plated 1 ml/well into 24-well tissue culture plates. After a 24 hour incubation in a 5% CO₂, 37°C humidified incubator, the media was aspirated, the wells were washed with serum free media, and the cells were supplemented with media containing 0.1% FBS, and incubated for 24 hours. Cells were sequentially treated with antibodies, GAGs, and growth factors as appropriate. Sodium chlorate was added at 50 mM [30]. Antibodies to VEGFR2 or VEGFR3 were added to yield a final dilution of 1:100. All GAGs were initially added to over a range of concentrations from 1 ng/ml to 100 μ g/ml. Heparin, UDS, and DS DT were subsequently added at 1 μ g/ml unless otherwise noted. FGF1, FGF2, FGF7 and VEGF were added at 10 ng/ml unless otherwise noted. Cells were then incubated for 72 hours. Wells were then washed twice with PBS and treated with 0.5 ml trypsin-EDTA/well and incubated for 10 minutes at 37°C. Whole cell number was determined using an electronic cell counter.

RT-PCR. Five μ g of total RNA was isolated from NBT-II cells using Trizol reagent (Life Tech, Rockville, MD) followed by reverse transcription with random hexamers. Specific oligomers were designed based on the published sequences of FGFR isoforms in order to detect their expression. Sequences of primer pairs corresponding to distinct FGFR isoforms were as follows:

FGFR1b: 5'-TGG AGC AAG TGC CTC CTC-3' and 5'-ATA TTA CCA CTT CGA TTG GTC-3'; FGFR1c: 5'-TGG AGC TGG AAG TGC CTC CTC-3' and 5'-GTG ATG GGA GAG TCC GAT AGA-3'; FGFR2b: 5'-GTC AGC TGG GGT CGT TTC ATC-3' and 5'-CTG GTT GGC CTG CCC TAT ATA-3'; FGFR2c: 5'-GTC AGC TGG GGT CGT TTC ATC-3' and 5'-GTG AAA GGA TAT CCC AAT AGA-3'; FGFR3b: 5' GTA GTC CCG GCC TGC GTG CTA-3' and 5'-GAC CGG TTA CAC AGC CTC GCC-3'; FGFR3c: 5'-GTA GTC CCG GCC TGC GTG CTA-3' and 5'-TCC TTG CAC AAT GTC ACC TTT-3'; and FGFR4: 5'-CCC TGC CGG GAT CGT GAC CCG-3' and 5'-TCG AAG CCG CGG CTG CCA AAG-3'. Sequences of primer pairs corresponding to distinct VEGFR isoforms were as follows: VEGFR1: 5'-CGG ACA CTC CCG GGA GGT AGT-3' and 5'-CTT CTG TCG AGT AGG GGA-3'; VEGFR2: 5'-TGC GGG CCA GGG ACG GAG AAG-3' and 5'-CTA GTT ACT ACT TTG GAT AGT-3'; and VEGFR3: 5'-CGG GCG CTG CGC TGA ACC GGC-3' and 5'-TCG ACA TGG GGT TCT TCA GTG-3'. To control for total cell protein, RT-PCR was also performed on β -actin using the primers 5'-GCC AGC TCA CCA TGG ATG ATG ATA T-3' and 5'-GCT TGC TGA TCC ACA TCT GCT GGA A-3'. PCR was performed using the Advantage-GC cDNA kit from Clontech as per manufacturer's instructions (Palo Alto, CA). Prior to experimental use, primers were confirmed to detect and have specificity towards given receptor isoforms.

Whole cell ELISA. ELISA was performed using whole cells to quantify relative levels of kinase activity. NBT-II cells were grown until confluence in 75 cm² flasks. Each flask was washed with 20 ml PBS, and treated with 3 ml trypsin-EDTA at 37°C for 3-5 minutes, until cells detached. Cells were centrifuged for 3 minutes at 195 x g. The supernatant was aspirated, and the cells were resuspended in 10 ml media. The cell density was measured using an electronic cell counter, and the suspension was diluted to 50,000 cells/ml. 100 mm dishes were supplemented with 10 ml cell suspension per dish. After a 24 hour incubation, the media was aspirated, the dishes washed with serum free media, and the cells supplemented with media containing 0.1% FBS. After a 24 hour incubation, dishes were treated with PBS, 10 μ g/ml heparin, or 10 μ g/ml DS DT. Subsequently, cells were treated with 10 ng/ml FGF7, 10 ng/ml VEGF, or both. Cells were incubated for 30 minutes (for Erk1, Erk2, phospho-Erk1/2, Mek1, Mek2, phospho-Mek1/2, Akt1/2, and phospho-Akt1/2/3) or 24 hours (for VEGF, VEGF-C, and VEGF-D). Media was aspirated and cells were homogenized per manufacture instructions.

Total protein concentration was determined by Bradford assay. An equivalent protein concentration from cell extract was added to 96-well plates previously incubated for 1 hour with primary antibodies to Erk1, Erk2, phospho-Erk1/2, Mek1, Mek2, phospho-Mek1/2, Akt1/2, phospho-Akt1/2, VEGF, VEGF-C, or VEGF-D. The cell extract was incubated on the plates for 1 hour, after which, wells were washed twice, and supplemented with the same primary antibody (1:100) as was in the well. Wells were incubated 1 hour, washed twice, and treated with HRP-conjugated secondary antibody (1:500). Plates were incubated for 30 minutes, washed twice, and incubated in with TMB One Solution (Promega, Madison, WI). The reaction was quenched with 3 M sulfuric acid, and the plates were analyzed using a UV plate reader at 450 nm. Data was quantified by comparing to a standardized curve with varying concentrations of protein from untreated cells.

Chapter 7. FGF1 is essential for FGF2 and FGF7 regulation of epithelial monolayer integrity

7.0 Summary

Members of the FGF family have a protective effect in the colonic epithelium, but can serve to support angiogenesis and promote bowel wall thickening in inflammatory bowel disease (IBD). While FGFs have been demonstrated to reduce inflammation in cellular and animal models of IBD, this success has not been recapitulated in humans. Using FGF2 and FGF7 as model FGFs because of their established role in IBD, as well as the wealth of biochemical information available for these ligands, we explored how FGFs exert their effects on the colonic epithelium. Caco-2 and T84 cells predominantly expressed FGFR3b, through which FGF1, but neither FGF2 nor FGF7, can induce a cellular response. FGF2 and FGF7, however, induced cellular responses that were dependent on FGFR3b and its downstream signaling. The activities of FGF2 and FGF7 were associated with increases in paracellular flux and alterations in the distribution of the tight junction proteins occludin and zona occludens-1 (ZO-1). FGF1, secreted by both Caco-2 and T84 cells, was necessary for FGF2 and FGF7 activity. The ability of FGF2 and FGF7 to induce cellular response may be enabled by FGF1 signaling through FGFR3b, facilitating syndecan clustering by FGF2 and FGF7. FGF1 may serve an essential role in regulating FGF2 and FGF7 in the colon. FGF1 expression by colonic epithelial cells would enable FGF2 and FGF7 to promote epithelial maintenance and repair, while its downregulation could lead to the angiogenesis and bowel wall thickening associated with FGF activity within the lamina propria in IBD.

7.1 Introduction

The FGF family consists of at least 23 members, all of which bind to the HSGAG component of HSPGs and to at least one of five high affinity cell surface FGFRs [153, 178, 396, 445]. While FGFs are best known for their role in angiogenesis [310], FGF2, FGF7, FGF10, and FGF20, have each been implicated as having a potential role in regulating the severity and progression of IBD [49, 68, 169, 205]. Angiogenic factors including FGFs and vascular endothelial growth factor not only determine the susceptibility of the IBD colonic mucosa to injury but also increase blood vessel formation and bowel wall thickening [25, 91, 216].

FGFs are released by colonic intraepithelial $\gamma\delta$ T cells as well as by fibroblasts and smooth muscle cells of the lamina propria to maintain and repair the colonic epithelium [68, 126, 342]. In addition to their angiogenic functions, FGFs stimulate the proliferation and migration of intestinal epithelial cells, important for wound healing [132, 187, 459]. FGF2 and FGF7 specifically promote intestinal epithelial cell growth and wound healing [93]. FGF2 can accelerate gastrointestinal wound healing and resist insults that lead to colonic inflammation [132, 459]. FGF7 is found in the colonic mucosa of IBD patients and reduces the inflammatory response [55, 125]. The cellular mediated effects of these ligands, however, have been associated with FGFR3b, in cells such as Caco-2 cells [215]. FGF1 and FGF9 bind and promotes a downstream response through FGFR3b [66]. FGF2 promotes cellular responses through FGFR1c, FGFR3c, and FGFR4, while FGF7 exclusively requires FGFR2b [348]. The mechanism by which FGF2 and FGF7 produce their effects in the colon, however, is not clear.

Although various FGF family members reduce the severity of colitis and promoted healing in IBD both *in vitro* and *in vivo* [300, 525], little therapeutic benefit has been observed in human studies [415]. Understanding the cellular mechanism by which FGFs can induce their protective and therapeutic responses in the colon can shed insight into their role in epithelial repair as well as in bowel wall thickening. Furthermore, mechanisms elucidated in the colon may provide insight into FGF activity in other physiological or pathological settings. We therefore investigated how FGF2 and FGF7 promote cellular mediated responses in colonic epithelial cell lines. These FGFs were employed as they are better characterized biochemically than other FGFs that have shown a potential therapeutic benefit in IBD [169, 348].

7.2 Results and Discussion

7.2.1 Caco-2 and T84 cells express FGFR3b

In order to explore FGF activity on colonic epithelial cells, we first characterized the FGFR expression profile. RT-PCR was performed for FGFR1b, 1c, 2b, 2c, 3b, 3c, and 4, on Caco-2 cells. The primer pairs used to detect each isoform were demonstrated to specifically detect that FGFR isoform and not show cross-reactivity with other isoforms using BaF3 cells specifically transfected with each FGFR [30, 31]. Both Caco-2 and T84 cells expressed FGFR3b (**Figure 7.1A**). Caco-2 cells also potentially expressed FGFR4, and T84 cells expressed FGFR1c. FGFR4, however, was not expressed by T84 cells and FGFR1c was not expressed by Caco-2 cells. The expression of the FGFR3b protein in both Caco-2 and T84 cells was confirmed by FACS (**Figure 7.1B**), as well as by immunohistochemistry (**Figure 7.1C**). While the percentage of positive cells in FACS analysis did not correlate with the staining pattern observed with immunohistochemistry, this result is likely due to substantial digestion of cell surface proteins with the long incubation in trypsin required to detach the cells from

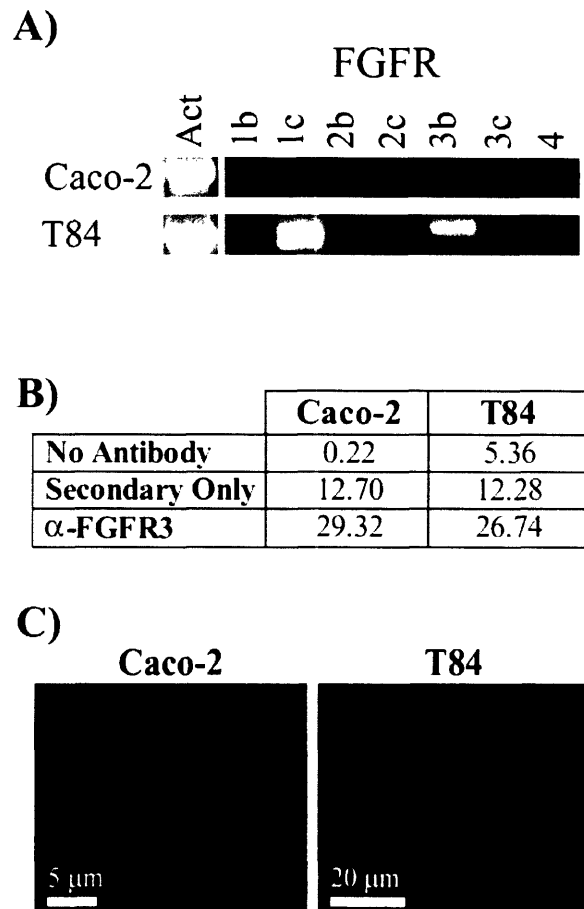


Figure 7.1. Caco-2 and T84 cells express FGFR3b. A) RT-PCR on Caco-2 and T84 cells was performed using primers specific to FGFR isoforms (1b, 1c, 2b, 2c, 3b, 3c, and 4) and to β -actin (Act), the positive control. B) FACS was performed on Caco-2 and T84 cells. Cells were stained using a rabbit anti-human primary antibody to FGFR3, and a goat anti-rabbit antibody conjugated to FITC secondary antibody. Data is presented as the percentage of total cells that exhibited positive expression. C) Immunohistochemistry for FGFR3 was performed on Caco-2 and T84 cells. Cells were stained using a rabbit anti-human FGFR3 primary antibody, and a goat anti-rabbit FITC-conjugated secondary antibody. Scale bars are as indicated.

culture flasks. FGFR3b expression was observed nonetheless using both methods. Additionally, Caco-2 cells have been previously demonstrated to express FGFR3b [215].

7.2.2 FGF2 and FGF7 induce cellular mediated responses in Caco-2 and T84 cells

Both FGF2 and FGF7 promote cellular mediated activity in intestinal epithelial cells, which has been associated with FGFR3b [93, 215]. The effects of FGF2 and FGF7 were investigated on intestinal epithelial cells using transepithelial resistance (TER) alterations as an output. TER is a measure associated in monolayer formation and integrity [98]. Caco-2 and T84 cells form monolayers with epithelial resistance mediated by tight junctions (TJs) [9, 516]. Both FGF2 and FGF7 significantly reduced TER (**Figure 7.2A**). FGF2 inhibited TER increases by $67.2 \pm 25.8\%$ ($p < 0.05$) in Caco-2 cells and by $43.4 \pm 16.6\%$ ($p < 0.04$) in T84 cells. FGF7 inhibited TER increases by $61.4 \pm 17.3\%$ ($p < 0.02$) in Caco-2 cells and by $54.6 \pm 7.6\%$ ($p < 0.02$) in T84 cells. The capacity of FGF2 and FGF7 to induce cellular mediated responses in Caco-2 and T84 cells was confirmed by measuring whole cell proliferation (**Figure 7.2B**). FGF2 increased whole cell number by $20.2 \pm 7.4\%$ ($p < 0.0003$) in Caco-2 cells and by $24.8 \pm 8.8\%$ ($p < 5 \times 10^{-5}$) in T84 cells. FGF7 increased whole cell number by $16.4 \pm 8.9\%$ ($p < 0.003$) in Caco-2 cells and by $11.4 \pm 3.8\%$ ($p < 0.006$) in T84 cells.

The ability of FGF2 and FGF7 to reduce TER was further examined by observing its effects over different time scales. FGF2 and FGF7 reduced TER substantially after 24 hours and 48 hours in both Caco-2 cells (**Figure 7.2C**) and T84 cells (data not shown). With FGF2 and FGF7 were initially and again after 2 days, and with TER measured initially, at day 2, and at day 5, the ability of FGF2 and FGF7 to reduce TER was evident after both day 2 and day 5 in both Caco-2 cells (**Figure 7.2D**) and T84 cells (**Figure 7.2E**). On day 5, FGF2 and FGF7 reduced resistance by $43.6 \pm 11.1\%$ ($p < 0.007$) and $44.4 \pm 8.7\%$ ($p < 0.003$) respectively compared to untreated Caco-2 cells, and $41.7 \pm 8.1\%$ ($p < 0.007$) and $37.3 \pm 3.5\%$ ($p < 0.0002$) respectively compared to untreated T84 cells. The effect of the two ligands was not significantly distinct in either Caco-2 cells ($p > 0.93$) or T84 cells ($p > 0.45$).

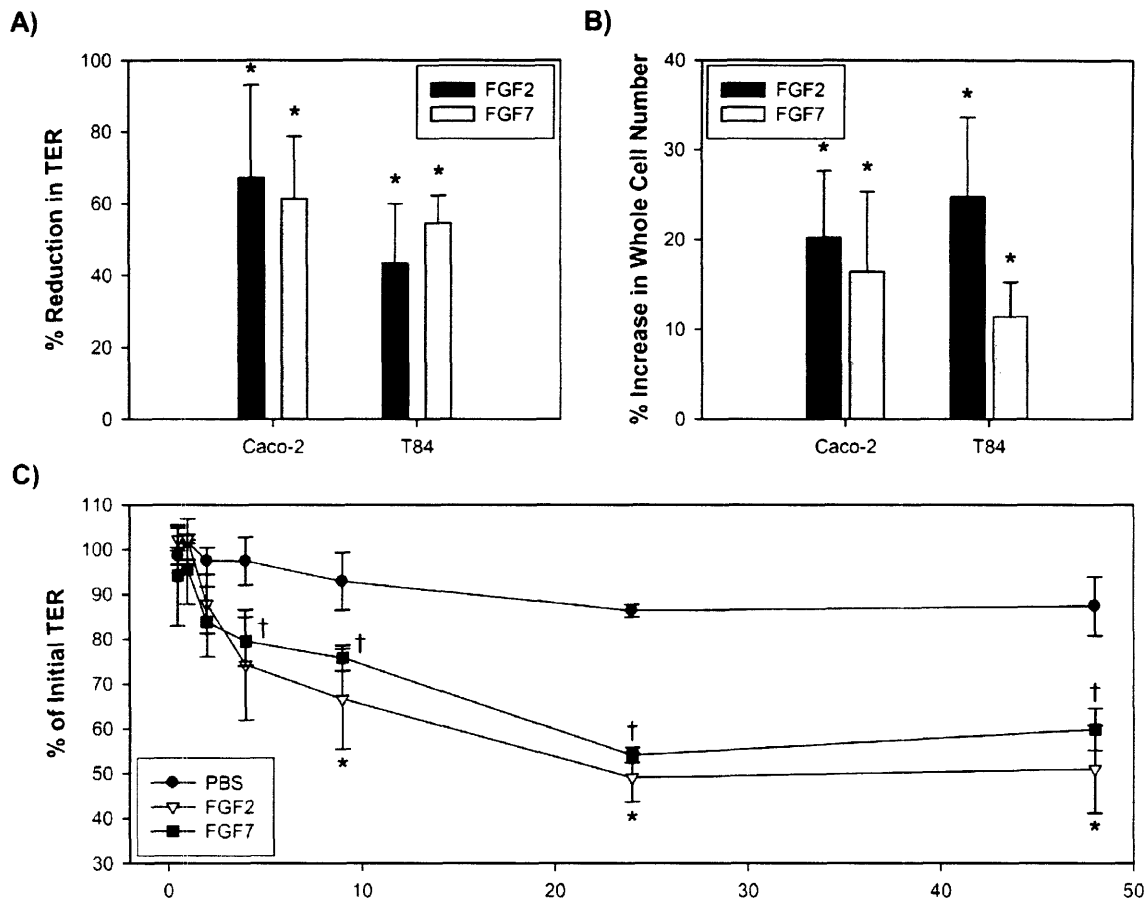


Figure 7.2. FGF2 and FGF7 induce cellular responses in Caco-2 and T84 cells. A) The ability of FGF2 and FGF7 to inhibit TER increases was determined three days after the addition of ligand. Data is presented as the percent reduction in TER compared to PBS treated cells (not shown) over the same time period. * denotes $p < 0.05$ for the experimental point compared to the PBS control. B) Caco-2 and T84 cells were plated at 5×10^4 cells/well. Cells were treated with PBS, FGF2, FGF7, and whole cell number was determined after three days. Data is presented as percent reduction in whole cell number controlled to the PBS control (not shown). * denotes $p < 0.05$ for the experimental point compared to the PBS control. C) Caco-2 monolayers were treated with PBS, FGF2 or FGF7, and the reduction in TER was determined over 48 hours. Data is presented as the percent of initial TER over time. * denotes $p < 0.05$ for FGF2 compared to the PBS control. † denotes $p < 0.05$ for FGF7 compared to the PBS control. D) Caco-2 and E) T84 monolayers were treated with PBS, FGF2 or FGF7 on days 0 and 2, and TER was measured over time. * denotes $p < 0.05$ for FGF2 compared to the PBS control. † denotes $p < 0.05$ for FGF7 compared to the PBS control.

7.2.3 FGF2 and FGF7 promote epithelial monolayer dysfunction

FGF2 and FGF7 promoted both TER inhibition and whole cell proliferation. The reduction in TER could therefore be attributed to increases in paracellular flux. To confirm the observed cellular mediated effects induced by FGF2 and FGF7, paracellular flux was measured

using a 3 kDa dextran conjugated to FITC (**Table 7.1**). FGF2 and FGF7 both significant increased flux in Caco-2 cells compared to PBS treated monolayers ($p < 0.003$). FGF7 increased flux significantly more than FGF2 ($p < 0.04$). Similarly, FGF2 and FGF7 both significant increased flux in T84 cells ($p < 0.03$).

	PBS	FGF2	FGF7
Caco-2	20.28 ± 4.72	47.82 ± 4.64	117.14 ± 25.36
T84	7.99 ± 0.22	37.21 ± 10.25	33.39 ± 9.24

Table 7.1. Flux across Caco-2 and T84 monolayers. Monolayers were grown for 15 days. 100 ng/ml ligand (FGF2 or FGF7) or 10 μ l PBS was added on days 10 and 12. Flux was measured by the passage of 3 kDa-dextran conjugated to FITC on day 15. Data is reported as a function of emission at 530 nm over time, averaged over three experiments.

The increases in paracellular flux after ligand addition are consistent with TER decreases associated with cell separation. To confirm this, immunostaining for occludin (**Figure 7.3**) and ZO-1 (data not shown), which are both components of TJs, was performed. Application of either FGF2 or FGF7 induced ruffling of cell membranes in both Caco-2 and T84 cells, consistent with alterations to TJs.

FGF2 and FGF7 reduce TER, increase paracellular flux, and induce membrane ruffling. These findings are consistent with disruption of cell-cell contacts, reducing the total monolayer resistance and integrity [296]. Cell-cell contacts are mediated through apically located TJs and adjacent adherens junctions (AJs) [117]. Both types of junctions are important in regulating monolayer integrity, paracellular permeability, cell proliferation, and cell differentiation [165, 295, 513]. TJs and AJs can be broken down, internalized, and reorganized in response to extracellular cues including proliferative, inflammatory, and pathological stimuli [165, 171, 337]. The reduction of cell-cell contacts observed in response to FGF2 and FGF7 suggests an alteration in the properties of TJs and AJs. Immunohistochemistry for occludin and ZO-1 confirms that the cellular effects of FGF2 and FG7 involve TJs. TJs, however, can be altered without effects observed in AJs [181]. This study therefore provides the first demonstration that FGF family members can alter TJs. The ability of FGFs to affect TJs is consistent with their capacity to enable proliferation, migration, and cell-cell interactions, all of which are critical not only in maintaining and restoring the colonic epithelium, but also in angiogenesis.

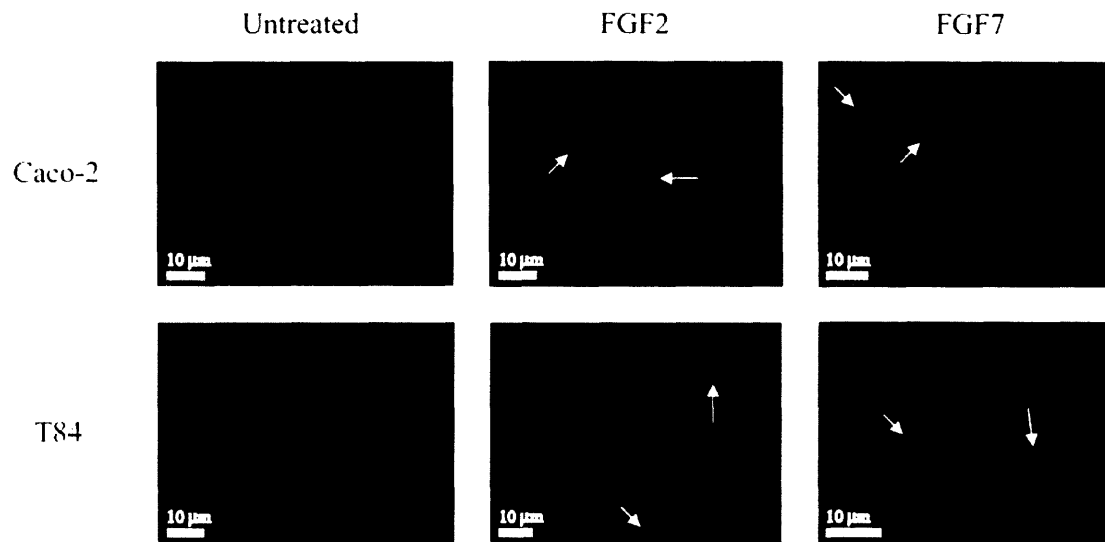


Figure 7.3. FGF2 and FGF7 induce membrane ruffling in Caco-2 and T84 cells. Caco-2 and T84 cells stained for ocludin were visualized by fluorescence microscopy. Scale bars represent 10 μm . Arrows illustrate regions of membrane ruffling.

7.2.4 FGFR3b is necessary for FGF2 and FGF7 to reduce TER

The cellular mediated effects of FGF2 and FGF7 have been associated with FGFR3b [215]. Therefore, we next investigated whether FGFR3b was necessary for FGF2 and FGF7 to reduce TER. Antibodies to FGFR3 prevented both FGF2 and FGF7 from reducing TER in both Caco-2 cells (**Figure 7.4A**) and T84 cells (**Figure 7.4B**). The same antibody was previously confirmed to inhibit responses through FGFR3b in transfected BaF3 cells (data not shown). Antibodies to FGFR1, however, did not prevent FGF2 or FGF7 from reducing TER in either Caco-2 cells (**Figure 7.4C**) or T84 cells (**Figure 7.4D**). The importance of the FGFR3b receptor was further examined using LY294002 to inhibit phosphoinositol 3-kinase (PI3K), which is downstream of FGFRs [309]. Treatment with LY294002 eliminated the ability of FGF2 and FGF7 to reduce TER in Caco-2 cells (**Figure 7.4E**) and T84 cells (**Figure 7.4F**). Inhibition of Mek/Erk with PD98059 and inhibition of p38 with SB203580, failed to eliminate the ligand mediated inhibition of TER (data not shown). Mek/Erk activity is associated with the activities of FGF2 via FGFR1 [21, 31].

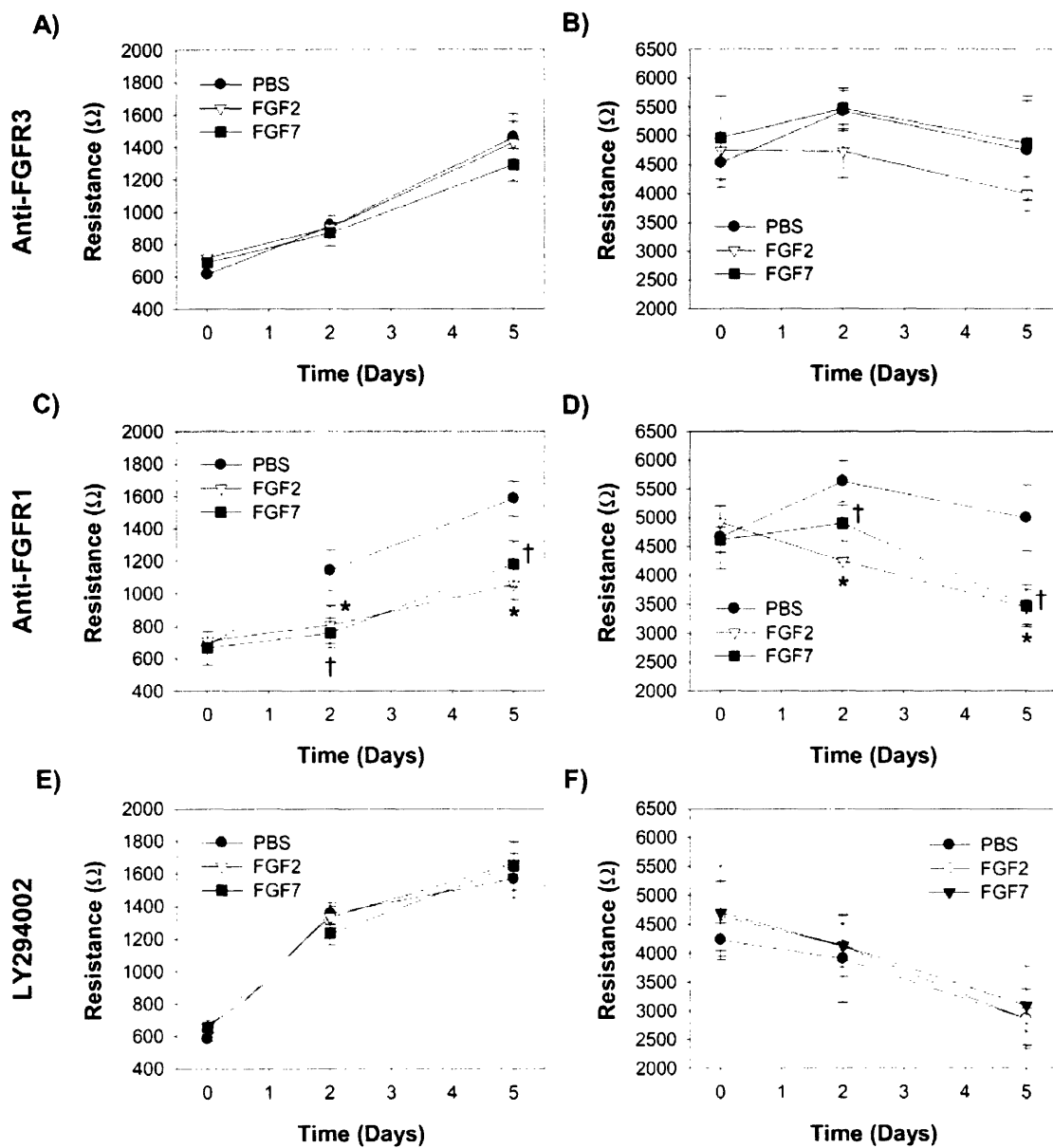


Figure 7.4. FGFR3 is necessary for FGF2 and FGF7 to reduce TER. TER was measured in Caco-2 (A, C, and E) and T84 (B, D, and F) cells after administration of PBS, FGF2, or FGF7 along with anti-FGFR3 antibodies (A and B), anti-FGFR1 antibodies (C and D), or LY294002 (E and F). Data is presented as resistance (in ohms) as measured on day 0 and day 2, and on day 5. Antibodies, kinase inhibitors, FGF2 and FGF7 were added at the same time on both day 0 and day 2. * denotes $p < 0.05$ for FGF2 compared to the PBS control. † denotes $p < 0.05$ for FGF7 compared to the PBS control.

7.2.5 FGF1 reduces TER in Caco-2 and T84 cells

While FGFR3b is necessary for FGF2 and FGF7 to reduce TER, neither FGF2 nor FGF7 supports mitogenesis through this receptor [348]. FGF1, however, can support mitogenesis through FGFR3b [348]. We therefore investigated whether FGF1 could induce a biological response in Caco-2 cells and T84 cells. FGF1 reduced TER in Caco-2 cells (**Figure 7.5A**) and T84 cells over 48 hours similar to FGF2 and FGF7. At 48 hours, FGF1 reduced TER by $45.1 \pm 5.2\%$ ($p < 0.004$) in Caco-2 cells and by $22.7 \pm 3.2\%$ ($p < 0.0008$) in T84 cells. Over three days, FGF1 inhibited increases in TER by $35.1 \pm 12.3\%$ ($p < 0.006$) in Caco-2 cells and by $30.1 \pm 1.5\%$ ($p < 0.0001$) in T84 cells (**Figure 7.5B**). FGF1 also significantly reduced TER after day 0 and day 2 doses on day 5 in both Caco-2 ($p < 0.009$) and T84 cells ($p < 0.006$). Boiled FGF1 did not reduce TER (data not shown). FGF1, however, did not induce the proliferation of either Caco-2 cells ($p > 0.68$) or T84 cells ($p > 0.11$) over three days (**Figure 7.5C**).

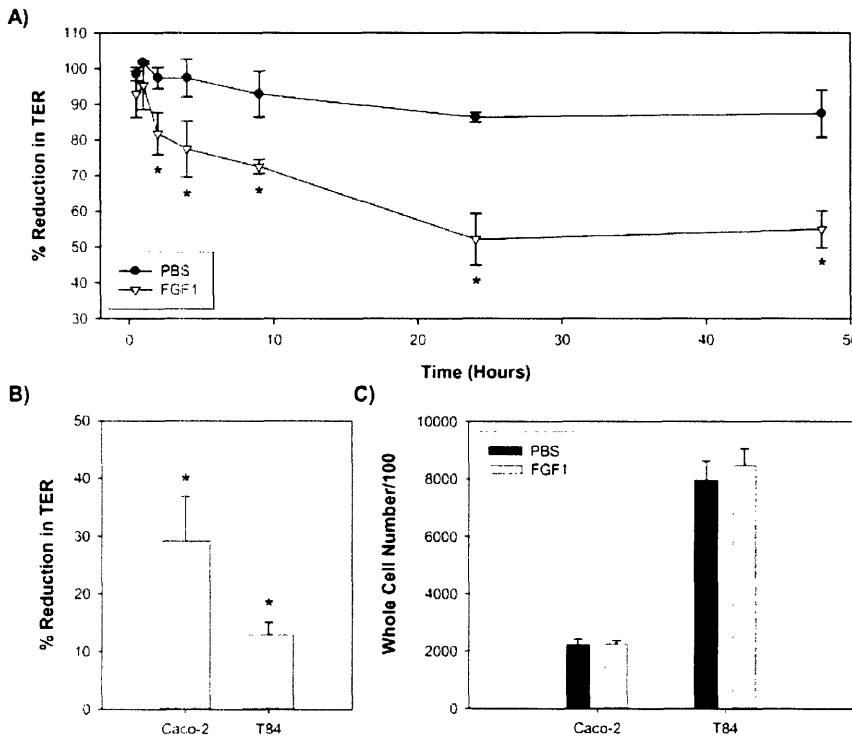


Figure 7.5. FGF1 elicits cellular responses in Caco-2 and T84 cells. A) Caco-2 monolayers were treated with PBS, FGF2 or FGF7, and the reduction in TER was determined over 48 hours. Data is presented as the percent reduction in TER over time. * denotes $p < 0.05$ for FGF1 compared to the PBS control. B) The ability of FGF1 to reduce TER increases was determined 72 hours after the addition of ligand. Data is presented as the percent reduction in TER compared to PBS treated cells over the same time period. * denotes $p < 0.05$ for the experimental point compared to the PBS control. C) Caco-2 and T84 cells were plated at 5×10^4 cells/well. Cells were treated with PBS or FGF1, and whole cell number was determined after three days. Data is presented as whole cell number/100.

7.2.6 FGF1, FGF2, and FGF7 have identical receptor dependence in Caco-2 and T84 cells

We next examined whether FGF1 reduced TER through FGFR3b. Antibodies to FGFR3, but not those to FGFR1, prevented reductions in TER after FGF1 administration (data not shown). Furthermore, the use of the PI3K inhibitor LY294002 eliminated the ability of FGF1 to reduce TER (data not shown). These results recapitulated those observed with FGF2 and FGF7, demonstrating that FGF1, FGF2, and FGF6 all require FGFR3b to induce a cellular mediated response.

In addition to the high-affinity cell surface tyrosine kinase receptor, FGF activity is also influenced by low-affinity HSGAG receptors [153, 348, 396]. Therefore, we examined whether FGF2 and FGF7 have the same low-affinity receptor requirements to induce a cellular mediated response as FGF1. Pretreatment of cells with sodium chlorate, which prevents heparan sulfate biosynthesis [114, 395], was used to investigate the role of cell surface HSGAGs in conferring reductions in TER. Sodium chlorate treatment eliminated the ability for FGF1 ($p > 0.69$ for Caco-2 cells; $p > 0.62$ for T84 cells), FGF2 ($p > 0.34$ for Caco-2 cells; $p > 0.22$ for T84 cells), and FGF7 ($p > 0.28$ for Caco-2 cells; $p > 0.97$ for T84 cells) to reduce TER in Caco-2 cells (**Figure 7.6A**) and T84 cells (**Figure 7.6B**). FGF1, FGF2, and FGF7, therefore, have the same high-affinity and low-affinity receptor requirements to promote epithelial monolayer dysfunction.

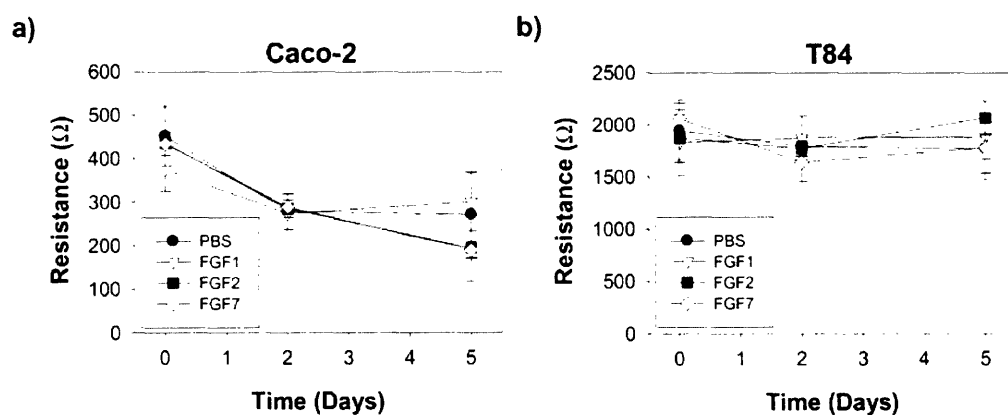


Figure 7.6. Cell surface HSGAGs are necessary for FGF-mediated changes in TER. TER was measured in Caco-2 (A) and T84 (B) cells supplemented with 50 mM sodium chlorate. Sodium chlorate was added 24 hours prior to day 0, on day 0, and on day 2. PBS and FGFs were added on day 0 and on day 2. Data is presented as resistance (in ohms) averaged over three experiments. * denotes $p < 0.05$ for FGF1 compared to PBS. † denotes $p < 0.05$ for FGF2 compared to PBS. § denotes $p < 0.05$ for FGF7 compared to PBS.

The requirement of cell surface HSGAGs for FGF1, FGF2 and FGF7 activity is consistent with the possibility of syndecans serving an essential role in FGF2 and FGF7 inducing a cellular response even though in the absence of a cell surface receptor that could support their activity. Syndecans are a family of HSPGs that interact with ligands, including FGFs, through their core proteins and HSGAG side chains [81]. Syndecan clustering and associated actin stress fiber formation reduces monolayer integrity in endothelial cells [98]. The conserved cytoplasmic domains of syndecans interact with ZO-1 and other PSD95/DLG/ZO-1 (PDZ) proteins [81, 121, 160, 530]. Correspondingly, both FGF2 and FGF7 do alter the distributions of the TJ proteins occludin and ZO-1 (**Figure 3**).

7.2.7 FGF1 is necessary for FGF2 and FGF7 to induce cellular mediated responses

Since each of FGF1, FGF2, and FGF7 require the same receptor to induce a cellular mediated response, but only FGF1 can induce mitogenesis through the high-affinity cell surface receptor FGFR3b [348], we investigated whether FGF1 was essential for other FGFs to promote a cellular mediated response. Treating cells with ammonium tetrathiomolybdate TM, which inhibits the release of endogenous FGF1 [252], abrogated the reduction in TER induced by FGF2 ($p > 0.31$) and by FGF7 ($p > 0.12$) in Caco-2 cells (**Figure 7.7A**). The addition of exogenous FGF1, however, restored the ability of FGF2 and FGF7 to reduce TER in TM treated Caco-2 cells (**Figure 7.7B**). FGF2 elicited significant reduction in TER with FGF1 treatment after 9 hours ($p < 0.05$), 24 hours ($p < 0.03$), and 48 hours ($p < 0.005$). FGF7 elicited significant reduction in TER after 24 hours ($p < 0.004$) and 48 hours ($p < 0.004$).

These results suggest that FGF1 is necessary for FGF2 and FGF7 to induce a cellular mediated response. In order for FGF1 to be present for FGF2 and FGF7 to act, it must be produced by the Caco-2 and T84 cells themselves. We therefore explored whether Caco-2 and T84 cells expressed FGF1. Expression of FGF1 by Caco-2 cells (**Figure 7.7C**) and T84 cells (data not shown) was confirmed by immunohistochemistry. Treating cells with TM alters the distribution of FGF1 with Caco-2 cells (**Figure 7.7D**) and T84 cells (data not shown), retaining FGF1 closer to the nucleus, consistent with TM preventing the release of FGF1 [252] in Caco-2 and T84 cells.

The ability of TM to eliminate reductions in TER induced by FGF2 and FGF7 also extended to T84 cells. TM prevented FGF2 ($p > 0.25$) and FGF7 ($p > 0.23$) from reducing TER in T84 cells (**Figure 7.7E**). Additionally, FGF1 treatment restored TER reductions after 2 days ($p < 0.05$ for FGF2; $p < 0.04$ for FGF7) and 5 days ($p < 0.03$ for FGF2; $p < 0.02$ for FGF7) for both FGF2 and FGF7 (**Figure 7.7F**).

To validate that extracellular FGF1 is essential for FGF2 and FGF7 to reduce TER, cells were treated with antibodies to FGF1. The treatment of Caco-2 cells and T84 cells with antibodies to FGF1 also prevented FGF2 ($p > 0.13$ for Caco-2 cells; $p > 0.23$ for T84 cells) and FGF7 ($p > 0.08$ for Caco-2 cells; $p > 0.93$ for T84 cells) from reducing TER (data not shown). In order to further confirm the requirement of FGF1 for FGF2 and FGF7 cellular mediated responses, the effects of TM on whole cell proliferation were examined. TM eliminated the proliferative effect of FGF2 and FGF7 in both Caco-2 cells and T84 cells, while the addition of FGF1 again restored the proliferative capacity of these ligands in both cell types.

Eliminating FGF1 from the extracellular matrix with TM treatment [252], or neutralizing its activity prevented FGF2 and FGF7 from eliciting a cellular mediated response. Inhibition of components of the FGF1 pathway – the ligand, the receptor, or the downstream signal cascade – abrogated the ability of FGF2 and FGF7 to induce biological activity. Subsequently restoring FGF1 to the extracellular matrix enabled FGF2 and FGF7 to again impact cell function. FGF1 is therefore necessary and sufficient for FGF2- and FGF7-mediated activity in both Caco-2 and T84 cells.

Although FGF1-FGFR3b interactions are essential for FGF2 and FGF7 to induce cellular mediated responses, the mechanism for this activity is not clear. One potential mechanism is FGF1 activity through FGFR3b enabling syndecan clustering by other FGFs. FGF2 can induce cellular responses independent of FGFRs, through interactions with and internalization by HSPGs [71, 72]. The dependence of FGF2 and FGF7 on FGFR3b would therefore be for the requisite FGF1 signaling. Syndecans serving an essential role for FGF2 and FGF7 activity is consistent with the alterations in occludin and ZO-1 distributions [81, 121, 160, 530]. Furthermore, this mechanism is also supported by the ability of FGF2 and FGF7 to induce proliferation, unlike FGF1 (data not shown).

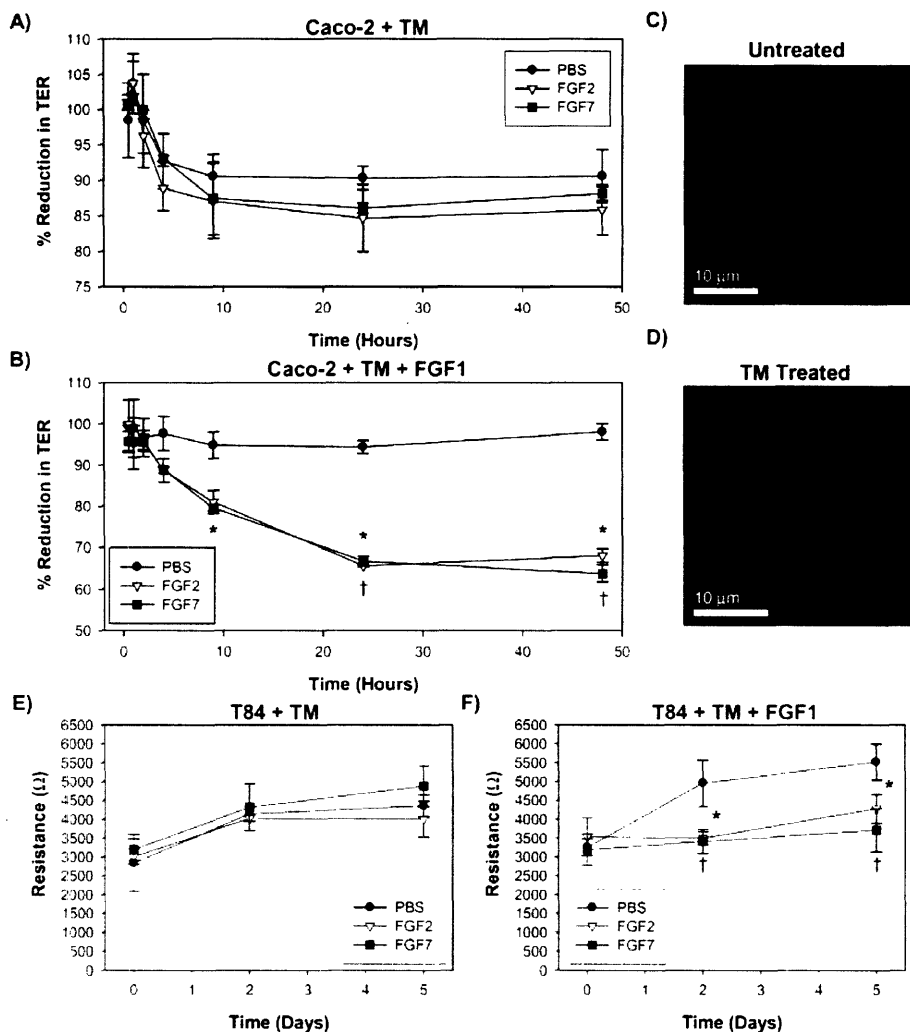


Figure 7.7. FGF1 is necessary for FGF2 and FGF7 reductions in TER. A) PBS, FGF2 or FGF7 was added to Caco-2 monolayers pretreated with TM, and the reduction in TER was determined over 48 hours. Data is presented as the percent reduction in TER over time. * denotes $p < 0.05$ for FGF2 compared to the PBS control. † denotes $p < 0.05$ for FGF7 compared to PBS. B) PBS, FGF2 or FGF7 was added to Caco-2 monolayers pretreated with TM and FGF1, and the reduction in TER was determined over 48 hours. Data is presented as the percent reduction in TER over time. * denotes $p < 0.05$ for FGF2 compared to the PBS control. † denotes $p < 0.05$ for FGF7 compared to PBS. C and D) Immunohistochemistry for FGF1 was performed on untreated Caco-2 cells (C) and Caco-2 cells treated with 200 μ M TM for 24 hours (D). E and F) TER was measured in T84 cells pretreated with TM (E) or both TM and FGF1 (F). TM and FGF1 were added 24 hours prior to day 0, day 0, and day 2. PBS, FGF2 and FGF7 were added at day 0 and day 2. Data is presented as resistance (in ohms) averaged over three experiments. * denotes $p < 0.05$ for FGF2 compared to PBS. † denotes $p < 0.05$ for FGF7 compared to PBS.

7.2.8 Therapeutic implications

The therapeutic role of FGFs in IBD has been extensively investigated. Each of FGF2, FGF7, FGF10, and FGF20 have shown some therapeutic benefit in attenuating the disease [49, 68, 169, 205]. The promising results observed in culture and in animal studies, however, have not been recapitulated in human studies [300, 415, 525]. This study sought to better understand the cellular mechanisms by which FGF family members induce cellular responses in the colon in order to shed insight into why FGFs have not had clinical success in treating IBD.

FGF1 is expressed by the normal intestinal epithelium and overexpressed in many colorectal adenomas and most colorectal cancers [103]. FGF1 autocrine signals promote epithelial cell survival [53]. The release of FGF2 and FGF7 enables protective and reparative functions by promoting angiogenesis, proliferation, and migration [50, 216]. In the unaffected colon, FGF2 and FGF7 may maintain and heal the epithelium in an FGF1-dependent manner, and directly promote an appropriate level of angiogenesis. In IBD, FGF2 levels increase correlated to the level of disease [49] and FGF7 is significantly elevated [125]. If the levels of FGF1, which can inhibit inflammation, were to decrease, FGF2 and FGF7 would retain their angiogenic role but potentially lose their ability to reduce inflammation and maintain the epithelium. The activity of FGFs in IBD has correspondingly been associated with increasing colonic angiogenesis as well as transmural wall thickness [91, 216]. FGF1 expression by colonic epithelial cells may serve as a critical switch, defining whether colonic FGFs inhibit inflammation or promote angiogenesis. Further work is necessary, however, to investigate the specific FGF1 expression profiles in IBD.

7.3 Significance

The activity of FGFs is typically associated with the dimerization of cell surface tyrosine kinase receptors. In this study, the activity of FGF2 and FGF7 was found to be dependent on FGF1, FGFR3b, and cell surface HSGAGs. FGF1 signaling through FGFR3b may enable the clustering of syndecans by FGF2 and FGF7. Consistent with this hypothesis, TJ protein distribution is altered by FGF2 and FGF7 signaling in this cell system, demonstrating for the first time that TJs can be altered by FGFs. This study demonstrates the importance of FGF1 for the

activity of other FGFs with known therapeutic roles in IBD. Furthermore, this study highlights the potential importance of syndecans in regulating inflammation in pathological settings such as IBD.

7.4 Experimental Procedures

Proteins and reagents. Recombinant human FGF1 was from Amgen (Thousand Oaks, CA). Recombinant human FGF2 was produced as described [250]. Recombinant human FGF7 was from Sigma (St. Louis, MO). Mouse recombinant collagen IV was from BD Biosciences (Bedford, MA). LY294002, PD98059, and SB203580 were from Promega (Madison, WI). Rabbit polyclonal anti-human FGF1, rabbit polyclonal anti-human FGFR1 and rabbit polyclonal anti-human FGFR3 were from Santa Cruz Biotechnology (Santa Cruz, CA). FITC conjugated goat anti-rabbit was from Molecular Probes (Eugene, OR). Caco-2 and T84 cells were from American Type Culture Collection (Manassas, VA). FBS was from Hyclone (Logan, UT). MEM, DMEM, Ham's F12 medium, McCoy's 5a medium, Hank's buffered saline solution (HBSS), PBS, RPMI-1640, L-glutamine, and penicillin/streptomycin, sodium pyruvate, HEPES, sodium bicarbonate, and non-essential amino acid solution were obtained from GibcoBRL (Gaithersburg, MD). BaF3 cells transfected with various FGFRs were generously provided by Dr. David Ornitz (Washington University, St. Louis, MO).

Cell culture. Caco-2 cells were maintained in MEM supplemented with 10% FBS and 15 mM HEPES. T84 cells were maintained in a 1:1 mixture of DMEM and F12 medium supplemented with 5% FBS, 1.2 g/L sodium bicarbonate, 2.5 mM L-glutamine, 15 mM HEPES, and 0.5 mM sodium pyruvate. All media was additionally supplemented with 100 mg/L penicillin and 100,000 U/L streptomycin. All cells were grown in 175 cm² flasks at 37°C in a 5% CO₂ humidified incubator. Caco-2 cells were passaged twice a week at confluence. T84 cells were passaged once a week, at confluence.

BaF3 cells transfected with various FGFRs were maintained as independent suspension cultures in propagation media composed of RPMI-1640 supplemented with 10% FBS, 100 µg/ml penicillin, 100 U/ml streptomycin, 1.5 mM L-glutamine, and 1 ng/ml mouse recombinant IL-3.

Cultures were grown in 75 cm² flasks at 37°C in a 5% CO₂ humidified incubator, and were passaged 1:10 by dilution three times a week.

RT-PCR. Five µg of total RNA was isolated from each of Caco-2 and T84 cells using Trizol reagent (Life Tech, Rockville, MD) followed by reverse transcription with random hexamers. Specific oligomers were designed based on published sequences in order to detect the expression of specific FGFR isoforms. Sequences of primer pairs corresponding to distinct FGFR isoforms were as follows: FGFR1b: 5'-TGG AGC AAG TGC CTC CTC-3' and 5'-ATA TTA CCA CTT CGA TTG GTC-3'; FGFR1c: 5'-TGG AGC TGG AAG TGC CTC CTC-3' and 5'-GTG ATG GGA GAG TCC GAT AGA-3'; FGFR2b: 5'-GTC AGC TGG GGT CGT TTC ATC-3' and 5'-CTG GTT GGC CTG CCC TAT ATA-3'; FGFR2c: 5'-GTC AGC TGG GGT CGT TTC ATC-3' and 5'-GTG AAA GGA TAT CCC AAT AGA-3'; FGFR3b: 5' GTA GTC CCG GCC TGC GTG CTA-3' and 5'-GAC CGG TTA CAC AGC CTC GCC-3'; FGFR3c: 5'-GTA GTC CCG GCC TGC GTG CTA-3' and 5'-TCC TTG CAC AAT GTC ACC TTT-3'; and FGFR4: 5'-CCC TGC CGG GAT CGT GAC CCG-3' and 5'-TCG AAG CCG CGG CTG CCA AAG-3'. To control for total cell protein, RT-PCR was also performed on β-actin using the primers 5'-GCC AGC TCA CCA TGG ATG ATG ATA T-3' and 5'-GCT TGC TGA TCC ACA TCT GCT GGA A-3'. PCR was performed using the Advantage-GC cDNA kit from Clontech as per manufacturer's instructions (Palo Alto, CA). Prior to experimental use, primers were confirmed to detect and have specificity towards given FGFR isoforms using BaF3 cells transfected with various FGFRs.

FACS analysis. Caco-2 and were grown just prior to confluence and T84 cells were grown to confluence. Cells were washed with 20 ml PBS and treated with 3.5 ml trypsin-EDTA per 175 cm² flask for 20-60 minutes at 37°C, until cells detached. The cells were then resuspended in 6.5 ml medium and pelleted. Cells were resuspended in PBS supplemented with 5% bovine serum albumin (BSA). Cell suspensions were filtered to remove clumps, and resuspended to a concentration of 5 x 10⁶ cells/ml based on the readings of an electronic cell counter. Aliquots of 100 µl cell suspension were kept on ice for the duration of the experiment. The primary

antibody, rabbit anti-human FGFR3, was added to cells at a 1:500 dilution, and incubated for 1 hour. After washing with PBS supplemented with BSA, the secondary antibody, goat anti-rabbit conjugated to FITC was added at a 1:250 dilution and incubated 30 minutes. Cells were washed with PBS supplemented with BSA, and FACS was performed using a Coulter Epics XL (Beckman Coulter, Miami, FL). Controls of no antibody, no primary antibody, and no secondary antibody were additionally performed.

Transepithelial resistance. Caco-2 cells were grown to just prior to confluence and T84 cells were grown to confluence. The apical chambers of transwell plates with 6.5 mm diameter and 3 μm pore size filters were pretreated with 50 μl of 45 $\mu\text{g/ml}$ collagen IV in 60% ethanol 24 hours prior to plating. Plates were incubated overnight at room temperature. At confluence, cells were washed with 20 ml PBS and treated with 3.5 ml trypsin-EDTA per 175 cm^2 flask for 20-60 min at 37°C, until cells detached. Cells were resuspended in 16.5 ml media appropriate to the cell type. Each apical chamber was supplemented with 82 μl cell solution. The basolateral chamber was filled with 1 ml propagation media. Filters were fed with new media every two days over the course of experiments.

Caco-2 and T84 cells were allowed to grow on transwells to form monolayers. Monolayer formation was examined every other day by light microscopy as well as by TER measurements using an EVOM ohmmeter (World Precision Instruments, Sarasota, FL). After monolayer formation, cells were treated with 100 ng/ml FGF1, 100 ng/ml FGF2, 100 ng/ml FGF7 an equivalent volume (10 μl) of PBS. TER measurements were made either after 72 hours or after each of 30 minutes, 1 hour, 2 hours, 4 hours, 9 hours, 24 hours, and 48 hours. To determine the effects of multiple additions of ligand, FGFs or PBS were added initially and again after 2 days, and TER measurements were made after 0, 2, and 5 days.

To probe the mechanism by which various FGFs induced cell mediated effects, various media treatments were employed. TM was added 24 hours prior to the addition of ligands to yield a final concentration of 200 μM , sufficient to prevent the release of FGF1 [252]. Similarly, sodium chlorate, which reduces cell HSPGs and the sulfation of associated HSGAGs, was added 24 hours prior to the addition of ligands to yield a final concentration of 50 mM [98, 448]. Antibodies and kinase inhibitors were added immediately prior to ligands. Antibodies to FGF1, FGFR1, and FGFR3 were added at a 1:100 dilution. Kinase inhibitors were added to yield final

concentrations of 50 μ M LY294002, 20 μ M PD98059, 1 μ M SB203580. All experiments were performed in triplicate.

BaF3 proliferation assay. The capacity for FGF2 and FGF7 to promote proliferative responses was performed as previously described with slight modification [31, 358]. BaF3 cells expressing FGFR1c or FGFR3c, previously verified by RT-PCR [30], were washed and resuspended to a density of 2×10^5 cells/ml in IL-3 deficient RPMI-1640. The cell suspension was added to each well of a 24 well plate, 1 ml/well. Each well was supplemented with FGF2 or FGF7 between 1 and 100 ng/ml. After a three day incubation at 37°C, 5% CO₂, proliferation was measured with an electronic cell counter. For antibody inhibition assays, antibodies to FGFR1 as well as those to FGFR3 were administered at a 1:100 just prior to the addition of ligand. FGFR1 and FGFR3 antibodies were also added to cells in the absence of ligand to ensure a lack of a direct biological response.

Caco-2 and T84 proliferation assays. Caco-2 cells were grown to just prior to confluence and T84 cells were grown to confluence. Each flask was washed with 20 ml PBS, and treated with 3 ml trypsin-EDTA at 37°C for 20-60 minutes until cells detached. Cells were centrifuged for 3 minutes at 195 x g. The supernatant was aspirated, and the cells were resuspended in 10 ml media. The cell density was measured using an electronic cell counter, and the suspension was diluted to 50,000 cells/ml. The suspension was plated 1 ml/well into 12-well tissue culture plates. After a 24 hour incubation in a 5% CO₂, 37°C humidified incubator, the media was aspirated, the wells were washed with serum free media, and the cells were supplemented with media containing 0.1% FBS. The wells were then supplemented with 10 μ l PBS, 50 mM sodium chlorate, or 200 μ M TM, and incubated for 24 hours. Subsequently, cells were supplemented with 100 ng/ml FGF1, FGF2, FGF7, or 10 μ l PBS, and incubated for 72 hours. Wells were then washed twice with PBS and treated with 0.5 ml trypsin-EDTA/well and incubated at 37°C until cells detached. Whole cell number was determined using an electronic cell counter. Data was averaged over three experiments, each consisting of four wells per condition.

Monolayer flux. Cells were plated on transwells as described. Media from the basolateral chamber was removed every other day and replaced with new media. Resistances were followed

for 10 days, and either 100 ng/ml FGF2, 100 ng/ml FGF7 or 10 μ l PBS were added on days 10 and 12. On day 15, media was removed from both the apical and basolateral chambers. The basolateral chamber was filled with 1 ml HBSS. FITC conjugated to 3 kDa dextran was added to the apical chamber in a volume of 100 μ l, at 1 mg/ml in HBSS. After 30, 60, and 90 minutes, 50 μ l was removed from the basolateral chamber and transferred to a 96 well plate, and 50 μ l HBSS was added to the basolateral chamber. Subsequently, the flux was determined by measurement of FITC-conjugated dextran that crossed the monolayer by measurement with a fluorimeter, stimulating at 480 nm and measuring emission at 530 nm.

Immunohistochemistry. To determine FGFR and FGF1 expression, Caco-2 cells were grown to just prior to confluence and T84 cells were grown to confluence on collagen coated glass slides. Cells were washed with PBS supplemented with 5% BSA. To stain for FGFR3, rabbit anti-human FGFR3 antibodies were added to cells at a 1:500 dilution, and incubated for 1 hour. Cells were washed with PBS supplemented with 5% BSA, and FITC-conjugated goat anti-rabbit antibodies were added and incubated for 30 minutes. Cells were washed with BSA-PBS, and examined using fluorescence microscopy. For FGF1 analysis, cells were treated with 200 μ M TM or 10 μ l PBS for 24 hours, formalin fixed, treated with goat anti-human FGF1 antibodies at a 1:200 dilution, and incubated for 4 hours. Cells were washed with PBS supplemented with 5% BSA, and Texas red-conjugated donkey anti-goat antibodies were added and incubated for 1 hour. Cells were washed with BSA-PBS, and examined using fluorescence microscopy.

To determine occludin and ZO-1 expression patterns, cells were plated on transwells as described for TER assays. Media from the basolateral chamber was removed every other day and replaced with new media. Resistances were measured for 10 days, and either 100 ng/ml FGF2, 100 ng/ml FGF7 or 10 μ l PBS were added on days 10 and 12. On day 15, media was removed from both the apical and basolateral chambers, and the apical chamber was washed twice with PBS. One ml of 1% (w/v) paraformaldehyde in cacodylate buffer was added to each well, the plates were incubated for 10 minutes at room temperature, and the wells were washed once in PBS. One ml permeabilization media, consisting of 0.2% Triton X-100 and 2% BSA in PBS, was added to each well. After a 10 minute incubation at room temperature, wells were washed three times. 20 μ l primary antibodies (rabbit polyclonal anti-human or occludin rabbit polyclonal anti-human ZO-1) diluted 1:20 in 1% goat serum, 0.25% sodium azide in PBS, were

added to the apical chamber of three wells per antibody per ligand, and plates were incubated 1 hour in a humidified chamber. Wells were washed in PBS for 10 minutes at room temperature, and 20 μ l goat anti-rabbit Texas red diluted 1:200 in 1% goat serum, 0.25% sodium azide in PBS was added to each well. After a 30 minute incubation in a dark, humidified chamber, wells were washed three times in PBS. Membranes were carefully removed from transwells and placed on coverslips. 10 μ l polyvinyl alcohol was added to each membrane, and the membranes were covered. Staining was then visualized by fluorescence microscopy. Controls of no antibody, primary antibody only, and secondary antibody only were performed. A Nikon HB10101AF fluorescence microscope was used and images were captured at room temperature using a Hitachi HVC20 camera and Scion image acquisition software. Images were processed using Adobe Photoshop 7.0 and Adobe Illustrator 10.0.

Statistical analysis. Results are expressed as mean \pm standard deviation. The Student's *t* test was used for statistical analysis. A *P* value of < 0.05 was considered statistically significant.

Chapter 8. Syndecan-1 is protective in inflammatory bowel disease

8.0 Summary

Various members of the FGF family have been demonstrated to have protective effects in cellular and animals models of IBD. The FGFR3b isoform is a predominant FGFR in the colonic epithelium. Although FGFR3b does not support the activity of FGF2 and FGF7, they do promote intestinal maintenance and repair. Previous work has demonstrated that the activities of FGF2 and FGF7 are dependent on the activity of FGF1. This study served to identify the mechanism by which FGF1 enabled FGF2 and FGF7 to promote a cellular response. FGF1 was found to induce the localization of syndecan-1, which co-localized with lipid rafts, to the nucleus. Wnt signaling was also affected by FGF2 and FGF7, consistent with a syndecan-1-dependent mechanism. These results not only identify syndecan-1 as a critical factor in enabling FGF2 and FGF7 activity, but also suggest that it may have a protective effect in IBD. Correspondingly, wild-type mice resist acute colitis much more effectively than syndecan-1 knock-out mice. Syndecan-1 is therefore an important protective factor in IBD.

8.1 Introduction

IBD is hypothesized to derive from an inappropriate and continuous activation of the mucosal immune system. The response may stem from defects in one or both of the intestinal epithelium and the mucosal immune system [380]. Failure to maintain epithelial integrity, either as a primary epithelial defect or secondary to inflammation, can lead to increased antigen uptake and the associated colitis phenotype [145, 177]. Epithelial repair is therefore essential in the resolution of colonic inflammation and therapy for IBD [169].

Release of FGF family members by colonic intraepithelial $\gamma\delta$ T cells helps to maintain and repair the colonic epithelium [68, 342]. The FGF family consists of at least 23 members all of which bind to the HSGAG component of HSPGs and to at least one of five high affinity cell

surface FGFRs [153, 178, 396, 445]. HSGAGs serve an important role in facilitating FGF and FGFR dimerization [402, 449]. Cell surface HSPGs, such as syndecans, are also essential modulators of physiological and pathological processes [5, 98, 262, 360]. Syndecans can regulate actin stress fiber formation [98], PDZ protein activity [81, 121, 160, 530], and Wnt-1 signaling [5]. Syndecan-1 expression is also regulated by inflammatory cytokines in IBD [88].

Various FGFs, including FGF2, FGF7, FGF10, and FGF20, regulate the severity and progression of IBD [49, 68, 169, 205]. While FGF2 and FGF7 promote intestinal epithelial cell growth and wound healing [93], the effects of these ligands have been associated with FGFR3b [215], which supports responses from FGF1 but neither FGF2 nor FGF7 [66, 348]. Previous work examined how FGF2 and FGF7 could induce a response in cell systems expressing FGFR3b, and revealed that FGF1, produced by the cells themselves, was necessary for their activity [Chapter 7]. This study examined the mechanism by which FGF2 and FGF7 induced a cellular mediated response. Syndecans, because of their ability of affect cell-cell contacts, their regulation by inflammatory cytokines, and their ability to shuttle FGFs to the nucleus [183], offer a potential route for FGF2 and FGF7 activity.

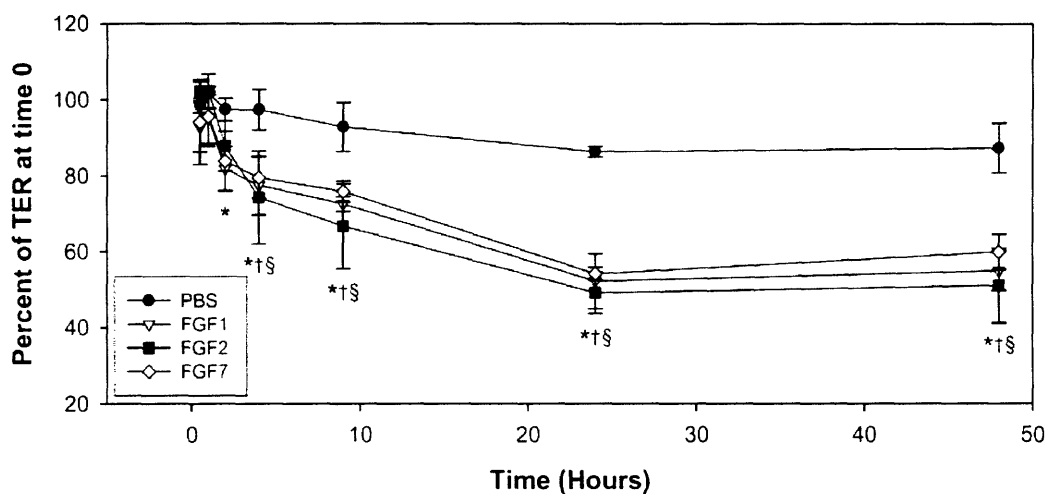


Figure 8.1. FGFs reduce TER in Caco-2 monolayers. Caco-2 cell monolayers were treated with PBS, FGF1, FGF2, or FGF7, and TER was measured over 48 hours. * denotes $p < 0.05$ for FGF1 treated cells compared to PBS treated cells. † denotes $p < 0.05$ for FGF2 treated cells compared to PBS treated cells. § denotes $p < 0.05$ for FGF7 treated cells compared to PBS treated cells.

8.2 Results and Discussion

8.2.1 FGF1 is necessary for FGF2 and FGF7 to reduce TER in Caco-2 cells

In order to explore how FGF1 enabled FGF2 and FGF7 activity in Caco-2 cells, the ability of each of the ligands to affect TER was first reproduced. Each of FGF1, FGF2, and FGF7 significantly reduced TER (**Figure 8.1**). Reductions in TER were evident 2 hours after FGF1 treatment ($p < 0.03$), and 4 hours after FGF2 or FGF7 treatments ($p < 0.05$). Significant reductions were evident at all subsequent time points examined ($p < 0.04$). The magnitude of TER reduction elicited by FGF1, FGF2, and FGF7, however, was not significantly different ($p > 0.20$). Each of FGF1, FGF2, and FGF7 could therefore reduce TER, consistent with previous findings [Chapter 7].

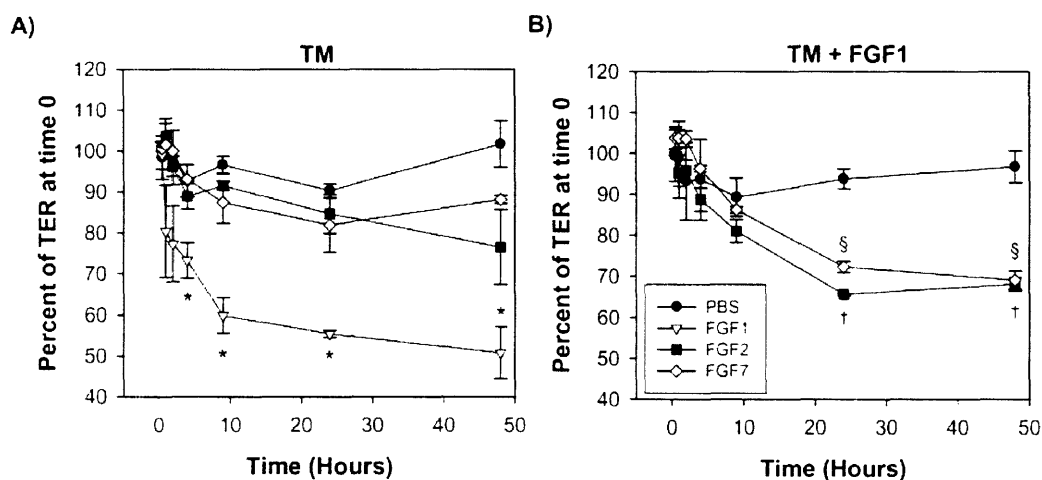


Figure 8.2. FGF1 is necessary for FGF2 and FGF7 reductions in TER. Caco-2 cell monolayers were pretreated with TM. A) Cells were treated with PBS, FGF1, FGF2, or FGF7, and TER was measured for 48 hours. * denotes $p < 0.05$ for FGF1 treated cells compared to PBS treated cells. B) Cells were treated with FGF1 along either FGF2 or FGF7. Control cells were treated with TM, but not FGF1. TER was measured over 48 hours. † denotes $p < 0.05$ for FGF2 treated cells compared to PBS treated cells. § denotes $p < 0.05$ for FGF7 treated cells compared to PBS treated cells.

TM was subsequently used to confirm the requirement of FGF1 for FGF2 and FGF7 to reduce TER. Treating cells with TM, which inhibits the release of endogenous FGF1 [252], abrogated the reduction in TER induced by FGF2 ($p > 0.13$) and by FGF7 ($p > 0.17$) at all time points (**Figure 8.2A**). FGF1, however, still elicited significant reductions in TER with TM

treatment at all time points beginning at 4 hours ($p < 0.05$). The addition of exogenous FGF1, however, restored the ability of FGF2 and FGF7 to reduce TER in TM treated Caco-2 cells (**Figure 8.2B**). FGF2 and FGF7 both significantly reduced TER after 24 hours ($p < 0.04$) and 48 hours ($p < 0.04$). Since supplementing TM-treated cells with FGF1 cells reduces TER, the effects of FGF2 and FGF7 in the presence of TM and FGF1 were compared to TM-treated cells. These results confirm previous findings that FGF1 is necessary for FGF2 and FGF7 to reduce TER in Caco-2 cells.

8.2.2 Cell surface HSPGs are necessary for FGF2 and FGF7 to reduce TER

FGF-induced TER reductions were demonstrated to result from increased paracellular flux and reduce cell-cell contacts [Chapter 7]. To examine the effects of FGFs on cell-cell interactions over time, immunostaining for the TJ protein ZO-1 was performed (**Figure 8.3**). FGF2 and FGF7 induced notable membrane ruffling at 1 hour, 4 hours, 24 hours, and 48 hours, confirming that the reductions in TER over time are associated with disruption of cell-cell contacts.

Cell-cell contacts are formed by both apical TJs and adjacent AJs [117]. While both TJs and AJs are important in regulating monolayer integrity, TJs interact with cell surface HSPGs. Specifically, ZO-1 and other PDZ proteins interact with the conserved cytoplasmic domains of syndecans, a family of HSPGs [81, 121, 160, 530]. As the HSGAG component of HSPGs interacts with FGFs, cell surface syndecans could offer a potential mechanism by which FGFs affect TJs and therefore TER.

The ability of FGF2 and FGF7 to promote actin stress fiber formation was additionally investigated. Both FGF2 and FGF7 induced actin stress fiber formation (**Figure 8.3**). Monolayer integrity can be reduced by syndecan clustering and associated actin stress fiber formation [98]. The ability of FGF2 and FGF7 to reduce TER, alter TJ proteins such as ZO-1, and induce stress fiber formation is consistent with a syndecan-mediated mechanism.

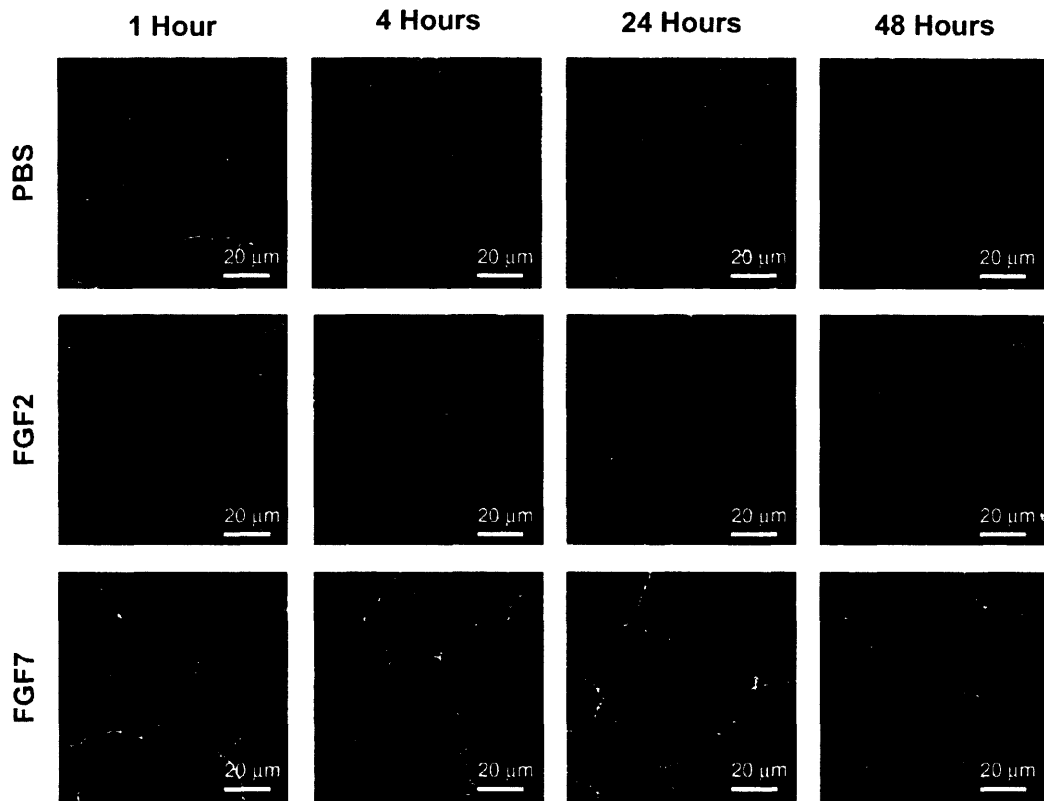


Figure 8.3. FGF2 and FGF7 affect ZO-1 as well as actin stress fiber formation. Caco-2 cell monolayers were treated with PBS, FGF2, or FGF7. Immunohistochemistry was performed for ZO-1 (green) and F-actin (red). Images were captured by confocal microscopy. Scale bars are as indicated.

Cell surface HSPGs, including syndecans, are protein-HSGAG conjugates [427]. To investigate the importance the role of the HSGAG component of cell surface HSPGs in mediating TER reductions, cells were pretreated with sodium chlorate, which prevents heparan sulfate biosynthesis [114, 395]. Sodium chlorate treatment abrogated the ability of FGF1 ($p > 0.49$), FGF2 ($p > 0.38$), and FGF7 ($p > 0.16$) to reduce TER compared to PBS treatment (**Figure 8.4A**). With the addition of heparin (**Figure 8.4B**), FGF1 reduced TER compared to PBS at 9 hours ($p < 0.003$) and at 24 hours ($p < 0.004$). The ability of FGF2 ($p > 0.08$) and FGF7 ($p > 0.16$) to reduce TER, however, was not restored with heparin. While HSGAGs are necessary for each of FGF1, FGF2, and FGF7 to reduce TER, the requirements for FGF1 differ from those of FGF2 and FGF7. HSGAGs free in the ECM are not sufficient for FGF2 and FGF7 to reduce TER, but are for FGF1. These findings suggest that the HSGAG component of cell surface HSPGs, however, is necessary for FGF2 and FGF7 to reduce TER.

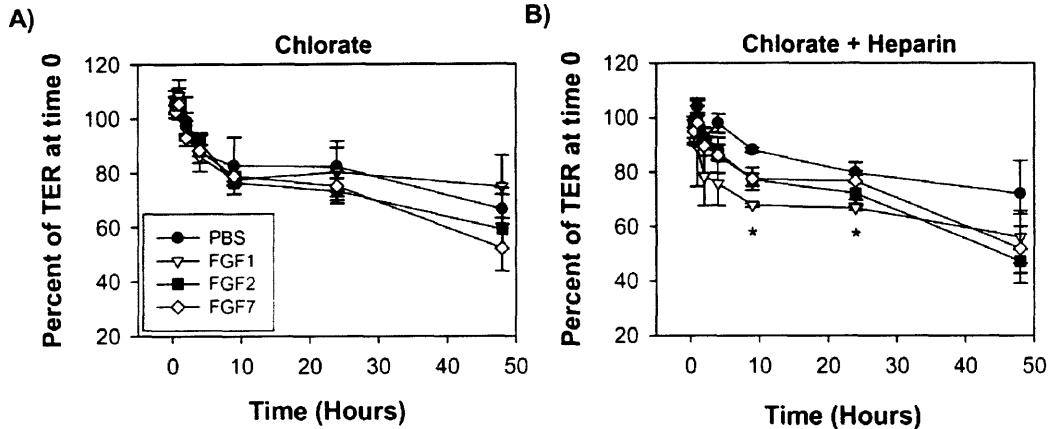


Figure 8.4. Cell surface HSGAGs are necessary for FGF2 and FGF7 reductions in TER. Caco-2 cell monolayers were pretreated with sodium chlorate. A) Cells were treated with PBS, FGF1, FGF2, or FGF7, and TER was measured over 48 hours. B) Cells were treated with heparin as well as PBS, FGF1, FGF2, or FGF7, and TER was measured over 48 hours. * denotes $p < 0.05$ for FGF1 treated cells compared to PBS treated cells.

To verify the importance of cell surface HSPGs, Caco-2 cells were treated with PMA, which activates PKC, and as a result, accelerates the shedding of syndecan-1 and syndecan-4 [128]. After PMA treatment (**Figure 8.5**), FGF1 reduced TER after 9 hours ($p < 0.03$), 24 hours ($p < 0.008$), and 48 hours ($p < 0.02$). Neither FGF2 ($p > 0.07$) nor FGF7 ($p > 0.35$), however, reduced TER in PMA treated Caco-2 cells at any time point. Loss of cell surface syndecan-1 and syndecan-4 by PMA-induced shedding therefore prevents FGF2 and FGF7 activity, but not that of FGF1.

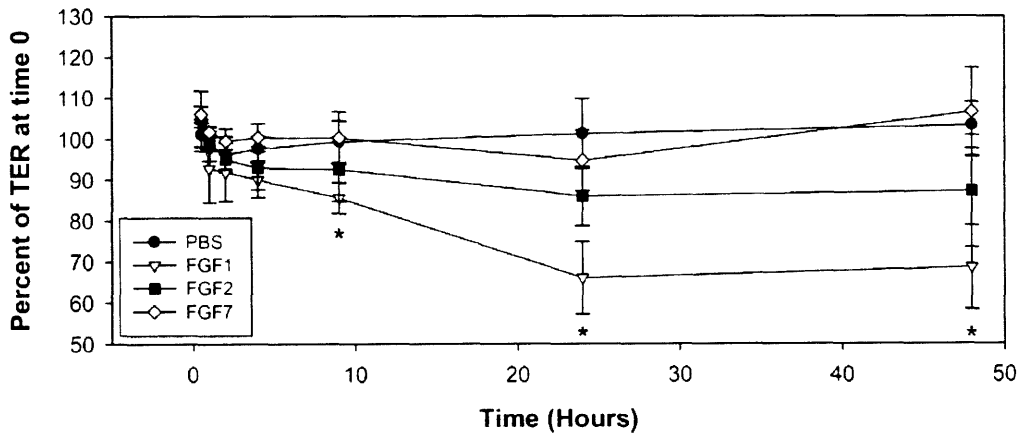


Figure 8.5. Cell surface HSPGs are necessary for FGF2 and FGF7 reductions in TER. Caco-2 cell monolayers were pretreated with PMA, and subsequently, PBS, FGF1, FGF2, or FGF7 was added. TER was measured over 48 hours. * denotes $p < 0.05$ for FGF1 treated cells compared to PBS treated cells.

These results demonstrate that cell surface HSPGs are necessary for FGF2 and FGF7 to reduce TER. The HSGAG component of the HSPG is necessary likely to mediate ligand binding [396]. The ability of FGF2 and FGF7 to induce membrane ruffling and promote actin stress fibers formation confirms the importance of the protein component of the HSPG as the cytoplasmic domains of syndecans interact with ZO-1 and other PDZ proteins [81, 121, 160, 530]. The effects on ZO-1 and TJs additionally suggest that the involved HSPGs are most likely syndecans. Syndecan-1 and syndecan-4 clustering promotes actin stress fiber formation [98]. Furthermore, PMA promotes syndecan-1 and syndecan-4 shedding [128], preventing FGF2- and FGF7-mediated reductions in TER. Taken together, the necessary HSPG for FGF2 and FGF7 to reduce TER is likely either syndecan-1 or syndecan-4.

8.2.3 FGF2 and FGF7 alter syndecan-1 localization

The effects of FGF1, FGF2, and FGF7 on syndecan-1 distribution were next examined. One hour after FGF2 and FGF7 treatment, syndecan-1 was primarily localized around the nucleus (**Figure 8.6A**). This finding was seen substantially less with FGF1 treatment and was absent after PBS treatment. After 24 hours, FGF2 and FGF7 treated cells reveal a moderately enhanced cytoplasmic and membrane-associated distribution of syndecan-1 than FGF1 treated cells. Glypican-1, another HSPG, was not affected by FGF1, FGF2, or FGF7 (data not shown). The nuclear localization of syndecan-1 is of particular note as HSPGs have been hypothesized to serve as a shuttle to transport heparin-binding growth factors, specifically including FGF2, to the nucleus [183]. As a result, transport of syndecan-1 with bound growth factors could serve as a mechanism by which Caco-2 cells could respond to FGF2 and FGF7 even though the cell surface tyrosine kinase receptors expressed cannot support a response from these ligands [348].

While syndecan-1 may enable FGF2 and FGF7 to induce a cellular response, FGF1 is necessary for FGF2 and FGF7 to reduce TER. One potential explanation is that FGF1 may activate processes that allow syndecan-1 to serve its role facilitating FGF2 and FGF7 activity. HSPGs can be localized within lipid rafts, creating high local concentrations of binding sites for heparin-binding growth factors such as FGF2, promoting ligand association and inhibiting dissociation [71]. We therefore investigated the localization of caveolin-1, a marker for lipid rafts [473], after FGF1 treatment. PBS did not induce the nuclear localization of syndecan-1 or caveolin-1 (**Figure 8.6B**). Four hours after administration of FGF1, however, caveolin-1 was

localized surrounding the nucleus. Furthermore, caveolin-1 and syndecan-1 did co-localize near the nucleus.

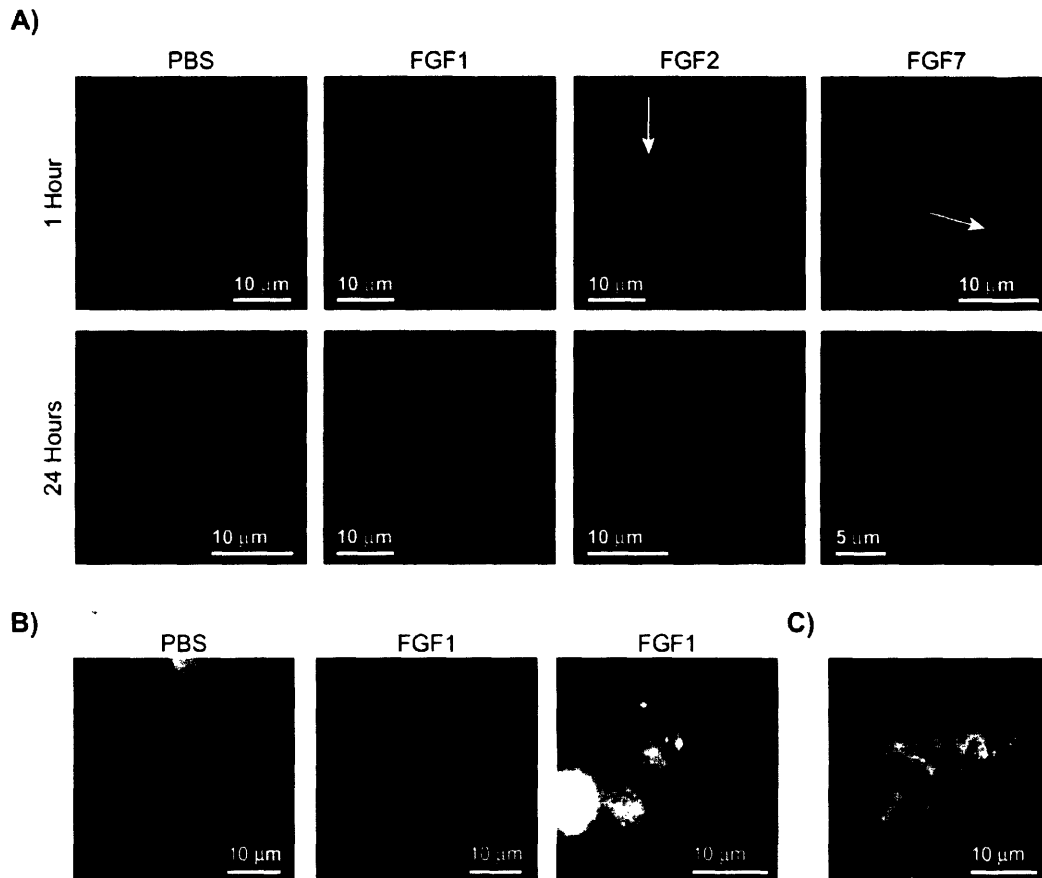


Figure 8.6. FGFs alter syndecan-1 localization. A) Caco-2 cell monolayers were treated with PBS, FGF1, FGF2, or FGF7 for 1 or 24 hours. Immunohistochemistry was performed for syndecan-1 (green) and DAPI (blue). Images were captured by fluorescence microscopy. Scale bars are as indicated. B) Caco-2 cell monolayers were treated with PBS (left) or FGF1 (middle and right) for 4 hours, and images were captured by fluorescence microscopy. Immunohistochemistry was performed for syndecan-1 (green), caveolin-1 (red) and DAPI (blue). The left image shows an overlay of staining for syndecan-1, caveolin-1 and DAPI after PBS treatment. The middle panel represents staining for caveolin-1 and DAPI after FGF1 treatment. The right image shows an overlay of staining for syndecan-1, caveolin-1 and DAPI after FGF1 treatment. Scale bars are as indicated. C) Caco-2 monolayers were treated with FGF1 for 24 hours, and immunohistochemistry was performed for FLAER (green), syndecan-1 (red) and DAPI (blue). Images were captured by fluorescence microscopy. Scale bars are as indicated.

To confirm the ability of FGF1 to promote syndecan-1 association with lipid rafts, immunohistochemistry was performed for syndecan-1 and glycosylphosphatidylinositol (GPI)-anchored proteins. FLAER, an Alexa-488 conjugated inactive variant of the protein proaerolysin, detects GPI-anchored proteins [52, 469]. Syndecan-1 and GPI-anchored proteins

were found to exhibit co-localization at the membrane and within the cytoplasm (**Figure 8.6C**). The co-localization of syndecan-1 and GPI-anchored proteins is consistent with syndecan-1 in the cytoplasm originating from regions rich in lipid rafts [470].

The data presented reveals that FGF2 and FGF7 activity is associated with syndecan-1 translocation to the nucleus. Syndecan-1 may enable FGF2 and FGF7 reductions in TER by binding the ligands and shuttling them to the nucleus [183], serving to bypass the cell surface FGFRs that do not support their activity [348]. The ability of syndecan-1 to translocate FGF2 and FGF7 may be promoted by FGF1. FGF1 promotes the localization of lipid rafts to the nucleus, and syndecan-1 co-localizes with these lipid rafts. As such, FGF1 activity may cause syndecan-1 to move to the nucleus by causing lipid rafts to translocate them. FGF2 and FGF7, prior to this activity, could be bound by the HSGAG component of syndecan-1, and with FGF1 activity, they would be specifically induced to be brought to the nucleus, where they could initiate signaling.

8.2.4 FGF2 and FGF7 alter Wnt signaling

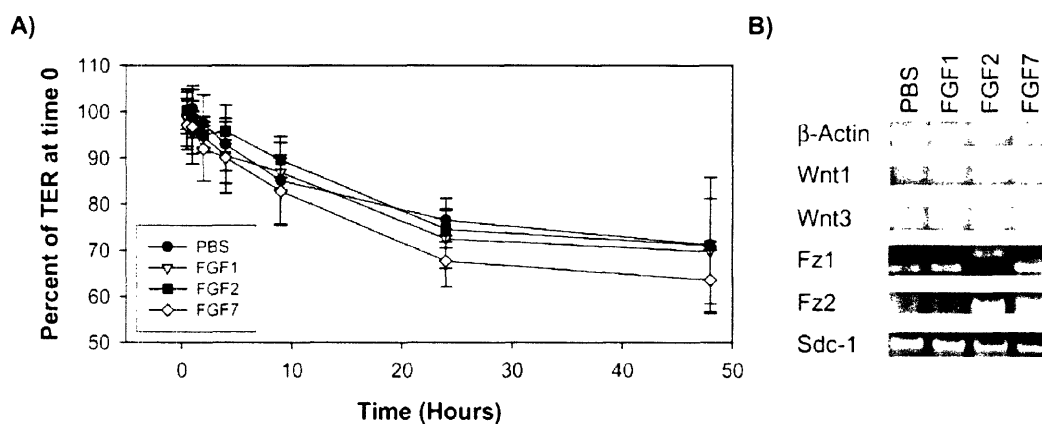


Figure 8.7. Wnt signaling is necessary for FGF2 and FGF7 reductions in TER. A) Caco-2 cell monolayers were treated with anti-Fz1 antibodies, as well as PBS, FGF1, FGF2 or FGF7. TER was measured over 48 hours. B) RT-PCR was performed on Caco-2 cells after treatment with PBS, FGF1, FGF2 or FGF7.

Syndecan-1 is known to modulate Wnt signaling [5]. Should syndecan-1 serve as a critical factor by which FGF1 enables FGF2 and FGF7 to elicit cellular mediated responses in Caco-2 cells, Wnt signaling would also likely be affected. Wnt signaling is initiated by the Wnt ligand binding to Frizzled (Fz) protein receptors as well as lipoprotein receptor-related proteins [329]. Initiation of the Wnt cascade results in the cytoplasmic accumulation of β -catenin, which

binds to a protein complex including T cell factor/lymphoid enhancer factor (TCF/LEF) transcription factors and induces gene expression [56, 329]. To promote cellular responses, Wnt inhibits glycogen synthase-3 β , thereby stabilizing β -catenin and causing its cytoplasmic localization from being sequestered by proteins including E-cadherin [329]. Slug/Snail family proteins, induced by signaling by a variety of growth factors including FGFs, inhibit E-cadherin transcription [73]. Their activity can reduce cell-cell adhesion concomitantly with the accumulation of cytoplasmic β -catenin [73, 329].

To investigate the potential involvement of the Wnt pathway, Caco-2 cells were supplemented with anti-Fz antibodies. Treating Caco-2 cells with anti-Fz antibodies prevented FGF1 ($p > 0.26$), FGF2 ($p > 0.51$), and FGF7 ($p > 0.16$), from reducing TER (**Figure 8.7A**). RT-PCR was performed to confirm the expression of members of

	PBS	FGF1	FGF2	FGF7
Wnt1	1.0	2.2	2.7	5.1
Wnt3	1.0	1.3	1.3	1.2
Fz1	1.0	1.5	1.1	2.4
Fz2	1.0	0.7	1.7	1.6
Sdc-1	1.0	1.3	0.9	0.6

Table 8.1. FGFs increase Wnt1 expression. Intensity of RT-PCR images was quantified using NIH ImageJ. Data was normalized to the intensity of expression after PBS treatment, which was defined as 1.0.

the Wnt-signaling cascade. Specifically, RT-PCR demonstrated the expression of Wnt1, Wnt3, Fz1, Fz2, and syndecan-1 (the protein produce by the Sdc-1 gene; **Figure 8.7B**). No expression of Wnt2, Wnt3A, or Fz10 was detected by RT-PCR (data not shown). The expression of Fz1 was further confirmed by immunohistochemistry (data not shown). Of note, the RT-PCR data suggested that Wnt1 expression was increased with FGFs. Band intensity was therefore quantified using NIH ImageJ. FGF1, FGF2, and FGF7 all increased Wnt1 expression (**Table 1**). FGF2 and FGF7 also both increased Fz2 expression, while only FGF7 increased and Fz1 expression.

E-cadherin, associated with Wnt activities, is the prototypical and best characterized AJ protein [369]. We next investigated whether E-cadherin distribution was affected by FGFs. FGF2 and FGF7 altered E-cadherin localization after 1 hour (**Figure 8.8A**), while PBS and FGF1 did not. After 24 hours, E-cadherin exhibited exhibit notably more cytoplasmic localization with FGF2 and FGF7 treatments than at 1 hour, and more than PBS and FGF1 treatment at 24 hours. FGF2 and FGF7 therefore affect AJs, suggesting that when these ligands

are brought to the nucleus, they may activate distinct processes from FGF1. Furthermore, the Wnt pathway may be affected by FGF2 and FGF7.

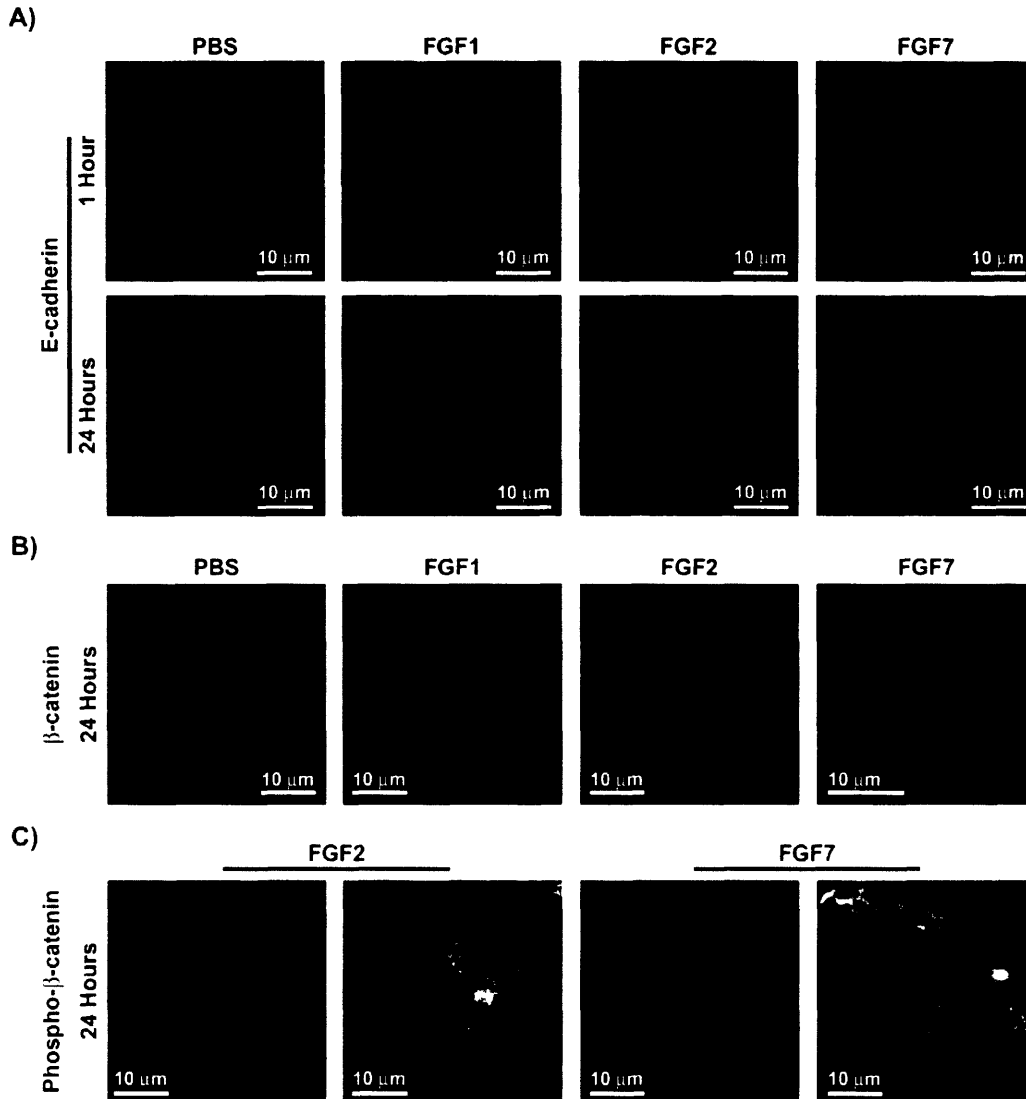


Figure 8.8. FGFs affect the Wnt signaling cascade. Caco-2 cell monolayers were treated with PBS, FGF1, FGF2, or FGF7 for 1 or 24 hours. A) Immunohistochemistry was performed for E-cadherin (green) and DAPI (blue). Images were captured by fluorescence microscopy. Scale bars are as indicated. B) Immunohistochemistry was performed for β -catenin (red) and DAPI (blue). Images were captured by fluorescence microscopy. Scale bars are as indicated. C) Immunohistochemistry was performed for E-cadherin (green), phospho- β -catenin (red) and DAPI (blue). Images were captured by fluorescence microscopy. Scale bars are as indicated.

To further probe the involvement of Wnt signaling, the effects of PBS, FGF1, FGF2, and FGF7 on β -catenin localization were examined. After 24 hours, FGF2 and FGF7 induced

markedly increased cytoplasmic β -catenin compared to PBS treatment, which clustered around the nucleus (**Figure 8.8B**). FGF1 treatment yielded potentially reduced levels of cytoplasmic β -catenin compared to PBS treatment. Phosphorylated β -catenin also clustered around the nucleus after Caco-2 cells were treated with FGF2 and FGF7 (**Figure 8.8C**), which was not observed with PBS or FGF1 (data not shown). Of note, much of the detected phosphorylated β -catenin appeared in distinct locations from E-cadherin, consistent with β -catenin being sequestered to the cytoplasm from E-cadherins. Furthermore, FGF2 and FGF7 increased TCF/LEF activity compared to PBS and FGF1 (data not shown). Taken together, these results suggest that FGF2 and FGF7 activity is associated with Wnt signaling, which supports the involvement of syndecan-1 in enabling FGF2 and FGF7 to promote cellular responses. Although syndecan-4 was not specifically investigated, Wnt signaling is associated with syndecan-1 [5], suggesting that this HSPG is the more likely factor. Nonetheless, syndecan-4 may also facilitate FGF2 and FGF7 activity.

8.2.5 Syndecan-1 is protective in IBD

The data presented suggests that syndecan-1 enables FGF2 and FGF7 to reduce TER in Caco-2 cells even though they do not express the corresponding cell surface FGFRs. FGF1 uses a distinct pathway, most likely via FGFR3b, which is expressed by Caco2 cells [215], and which supports FGF1 activity [348]. Given that FGF2 and FGF7 promote intestinal epithelial cell growth, wound healing, and reduce the inflammation associated with IBD [55, 93, 459], as well as the importance of syndecan-1 to promote the activities of these growth factors in Caco-2 cells, we next examined whether syndecan-1 had a protective effect in IBD. Wild-type and *Sdc-1* (the gene for syndecan-1) knock-out mice were administered drinking water with 10% dextran sodium sulfate (DSS) to induce an acute colitis. The DSS model promotes an acute disease that substantially affects survival. *Sdc-1* knock-out mice, whose survival was not different from wild-type mice in an unmodified environment (data not shown), were notably more susceptible to DSS than wild-type mice (**Figure 8.9A**). In *Sdc-1* knock-out mice, all mice had died by 7 days of ingesting DSS-water, while 40% of the wild-type mice survived for 8 days. The surviving mice exhibited no significant weight change over the course of the experiment or significant weight difference between the groups at any time point (**Figure 8.9B**). Syndecan-1 therefore appears to have a protective effect in acute IBD.

The data presented demonstrated that syndecan-1 is a specific cell surface HSPG that has a pivotal role in IBD. Syndecan-1 can enable the activity of FGFs in the absence of cognate cell surface FGFRs, likely by promoting ligand translocation to the nucleus [183]. Furthermore, the action of syndecan-1 is associated with alterations in cell-cell contacts through both TJs and AJs, which are important in processes essential for maintaining and healing the epithelial [165, 295, 513]. These activities, as well as effects on Wnt signaling, associated with syndecan-1 [5] present potential mechanisms by which this HSPG may induce protective effects in IBD. Further work is necessary, however, to determine if syndecan-1 is protective in other IBD models, including inflammatory cell mediated and chronic [39, 380]. Additionally, methods to enhance syndecan-1 expression warrant further study for their potential in ameliorating IBD.

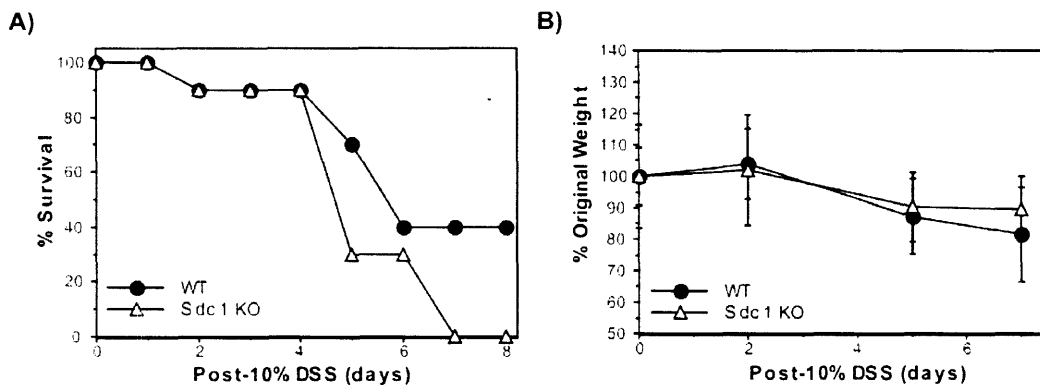


Figure 8.9. Syndecan-1 increases survival in an inflammatory bowel disease mouse model. Wild-type and syndecan-1 knock-out (Sdc1 KO) mice were administered 10% DSS in their drinking water. A) Overall survival was measured over eight days. B) Weight of surviving rats was measured over seven days.

8.3 Significance

Previous studies demonstrated that FGF2 and FGF7 induce cellular mediated responses in Caco-2 cells, which express a cell surface FGFR that does not support the activity of these FGFs. FGF1, however, was previously found to be necessary for FGF2 and FGF7 to induce a cellular mediated response. This study served to identify the mechanism by which FGF1 enables FGF2 and FGF7 activity. The data presented demonstrates that FGF2 and FGF7 are dependent on cell surface HSPGs, while FGF1 is not. Syndecan-1 was found to translocate to the nucleus, a mechanism which has been previously validated by which FGFs can induce a cellular response.

Of note, FGF1 promotes the clustering of syndecan-1 with lipid rafts, which together co-localize around the nucleus. This may therefore serve as the mechanism by which FGF1 enables FGF2 and FGF7 to induce cellular responses. Unlike FGF1, both FGF2 and FGF7 also affect the Wnt pathway, which has important implications in the colon, especially regarding cell transformation and tumor growth. Furthermore, these studies identify syndecan-1 as a potentially important modulator in IBD. Correspondingly, the presence of syndecan-1 was found to have a substantial protective effect in acute colitis. This study therefore demonstrates that syndecan-1 is a key factor with therapeutic potential in IBD, warranting further investigation.

8.4 Experimental Procedures

Cell Culture. Caco-2 cells (American Type Culture Collection, Manassas, VA) were maintained in MEM (GibcoBRL, Gaithersburg, MD) supplemented with 10% FBS (Hyclone, Logan, UT), 15 mM HEPES, 100 mg/L penicillin and 100,000 U/L streptomycin (GibcoBRL). Cells were grown in 175 cm² flasks at 37°C in a 5% CO₂ humidified incubator. Caco-2 cells were passaged twice a week at confluence. T84 cells were passaged once a week, at confluence.

RT-PCR. Five µg of total RNA was isolated from Caco-2 cells using Trizol reagent (Life Tech, Rockville, MD) followed by reverse transcription with random hexamers. Specific oligomers were designed based on published sequences in order to detect the expression of specific human Wnt, Fz, and syndecan isoforms. Sequences of primer pairs were as follows: Wnt-1: 5'-CAC GAC CTC GTC TAC TTC GAC-3' and 5'-ACA GAC ACT CGT GCA GTA CGC-3' [69]; Wnt-2: 5'-CAT GGT GGT ACA TGA GAG CTA C-3' and 5'-GGC AAA TAC AAC TCC AGC TGA G-3' [220]; Wnt-3: 5'-GAG AGC CTC CCC GTC CAC AG-3' and 5'-CTG CCA GGA GTG TAT TCG CAT C-3' [221]; Wnt-3a: 5'-CAG GAA CTA CGT GGA GAT CAT G-3' and 5'-CCA TCC CAC CAA ACT CGA TGT C-3' [221]; Fz-1: 5'-GAA CTT TCC TCC AAC TTC ATG GC-3' and 5'-CAT TTC CAT TTT ACA GAC CGG-3' [391]; Fz-2: 5'-GGT GAG CCA GCA CTG CAA GAG-3' and 5'-CCT AAA AGT GAA ATG GTT TCG ATC G-3' [391]; Fz-10: 5'-ACA CGT CCA ACG CCA GCA TG-3' and 5'-ACG AGT CAT GTT GTA GCC GAT G-3' [391]; and Syndecan-1/Sdc-1/CD138: 5'-CTT CAC ACT CCC CAC ACA GA-

3' and 5'-TCC TGT TTG GTG GGC TTC TG-3' [334]. To control for total cell protein, RT-PCR was also performed on β -actin using the primers 5'-GCC AGC TCA CCA TGG ATG ATG ATA T-3' and 5'-GCT TGC TGA TCC ACA TCT GCT GGA A-3' [31]. PCR was performed using the Advantage-GC cDNA kit from Clontech as per manufacturer's instructions (Palo Alto, CA).

Transepithelial resistance. Caco-2 cells were grown to just prior to confluency. The apical chambers of transwell plates with 6.5 mm diameter and 3 μ m pore size filters were pretreated with 50 μ l of 45 μ g/ml mouse recombinant collagen IV (BD Biosciences, Bedford, MA) in 60% ethanol 24 hours prior to plating. Plates were incubated overnight at room temperature. Just prior to confluency, cells were washed with 20 ml PBS and treated with 3.5 ml trypsin-EDTA per 175 cm² flask for 20-60 min at 37°C, until cells detached. Cells were resuspended in 16.5 ml media appropriate to the cell type. Each apical chamber was supplemented with 82 μ l cell solution. The basolateral chamber was filled with 1 ml propagation media. Filters were fed with new media every two days over the course of experiments.

Caco-2 cells were allowed to grow on transwells to form monolayers. Monolayer formation was examined every other day by light microscopy as well as by TER measurements using an EVOM ohmmeter (World Precision Instruments, Sarasota, FL). After monolayer formation, cells were treated with 100 ng/ml recombinant human FGF1 (Amgen, Thousand Oaks, CA), 100 ng/ml recombinant human FGF2 [250], 100 ng/ml recombinant human FGF7 (Sigma, St. Louis, MO), or an equivalent volume (10 μ l) of PBS. TER measurements were made after each of 30 minutes, 1 hour, 2 hours, 4 hours, 9 hours, 24 hours, and 48 hours.

To probe the mechanism by which various FGFs induced cellular mediated effects, various media treatments were employed. TM was added 24 hours prior to the addition of ligands to yield a final concentration of 200 μ M, sufficient to prevent the release of FGF1 [252]. Sodium chlorate, which reduces cell HSPGs and the sulfation of associated HSGAGs, was added 24 hours prior to the addition of ligands to yield a final concentration of 50 mM [98, 448]. Heparin (Celsus, Cincinnati, OH) was added at a concentration of 500 ng/ml concurrently with ligands. PMA (100 ng/ml; Sigma, St. Louis, MO), which activates PKC, and promotes syndecan shedding [128], was added 2 hours prior to ligands and again, 24 hours after. Goat anti-human Fz-1 (Santa Cruz Biotechnology, Santa Cruz, CA) was added with ligands at a 1:100 dilution. All experiments were performed in triplicate.

Immunohistochemistry. Caco-2 cells were grown to just prior to confluency on collagen IV coated glass slides. Cells were treated with PBS, FGF1, FGF2, and FGF7, and were incubated at 37°C in a 5% CO₂ humidified incubator for 1 hour, 4 hours, 24 hours or 48 hours, as noted. Cells were washed with PBS, fixed with 3.7% formalin for 10 minutes, and washed again with PBS. Cells were treated with 0.1% Triton x-100 for 5 minutes to extract lipids. Cells were washed with PBS, and preincubated with PBS supplemented with 1% BSA. Primary antibodies were added for 4 hours at room temperature, and cells were washed with PBS. Primary antibodies used were as follows: rabbit anti-human ZO-1 (1:160; Zymed Laboratories, San Francisco, CA); mouse anti-human syndecan-1 (1:300; Santa Cruz Biotechnology); goat anti-human Fz-1 (1:125; Santa Cruz Biotechnology); rabbit anti-human caveolin-1 (1:250; Santa Cruz Biotechnology); goat anti-human glypican-1 (1:100; Santa Cruz Biotechnology); mouse anti-human E-cadherin (1:250; Zymed Laboratories); rabbit anti-human β -catenin (1:125; Cell Signaling Technology, Beverly, MA); and rabbit anti-human phospho- β -catenin (Ser33/37/Thr41; 1:125; Cell Signaling Technology).

Cells were then treated with secondary antibodies, Texas Red-labeled phalloidin (Molecular Probes, Eugene, OR), or FLAER-FL1 (1:400; Protox Biotech, Victoria, BC, Canada) as appropriate for 1 hour in the dark at room temperature. Secondary antibodies used were as follows: FITC-labeled chicken anti-rabbit (for ZO-1; 1:100; Molecular Probes); Texas Red-labeled goat-anti mouse (for syndecan-1; 1:400; Molecular Probes); FITC-labeled donkey anti-mouse (for syndecan-1; 1:400; Molecular Probes); FITC-labeled rabbit anti-mouse (for syndecan-1 and E-cadherin; 1:500; Molecular Probes); Texas Red-labeled rabbit anti-goat (for Fz-1; 1:200; Jackson ImmunoResearch Laboratories, West Grove, PA); Texas Red-labeled goat anti-rabbit (for caveolin-1, β -catenin and phospho- β -catenin; 1:500; Molecular Probes); and Texas Red-labeled donkey anti-goat (for glypican-1; 1:80; Research Diagnostics, Flanders, NJ).

Cells, except those stained with phalloidin, were washed with PBS and stained with DAPI for 5 minutes at room temperature (Molecular Probes). Controls of no antibody, primary antibody only, and secondary antibody only were performed. Cells were examined by confocal microscopy (ZO-1 and phalloidin only), or by fluorescence microscopy. A Nikon HB10101AF fluorescence microscope was used and images were captured at room temperature using a

Hitachi HVC20 camera and Scion image acquisition software. Images were processed using Adobe Photoshop 7.0 and Adobe Illustrator 10.0

TCF/LEF assay. Caco-2 cells were seeded in 12 well plates such that they would reach 90% confluency in 4 days. Two days after plating, Caco-2 cells were transiently transfected with the TOPFLASH (contains 4 TCF/LEF binding elements) luciferase promoter construct (Promega, Madison, WI) as well as a thymidine kinase driven renilla luciferase construct (Promega) as a transfection control vector. Each well was transfected with 1.5 µg DNA using Superfect transfection reagent (Promega). Twenty-four hours after transfection, Caco-2 cells were treated with PBS, FGF1, FGF2, or FGF7, for 1 hour, 4 hours, or 24 hours. The Caco-2 cells were processed using a dual-luciferase assay system to measure luciferase activity from both the TOPFLASH constructs and the renilla constructs. All results were standardized to the relative transfection efficiencies as observed from the renilla values.

DSS acute colitis model. Mice with knock-outs of Sdc-1, the gene for syndecan-1, were produced as previously described [5, 262, 360]. Disease was induced by *ad libitum* administration of 10% DSS in the drinking water [55]. Survival and the weight of surviving mice were measured over time. Ten wild-type and 10 Sdc-1 knock-out mice were used for experiments.

Statistical analysis. Results are expressed as mean ± standard deviation. The Student's *t* test was used for statistical analysis. A *P* value of < 0.05 was considered statistically significant.

Section 3. Internalization of Heparin

Overview:

Section 3 describes the development of poly(β -amino ester)-heparin conjugates. These conjugates can enable cellular uptake of heparin by endocytosis, preferentially into cancer cells. After entry into cells, conjugates alter cellular responses, leading to apoptotic cell death. The selectivity for cancer cells coupled with their ability to induce cell death makes poly(β -amino ester)-heparin conjugates a viable potential anti-cancer agent. While poly(β -amino ester)-heparin conjugates are effective on most cancer cell lines, one notable exception is with Burkitt's lymphoma, a cancer associated with the Epstein-Barr virus, where they induce proliferation. Using the conjugates as a tool aided in the identification of cell surface heparin/heparan sulfate-like glycosaminoglycans as critical modulators of cell growth. The depolymerization of Burkitt's lymphoma cell surface heparin/heparan sulfate-like glycosaminoglycans with heparinases was subsequently found to be an effective way to inhibit their growth. Finally, the ability of poly(β -amino ester)-heparin conjugates to inhibit cancer cell growth was validated *in vivo*, where it additionally has no anticoagulant effects and no detectable toxicity. Poly(β -amino ester)-heparin conjugates therefore offer a new potential therapeutic modality to treat cancer. Furthermore, selectivity based on the rate of endocytosis is an effective means to target cancer cells.

Chapter 9. Poly(β -amino ester)s promote cellular uptake of heparin and cancer cell death

This report was previously published in *Chemistry and Biology* in 2004. See reference [32] for details. All figures in this chapter were adapted from the original publication.

9.0 Summary

Heparin/heparan sulfate-like glycosaminoglycans (HSGAGs) are involved in diverse cellular processes in the ECM. The biological effect of HSGAGs depends on disaccharide content and physiological location within the ECM. HSGAGs are also brought into cells during membrane transcytosis and growth factor signaling while protein bound. This study serves to probe the impact of free HSGAGs within the cell by using heparin as a model HSGAG. A library of poly(β -amino ester)s (PAEs), which internalize DNA, was examined for the capacity of its members to internalize heparin. Fourteen polymers enabled heparin internalization. The most efficacious polymer reduced murine melanoma cell growth by 73%. No GAG was as efficacious as highly sulfated, full-length heparin. Internalized heparin likely interferes with transcription factor function and subsequently induces apoptotic cell death. Therefore, internalized heparin is a novel mechanism for inducing apoptosis of cancer cells.

9.1 Introduction

The role of HSGAGs in influencing biological processes has been defined by their function in the ECM. HSGAGs are found as the GAG component of HSPGs. Depending on the core protein, HSPGs are either free in the ECM or at the cell-ECM interface [427]. Interactions between HSGAGs and other ECM components regulate important physiological and pathological processes, including normal development, wound healing, and tumor progression [77, 370].

HSGAGs can regulate such a wide variety of cell processes because of their information-rich nature [108]. The HSGAG polysaccharide is composed of a disaccharide repeat unit consisting of a glucosamine linked to either an iduronic acid or a glucuronic acid. Potential 2-O sulfation on the uronic acid, 6-O and 3-O sulfation of the glucosamine, and an unmodified, acetylated, or sulfated amine lead to 48 potential disaccharide units that compose the 10–100-mer HSGAG chain [370]. In addition to the information content inherent in the polysaccharide chain [38], the relative biological location of both the HSGAG and the HSPG influences function. The tumorigenicity of an HSGAG chain is distinct whether it is free in the ECM or attached to an HSPG on the cell surface [274, 448].

In normal function, HSGAGs are brought into the cell in a controlled fashion. For example, HSGAGs bind to FGF2 and FGFR1 to form an internalized ternary complex [365, 448]. HSGAGs may facilitate the localization of the FGF-FGFR-HSGAG complex to the nucleus, where it impacts cell function [183]. Nonetheless, the role of free HSGAGs within the cell has not been established. PAEs are a class of cationic polymers that bind to DNA and enable its internalization by endocytosis [285, 286]. The low toxicity of this set of polymers compared to other cationic polymers that can also bind and internalize DNA, including poly(lysine) and poly(ethylene imine) [51, 285], provides an optimal method for investigating the potential for the internalization of HSGAGs with heparin as a model HSGAG, as well as a useful tool for understanding the effects of free HSGAGs within the cell.

The capacity of the PAEs to bind DNA and enable internalization, presumably by forming a conjugate with a net positive charge to promote endocytosis [210, 285], makes heparin binding and internalization rational. Herein, we investigated the capacity of PAEs to bind and internalize heparin, as well as the resultant cellular effects. We found that, although most polymers can bind heparin, only a small subset enables efficient internalization. Entry of heparin into cells promotes cell death, which is limited primarily by the rate at which cells internalize the polymer-heparin conjugate. The magnitude of cell death is maximal with PAEs conjugated to heparin rather than to other GAGs. We found that internalized heparin promotes spermine influx, a general increase in transcription factor levels in both the nucleus and cytosol, and apoptotic cell death.

9.2 Results

9.2.1 PAEs bind heparin

PAEs have been previously demonstrated to efficiently bind DNA [285, 286]. The interaction between this class of polymers and DNA is thought to be primarily mediated through electrostatic interaction between the anionic DNA and the cationic polymers. azure A is a cationic dye that binds to sulfate groups on heparin [502]. We examined polymer-heparin binding by determining if polymers could compete with azure A for binding sites on heparin. The ability of PAEs to displace Azure A was initially examined for five polymers with variable DNA binding efficiencies over a range of polymer:heparin (w/w) ratios. All five polymers displaced heparin. The optimal ratios for these five polymers were at either 5:1 or 20:1. The 70 PAEs that had been previously demonstrated to be water soluble from an initial screening group of 140 [286] were then tested for their ability to bind heparin. Of the 70 polymers tested, 64 bound heparin to some degree at a 5:1 (w/w) polymer:heparin ratio, and all 70 bound heparin at a 20:1 ratio in 25 mM sodium acetate. When dissolved in PBS, only 57 polymers bound heparin at a 5:1 (w/w) ratio, and 63 did so at a 20:1 (w/w) ratio. pH affects not only the rate at which PAEs degrade but also their ability to directly bind DNA [285]. The reduced ability of PAEs to bind heparin at a higher pH is consistent with DNA's reduced ability to do so.

9.2.2 Select PAEs enable internalization of heparin

To determine if PAE binding to heparin would enable internalization into cells, as is the case for PAE-DNA conjugates [4, 285, 286], we employed fluorescein-labeled heparin. Conjugates of polymer and fluorescein-labeled heparin were formed in 25 mM sodium acetate for each of the 70 water-soluble polymers at a 20:1 (w/w) polymer:heparin ratio. The conjugates were incubated with SMCs, BAECs, and NIH 3T3 cells for 24 hr, and internalization was detected by fluorescence microscopy. A group of 14 polymers composed of diacrylate "A" and amine "5" (A5), A8, A11, B6, B9, B11, B14, C4, C12, D6, E7, E14, F20, and G5 (**Figure 9.1**) enabled passage of heparin across the cell membrane; this heparin passage sufficiently met the criteria detailed in Experimental Procedures. The structures of A5 and B6 can be seen in **Figure**

9.1C. The chemical properties of the various polymers examined and the complexes formed with them have been reported previously [4, 286].

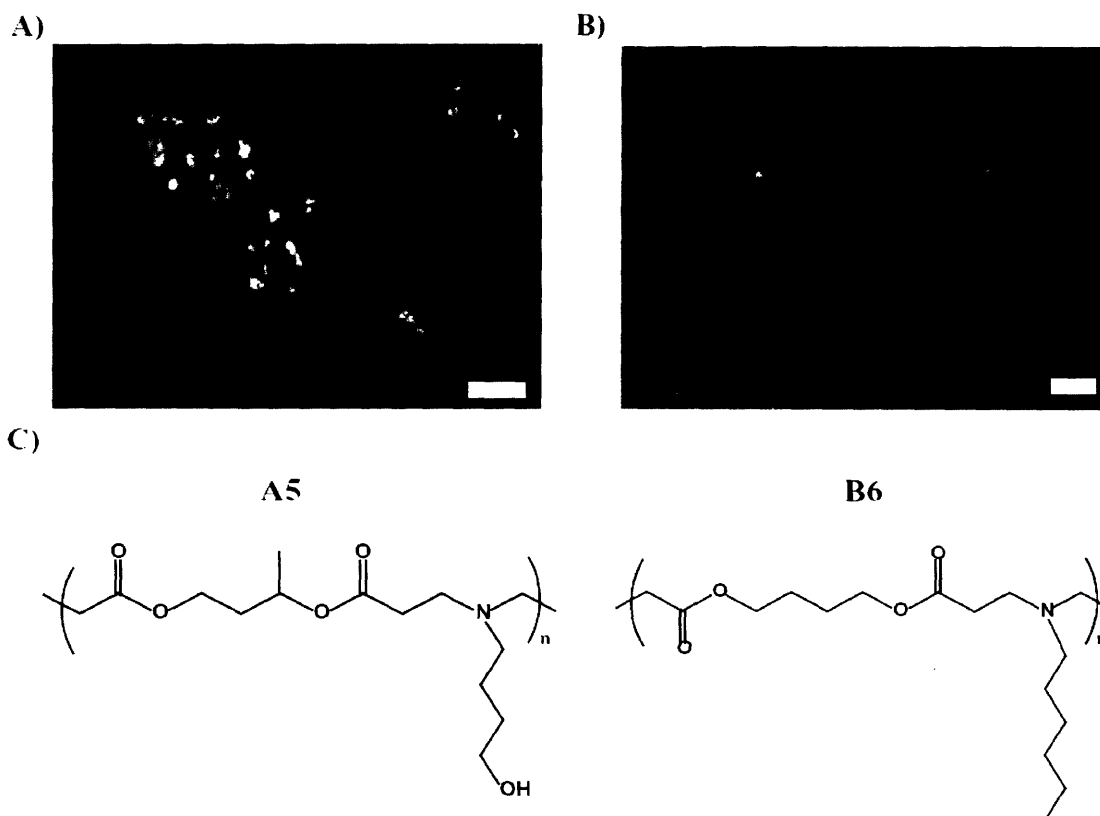


Figure 9.1. Select PAEs enable internalization of heparin. (A and B) SMCs were incubated with conjugates of fluorescein-labeled heparin and various polymers. Fluorescence microscopy images of polymers (A) A5 and (B) B6 are shown. Images are presented as an overlay of fluorescence onto light microscopy. Scale bars represent 10 μm . (C) Polymers A5 and B6.

9.2.3 Internalized heparin inhibits B16-F10 growth

We treated B16-F10 cells with polymer-heparin complexes to investigate if internalized heparin could influence cell processes. Polymer-heparin complexes were formed at a polymer:heparin ratio of 20:1 (w/w) with each of the 14 polymers that enabled heparin internalization. Cells were treated with enough complexes to produce a heparin concentration of 500 ng/ml. Internalization of heparin caused a polymer-specific and polymer-dependent response in terms of B16-F10 proliferation (**Figure 9.2A**). A5-heparin induced a $58.28\% \pm 12.97\%$ reduction in cell number in treated versus untreated cells; this reduction was significantly greater

than that induced by any other polymer-heparin conjugate tested ($p < 0.008$). Heparin alone inhibited cell growth $2.40\% \pm 10.33\%$.

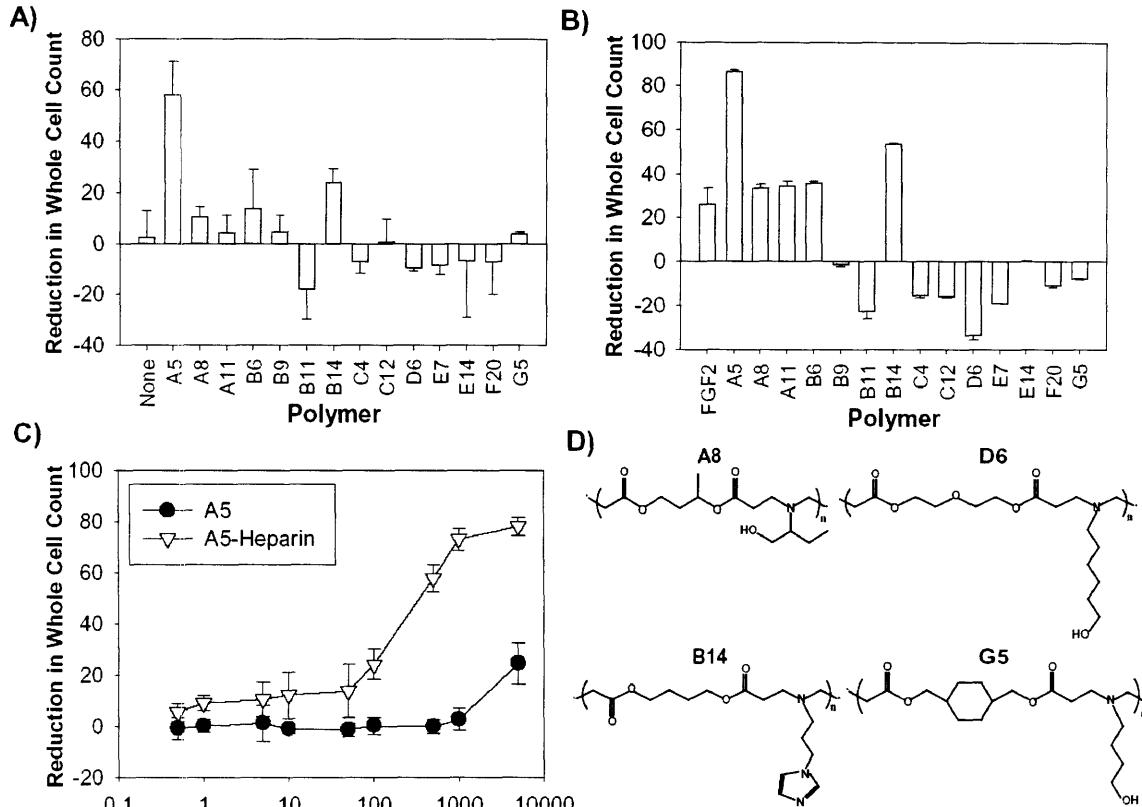


Figure 9.2. A5-Heparin reduces B16-F10 growth. B16-F10 cells were treated with polymer heparin conjugates (A) alone or (B) with 5 ng/ml FGF2. Data were normalized as percent reduction in the whole-cell count compared to untreated cells. (C) B16-F10 cells were treated with A5-heparin at a 20:1 (w/w) ratio or with equivalent amounts of A5 alone. The whole-cell count was converted to a percent reduction compared to that of untreated cells. (D) Chemical structures of four polymers that had notable cellular effects after conjugation to heparin.

To examine whether the observed conjugate-induced effects were related to FGF2 cell-mediated responses, we added each of the 14 polymer-heparin complexes and 10 ng/ml FGF2 to the cells. In the presence of FGF2, A5-heparin reduced the whole-cell number by $86.51\% \pm 1.05\%$ in treated compared to untreated cells. Given that FGF2 alone produced a $26.28\% \pm 7.23\%$ inhibition, the increased magnitude of the inhibitory effect appears to be additive (**Figure 9.2B**). FGF2 generally promoted inhibition across polymers in an additive manner. D6 provides

a notable exception in that cell number inhibition *decreased* from $-9.51\% \pm 1.13\%$ to $-33.97\% \pm 1.47\%$.

We next examined the dose dependence of A5-heparin. The capacity of A5-heparin conjugates to reduce the whole-cell number increased with concentration (**Figure 9.2C**). The addition of 5 $\mu\text{g/ml}$ heparin and 100 $\mu\text{g/ml}$ A5 reduced the whole-cell number by $24.58\% \pm 7.98\%$ ($p < 0.004$). At 1 $\mu\text{g/ml}$ heparin, A5-heparin reduced cell numbers by $73.14\% \pm 2.75\%$. The amount of polymer used in the conjugate was the highest amount of polymer alone that did not have a significant effect.

9.2.4 Internalized heparin affects cell processes

To determine if the conjugate-mediated effects were due to nonspecific cytotoxicity, we examined whether specific cell processes were affected. The effects of internalized heparin on six transcription factor levels in B16-F10 cells were determined. We found a general alteration of specific transcription factors in both the nucleus and the cytoplasm (**Figures 9.3A and 9.3B**). The most striking effect was seen in DP-1 in the nucleus and the cytoplasm, where levels were elevated 2.18 ± 0.12 -fold and 2.72 ± 0.03 -fold, respectively. Nuclear E2F-1 and Sp-1 were both initially lower than the control but then corrected toward the control. Nuclear p107, Rb, and E2F-2 all showed initial increases compared to the control but subsequently declined. After 4 hr, Rb decreased substantially below the control level. Cytoplasmic p107 and E2F-2 were initially elevated but then returned to near baseline levels. Levels of E2F-1, Rb, and Sp-1 were substantially elevated over time, although Rb did show a relative decrease between 1 hr and 4 hr. The measured levels for the six transcription factors showed an average elevation of 1.20- and 1.63-fold in the nucleus and cytoplasm, respectively, after 4 hr. Without DP-1, the increases were 1.01-fold for nuclear transcription factors and 1.41-fold for cytoplasmic transcription factors.

To examine the occurrence of individual HS epitopes within the HSGAGs present on and around B16-F10 cells, we used a panel of 10 anti-HS antibodies for immunocytological staining of fixed cell cultures. Most antibodies showed strong staining for HS on the cell surface and in the ECM. Antibodies HS4C3 and RB4CD12 showed differential staining patterns between A5-heparin and heparin alone (**Figure 9.3C**).

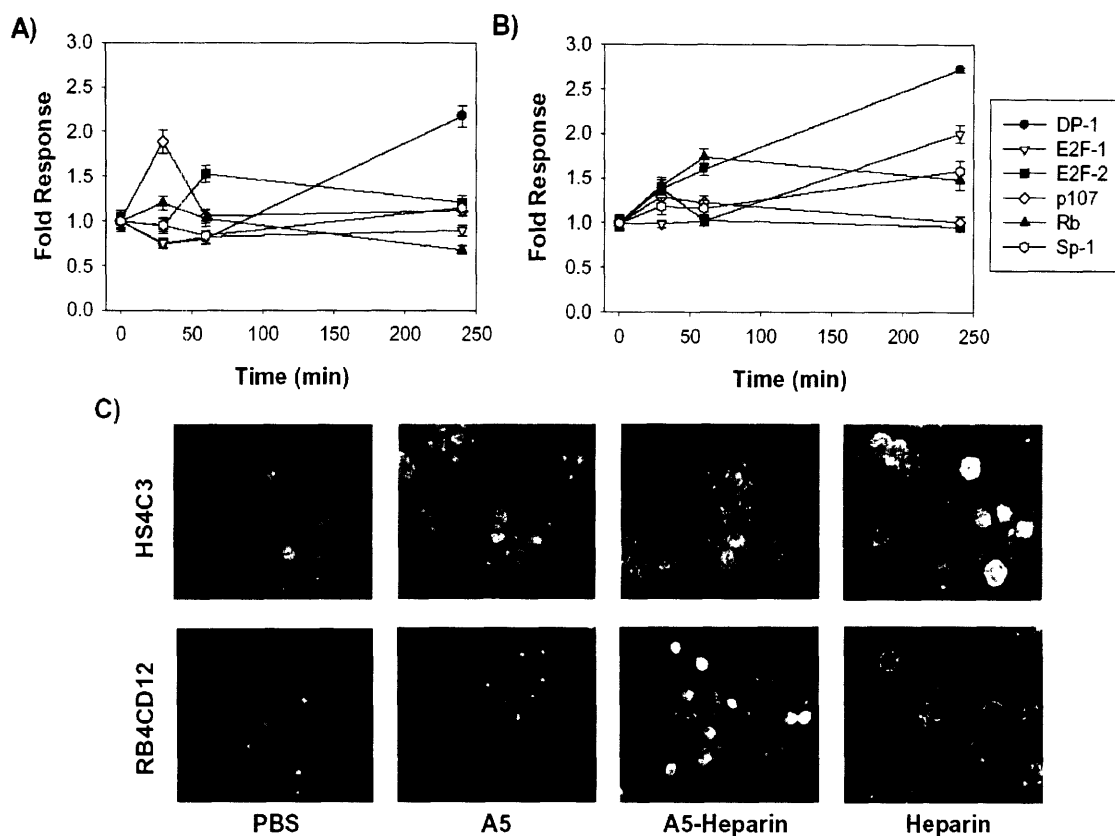


Figure 9.3. A5-Heparin affects cellular processes. B16-F10 cells were treated with A5-heparin conjugates at a 20:1 (w/w) ratio. (A) Nuclear and (B) cytosolic transcription factor levels were determined after incubation with conjugates for different time periods. Data are normalized to untreated cells with results presented as the relative increase in magnitude compared to untreated cells. (C) Immunohistochemistry of B16-F10 cells after treatment with PBS, A5, A5-heparin conjugates, or heparin with antibodies specific to HS moieties.

9.2.5 Growth-inhibitory effects are GAG specific

To investigate whether the growth-inhibitory effect was specific to heparin or generalized to GAGs of various size, charge, and composition, heparan sulfate (HS), enoxaparin, low molecular-weight heparin (LMWH) of two activity levels, and two forms of CS were tested for their ability to bind A5 and to produce a biological effect in B16-F10 cells via proliferation assays. The composition of the HSGAGs was determined by capillary electrophoresis-based compositional analysis as described [30, 31]. Heparin, enoxaparin, and high-activity LMWH had the highest quantities of sulfate groups, averaging 2.32, 2.41, and 2.35 sulfates per disaccharide, respectively (**Figure 9.4A**). HS had only 0.43 sulfates per disaccharide. CS-A was primarily 4-O sulfated, with the corresponding peak constituting 98.2% of total peak area. CS-C was primarily 6-O sulfated but contained some 4-O sulfated disaccharides, as well as three forms

of disulfated disaccharides. This collection of GAGs, therefore, allowed for the examination of sulfation degree, length, and saccharide type.

A)

Disaccharide	Heparin	HS	Enoxparin	High Activity LMWH	Low Activity LMWH
U ₂ S ₁ H _{NS,6S}	58.13	1.05	63.00	57.97	0.31
U ₂ S ₁ H _{NS}	5.84	0.73	3.95	4.19	60.25
UH _{NS,6S}	13.74	2.13	14.82	17.04	31.50
U ₂ S ₁ H _{NAc,6S}	1.97	0.48	1.47	1.63	10.27
UH _{NS}	4.09	15.01	2.75	3.51	0.97
U ₂ S ₁ H _{NAc}	0.90	0.26	0.67	0.20	0.12
UH _{NAc,6S}	9.31	18.19	7.87	11.46	0.65
UH _{NAc}	3.86	61.66	2.70	0.79	2.09

B)

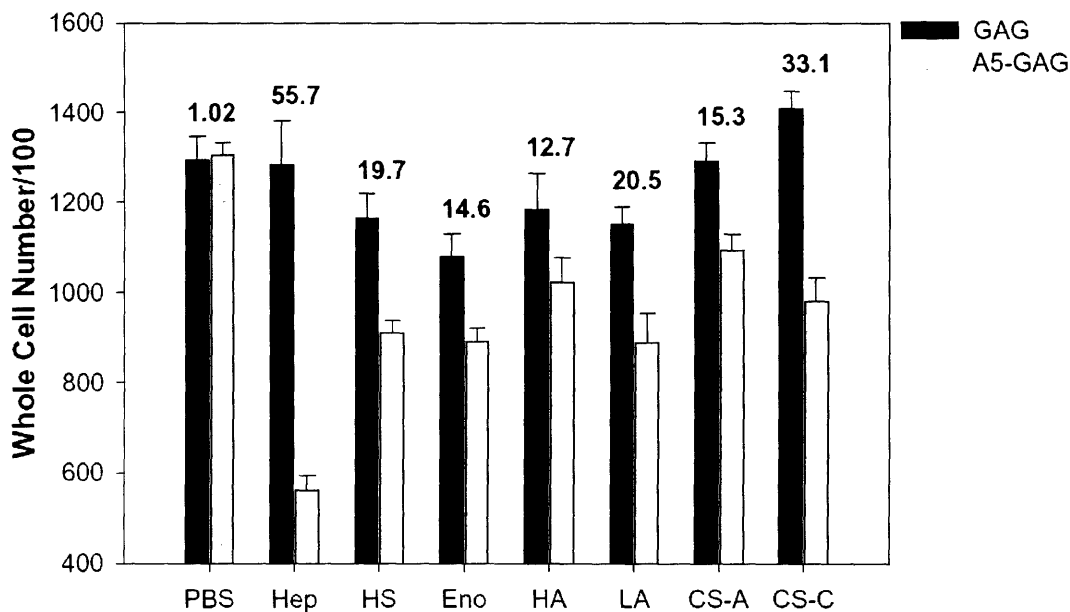


Figure 9.4. Heparin induces greater growth inhibition than other GAGs. (A) The disaccharide composition of the various pools was determined by capillary electrophoresis after complete digestion by heparinases. Numbers represent the percentage of each given disaccharide. Not included is the undigestible 4-7 tetrasaccharide, which represents the deviation of the sum of each column from 100. (B) B16-F10 cells were treated with GAGs (black bars) and A5-GAG conjugates (gray bars; 20:1, w/w). Hep, Eno, HA, LA, CS-A, and CS-C refer to heparin, enoxparin, high-activity LMWH, low-activity LMWH, CS A, and CS C respectively. Data are expressed as a whole-cell number/100. Numbers represent the percent change in the whole-cell number for the A5-GAG conjugate compared to GAG alone.

The azure A binding assay demonstrated that A5 bound to all of the GAGs employed at a 20:1 (w/w) A5:heparin ratio in 25 mM sodium acetate. The minimum amount of polymer required for complete binding was higher for GAG species with more sulfates per disaccharide.

Correspondingly, A5 (as well as other polymers) bound full-length heparin and highly-sulfated LMWHs with similar efficiency. Heparin induced the greatest reduction in the B16-F10 cell number ($p < 5 \times 10^{-5}$; **Figure 9.4B**) of the A5-GAG conjugates (20:1, w/w; 500 ng/ml GAG). The undersulfated HS produced only a $19.70\% \pm 4.01\%$ reduction compared to that of $53.73\% \pm 5.80\%$ for heparin. The shorter chain enoxaparin and LMWHs also produced reductions in cell number that were lower in magnitude than full-length heparin. It is noteworthy that, compared to other polymers that enabled conjugate internalization, A5 also promoted the maximal cell-mediated effect for LMWHs. Each of the two species of CS had less of an effect than heparin. The $33.12\% \pm 5.51\%$ reduction induced by CS-C is significantly greater than the $15.28\% \pm 4.52\%$ reduction induced by CS-A ($p < 0.0002$) and the reduction induced by HS ($p < 0.001$).

9.2.6 Internalized heparin promotes a cell-specific response

We examined if A5-heparin affected other cell types. The proliferative effects of A5-heparin (20:1, w/w; 1 $\mu\text{g/ml}$ heparin) were examined in SMCs, BAECs, FGFR1c-transfected BaF3 cells, SW-1088, SK-ES-1, Panc-1, SK-ES-1, and B16-BL6 by whole-cell proliferation. The A5-heparin conjugate had a minimal effect on SMCs ($3.84\% \pm 3.33\%$), BAECs ($-1.09\% \pm 1.94\%$), transfected BaF3 cells ($14.52\% \pm 4.05\%$), B16-BL6 cells ($-8.92\% \pm 12.36\%$), and Panc-1 cells ($-2.74\% \pm 5.41\%$), but it did elicit a significant reduction in the whole-cell number of SK-ES-1 ($53.79\% \pm 7.85\%$) and SW-1088 ($23.76\% \pm 8.89\%$) cells. Proliferation assays were also performed in the presence of each of 10% FBS, 50 mM sodium chlorate, and 5 ng/ml FGF2 (50 ng/ml for transfected BaF3 cells). The presence of FBS significantly reduced the effect of the conjugate. Sodium chlorate, which abrogates cell surface HSPGs [448], reduced the growth-inhibitory effects of A5-heparin in SK-ES-1 and SW-1088 cells (**Figure 9.5A**). The effect of A5-heparin in the presence of FGF2 was not significantly different from the summed changes induced separately by conjugate and-FGF2.

The cell-specific effects of A5-heparin raised the question as to why certain cells were more affected. The results could not be directly attributed to cell turnover rate because transfected BaF3 cells and SMCs, which are not susceptible to A5-heparin conjugate-mediated reductions, have a faster turnover rate than SW-1088 cells, which are susceptible. Given that the polymer likely enables internalization by promoting endocytosis [285], we investigated whether internalization rates could be the source of the differential effects observed. Fluorescein-

conjugated heparin was used for measuring internalization rates in SMCs, B16-BL6 cells, and B16-F10 cells. B16-F10 cells show internalization of heparin within 1 hr (**Figure 9.5B**). Neither SMCs nor B16-BL6 cells showed significant internalization within 6 hr, although all three cell lines demonstrated internalized conjugate after 24 hr. These results confirm the cell-specific nature of A5-heparin conjugate-mediated inhibition of proliferation and suggest that selectivity is related to the complexes' rate of uptake.

A)

A5-Heparin	B16-F10	SK-ES-1	SW-1088	BaF3
Unsupplemented	58.28 ± 12.97	53.79 ± 7.85	23.76 ± 8.89	14.59 ± 4.05
FGF2	86.51 ± 1.05	48.12 ± 12.21	21.67 ± 11.47	14.52 ± 10.70
Chlorate	54.39 ± 11.06	31.71 ± 19.18	3.36 ± 6.00	N/A

B)

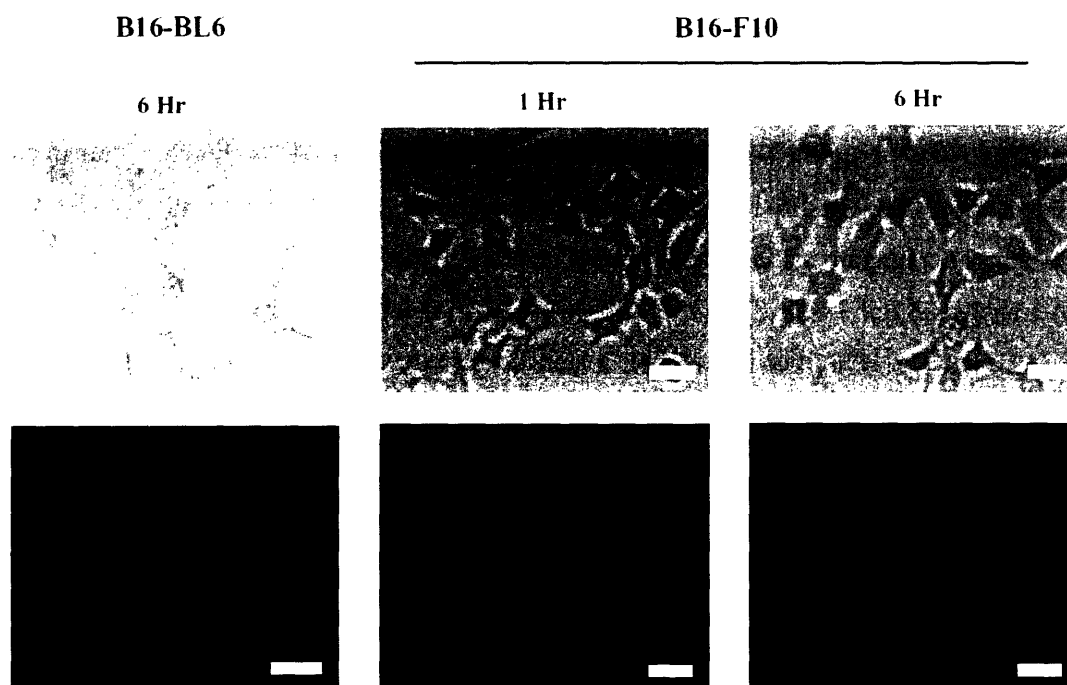


Figure 9.5. A5-Heparin exhibits cell selectivity. Cells were treated with A5-heparin (20:1, w/w, 1 µg/ml heparin) supplemented with PBS, FGF2, or sodium chlorate. Data are presented as a percent of the whole-cell count compared to the count for treatment without A5-heparin. Transfected BaF3 cells were not examined in the presence of chlorate as a result of the lack of cell surface GAGs. (B) B16-BL6 and B16-F10 cells were treated with A5-fluorescein-labeled heparin conjugates heparin (20:1, w/w, 1 µg/ml heparin). Cells were imaged with light microscopy, and fluorescein was visualized with fluorescence microscopy. Scale bars represent 10 µm.

9.2.7 Internalized heparin induces cell death

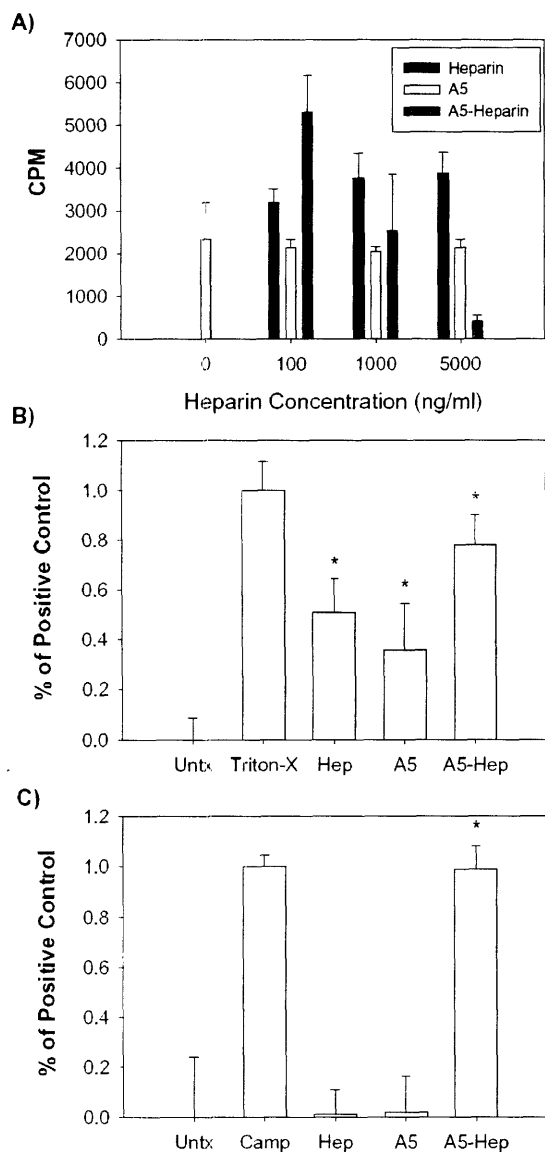


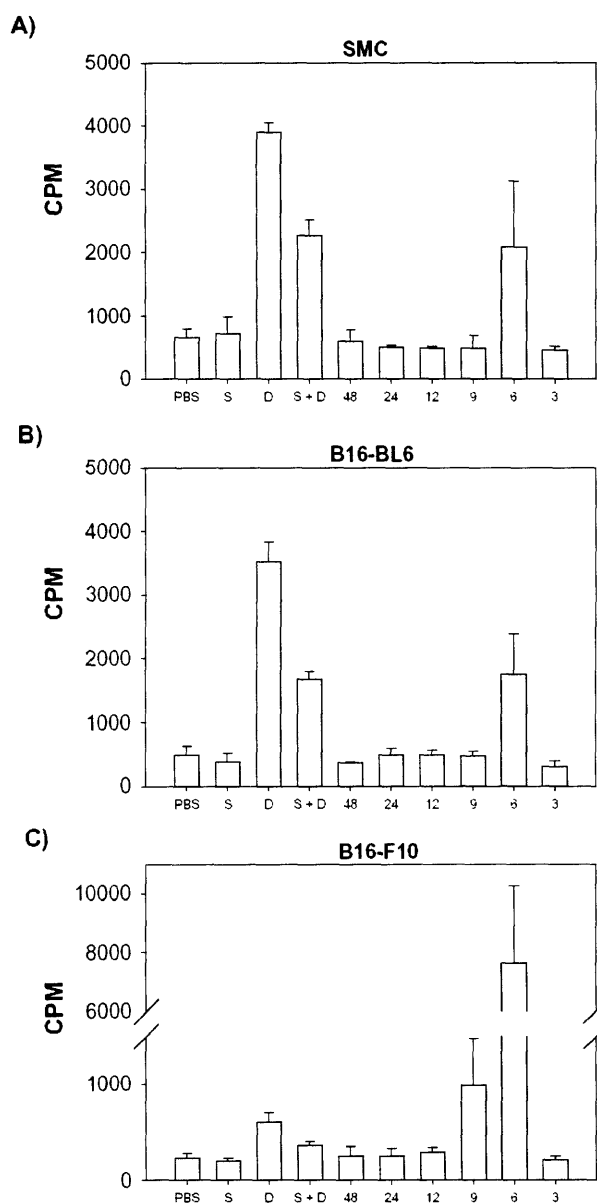
Figure 9.6. A5-Heparin induces cell death. B16-F10 cells were treated with A5-heparin conjugates at a 20:1 (w/w) ratio or with equivalent concentrations of A5 or heparin clone. (A) ³H-thymidine incorporation was measured as CPM over a range of heparin concentrations. A concentration of 0 ng/ml represents untreated cells. (B) Cytotoxicity measured by an LDH assay was determined at a 1 µg/ml heparin. Untx and Hep represent untreated and heparin treated cells, respectively. Data are presented as the percent of the positive control, determined as follows: (experimental point – negative control)/(positive control – negative control). Where untreated is the negative control and Triton-X is the positive control. (C) Apoptotic activity measured by caspase-3/-7 assays was determined at a heparin concentration of 1 µg/ml. Untx, Camp, and Hep represent untreated, camptothecin, and heparin, respectively. Data are presented as the percent of the positive control, where untreated is the negative control, and camptothecin is the positive control. An asterisk denotes $p < 0.05$ compared to the negative control.

We next sought to determine whether internalization of heparin by A5 affects specific cell processes and thus reduces the whole-cell number. We used ³H-thymidine incorporation to measure DNA synthesis in B16-F10 cells after the application of A5-heparin. The mitogenic response followed a dose-response curve, wherein low concentrations of A5-heparin *promote* ³H-thymidine incorporation and high doses inhibit it (**Figure 9.6A**). None of the equivalent A5 concentrations (20-fold greater than the heparin concentration), including the highest concentration tested, 100 µg/ml, elicited a change in mitogenesis.

The mechanism by which A5-heparin conjugates induced their effects was also examined with a lactic-acid dehydrogenase (LDH) cytotoxicity assay and a caspase-3/-7 apoptosis assay. Heparin, A5, and A5-heparin all significantly increased LDH detection compared to that in the untreated condition (**Figure 9.6B**). Heparin, A5, and A5-heparin elicited responses that were $50.70\% \pm 13.81\%$, $35.69\% \pm 18.94\%$,

and $77.93\% \pm 11.91\%$, respectively, of that caused by Triton-X, the positive control. A5-heparin conjugate activated caspase-3/-7 levels to an extent comparable to that of camptothecin, the positive control (**Figure 9.6C**). Compared to PBS, neither heparin nor A5 alone promoted a significant elevation of caspase activity, thereby suggesting that the conjugation of A5 and heparin promoted apoptosis in a way unobserved with either component alone.

9.2.8 A5-Heparin promotes early spermine incorporation



Spermine incorporation was investigated not only because cell surface HS binds to the spermine transporter, which promotes the uptake of spermine, but also because cellular proliferation is dependent on an adequate supply of polyamines [26, 27]. To this end, ^{14}C -spermine incorporation was measured over time subsequent to A5-heparin administration in SMCs and B16-BL6 and B16-F10 cells. SMCs and B16-BL6 cells showed a significant influx of ^{14}C -spermine at the 6 hr time point (**Figure 9.7**). The magnitude of this effect was 43.97% and 41.83% of that induced by difluoromethylornithine (DFMO) in SMCs and B16-BL6 cells, respectively. However, we observed an influx of ^{14}C -spermine that

Figure 9.7. A5-Heparin induces spermine incorporation at 6 hours. Incorporation of ^{14}C -spermine was measured over time after treatment of (A) SMCs, (B) B16-BL6 cells, and (C) B16-F10 cells with A5-heparin conjugates (20:1, w/w, 1 $\mu\text{g}/\text{ml}$). S and D denote 5 μM spermine and 5 mM DFMO, respectively. Numbers along the x-axis reflect conjugate incubation time. Data are presented as CPM.

was 19.61-fold greater than that observed with DFMO at 6 hr in B16-F10 cells. Furthermore, at the 9 hr time point, B16-F10 cells had 2-fold greater incorporation.

9.3 Discussion

9.3.1 Cationic polymers can bind and internalize heparin

The internalization of HSGAGs into cells has been seen as an event involved with specific processes, including growth factor signaling and membrane transcytosis. HSGAGs bind to FGF2 and FGFR1 to form a ternary complex that is internalized by endocytosis [365, 448]. HSGAGs can also facilitate membrane transcytosis, such as at the blood-brain barrier [89]. The function of HSGAGs in these cases is to regulate the biological response to and the localization of growth factors. The specific internalization of heparin as a model HSGAG could therefore, theoretically, be used for modulating cell processes involving HSGAGs within the confines of the cell.

Herein, we utilized PAEs, a class of polymers that interact with DNA via a charge-mediated mechanism. PAEs are an ideal class of polymers for delivery of DNA as a result of their low toxicity compared to that of other polymeric methods of DNA delivery, their rapid biodegradability into biologically inert compounds, and their simple synthesis [285, 286]. The primary anionic region of heparin is in the sulfate groups at the N-, 2-O, 3-O, and 6-O positions on the disaccharides that compose heparin. The high quantity of sulfate groups on heparin confers a greater negative charge than DNA [377]. Because of this, of the 70 water-soluble PAEs from a screening library of 140, all bound heparin at a 20:1 w/w ratio in optimal conditions (25 mM sodium acetate, pH 5.0). Substantial binding is similarly facilitated at suboptimal conditions. However, only a small subset of these polymers enable internalization of heparin into cells. The fact that PAEs do not enable heparin internalization as well as DNA is not surprising, however, given that a net positive charge, which may trigger endocytosis by promoting interactions with the negatively charged cell membrane, would be more difficult to achieve with a more anionic biopolymer [210]. Correspondingly, the PAEs that mediated the highest levels of DNA internalization had the most positive zeta potentials [4]. The fact that PAEs do not enable heparin internalization as well as DNA is consistent with a net positive charge required for endocytosis.

Although lysosomal escape was not specifically examined here, cationic surfaces promote interactions with the lysosome membrane and subsequent release into the cytosol [359]. Therefore, the positive zeta potentials are consistent with lysosomal escape. Apoptotic bodies visible in cultures after the addition of fluorescein-heparin conjugated to polymers uniformly exhibited fluorescence (**Figure 9.1**), suggesting even distribution of the conjugates throughout the cytosol. Furthermore, we surmise that the A5-heparin conjugate must escape into the cytosol to significantly alter the activities of transcription factors and caspases.

9.3.2 Internalized heparin affects cell processes

The 14 PAEs that internalized heparin had distinct response levels when examined in a whole-cell proliferation assay. Polymer A5 was used because the magnitude of change in the whole-cell number was greatest, suggesting either the presence of the highest quantity of internalized heparin or the most robust response induced by the internalized complex. The ability of A5-heparin conjugates as opposed to heparin or A5 alone, to affect the whole-cell number, transcription factor levels, and the HSGAG epitopes present on and around the cell, is consistent with internalization of the complex. Furthermore, complexes formed with PAEs that were shown by assays performed herein to bind but not internalize heparin had no effect on the whole-cell number.

The cellular response to A5-heparin was found to be cell specific (**Figure 9.5A**). In general, noncancerous cells produced a lower magnitude of effect than cancer cells. The upregulation of huntingtin-interacting protein-1, a cofactor in clathrin-mediated endocytosis, has been associated with various epithelial cancers [394, 410]. Endocytic rate has been demonstrated to govern cell sensitivity to exogenous agents [22]. Correspondingly, B16-F10 cells, which exhibited the greatest magnitude of response to A5-heparin conjugates, showed a much faster rate of conjugate internalization than other cells, in which less pronounced responses were induced (**Figure 9.5B**). Spermine incorporation, which is greatly increased in susceptible cells, showed maximal effects after 6 hr. SMCs and B16-BL6 cells did not show significant internalization at this time and, correspondingly, elicited lower levels of spermine incorporation (**Figure 9.7**). B16-F10s, which internalized A5-heparin conjugates within 1 hr, showed much greater levels of spermine incorporation. Cell selectivity therefore seems dependent on internalization rate.

9.3.3 Full-length heparin promotes the greatest biological response

The biological effect of internalized GAGs is not limited to heparin. Compared to GAG or polymer A5 alone, heparin, HS, LMWHs, and CS each induced some reduction in the whole-cell number. Full-length heparin, however, induced the largest effect. Heparin has the highest charge density of the four full-length GAGs tested. High-activity LMWH, however, has a similar charge density to, but a smaller biological effect than, full-length heparin. Although the relative amount of each internalized GAG was not quantified, these results suggest that high molecular weights and higher charge densities confer greater activity. Correspondingly, partial digestion of heparin with hepl [31], which cleaves highly sulfated regions of HSGAGs prior to conjugation with polymer A5, reduces the magnitude of effect observed. Although hepIII digestion, which targets undersulfated regions, also reduces the magnitude of response, the reduction is less than that observed with hepl treatment (data not shown).

9.3.4 Internalized heparin induces apoptosis

Reduction of the whole-cell number does not directly explain the mechanism of action or distinguish between general toxicity and controlled alterations to cell processes. We therefore sought to probe how internalized heparin induced cellular effects. We hypothesized that internalized heparin induces cell-mediated responses by affecting cell processes normally involving heparin, altering cell functions by the degree of negative charge in the cell, or preventing transcription factor binding.

FGF2 has an essential autocrine role in melanoma [158]. Furthermore, the FGF-FGFR complex is stabilized, and heparin promotes downstream signaling [449, 486]. The FGF2 system therefore provides an ideal approach for examining if internalized heparin alters cell processes normally involving heparin. The effects of A5-heparin conjugates in the presence of FGF2 did not yield a reduction in the whole-cell number that was distinct from the sum of the independent effects of the conjugates and FGF2. The affect of conjugates in the presence of FGF2 was similarly additive in all cell lines examined. Furthermore, when normalized to the effects of FGF2 alone the affects of internalized heparin are identical on BaF3 cells as well as those transfected with FGFR1 (data not shown). Taken together, these results suggest internalized heparin does not directly affect FGF2 signaling.

The Rb pathway is another critical pathway in the development of melanoma [217]. The mutation of Rb and other tumor suppressor proteins, including p107, causes an increase in the number of free E2F family members present [168]. We found that internalized heparin led to an upregulation of nuclear E2F-2 and cytoplasmic E2F-1. Furthermore, Rb was upregulated in the cytoplasm but downregulated in the nucleus. The levels of p107 were generally unchanged. DP-1 is not typically associated with melanomas but has been found to be upregulated in complexes with E2F [70]. Sp-1, which is similarly not thought of as important in melanomas, was upregulated in tumors, including glioblastomas [244]. With the exception of elevated levels of Rb found in the cytoplasm, the internalization of heparin promotes a cellular response that is in accordance with *promoting* melanoma growth.

Heparin internalization places a substantial quantity of a highly charged compound into cells. Although this could adversely affect cells by a nonspecific process, controlled internalization of 0.15 M trehalose actually *protects* cells from environmental changes [107]. With the addition of 1 μg heparin to 5×10^4 cells, each cell could receive up to 20 pg of internalized heparin, or ~ 0.13 M heparin, suggesting that a purely osmotic effect is unlikely. Furthermore, HA-LMWH, which has the same charge density as full-length heparin, has a much lower capacity to reduce the whole-cell number. Therefore, nonspecific charge-mediated effects do not appear to be the source of the observed biological response.

Oligosaccharides have previously been demonstrated to bind transcription factors [96]. Additionally, heparin is used for assessing the binding strength of delivery systems to DNA because the greater charge density of heparin can compete with and force charged molecules off of DNA. We found a generalized upregulation of transcription factors in both the cytosol and the nucleus. Because an ELISA technique was used for quantifying transcription factor levels, heparin could apparently increase transcription factor levels by competing with and forcing transcription factors off of DNA and thereby freeing the binding sites. Antithrombin III, however, prevents NF- κ B activation and the subsequent production of growth factors and cytokines in a heparin-dependent manner [339]. Internalized heparin therefore likely inhibits transcription factor activity either by preferentially binding DNA or by inhibiting transcription factor activation. The alterations in mitogenic response and caspase-3/-7 activity (**Figure 9.6**) are consistent with specific cell processes being affected to induce apoptosis. These results suggest

that internalized heparin reduces cell numbers by inducing apoptotic cell death via a transcription factor-mediated mechanism.

This report details a novel mechanism by which large, highly charged polysaccharides can be delivered into cells. This delivery induces a cell-specific apoptotic response, based primarily on the rate at which complexes are internalized. Because certain cancers have a higher endocytic rate, the use of internalized heparin may offer a novel approach for treating cancers. Additionally, because heparin can bind several growth factors and cytokines, delivery of heparin could serve as a platform for the development of combination therapies to treat cancer. Further work is still necessary to elucidate the specific mechanism by which internalized heparin induces apoptosis as well as to elucidate its efficacy in other cancers.

9.4 Significance

HSGAGs are anionic biopolymers involved in diverse cellular processes in the extracellular matrix. Heparin is a prototypical HSGAG that is more negatively charged than other HSGAGs as a result of the high quantity of sulfate groups found on the composite disaccharides. A library of polymers, PAEs, which interact with DNA via a charge-mediated mechanism and enable its internalization, were used for investigating the impact of free heparin within the cell. HSGAGs are normally internalized but are protein bound in the process. All water-soluble polymers bound heparin but only 14 allowed for heparin internalization. Of importance, cationic polymers that sufficiently bind heparin can promote its uptake into cells. Fewer PAEs enabled internalization of heparin than of DNA, which is consistent with conjugate endocytosis requiring a net positive charge. Only a subset of polymers that can internalize DNA would be sufficiently cationic to internalize the more anionic heparin. Polymers developed for intracellular delivery of anionic compounds therefore need a sufficient positive charge to compensate for the molecule delivered. Furthermore, the uptake of heparin into the cell induces apoptotic cell death that is preferential to specific cell types because of internalization rates. Cancer cells, which have a faster endocytic rate than noncancerous cells and correspondingly take up polymer-heparin conjugate more quickly, are typically more susceptible to the effects of polymer-heparin conjugates. Although targeting cancer based on endocytic rate alone would

likely affect macrophages and neutrophils as well, local delivery could allow for induction of cancer cell death with minimal effects to surrounding tissues. Therefore, internalizing heparin with poly(β -amino ester)s offers a new approach to induce cancer cell death.

9.5 Experimental Procedures

Proteins and reagents. Porcine intestinal mucosa heparin was from Celsus Laboratories (Columbus, OH). FBS was from Hyclone (Logan, UT). MEM, DMEM, RPMI-1640, L-15, PBS, L-glutamine, and penicillin/streptomycin were obtained from GibcoBRL (Gaithersburg, MD). Mouse recombinant IL-3 was from R & D Systems (Minneapolis, MN). B16-BL6, B16-F10, Panc-1, SK-ES-1, and SW-1088 cells were from the American Type Culture Collection (Manassas, VA). DTT and the protease inhibitor cocktail were from Sigma (St. Louis, MO). BaF3 cells transfected with FGFR1c [30] were generously provided by Dr. David Ornitz (Washington University, St. Louis, MO). NIH 3T3 cells were generously provided by Dr. Matthew Nugent (Boston University School of Medicine, Boston, MA).

Polymer-heparin conjugate synthesis. Polymers were prepared and conjugated to heparin via a similar method as that described for DNA [286]. Each polymer is named by its composite diacrylate (A–F) and amine (1–20). In brief, polymers were dissolved via vortexing in 25 mM sodium acetate (pH 5.0) and then mixed with heparin in 25 mM sodium acetate (pH 5.0) to produce the desired polymer:heparin ratio (w/w). The mixture was shaken for 30 min at room temperature. Complexes were stored at 4°C until use, which was no greater than 3 hr after conjugation.

Azure A heparin binding assay. The individual effects of heparin and polymer on the azure A colorimetric assay were first established. Azure A was dissolved in sodium acetate (pH 5.0) to produce a 0.2% (w/v) solution. Heparin and each of the 70 library-derived polymers that are soluble in sodium acetate (pH 5.0) [286] were dissolved in it to produce solutions ranging between 10 ng/ml and 1 mg/ml. Each sample at each concentration was mixed thoroughly at a 1:1 ratio with azure A in a final volume of 1 ml, and the absorbance was determined at 596 nm [238].

For polymer-azure A competition assays, 250 μ l of 20 μ g/ml heparin in 25 mM sodium acetate (pH 5.0) was mixed with 250 μ l of each of the 70 polymers in 25 mM sodium acetate to yield a final polymer:heparin ratio (w/w) of 1:1, 5:1, 10:1, or 20:1. Each 500 μ l solution was shaken for 30 min at room temperature to allow for conjugation and then supplemented with 500 μ l azure A solution. The resultant solution was incubated for 5 min at room temperature and mixed thoroughly, and the absorbance was measured at 596 nm. The amount of free heparin capable of binding azure A after polymer:heparin complexes were produced was determined by comparison of the resulting A_{596} to a standard heparin curve.

Cell culture. SMCs were isolated as described [331]. SMCs, BAECs, NIH 3T3 mouse fibroblast cells, and Panc-1 human pancreatic adenocarcinoma cells were maintained in DMEM supplemented with 10% FBS. B16-BL6 and B16-F10 mouse melanoma cells were maintained in MEM supplemented with 10% FBS. SK-ES-1 human anaplastic osteosarcoma cells were maintained in 5a media supplemented with 15% FBS. SW-1088 human astrocytoma cells were maintained in L-15 media supplemented with 10% FBS. All media were supplemented with 100 μ g/ml penicillin, 100 U/ml streptomycin, and 500 μ g/ml L-glutamine. Adhesion cells were grown in 75 cm² flasks or 150 cm² dishes at 37°C in a 5% CO₂ humidified incubator and passaged 2–3 times per week at confluence.

FGFR1c-transfected BaF3 cells were maintained as suspension cultures in RPMI-1640 supplemented with 10% FBS and 500 ng mouse recombinant IL-3. Cultures were grown in 75 cm² flasks at 37°C in a 5% CO₂ humidified incubator and passaged at a 1:10 dilution three times a week.

Conjugate internalization. Fluorescein-conjugated heparin (Molecular Probes, Eugene, OR) was complexed with polymers as for unconjugated heparin. BAECs, SMCs, and NIH 3T3 cells were grown until confluent, washed with PBS, treated with 4 ml trypsin-EDTA per 150 cm² tissue culture dish at 37°C for 3–5 min, and collected with 10 ml media. The suspension was pelleted and resuspended in 10 ml proliferation media. Cell concentration was determined with an electronic cell counter, and the solution was diluted to 5×10^4 cells/ml. Wells of 96-well plates were supplemented with 100 μ l of cell suspension. For each cell type, three wells per polymer were treated with polymer-heparin conjugates at a 20:1 (w/w) ratio to yield a final

heparin concentration of 500 ng/ml. Three wells were treated with an equivalent amount of polymer alone. Three wells for each cell type were treated with fluorescein-labeled heparin. Three wells per cell type contained untreated cells. The plates were incubated for 24 hr at 37°C and 5% CO₂ and visualized with fluorescence microscopy. Conjugates were defined as having enabled heparin internalization if 80% of cells showed fluorescence colocalized with cells in 7 of 10 high-powered fields in each of the three wells for the given conjugate, and less than 20% of cells treated with labeled heparin alone in 7 of 10 high-powered fields for each of the three wells showed similar colocalization of fluorescence with cells.

For evaluation of internalization rates, SMCs, B16-BL6 cells, and B16-F10 cells were seeded at 5×10^4 cells/ml in 24-well plates. Three wells for each cell type were treated with 10 μ l PBS, A5-fluorescein-labeled heparin conjugates (20:1, w/w; 1 μ g/ml), fluorescein-labeled heparin (1 μ g/ml), or uncomplexed A5 alone (20 μ g/ml). Cells were visualized with fluorescence microscopy every hour for 6 hr and again after 24 hr. Requirements for defining internalization were as described. Digital images were processed with Adobe Illustrator 10.0 and Adobe Photoshop 7.0.

Whole-cell proliferation assay. Adhesion cells (B16-F10, B16-BL6, SMCs, BAECs, NIH 3T3, SK-ES-1, Panc-1, and SW-1088) were seeded in 24-well plates at 1 ml/well as well as in 6-well plates at 3 ml/well, both at a density of 5×10^4 cells/ml. The plates were incubated for 24 hr at 37°C and 5% CO₂. The cells were then washed with PBS and supplemented with media as appropriate. Cells were treated with PBS, heparin, polymer, or polymer-heparin conjugate in 10 μ l quantities at appropriate concentrations. Cells were incubated at 37°C and 5% CO₂ for 72 hr. Subsequently, each well was treated with 500 μ l (24-well plates) or 1 ml (6-well plates) trypsin-EDTA for 5–15 min at room temperature, and 400 μ l was used for counting the cell number with an electronic cell counter. Assays were performed in the presence of 0.1% FBS supplemented with PBS, 5 ng/ml FGF2, or 50 mM sodium chlorate. Panc-1 cells were only tested in 10% FBS. The effects of conjugates were normalized to that of cotreatment without conjugates.

Proliferation assays on transfected BaF3 cells were performed as described [358] with slight modification. Cells were collected from 75 cm² flasks, washed three times with FBS-deficient media, and resuspended in 10 ml FBS-deficient media. Cells were diluted to 1×10^5 cells/ml based on the reading of an electronic cell counter and plated 1 ml/well in 24-well plates.

Wells were treated with PBS, heparin, polymer, or polymer:heparin conjugate in 10 μ l volumes and incubated for 72 hr at 37°C and 5% CO₂. Cell counts were determined with an electronic cell counter. The conditions employed were similar to those used for adherent cells except that FGF2 was applied at a concentration of 50 ng/ml [358]. The effects of the conjugate were normalized to the no-conjugate condition.

Immunohistochemistry. B16-F10 cultures were washed three times with PBS, dried overnight, and stored at -80°C until use. Cell cultures were rehydrated in PBS for 10 min. After being blocked for 20 min in PBS containing 0.1% (w/v) BSA, cultures were incubated with c-Myc-tagged and VSV-tagged anti-HS antibodies (AO4B05, AO4B08, AO4F12, HS4A5, HS4C3, RB4CD12, RB4CB9, RB4EA12, EW4A11, and EW4G2) overnight [481, 482]. Bound antibodies were visualized with either an anti-c-Myc-chicken monoclonal antibody (A21281; Molecular Probes) for 90 min and then an Alexa 594-conjugated goat anti-chicken IgG antibody for 60 min (A11042; Molecular Probes), or a Cy-3-labeled anti-VSV monoclonal antibody (9E10; Sigma). Cultures were washed three times for 10 min (each time) with PBS after each incubation. Finally, cultures were fixed in 100% methanol, dried, and embedded in Mowiol (10% [w/v] in 0.1 M Tris-HCl [pH 8.5]/25% [v/v] glycerol/2.5% [w/v] NaN₃). As a control, primary, secondary, or conjugated antibodies were omitted. All incubations were performed at ambient temperature (21°C) with antibody titers of half the dilution factor at which signal was abolished. Photographs were taken with a constant aperture and shutter time on a Zeiss Axioskop immunofluorescence microscope (Göttingen, Germany) equipped with a Kodak KAF 1400 CCD. Digital images were processed with Adobe Photoshop 7.0.

Mitogenic assay. B16-F10 cells were plated in 24-well plates at 5×10^4 cells/ml in 1 ml/well. Cells were serum starved for 24 hr. Polymer-GAG conjugates were added in 10 μ l volumes and incubated for 20 hr. Cells were incubated with 1 μ Ci/ml ³H-thymidine (Perkin Elmer, Wellesley, MA) for 4 hr, washed with PBS, and treated with 500 μ l of 1 M NaOH per well. The contents of each well were transferred to 7 ml scintillation vials containing 5 ml scintillation fluid and counted with a scintillation counter. Data are reported as CPM.

Transcription factor and cell death assays. For assessing the affects on transcription factors, B16-F10 cells were seeded at 5×10^4 cells/ml in 6-well plates in propagation media. Cells were serum starved and subsequently treated with PBS, A5 (20 $\mu\text{g/ml}$), heparin ($\mu\text{g/ml}$), or A5-heparin formulated at a 20:1 ratio (w/w). ELISA for transcription factors DP-1, E2F-1, E2F-2, p107, Rb, and Sp-1 proceeded according to the manufacturer's protocol (BD Biosciences, Palo Alto, CA). The relative change in transcription factor levels was measured with a spectrophotometric plate reader at 655 nm.

The LDH cytotoxicity assay (Roche, Basel, Switzerland) and the Caspase-3/7 apoptosis assay (Roche) were performed according to the manufacturers' instructions. B16-F10, B16-BL6, NIH 3T3, Panc-1, SK-ES-1, and SW-1088 cells were grown to confluence in 150 cm^2 dishes. Cells were trypsinized, pelleted, and resuspended in media. Cell concentration was determined with an electronic cell counter. The cell suspension was diluted, and cells were plated in 96-well plates as appropriate. The assays proceeded as described, and the results were determined with a spectrophotometric plate reader.

Spermine incorporation assay. Spermine incorporation was determined as described [27] with slight modification. SMCs, B16-BL6 cells, and B16-F10 cells were seeded at 5×10^4 cells/ml in 24-well plates in propagation media. Cultures were grown for 24 hr, washed twice with PBS, and supplemented with FBS-deficient media with 5 μM ^{14}C -spermine (Amersham Biosciences, Piscataway, NJ). Cells were immediately treated with PBS, heparin (1 $\mu\text{g/ml}$), A5 (20 $\mu\text{g/ml}$), or A5:heparin (20:1, w/w). Cells were treated with 5 mM DFMO, 5 μM spermine, or both DFMO and spermine as controls. After 3, 6, 9, 12, 24, and 48 hr incubations, cells were chilled and washed with ice-cold FBS-deficient media containing 1 mM spermine. Cells were lysed with 0.5 ml NaOH, which was then added to 5 ml scintillation fluid, and incorporation was determined with a scintillation counter.

Chapter 10. HSGAGs as tools and targets for Burkitt's lymphoma

10.0 Summary

Burkitt's lymphoma (BL) is a B-cell tumor associated with the Epstein-Barr virus (EBV). HSGAG-binding proteins and cell surface HSPGs are associated with a worse patient prognosis, increase EBV gene expression, and promote apoptotic cell death, and. We examined whether HSGAGs could be used to influence BL cell growth. Exogenous heparin inhibited Daudi cell growth >30%, but this effect was eliminated by the presence of serum. Heparin internalized with PAEs has been demonstrated to induce cancer cell death, but was found to promote Daudi cell proliferation $55.2 \pm 2.9\%$. These effects were PI3K-, Erk/Mek- and cell surface HSGAG-dependent. We therefore investigated whether cell surface HSGAGs would be an effective target to inhibit Daudi cell growth. Heparinase I digestion inhibited proliferation by $49.7 \pm 10.4\%$. Heparinase III and protamine sulfate additionally reduced cell growth. This data demonstrates that cell surface HSGAGs can be used to inhibit BL growth, and are therefore novel potential therapeutic target.

10.1 Introduction

BL is a highly malignant B-cell tumor characterized by a chromosomal translocation that causes constitutive activation of *c-myc* through its juxtaposition with immunoglobulin loci [237]. A translocation to the IgH enhancer, t(8:14); the Ig κ locus, t(2:8); or the Ig λ locus, t(8:22); is critical in the initiation of BL, leading to a reduction in ubiquitin conjugates and apoptotic activity as well as [147, 236]. Gene products of the EBV are involved in promoting the tumorigenicity of BL, facilitating the deregulation of *c-myc* [412, 413].

While chromosomal translocations initiate the disease, mounting evidence suggests that other factors, including extracellular matrix components such as HSGAGs, may be important regulators of BL. The EBV oncoprotein, latent membrane protein (LMP) 1, for example, induces the extracellular release of FGF2 from epithelial cells [498]. The expression of FGF2, whose activity is regulated by HSGAGs, is associated with a worse prognosis in patients with BL [180, 358]. The expression of syndecan-1, a cell surface HSPG, is correlated with the onset and proliferation of lymphoma [436]. PMA, which promotes the shedding of syndecan-1 and syndecan-4 [128], induces the lytic cycle of EBV genes as well as cell apoptosis [193]. Transforming growth factor (TGF)- β , whose activity is also modulated by HSGAGs, elicits the same effects as PMA [64, 192, 287]. Taken together, these findings suggest that HSGAGs may be important regulators of BL proliferation and cell death.

The ability of HSGAGs to regulate several diverse processes associated with BL derives from the 48 potential disaccharide units that compose the 10-100-mer HSGAG [370]. The specific arrangement of disaccharides allows for the regulation of a wide range of cell processes [38, 108, 196]. HSGAGs are linear polysaccharides found as the GAG component of HSPGs, which are found at the cell surface or free in the ECM [427]. The tumorigenicity of an HSGAG chain is distinct whether it is free in the ECM or attached to an HSPG on the cell surface [274]. Polymer-mediated internalization of heparin can promote tumor cell death in cells not affected by heparin alone [32]. Since each of the disaccharide composition and the HSGAG location make important contributions to the cellular response elicited, both aspects must be examined to understand the potential of HSGAGs as important regulators of BL growth.

In this study, we examined the ability of HSGAGs to influence BL cell proliferation. Exogenous heparin alone inhibited Daudi cell growth by inducing apoptosis. The growth inhibitory effects of heparin were abrogated, however, by serum. Internalization of heparin by PAEs, typically induces cancer cell death [32], but was found to induce proliferation of Daudi cells. The internalized heparin effect was dependent on cell surface HSGAGs and the downstream signaling cascades were associated with cell surface HSPG activity. In the presence of serum, high dose protamine sulfate, hepl, and heplIII all inhibited cell growth. These results demonstrate the importance of HSGAGs in the proliferation of BL cells, and suggest that HSGAGs may be potential therapeutic targets.

10.2 Results and Discussion

10.2.1 Heparin inhibits BL cell proliferation

A wealth of evidence has demonstrated that HSGAGs can modulate cancer cell growth [38, 131, 427]. Since HSGAG binding proteins and HSPGs are intimately connected with both the lytic cycle of EBV genes and BL cell apoptosis [193, 436, 498], we surmised that HSGAGs may also effectively regulate BL proliferation, control of which could yield potential therapeutic agents or identify important cellular targets. To examine the effect of HSGAGs on BL cells, Daudi cells, a BL cell line that contains the EBV genome and a subset of latent proteins [235, 323], were treated with heparin. Heparin treatment reduced whole cell number in a dose-dependent manner. The maximal reduction in whole cell number of $33.8 \pm 9.1\%$ ($p < 7 \times 10^{-4}$) compared to PBS was observed at $1 \mu\text{g/ml}$ heparin (**Figure 10.1**). The initial experiments were performed in the absence of serum. To examine if heparin could be effectively used as an agent to inhibit BL cell growth, Daudi cells in serum supplemented media were treated with heparin. In the presence of serum, the growth inhibitory capacity of free heparin was reduced to $7.7 \pm 9.9\%$, which was no longer a significant inhibitory effect ($p > 0.12$).

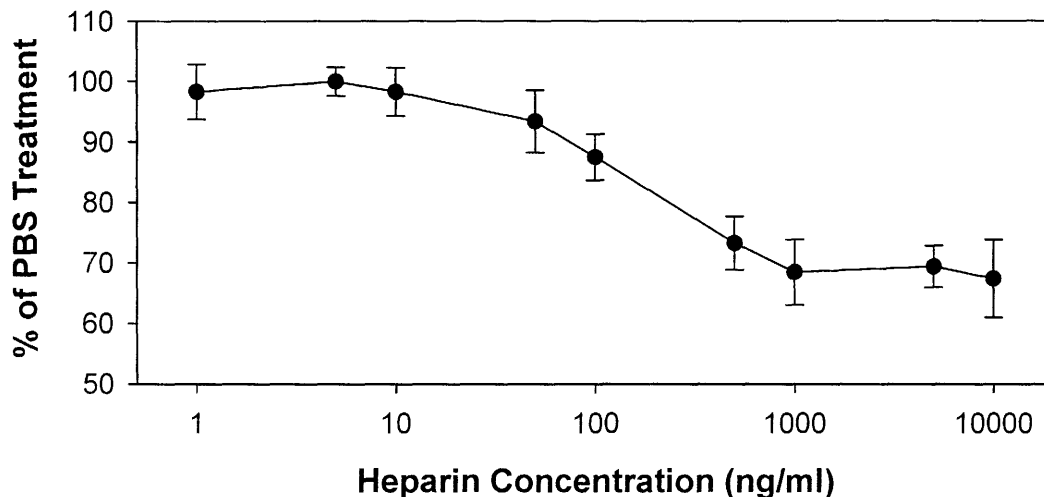


Figure 10.1. Heparin inhibits Daudi proliferation. A) Daudi cells were treated with PBS or heparin over a range of concentrations. Whole cell number was determined after three days, normalized to PBS treatment and presented as percent reduction in total cell number.

10.2.2 Polymer 1-heparin conjugates promote BL cell proliferation

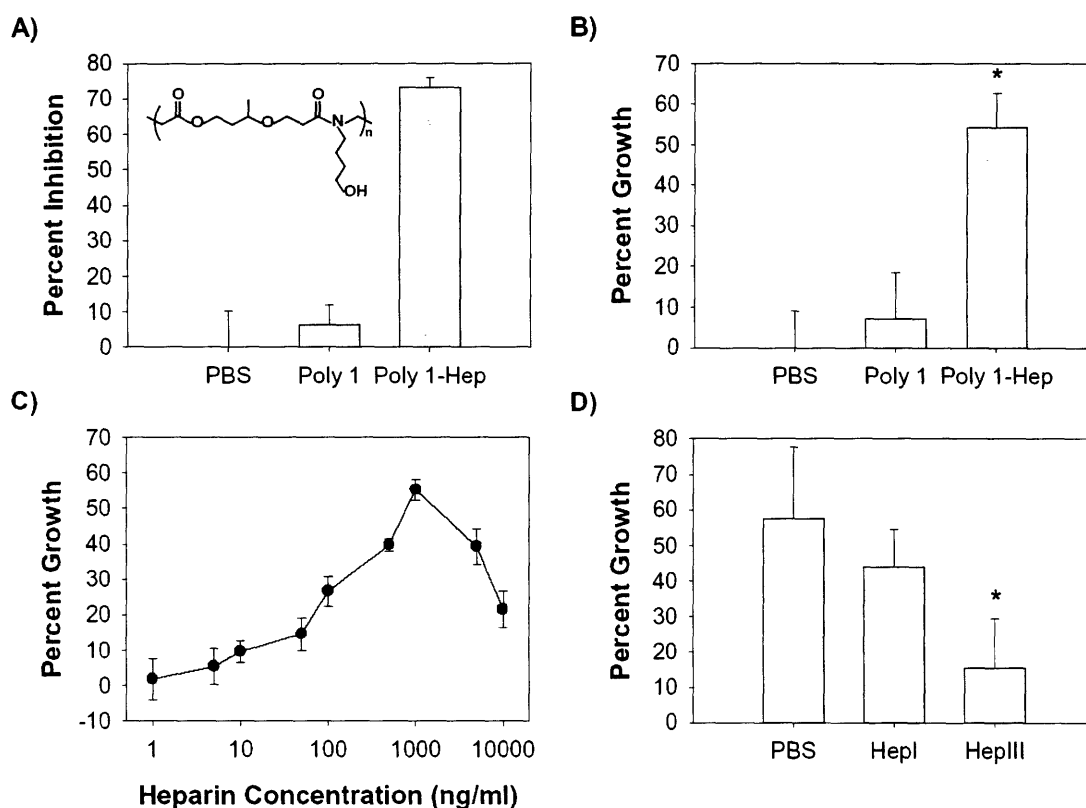


Figure 10.2. Polymer 1-heparin induces Daudi proliferation. A) B16-F10 cells were treated with PBS, 20 $\mu\text{g/ml}$ polymer 1, or polymer 1-heparin (20:1 ratio, w/w, 1 $\mu\text{g/ml}$ heparin). Whole cell number was determined after three days, and the result was normalized to PBS treatment and presented as percent reduction in total cell number. The chemical structure of polymer 1 is inlayed within (A). B) Daudi cells were treated with PBS, 20 $\mu\text{g/ml}$ polymer 1, or polymer 1-heparin (20:1 ratio, w/w, 1 $\mu\text{g/ml}$ heparin). Whole cell number was determined after three days, and the result was normalized to PBS treatment and presented as percent increase in cell number. * denotes $p < 0.05$ compared to PBS treated cells. C) Daudi cells were treated with polymer 1-heparin (20:1, w/w) over a range of heparin concentrations. Whole cell number was determined after three days. Data is expressed as percent growth compared to PBS treatment. D) Heparin was pretreated with PBS, hepI, or hepIII, and conjugated with polymer 1. Whole cell number data, obtained after three days, is presented as percent increase in whole cell number compared to treatment with PBS alone. PBS, hepI, and hepIII refer to the treatment of heparin prior to conjugation with polymer 1. * denotes $p < 0.05$ compared to polymer 1 conjugated with PBS treated heparin.

Internalizing heparin using polymer 1 induces cell death in several cancer cell lines that heparin, including those that are not effected by unbound heparin [32]. For example, polymer 1-heparin conjugates reduce whole cell number by $73.1 \pm 2.8\%$ in B16-F10 murine melanoma cells, while heparin alone had no significant effect (**Figure 10.2A**). In Daudi cells, however, polymer 1-heparin induced a $58.2 \pm 8.6\%$ increase in whole cell number compared to PBS

treated cells ($p < 2 \times 10^{-5}$; **Figure 10.2B**). Polymer **1** alone had no significant effect ($p > 0.38$). Internalization of polymer **1**-heparin conjugates was verified by fluorescence microscopy (data not shown). To verify the proliferative response, a dose-response curve for polymer **1**-heparin treatment of Daudi cells was subsequently generated (**Figure 10.2C**). The proliferative capacity of polymer **1**-heparin was dose-dependent with a maximal proliferative capacity of $55.2 \pm 2.9\%$ observed at $1 \mu\text{g/ml}$ heparin ($20 \mu\text{g/ml}$ polymer **1**). Notably, administration of polymer **1**-heparin at concentrations greater than $1 \mu\text{g/ml}$ produced less of a proliferative response.

To ensure that the heparin component was essential for the induced proliferation and to probe the structural components of heparin important in promoting proliferation, heparin was partially digested with heparinases [31] prior to conjugation. Heparinase treatments did not prevent binding to polymer **1**, as confirmed using an azure A competition assay. Digestion of heparin with hepl elicited $44.1 \pm 10.4\%$ proliferation (**Figure 10.2D**), which was not significantly less than PBS treated heparin ($p > 0.13$). Digestion with hepIII, however, produced a proliferative response ($15.5 \pm 14.0\%$) significantly less than that of PBS treated heparin ($p < 5 \times 10^{-7}$), and not significantly greater than PBS treatment of Daudi cells alone ($p > 0.11$). These results demonstrate that the proliferative capacity of polymer **1**-heparin requires the HSGAG component, based on the substrate specificity of the heparinases [104]. Furthermore, digestion with hepIII reduces the presence of domains that effectively modulate BL growth.

Daudi cells are the only cells identified to date in which growth is promoted by polymer-mediated heparin internalization. Of note, the HSGAG component digested by hepIII was the essential factor in changing growth rates, while in cells where internalized heparin promotes cell death, the HSGAG component digested by hepl is critical for inducing apoptosis [32]. Since the HSGAG component responsible for inducing Daudi proliferation is distinct from that essential for growth inhibition, we next sought to understand what cellular pathways could be involved in mediating proliferation. The cellular effects were first examined by MTS assay, in which a tetrazolium salt is used to detect mitochondrial integrity, by LDH assay, which serves as a measure of cell death. Polymer **1**-heparin produced a dose response curve by MTS assay that mimicked the whole cell count data (**Figure 10.3A**), with a maximal response that was $65.4 \pm 12.5\%$ greater than the PBS control, at $1 \mu\text{g/ml}$ heparin. The LDH cytotoxicity assay demonstrated a progressive increase LDH release with polymer **1**-heparin concentration, with no observed plateau (**Figure 10.3B**). At the maximum dose of $10 \mu\text{g/ml}$ heparin a cytotoxic

response $75.41 \pm 6.56\%$ of that induced by Triton-x, the positive control, was observed. Polymer 1-heparin therefore increases cell proliferation and cell turnover.

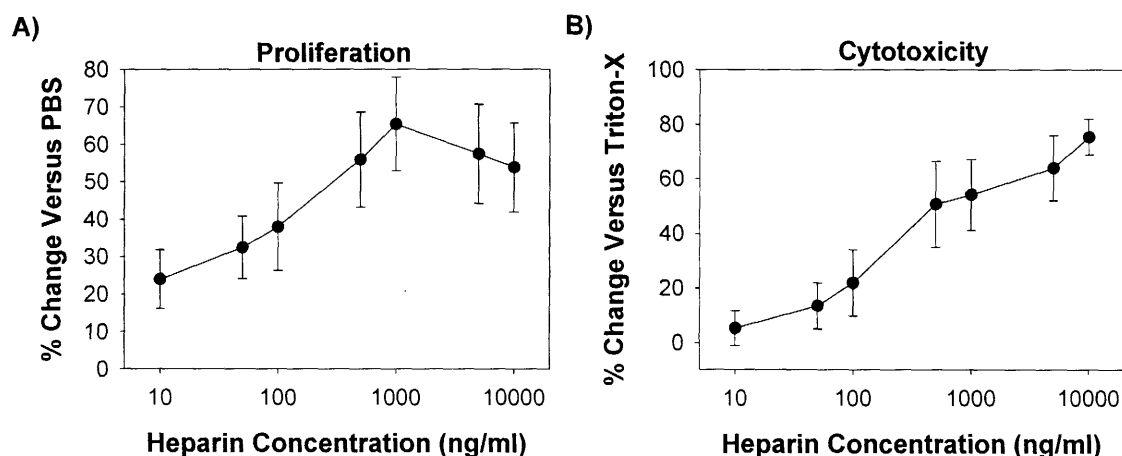


Figure 10.3. Polymer 1-heparin promotes both proliferation and cell death. Daudi cells were treated with polymer 1-heparin (20:1. w/w, 1 $\mu\text{g/ml}$ heparin) over a range of heparin concentrations. A) Proliferation was measured by MTS assay. Data was normalized as a percent change from the untreated condition. B) Cytotoxicity was measured by LDH assay. Data was converted to a percentage of the change induced by Triton-x, the positive control, relative to PBS treatment, the negative control.

To examine if the increase in cell death was a function of merely increased cell number from induced proliferation or of a distinct process, we examined the cellular response to polymer 1-heparin using a caspase-3/-7 apoptosis assay. Increasing concentrations of polymer 1-heparin promoted progressively higher levels of caspase-3/-7 activity (**Figure 10.4**). At the highest concentration examined, polymer 1-heparin induced an apoptotic response that was $19.83 \pm 2.77\%$ of that induced by camptothecin, the positive control. The cellular effects of unbound heparin were also examined by the caspase-3/-7 apoptosis assay. Heparin concentrations of 1 $\mu\text{g/ml}$ elicited the maximal response observed of $41.5 \pm 2.1\%$ of that induced by camptothecin. The finding that unbound heparin promotes apoptosis may shed insight into why at heparin concentrations greater than 1 $\mu\text{g/ml}$, polymer 1-heparin induced proliferation decreased, as measured by both whole cell counts and the MTS assay. PAEs separate from anionic substances with half-lives between 6 and 72 hours [285, 286]. If the conjugate has entered the cell, the released heparin likely contributes to the induction of cell death [32]. At the highest concentrations, sufficient unbound heparin is likely present to induce apoptosis.

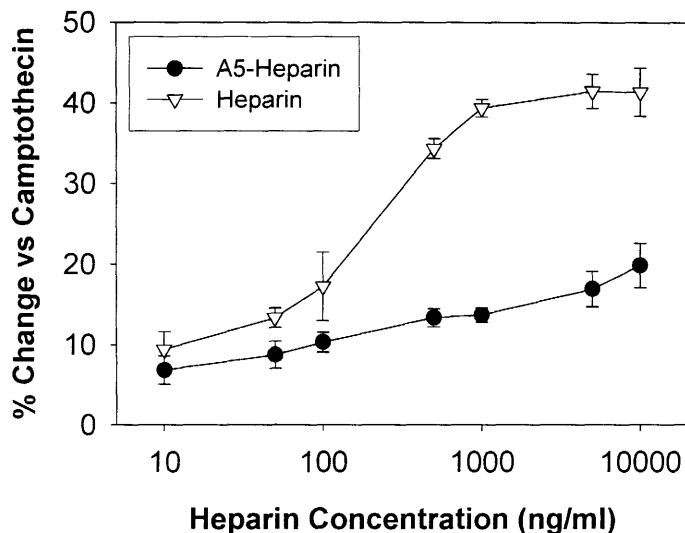


Figure 10.4. Heparin induces cell death through apoptosis. Daudi cells were treated with polymer 1-heparin (20:1, w/w, 1 $\mu\text{g/ml}$ heparin) or 1 $\mu\text{g/ml}$ heparin. Apoptosis was measured using a caspase-3/-7 assay. Data was converted to a percentage of the change induced by camptothecin, the positive control, relative to PBS treatment, the negative control.

10.2.3 Cell surface HSGAGs are necessary for polymer 1-heparin induced proliferation.

We next examined specific cellular pathways to understand by what mechanism polymer 1-heparin could be promoting proliferation. BL growth and pathogenesis can be influenced by FGF2 [180, 498], which induces the phosphorylation of PI3K and Erk/Mek [343, 344]. Kinase inhibitors were used to probe whether polymer 1-heparin could promote proliferation via these pathways. Both the PI3K inhibitor LY294002 and the Erk/Mek inhibitor PD98059 abrogated the proliferative response of polymer 1-heparin. Polymer 1-heparin, however, induced proliferation with concurrent inhibition of p38 by SB203580 ($p < 0.005$). Neither LY294002 ($p > 0.39$) nor PD98059 ($p > 0.64$) alone had a direct effect on Daudi whole cell number. These results suggest that PI3K and Erk/Mek are necessary for the proliferative response induced by polymer 1-heparin.

Daudi cells were subsequently treated with FGF2 and sodium chlorate. Should the FGF2 pathway be important in promoting Daudi proliferation, FGF2 alone should increase whole cell number, and the combination of FGF2 and polymer 1-heparin could be additive. Nonetheless,

FGF2 did not significantly increase Daudi proliferation or augment increases in whole cell number with polymer 1-heparin ($p > 0.71$; **Table 10.1**). Treatment with sodium chlorate, which prevents heparan sulfate biosynthesis [114, 395], did, however, prevent polymer 1-heparin from inducing a proliferative response. Chlorate treatment alone did not significantly affect whole cell number ($p > 0.05$). Cell surface HSGAGs are therefore necessary for polymer 1-heparin induced proliferation.

	PBS	FGF2	Chlorate
PBS	100.0 ± 12.1	100.0 ± 11.3	100.0 ± 11.4
Polymer 1	107.2 ± 15.0	129.1 ± 12.7	120.7 ± 8.7
Polymer 1-Heparin	154.2 ± 11.4	159.8 ± 16.6	<i>92.0 ± 13.7</i>
Heparin	66.2 ± 12.1	65.6 ± 11.9	69.2 ± 12.3

Table 10.1. Polymer 1-heparin proliferation requires cell surface HSGAGs. Daudi cells were pretreated with PBS, 50 mM sodium chlorate, or 10 ng/ml FGF2, and subsequently supplemented with PBS, polymer 1, polymer 1-heparin (20:1, w/w, 1 µg/ml heparin), or 1 µg/ml heparin. Whole cell number was determined after 72 hours, and normalized as the percent of the whole cell number after PBS treatment. Data is presented as the percent of cells present compared to PBS treatment. Italics denote $p < 0.05$ induced by a media supplement for a given treatment compared to the same treatment with PBS.

The requirement of cell surface HSGAGs for polymer 1-heparin-mediated proliferation is of note. Both the Erk and Wnt/ β -catenin pathways are activated and involved in proliferation downstream of Wnt signaling [518]. Additionally, LMP2A promotes PI3K activity, which is necessary for the nuclear translocation of β -catenin [315]. The overactivation of these pathways promotes EBV-mediated malignancy [316, 434]. Syndecan-1, a cell surface HSPG, modulates Wnt signaling, and can play an important role in regulating cancer development downstream of Wnt [5]. These results suggest that polymer 1-heparin may induce proliferation by influencing signal cascades downstream of cell surface HSPGs, including PI3K, Erk/Mek, and Wnt/ β -catenin. More importantly, however, these findings suggest that cell surface HSGAGs are a potential target to prevent BL cell growth.

10.2.4 Targeting BL cell surface HSGAGs maximally inhibits proliferation

We next examined whether cell surface HSGAGs could be effectively targeted to inhibit proliferation. We first attempted to directly prevent HSGAG activity without changing the HSGAGs in the ECM. Daudi cells in serum supplemented media supplemented were treated with protamine sulfate, a protein that is clinically used to counteract the effects of heparin by

preventing heparin binding to proteins rather than promoting its degradation [76, 465]. Protamine sulfate had no effect at concentrations less than 1×10^5 ng/ml (**Figure 10.5**). At 1×10^5 ng/ml, however, protamine sulfate induced a $12.9 \pm 2.8\%$ reduction in whole cell number ($p < 3 \times 10^{-6}$).

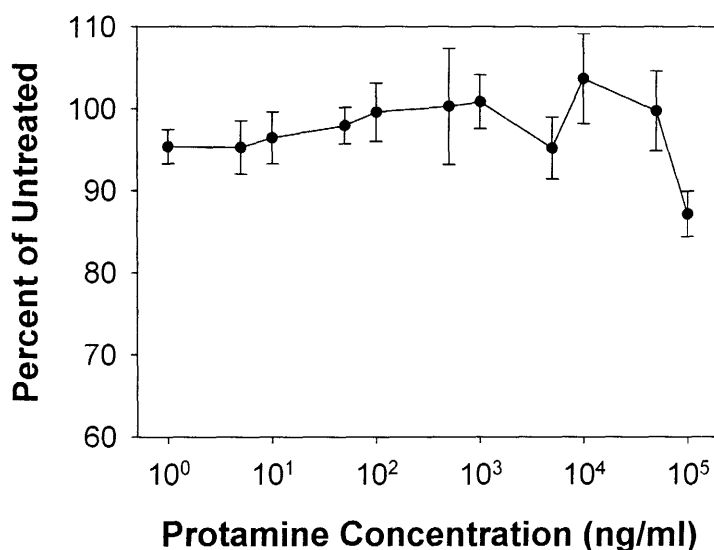


Figure 10.5. Protamine sulfate inhibits Daudi proliferation at high concentrations. Daudi cells in propagation media were treated with protamine sulfate over a range of concentrations, and whole cell number was determined after three days. Data is expressed as the percentage of the whole cell number after PBS treatment. * denotes $p < 0.05$ compared to PBS treatment.

Since only high concentrations of protmine sulfate inhibited proliferation, we next attempted to directly digest cell surface HSGAGs. Cells were treated with heparinases, which differentially digest HSGAGs based on the distribution of sulfate groups. Specifically, hepI digests highly sulfated regions and hepIII digests undersulfated regions [104]. Daudi cells in serum supplemented media were treated with heparinases for 24, 48, or 72 hours. Both hepI and hepIII inhibited proliferation in a dose-dependent manner. For hepI treatments (**Figure 10.6A**), incubations for 24 hours were more efficacious than those for 48 or 72 hours at concentrations of $50 \mu\text{U/ml}$ ($p < 3 \times 10^{-5}$) and $500 \mu\text{U/ml}$ ($p < 6 \times 10^{-5}$). Furthermore, the $49.7 \pm 10.4\%$ inhibition obtained with $500 \mu\text{U/ml}$ was significantly greater than the maximal inhibitory effect, $33.7 \pm 14.5\%$, obtained with hepIII ($p < 0.05$; **Figure 10.6B**). The time of incubation did not alter the inhibitory capacity of hepIII.

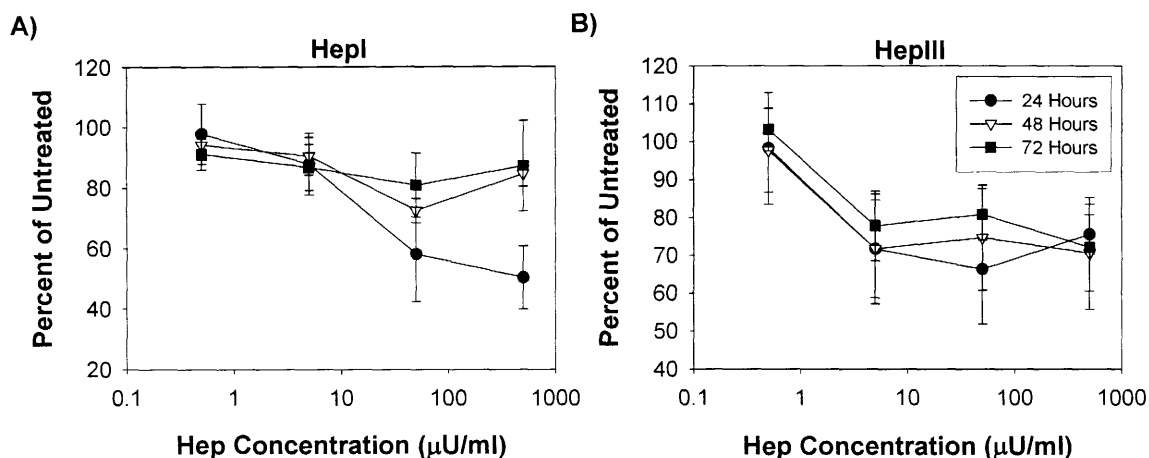


Figure 10.6. HepI inhibits Daudi proliferation. Daudi cells in propagation media (10% FBS) were treated with various concentrations of (A) hepl or (B) hepIII, and incubated for 24, 48, 72 hours. Cells were counted after the incubation, and cell number was normalized as the percent reduction in whole cell number compared to PBS treatment.

These findings reveal that treatment of BL cells with hepl provides an efficacious method to inhibit cell growth. HepIII digestion was demonstrated to eliminate the HSGAG elements essential to modulate proliferation, and correspondingly, treatment with hepIII inhibited proliferation less than hepl. Nonetheless, the ability of heparinases and high dose protamine sulfate to inhibit Daudi cell growth validates cell surface HSGAGs as an important and novel target that can be used to prevent BL growth. Future work focusing on how best cell surface HSGAGs can be used to inhibit BL proliferation will ultimately establish the therapeutic value of this target.

10.3 Significance

BL is a highly malignant B-cell cancer. HSPGs and HSGAG-binding proteins play an important role in determining the progression of this cancer as well as patient prognosis. HSGAGs may therefore be useful targets for the treatment of this cancer. Although exogenous heparin can inhibit growth, its effects are abrogated by serum. Heparin internalized by conjugation to PAEs, which normally induces cancer cell death, promoted BL cell growth.

Using this new tool to impact cell function, the key elements by which internalized heparin promotes cell growth were probed. The induced proliferation was dependent on cell surface HSGAGs, PI3K activation, and Erk/Mek activity. These three elements are all intimately related to the Wnt/ β -catenin signal cascade, which is important in the pathogenesis of several cancers including BL. As a result, cell surface HSGAGs were identified as a potential therapeutic target. The ability of high dose protamine sulfate as well as heparinase treatment to inhibit proliferation validated this novel target. This report demonstrates that internalized heparin can serve as a new tool to probe cell function when heparin alone cannot. Furthermore, cell surface HSGAGs were identified and confirmed as a potential therapeutic target for BL.

10.4 Experimental Procedures

Polymer-heparin conjugate synthesis. A single polymer, “polymer 1,” was selected for this study based on previous screens of a 140-polymer library which identified an optimized PAE-heparin conjugate that elicited a maximal cellular mediated response [32]. Polymer 1 was prepared as described [286]. To form polymer 1-heparin conjugates, polymer 1 was dissolved with vortexing in 25 mM sodium acetate, pH 5.0, and mixed with porcine intestinal mucosa heparin (Celsus Laboratories, Columbus, OH) in 25 mM sodium acetate to produce a 20:1 polymer:heparin ratio (w/w). The mixture was shaken for 30 minutes at room temperature. The complexes were stored at 4°C until use, which was no more than 3 hours after conjugation.

Whole cell proliferation assay. Daudi human BL cells (American Type Culture Collection, Manassas, VA) were maintained as suspension cultures, grown in 75 cm² flasks at 37°C in a 5% CO₂ humidified incubator, and passaged 1:10 by dilution three times a week. Daudi cells were grown in propagation media composed of RPMI-1640 (GibcoBRL, Gaithersburg, MD), 10% FBS (Hyclone, Logan, UT), 100 μ g/ml penicillin, 100 U/ml streptomycin, and 500 μ g/ml L-glutamine (GibcoBRL).

Daudi cells were collected from 75 cm² flasks, washed three times, and resuspended into 10 ml FBS-deficient media or proliferation media as appropriate. Cells were diluted to 1×10^5 cells/ml based on the reading of an electronic cell counter, and plated 1 ml/well in 24-well plates.

Wells were treated with PBS, heparin, polymer 1, or polymer 1-heparin conjugate in 10 μ l volumes, and incubated for 72 hours at 37°C, 5% CO₂. Polymer 1-heparin conjugates were additionally supplemented with 50 μ M LY294002, 20 μ M PD98059, or 1 μ M SB203580, 50 mM sodium chlorate, or 10 ng/ml FGF2, as appropriate. Whole cell number was converted to a percent increase in whole cell number relative to PBS treatment unless otherwise indicated.

For digested heparin experiments, heparin at 20 μ g/ml in PBS was incubated with 5 mU/ml hepl, 5 mU/ml hepIII, or an equivalent volume of PBS for 30 minutes. Partial digestion was confirmed by UV spectroscopy at 232 nm [31]. Digested heparin was subsequently conjugated with polymer 1. Polymer 1 binding to the heparin fragments was confirmed using an azure A competition assay as described [32]. Daudi cells, plated at 1×10^5 cells/ml in 24-well plates, 1 ml/well, were treated with conjugates (20:1 ratio, w/w, 1 μ g/ml heparin) or an equivalent volume (10 μ l) of PBS. After incubating for 72 hours at 37°C, 5% CO₂, the resultant whole cell count was determined by electronic cell counter, and data was converted to a percent growth relative to Daudi treated with PBS alone.

To examine the effects of protamine sulfate and heparinases on Daudi growth, cells were collected from 75 cm² flasks, pelleted, and resuspended into 10 ml propagation media. Cells were diluted to 1×10^5 cells/ml based on the reading of an electronic cell counter, and plated 1 ml/well in 24-well plates. Protamine sulfate was added between 1 ng/ml and 100,000 ng/ml. HepI and hepIII were added between 0.5 and 500 μ U/ml for 24, 48, or 72 hours. Whole cell counts from were converted to percent reduction in whole cell number relative to PBS-treated cells.

Conjugate internalization. Fluorescein-conjugated heparin (Molecular Probes, Eugene, OR) was complexed with polymer 1. To determine whether polymer 1 conjugation enabled internalization, confluent Daudi cultures were washed in FBS-deficient media and resuspended in FBS-deficient media. Cells were diluted to 1×10^5 cells/ml based on the reading of an electronic cell counter, and plated 1 ml/well in 24-well plates. Polymer 1-heparin conjugates (20:1, w/w, 1 μ g/ml heparin), 20 μ g/ml polymer 1, 1 μ g/ml unconjugated fluorescein-labeled heparin, and an equivalent volume of PBS (10 μ l), were each added to four wells. Cells were incubated for 24 hours at 37°C, 5% CO₂, and visualized by fluorescence microscopy. Digital

images were captured using Scion Image and processed using Adobe Illustrator 10.0 and Adobe Photoshop 7.0.

Spectrophotometric assays. Daudi cells were grown to confluence in 75 cm² plates. Cells were washed and resuspended in FBS-deficient media. The cell suspension was diluted as appropriate based on the reading of an electronic cell counter and cells were plated in 96-well plates. The MTS proliferation assay (Promega, Madison, WI), the LDH cytotoxicity assay (Roche, Basel Switzerland) and the caspase-3/-7 apoptosis assay (Roche) were performed as per manufactures' instructions, and the results were determined using a spectrophotometric plate reader. MTS data was normalized as a percent change relative to PBS-treated cells. LDH data was normalized as the percent change of that induced by the positive control (Triton-x) relative to the negative control (PBS). Caspase-3/-7 data was similarly normalized as the percent reduction of that induced by the positive control (camptothecin), relative to the negative control (PBS).

Chapter 11. Heparin and internalized heparin: dual mechanisms to Inhibit prostate cancer growth

11.0 Summary

FGF family members play an important role in the growth and progression of prostate cancer. The activity of FGFs is modulated by HSGAGs, which interact with FGFs as well as their cell surface tyrosine kinase receptors. The ability of HSGAG to regulate prostate cancer growth was investigated. Heparin was found to prevent PC-3 cell growth. This growth inhibition was attributed to heparin preventing FGF2-mediated proliferation. PC-3 tumor growth was also inhibited by heparin *in vivo*. The ability of heparin conjugated to PAEs, which promote endocytosis preferentially into cancer cells and subsequent apoptotic cell death, was additionally examined. Internalized heparin inhibited PC-3 growth more efficaciously than heparin alone *in vitro*. *In vivo*, internalized heparin prevented PC-3 tumor growth. While heparin alone had an anticoagulant effect *in vivo*, associated with reducing cancer mortality in humans by preventing pulmonary embolism, no such effect was observed with PAE-heparin conjugates. Heparin and internalized heparin can each be used to effectively inhibit prostate cancer growth. The specific systemic response, however, is governed by whether heparin is free or bound to PAEs.

11.1 Introduction

In American men, prostate cancer is the most common cancer and second leading cause of cancer death [206]. The growth and progression of prostate cancers has been associated with the activities of FGF and the FGFR. FGF1 [95], FGF2 [151], FGF6 [404], FGF8 [94], and FGF9 [152], for example, have each been demonstrated to be produced by and to regulate the activity of prostate cancer cells. The corresponding FGFRs that can support signal transduction downstream of the various FGF are also expressed by prostate cancer cells [118, 151, 356, 407].

The presence of FGFs and FGFRs provides the basis for an autocrine loop by which FGF activity is through to enhance prostate cancer cell proliferation [356].

FGF2 and its receptor, FGFR1, have emerged as critical regulators of prostate cancer as well as benign prostatic hypertrophy [151, 152, 381, 403, 407]. The mechanism by which FGF2 affects cell behavior has been extensively studied. FGFs interact not only with cell surface tyrosine kinase FGFRs, but also the HSGAG component of HSPGs [153, 348, 396]. HSGAGs interact with both the ligand and the receptor, promoting ligand and subsequent receptor oligomerization, tyrosine kinase phosphorylation, and signal transduction [163, 213, 389, 511]. HSGAGs would be expected to modulate prostate cancer given the importance of FGFs and FGFRs.

Cancer growth, progression, and mortality can all be influenced by HSGAGs [196, 523]. The 48 disaccharide building blocks that compose the 10-100-mer HSGAG biopolymer allow HSGAGs to regulate a wide variety of important processes involved with cancer, including growth factor activity and angiogenesis [133, 196, 370]. When in the ECM, HSGAGs can bind growth factors and angiogenesis promoters, preventing their activity [116]. Heparin, a highly sulfated HSGAG, can reduce the mortality associated with cancer by preventing fatal pulmonary embolisms secondary to deep venous thrombosis [79, 523]. Nonetheless, the potential therapeutic use of HSGAGs in prostate cancer has not been examined.

In this study, we examined how HSGAGs influenced PC-3 growth, both *in vitro* and *in vivo*. Heparin was found to successfully inhibit cell growth by preventing FGF2-mediated proliferation. Sufficiently high doses of heparin also inhibited tumor growth *in vivo*. Additionally, we examined whether controlled internalization of heparin by conjugation to PAEs, which targets cancer cells based on their increased endocytic rate and induces apoptotic cell death [32], could also prevent PC-3 growth. Internalized heparin more effectively inhibited PC-3 growth *in vitro* than heparin, and was not permissive to *in vivo* tumor growth. Heparin can therefore be used in multiple ways to prevent prostate cancer growth.

11.2 Results and Discussion

11.2.1 Heparin inhibits PC-3 proliferation by preventing FGF2-mediated growth.

Human prostate cancer cells express FGFs as well as the appropriate FGFR isoforms to enable a cellular mediated response both *in vitro* and *in vivo* [82, 94, 95, 151, 152, 260, 403-405]. Autocrine FGF activity through cell surface FGFRs is common in human prostate cancer. Prostate cancer cells additionally switch their FGF and FGFR expression with invasion and malignancy [510]. FGF is thought to enhance prostate cancer cell proliferation.

PC-3 cells are androgen-insensitive and highly metastatic human prostate cancer cells, whose survival can be increased by FGF2 [322, 407]. FGF2 and FGFR1 are critical regulators of prostate cancer tumorigenicity [118]. HSGAGs are known to alter the growth and progression of cancers through a variety of mechanisms including via FGF2 [274]. Although HSGAGs serve to enhance the activity of FGF2 by promoting ligand dimerization, ternary complex formation, and downstream signal transduction [511], extracellular heparin can serve as a biological “sink,” binding FGFs and preventing cellular mediated responses [116]. Heparin could therefore be an effective tool to inhibit prostate cancer growth and progression.

To investigate whether HSGAGs could be used to inhibit human prostate cancer cell growth, PC-3 cells were treated with heparin, and the effect on proliferation was determined. Heparin reduced PC-3 whole cell number in a dose-dependent manner (**Figure 11.1A**), with a maximal effect of $21.0 \pm 4.4\%$ at 500 ng/ml. HS also reduced whole cell number in a dose-dependent manner. A maximal response of a $14.3 \pm 2.6\%$ reduction in whole cell number was observed at 1 $\mu\text{g/ml}$, the maximal concentration tested. Nonetheless, heparin elicited a more potent response than HS. To confirm the ability of HSGAGs to inhibit PC-3 growth, heparin was pretreated with PBS, hepl, or heplIII. Partial digestion was confirmed and quantified by UV spectroscopy at 232 nm [31]. PBS-treated heparin reduced whole cell number $17.8 \pm 2.5\%$ (**Figure 11.1B**), not significantly different from the cellular response elicited with heplIII digested heparin ($p > 0.45$). Hepl treated heparin only reduced whole cell number by $7.0 \pm 3.5\%$, significantly less than PBS-treated heparin ($p < 0.006$). Highly sulfated HSGAGs therefore elicit the greatest growth inhibitory response from PC-3 cells.

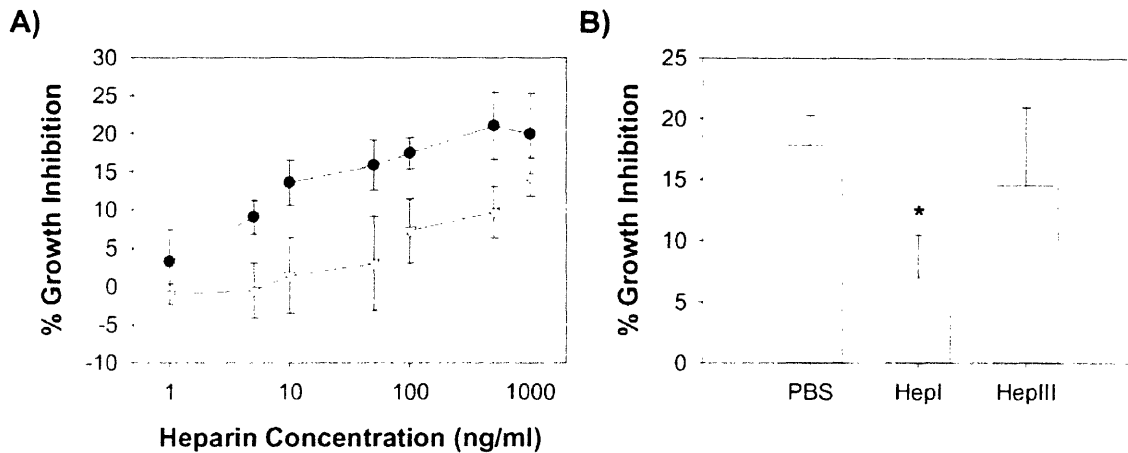


Figure 11.1. Heparin inhibits PC-3 proliferation. A) PC-3 cells were treated with various concentrations of heparin or HS. B) Heparin pretreated with PBS, hepl, or heplII was applied to PC-3 cells. Whole cell number was determined after a 72 hour incubation. Data was normalized to the final whole cell number of PBS-treated cells and presented as the percent reduction in final whole cell number.

We next sought to determine how heparin elicited its growth inhibitory effects. PC-3 cells produce FGF2, 80-90% of which remains in the cytoplasm while the other 10-20% is secreted into the ECM [82]. Heparin can inhibit the activity of angiogenic factors by preventing their interaction with cell surface HSGAGs [116]. To investigate whether heparin reduced whole cell number by inhibiting FGF2 activity, we first verified that PC-3 cells could respond to FGF2. RT-PCR demonstrated that PC-3 cells predominantly expressed FGFR1c (**Figure 11.2A**), which supports the activity of FGF2 [30, 348]. The addition of FGF2 induced the proliferation of PC-3 cells, with a maximal effect of $15.6 \pm 3.1\%$ observed with 100 ng/ml FGF2 (**Figure 11.2B**). To investigate whether heparin could reduce whole cell number by preventing FGF2 activity, PC-3 cells were treated with 100 ng/ml FGF2 and varying concentrations of heparin (**Figure 11.2C**). Heparin concentrations of 50 ng/ml and less permitted FGF2-mediated proliferation. At 100 ng/ml heparin, however, the increase in whole cell number was reduced to $7.7 \pm 3.0\%$, and at 500 ng/ml heparin, the cells responded as if no FGF2 had been added ($-0.9\% \pm 2.4\%$). Heparin can therefore prevent FGF2-mediated cell growth.

To confirm that heparin inhibited proliferation by preventing FGF2 activity, we next examined whether other techniques to block FGF2 and its downstream signaling would similarly reduce whole cell number. Correspondingly, treating PC-3 cells with antibodies to FGF2 ($56.6 \pm$

2.2%; $p < 1 \times 10^{-10}$) or to FGFR1 (58.2 ± 1.8 $p < 3 \times 10^{-12}$) reduced whole cell number. Furthermore, the addition of heparin failed to reduce whole cell number when cells were pretreated with antibodies to FGF2 (-5.0 ± 6.0 ; $p > 0.14$) or FGFR1 ($0.0 \pm 4.5\%$; $p > 0.99$). Antibodies to FGFR3 did not prevent heparin from reducing whole cell number ($p < 2 \times 10^{-6}$). The specificity of the various antibodies was confirmed (data not shown) by performing proliferation assays with BaF3 cells transfected with specific FGFRs [30, 33].

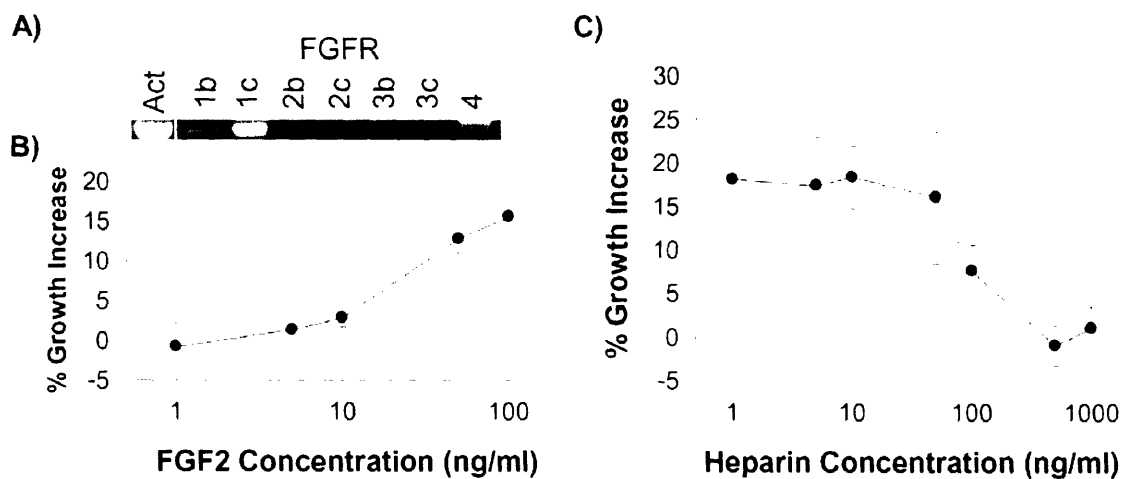


Figure 11.2. Exogenous heparin inhibits FGF2-mediated proliferation. A) RT-PCR was performed on PC-3 cells for actin (ACT) as well as FGFR isoforms (1b, 1c, 2b, 2c, 3b, 3c, and 4). B) Various concentrations of FGF2 were administered to PC-3 cells. C) PC-3 cells were treated with 100 ng/ml FGF2 and various concentrations of heparin. Whole cell number was determined after a 72 hour incubation. Data was normalized to the final whole cell number of PBS-treated cells and presented as the percent increase in final whole cell number.

Inhibition of processes downstream of FGF2, with LY294002, PD98059, or U0126, similarly prevented heparin-mediated growth inhibition. LY294002 inhibits PI3K, which is downstream of FGFRs [309]. PD98059 and U0126 inhibit Erk/Mek and Mek respectively, which are associated with the proliferative activities of FGF2 through FGFR1 [72]. The use of kinase inhibitors such as SB203580, which are not downstream of FGF2, however, had no effect. These findings provide additional evidence that heparin prevents FGF2 activity, thereby inhibiting PC-3 proliferation.

11.2.2 Heparin inhibits PC-3 cell growth *in vivo*.

Given the ability of heparin to inhibit PC-3 cell growth *in vitro*, we next examined its effects *in vivo*. PC-3 tumors were formed in the flanks of mice, allowed to grow, and heparin was injected intratumorally, either each experimental day or only once. Tumors were first injected with heparin each day ranging between 5 ng and 50 μ g per injection, for eight days. Heparin injections inhibited tumor growth compared to the vehicle (NaOAc) control (**Figure 11.3A**). Increasing amounts of heparin progressively increased the magnitude of the growth inhibitory effect of heparin up to 500 ng. Injections of greater amounts of heparin, however, did not inhibit PC-3 tumor growth to a greater extent.

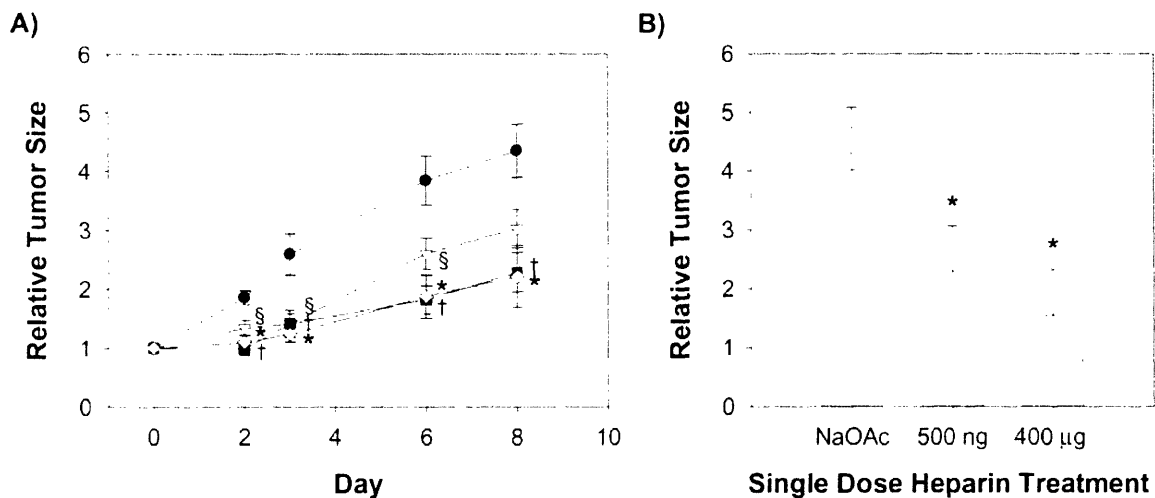


Figure 11.3. Heparin inhibits PC-3 tumor growth *in vivo*. PC-3 cells were injected into mouse flanks and allowed to grow to ~ 50 mm³ tumors. A) Tumors were treated with daily injections of NaOAc (the negative control), 5 ng, 50 ng, or 500 ng heparin, and tumor size was measured over eight days. * denotes $p > 0.05$ for tumors treated with 500 ng heparin compared to NaOAc. † denotes $p > 0.05$ for tumors treated with 50 ng heparin compared to NaOAc. § denotes $p > 0.05$ for tumors treated with 5 ng heparin compared to NaOAc. B) Tumors were injected only on day 0, with NaOAc (the negative control), 500 ng, or 400 μ g heparin. * denotes $p < 0.05$ for heparin treatment compared to the NaOAc control. Tumor volume was measured over eight days. Measurements on day 8 are presented. Data is presented as tumor size from day x /tumor size from day 0. A value of 1 denotes no growth. * denotes $p < 0.05$ compared to NaOAc.

The effects of single dose heparin was then determined (**Figure 11.3B**). PC-3 tumors were injected with heparin between 500 ng and 400 μ g (8 x 50 μ g). Treatment with 500 ng heparin significantly reduced tumor growth from 4.0 ± 1.1 -times the day 0 tumor (with NaOAc) to 2.3 ± 0.8 -times the day 0 tumor (with heparin treatment; $p < 0.05$). Increasing doses inhibited

tumor growth to a greater extent, with the most efficacious response observed with 400 μg , where final tumor volume was 1.6 ± 0.8 -times the size of the day 0 tumor, $\sim 61\%$ ($p < 0.02$) smaller than the NaOAc treated tumor. The highest dose of heparin therefore prevented tumor growth. No other single dose or repeated dose that was examined elicited this effect.

These results demonstrate that heparin effectively inhibits tumor growth. The importance of FGF-FGFR signaling has been well supported in cancer cell lines, in animal models, and in human tissues. The *in vitro* results demonstrate that heparin does inhibit FGF2 signaling and the same mechanism may enable *in vivo* prostate cancer growth inhibition. This mechanism was not confirmed in the *in vivo* experiments performed, but extensive evidence has previously validated this possibility [116, 356, 381]. Small molecule inhibitors of FGFR signaling have additionally shown preliminary success as a potential cancer therapy in clinical trials [251]. Especially as FGF2 release may be associated with more aggressive prostate cancers [82], the results presented suggest that heparin treatment may serve as an important therapeutic in prostate cancer, both by preventing tumor growth, and by preventing coagulation-related complications associated with cancer [79, 523].

11.2.3 Internalized heparin induces PC-3 cell death

Heparin itself has been demonstrated to have a wide range of potential roles in cancer growth and progression [427], and the data presented suggest potential therapeutic value in prostate cancer by inhibiting essential autocrine factors. The polydispersity of HSGAGs leads to a low percentage of sequences that regulate a given process and therefore, an increased potential for secondary, and possibly undesirable, activities [499]. Conjugating heparin with PAEs forms positively charged complexes that enable endocytosis, preferentially into cancer cells [32]. The selectivity of PAE-heparin conjugates for cancer cells is based on their increased rate of endocytosis relative to non-transformed cells, which is associated with the upregulation of factors found in epithelial tumors including those of the prostate and colon [394, 410]. We therefore investigated whether PAE-heparin conjugates would offer a more efficacious and potentially safer method to target cancer cells with heparin.

Initial studies with PAE-heparin conjugates focused on selected members of a 140-member polymer library [32, 286]. A subsequent library of 2350 polymers was constructed by the combinatorial addition of 94 amines and 25 diacrylates [7]. Nine polymers (C32, D94, E28,

F28, F32, U28, U32, JJ28, and JJ32) selected from previous screens to have the best *in vitro* transfection rates [7] were used to examine the effects of internalized heparin on PC-3 cells at polymer:heparin (w/w) ratios of 10:1, 20:1, 30:1, 40:1, and 60:1, all using a final heparin concentration of 1 $\mu\text{g/ml}$ [32]. The results of this screen identified three polymers that produced the greatest reduction in whole cell number: C32 (60:1), U 28 (60:1), and F32 (10:1). At the concentrations examined, polymer alone did not affect whole cell number (data not shown). The ability of these polymers to internalize heparin was subsequently verified by fluorescent microscopy using fluorescein-conjugated heparin [32]. These three polymers were tested specifically to validate the growth inhibition observed on the first screen (**Figure 11.4A**). C32 ($19.4 \pm 2.5\%$; $p < 6 \times 10^{-5}$), U28 ($20.1 \pm 6.6\%$; $p < 0.008$) and F32 (48.4 ± 3.2 ; $p < 6 \times 10^{-6}$) again showed substantial growth inhibition, with the greatest effects observed with F32.

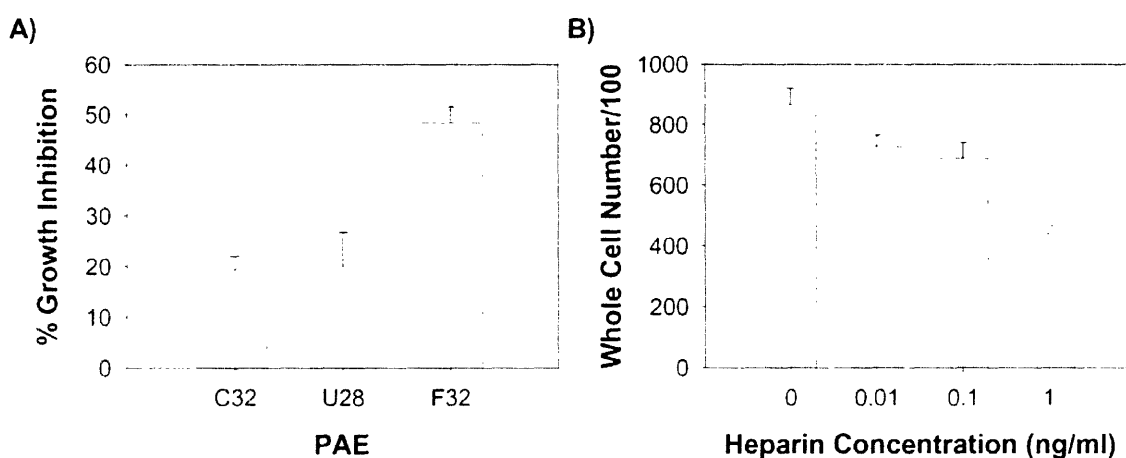


Figure 11.4. Internalized heparin inhibits PC-3 proliferation more efficiently than heparin alone. A) PAE-heparin conjugates were formed at 60:1 (w/w) for C32, 60:1 (w/w) for U28, and 10:1 (w/w) for F32 with 1 $\mu\text{g/ml}$ heparin, and used to treat PC-3 cells. B) F32 was conjugated at 10:1 (w/w) with heparin, and added to PC-3 cells at various heparin concentrations. Whole cell number was determined after a 72 hour incubation. Data was normalized to the final whole cell number of PBS-treated cells and presented as the percent reduction in final whole cell number.

A dose-response curve was produced using F32, which demonstrated that the ~50% growth inhibition observed could not be elicited by heparin concentrations less than 1 $\mu\text{g/ml}$ (**Figure 11.4B**). Furthermore, F32 alone at 10 $\mu\text{g/ml}$ did not alter whole cell counts. PC-3 cells were then treated with polymer-heparin conjugates for two hours, washed, and incubated for

three days in unsupplemented media to determine if increases in magnitudes of response were related to more rapid internalization, as previously demonstrated [32]. C32 and U28 had no effect, while F32 treatment for two hours reduced whole cell number by $10.0 \pm 0.8\%$ ($p < 0.02$).

11.2.4 Internalized heparin prevents PC-3 tumor growth

F32-heparin conjugates inhibited PC-3 cell growth not only better than the other polymer-heparin conjugates examined, but also more effectively than heparin alone. We therefore examined the effects of F32-heparin conjugates *in vivo*. PC-3 tumors were treated once with heparin (5 μg to 400 μg), F32-heparin (10:1, w/w polymer:heparin, 5 μg to 400 μg heparin), or NaOAc, and tumor volume was measured over 8 days. Liver function tests and complete blood counts were performed to identify any systemic toxicity associated with heparin or F32-heparin. No measure was significantly different than that observed with NaOAc treated rats. Consistent with previous data, heparin alone inhibited tumor growth in a dose-dependent manner, with the highest dose (1.7 ± 0.9 -times the original tumor volume) preventing significant tumor growth (Figure 11.5). F32-heparin conjugates effectively prevented tumor growth at each of 5 μg (1.5 ± 0.4 -times the original tumor volume), 50 μg (1.4 ± 0.5 -times the original tumor volume), and 400 μg (1.1 ± 0.3 -times the original tumor volume). Polymer alone had no significant effect on tumor size ($p > 0.63$). F32-heparin inhibited tumor growth significantly more than heparin alone at doses of 5 μg ($p < 0.005$) and 50 μg ($p < 0.004$). At 50 μg and 400 μg , tumors did not grow.

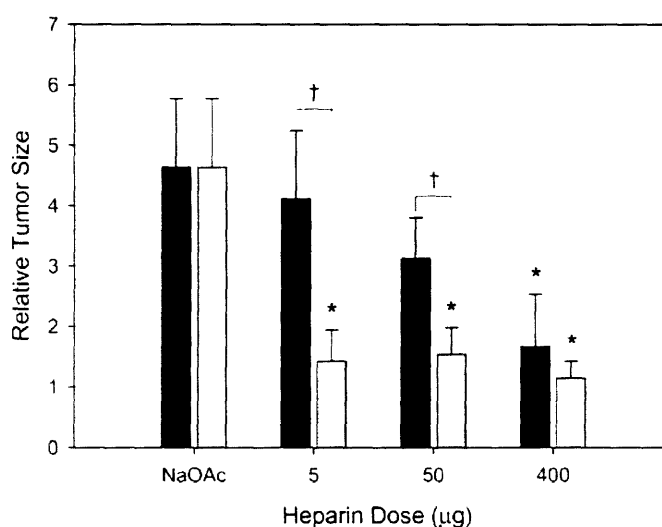


Figure 11.5. Internalized heparin prevents PC-3 tumor growth. PC-3 cells were injected into mouse flanks and allowed to grow to $\sim 50 \text{ mm}^3$ tumors. Tumors were injected once, with NaOAc (the negative control), 5 μg , 50 μg , or 500 μg heparin, or the equivalent amounts of heparin conjugated to F32 at a 10:1 polymer:heparin ratio (w/v). Tumor volume was measured over eight days. Measurements on day 8 are presented. Data is presented as tumor size from day x /tumor size from day 0. A value of 1 denotes no growth. * denotes $p < 0.05$ compared to NaOAc. † denotes $p < 0.05$ for heparin compared to polymer-heparin conjugates.

The anticoagulant effects of heparin and F32-heparin were additionally examined. Heparin reduces cancer-associated mortality through anticoagulant effects [79, 523]. Anti-Xa and anti-IIa activities were first measured *in vitro*. Heparin produced a Xa/IIa ratio of 1.3, consistent with previous findings [314]. Neither Xa nor IIa activity was detectable, however, with F32-heparin. The anticoagulant effects of heparin and F32-heparin were next examined *in vivo*. Serum was then collected from animals treated with heparin and F32-heparin, and the anticoagulant effects were determined. All doses of heparin had significant anticoagulant effects, while F32-heparin demonstrated no change in the anticoagulant profile of treated mice (data not shown). The coagulation assays additionally suggest that F32-heparin elicited the increased magnitude of response by heparin internalization rather than by slow-release. Should F32-heparin conjugates act through slow release of heparin, an anticoagulant effect would have been expected, albeit potentially less than that elicited by heparin alone. The absence of any detectable anticoagulant effect is not consistent with a slow-release mechanism. Furthermore, single dose heparin yielded a greater magnitude of response was than repeated doses. F32-heparin therefore increases the magnitude of growth inhibition in a slow release-independent manner, consistent with the previously validated heparin internalization mechanism [32].

Internalized heparin is therefore an effective way to prevent prostate cancer growth, both *in vitro* and *in vivo*, and thus warrants further investigation as a potential cancer therapeutic for prostate cancer as well as other cancers. The ability of internalized heparin to inhibit prostate cancer growth, better than heparin alone, validates the use of endocytic rate as a mechanism by which cancer cells can be targeted [32, 271]. Additionally, no side effects were detected by liver function tests, complete blood counts or coagulation assays. PAE-heparin conjugates therefore have increased anti-cancer activity *in vivo* with reduced side effects.

The data presented demonstrates that heparin can be harnessed to inhibit cancer growth by multiple mechanisms [271]. Heparin alone can prevent the activity of angiogenic and tumor growth promoting factors such as FGF2 [116], and therefore inhibit PC-3 growth *in vitro* and *in vivo*, while also exhibiting anticoagulant effects. As a result, heparin alone would serve as an important secondary anti-cancer agent by reducing tumor growth as well as potential coagulation-related mortality events [79, 523]. Conjugating heparin to PAEs can promote more potent growth inhibition without anticoagulant behavior. PAE-heparin conjugates would thus better function as a primary anti-cancer agent. Tailoring the delivery mechanism can therefore

change the anti-cancer behavior of heparin, an effect that can be harnessed to achieve a desired subset of therapeutic behaviors.

11.3 Significance

The importance of HSGAGs in regulating cancer growth, progression, and mortality has been a subject of increasing study. HSGAGs can regulate the activities of cancer cells through anticoagulant and growth factor pathways. Prostate cancer is notable because of the well defined involvement of FGFs and FGFRs. The ability of HSGAGs to modulate FGF activity suggests that HSGAGs may be important regulators of prostate cancer with potential therapeutic value. This study investigated the ability of heparin and internalized heparin to prevent prostate cancer growth both *in vitro* and *in vivo*. Correspondingly, heparin inhibited PC-3 cell and tumor growth, with high doses of heparin preventing increases in tumor size. Internalized heparin produced a greater degree of growth inhibition *in vitro*, and abrogated tumor growth at a dose ~10-fold lower than heparin alone. This finding demonstrates, for the first time, that internalized heparin is an effective method to target and kill cancer cells *in vivo*. Furthermore, no changes were observed in liver function tests or complete blood counts, validating both heparin and internalized heparin as potentially non-toxic approaches. Heparin, unlike internalized heparin, did have an anticoagulant effect. Taken together, these results suggest that heparin would be useful as a secondary agent in prostate cancer by inhibiting tumor growth as well as reducing coagulation related complications such as fatal pulmonary embolism secondary to deep venous thrombosis. Additionally, internalized heparin warrants further investigation as a potential primary anti-cancer agent for prostate cancer and other malignancy.

11.4 Experimental Procedures

Proteins and reagents. FBS was from Hyclone (Logan, UT). L-glutamine, penicillin/streptomycin, PBS, and Trizol reagent were obtained from GibcoBRL (Gaithersburg,

MD). Porcine intestinal mucosa heparin was from Celsus Laboratories (Columbus, OH). Recombinant human FGF2 was a gift from Scios, Inc. (Mountainview, CA). Recombinant heparinases were produced as described [326]. Kinase inhibitors LY294002, PD98059, SB203580, and U0126 were from Promega (Madison, WI).

Cell culture. PC-3 cells (American Type Culture Collection, Manassas, VA) were maintained in Ham's F12K medium (American Type Culture Collection) supplemented with 1.5 mg/mL sodium bicarbonate, 100 µg/ml penicillin, 100 U/ml streptomycin, 500 µg/ml L-glutamine and 10% FBS. Cells were grown in 75 cm² flasks at 37°C in a 5% CO₂ humidified incubator. Confluent cultures were split 1:3 to 1:6, two to three times per week.

Proliferation assays. PC-3 cells were grown until confluence in 75 cm² flasks. Each flask was washed with 20 ml PBS, and treated with 3 ml trypsin-EDTA at 37°C for 3-5 minutes, until cells detached. Cells were centrifuged for 3 minutes at 195 x g, the supernatant was aspirated, and the cells were resuspended in 10 ml media. The cell suspension was diluted to 50,000 cells/ml based on the readings of an electronic cell counter. The suspension was plated 1 ml/well into 24-well tissue culture plates. After a 24 hour incubation in a 5% CO₂, 37°C humidified incubator, the cells were washed with serum free media, supplemented with media containing 0.1% FBS, and incubated for 24 hours. Cells were treated with heparin, HS or FGF2 as appropriate. Heparin was added at 500 ng/ml unless otherwise noted. FGF2 was added at 100 ng/ml unless otherwise specified. Cells were then incubated for 72 hours. Wells were then washed twice with PBS and treated with 0.5 ml trypsin-EDTA/well and incubated for 10 minutes at 37°C. Whole cell number was determined using an electronic cell counter. Data was averaged over three experiments, each consisting of four wells per condition.

For antibody and kinase inhibitor experiments, antibodies and kinase inhibitors were added prior to HSGAGs or FGF2. Antibodies to FGF2, FGFR1, or FGFR3 were added to yield a final dilution of 1:100. Kinase inhibitors were added sufficient to yield final concentrations of 50 µM LY294002, 20 µM PD98059, 20 µM U0126, and 1µM SB203580.

To produce heparin digests, heparin was treated with PBS, hepI, or hepIII for 30 minutes, and boiled for 30 prior to addition to cells. Digestion was verified and quantified by UV

spectroscopy at 232 nm [31]. Digests were added to yield a final HSGAG concentration of 500 ng/ml.

Polymer-heparin conjugates. Nine polymers (C32, D94, E28, F28, F32, U28, U32, JJ28, and JJ32) were selected from a library of 2350 PAEs, as they enabled highly efficient DNA transfection [7]. Polymers were prepared as described [7]. To form conjugates, PAEs at 100 mg/ml in dimethyl sulfoxide were added to heparin in 25 mM NaOAc as appropriate to yield the desired PAE:heparin (w/w) ratio. The mixture was shaken gently at room temperature for five minutes, and diluted in PBS as appropriate for subsequent assays. Conjugates were used immediately after synthesis

A preliminary screen was performed on PC-3 cells by proliferation assay using the nine polymers described at polymer:heparin (w/w) ratios of 10:1, 20:1, 30: 1, 40:1, and 60:1. The three best formulations (polymer and ratio) were selected and analyzed further. From this, a single best polymer was selected for subsequent use. In vitro assessment of polymer activity was measured by proliferation assay with a heparin concentration of 1 µg/ml [32]. In vivo assessment was performed by intratumoral injection.

RT-PCR. A quantity of 5 µg of total RNA was isolated from PC-3 cells using Trizol reagent (Life Tech, Rockville, MD), and reverse transcription was performed with random hexamers. Specific oligomers were designed based on the published sequences of FGFR isoforms in order to detect their expression. Sequences of primer pairs corresponding to distinct FGFR isoforms were as follows: FGFR1b: 5'-TGG AGC AAG TGC CTC CTC-3' and 5'-ATA TTA CCA CTT CGA TTG GTC-3'; FGFR1c: 5'-TGG AGC TGG AAG TGC CTC CTC-3' and 5'-GTG ATG GGA GAG TCC GAT AGA-3'; FGFR2b: 5'-GTC AGC TGG GGT CGT TTC ATC-3' and 5'-CTG GTT GGC CTG CCC TAT ATA-3'; FGFR2c: 5'-GTC AGC TGG GGT CGT TTC ATC-3' and 5'-GTG AAA GGA TAT CCC AAT AGA-3'; FGFR3b: 5' GTA GTC CCG GCC TGC GTG CTA-3' and 5'-GAC CGG TTA CAC AGC CTC GCC-3'; FGFR3c: 5'-GTA GTC CCG GCC TGC GTG CTA-3' and 5'-TCC TTG CAC AAT GTC ACC TTT-3'; and FGFR4: 5'-CCC TGC CGG GAT CGT GAC CCG-3' and 5'-TCG AAG CCG CGG CTG CCA AAG-3'. To control for total cell protein, RT-PCR was also performed on β-actin using the primers 5'-GCC

AGC TCA CCA TGG ATG ATG ATA T-3' and 5'-GCT TGC TGA TCC ACA TCT GCT GGA A-3'. PCR was performed using the Advantage-GC cDNA kit from Clontech as per manufacturer's instructions (Palo Alto, CA). Prior to experimental use, primers were confirmed to detect and have specificity towards given FGFR isoforms using BaF3 cells transfected with various FGFRs [30, 31].

Measurement of anti-coagulant activity. *In vitro* anti-Xa and anti-IIa experiments were performed as described [457, 462-464]. The anti-Xa assay was performed by using S-2222 as the chromogenic substrate. The anti-IIa assay was performed by using S-2238 as the chromogenic substrate.

For *in vivo* assessment of Factor Xa and Factor IIa activity, mice were treated with heparin or F32-heparin and sacrificed by CO₂ asphyxiation within 24 hours. Cardiac puncture was used to collect ~500 µl blood per animal. For coagulation studies, blood was centrifuged the plasma was extracted, and the activities of plasma Factors Xa and IIa were measured. Plasma was diluted 1:150 in PBS to a final volume of 90 µl, and treated with 600 ng of chromogenic substrate for Factor Xa or for Factor IIa (Sigma, St. Louis MO) as appropriate in 10 µl PBS. Change in absorbance per second was measured at 405 nm.

In vivo tumor growth assays. Xenografts were generated in nude (nu/nu.c) Harlan (Indianapolis, Indiana) Sprague-Dawley rats via the subcutaneous injection of 5 x 10⁶ PC-3 human prostatic adenocarcinoma cells into each flank. Tumors were allowed to grow for 1 week until tumor volumes were approximately 50 mm³, and intratumoral injections were initiated (day 0). Only mice in which tumors on both sides were of similar size were used for the remainder of the experiment. Heparin was prepared in 2.5 mM sodium acetate in PBS, in a final volume of 100 µl. F32-heparin conjugates were produced as described at a 10:1 polymer:heparin (w/w) ratio, and diluted in PBS.

Three dosing regimens were employed. At least six mice were used for a given experimental point, predicted to yield p < 0.05 with power = 80%. First, heparin alone at various concentrations (5 ng – 50 µg) was injected into six mice per dose on day 0 and each subsequent day through the experimental end point (day 8). An equivalent volume of vehicle (referred to as

NaOAc) alone was injected into five mice. Second, six mice per dose were treated on day 0 with vehicle or heparin (500 ng to 400 μ g), and tumor size was measured over eight days. Finally, 10 mice per dose were treated once with vehicle, heparin (5 μ g – 400 μ g), or the equivalent amounts of heparin conjugated to F32 at a 10:1 polymer:heparin (w/w) ratio. Tumors were measured by caliper throughout the experiment, and volume was calculated as length x width x height x $\pi/6$. Liver function tests and complete blood counts were performed on all treated animals using blood collected via cardiac puncture.

Section 4. Novel Roles for Glycosaminoglycans

Overview:

Section 4 discusses two novel roles for glycosaminoglycans. First, cell surface heparin/heparan sulfate-like glycosaminoglycans are demonstrated to play an important role in microvascular permeability. Cationic proteins, such as those released during inflammation, initiate a cellular response through the heparinase III digestible glycosaminoglycan components of syndecan-1 and syndecan-4, by promoting their clustering and subsequent stress fiber formation. These results demonstrate, for the first time, that cell surface heparin/heparan sulfate-like glycosaminoglycans can serve as an important mediator of vascular permeability in inflammatory responses. Second, glycosaminoglycans were immobilized on substrates through direct deposition. This technique was demonstrated to produce stable surfaces based on the formation of hydrogen bonds between the glycosaminoglycans and the substrates. Immobilizing glycosaminoglycans elicits novel functions which are demonstrated to have important properties in regulating cancer growth, specifically promoting cancer cell adhesion to the surface while inhibiting growth and metastasis. Surfaces formed with heparin or heparinase III digested heparan sulfate have the most desirable properties, and may have therapeutic utility after surgeries for skin and ovarian cancer.

Chapter 12. Lung endothelial heparan sulfates mediate cationic peptide-induced barrier dysfunction: a new role for the glycocalyx

This report was previously published in *American Journal of Physiology: Lung Cell and Molecular Physiology* in 2003. See reference [98] for details. All figures in this chapter were adapted from the original publication.

12.0 Summary

The endothelial glycocalyx is believed to play a major role in microvascular permeability. We tested the hypothesis that specific components of the glycocalyx, via cytoskeletal-mediated signaling, actively participate in barrier regulation. With the use of polymers of arginine and lysine as a model of neutrophil-derived inflammatory cationic proteins, we determined size- and dose-dependent responses of cultured bovine lung microvascular endothelial cell permeability as assessed by transendothelial electrical resistance (TEER). Polymers of arginine and lysine >11 kDa produced maximal barrier dysfunction as demonstrated by a 70% decrease in TEER. Monomers of L-arginine and L-lysine did not alter barrier function, suggesting a cross-linking requirement of cell surface “receptors”. To test the hypothesis that GAGs are candidate receptors for this response, we used highly selective enzymes to remove specific GAGs before polyarginine (PA) treatment and examined the effect on TEER. Heparinase III attenuated PA-induced barrier dysfunction by 50%, whereas heparinase I had no effect. To link changes in barrier function with structural alterations, we examined actin organization and syndecan localization after PA. PA induced actin stress fiber formation and clustering of syndecan-1 and syndecan-4, which were significantly attenuated by heparinase III. PA-induced cytoskeletal rearrangement and barrier function did not involve myosin light chain kinase (MLCK) or p38 MAPK, as ML-7, a specific MLCK inhibitor, or SB-20358, a p38 MAPK inhibitor, did not alter PA-induced barrier dysfunction. In summary, lung endothelial cell heparan sulfate proteoglycans are key participants in inflammatory cationic peptide induced signaling that links cytoskeletal reorganization with subsequent barrier dysfunction.

12.1 Introduction

The aggregation of polymorphonuclear leukocytes (PMNs) is a hallmark of acute inflammation and represents a complex coordination of signals between microvascular endothelial cells and both circulating and adherent PMNs. Cytokines elaborated during infection and tissue injury activate both endothelial cells and PMNs, which promotes the sequence of PMN rolling, tethering, and ultimately, firm adhesion through the interaction of E- and P-selectins and vascular cell adhesion molecule-1 [261]. Subsequently, ligation of the β_2 -integrin receptor (CD11/18) complex on PMNs promotes the release of inflammatory peptides from azurophilic granules that further propagates the inflammatory response [43].

An important consequence of this inflammatory process is an increase in vascular endothelial permeability that results in tissue edema with attendant changes in microvascular hemodynamics, tissue oxygenation, and subsequent organ failure. In fact, microvascular dysfunction underlies the etiology of multiorgan failure after sepsis, trauma, burn injuries, solid organ transplant failure, and a host of autoimmune diseases [259, 284, 297]. Elucidating the fundamental mechanisms by which neutrophil-endothelial interaction produces subsequent changes in vascular permeability has important implications for attenuating the undesirable effects of inflammation.

Ligation of CD11/18 on PMNs initiates adhesion to microvascular endothelial cells and subsequent adhesion-dependent activation. Activated PMNs secrete cationic peptides such as heparin-binding protein/CAP37/azurocidin (HBP), elastase, and cathepsin G [43] that have been implicated in PMN-mediated vascular permeability changes, and inhibition of CD11/18-mediated adhesion of PMNs during acute lung injury [12, 218] prevents associated pulmonary edema. HBP/CAP37/azurocidin belongs to a family known as the serprocidins whose members include three active proteases (elastase, cathepsin G, and proteinase-3) and the inactive protease homolog HBP/CAP37. HBP has antimicrobial activities [368], has antiapoptotic effects in endothelium [341], and is a potent chemoattractant for monocytes and T cells [367]. Importantly, HBP/CAP37 has been reported to account for all of the vascular permeability-enhancing activity of activated neutrophils [146]. Whether receptors for HBP/CAP37 and other inflammatory

cationic peptides are present on the luminal surface of vascular endothelium has not been established. However, the strong cationic nature of HBP in conjunction with intrinsic heparin-binding characteristics suggests that a search for the HBP receptors could potentially include cell surface GAGs, including HSGAGs, implicating a component of the endothelial glycocalyx, a thick surface layer of proteoglycans whose anionic GAG side chains form an entangled meshwork on the cell surface [385]. The adsorption of serum proteins onto the GAG chains results in the formation of a gel-like layer that creates a direct physical barrier to both water and protein transport into the intercellular junction [84, 184]. In this study, we hypothesized that specific components of the glycocalyx may play an active role in barrier regulation through GAG-mediated interactions with soluble cationic ligands (like HBP), thereby activating signaling pathways associated with the cytoplasmic domain of the proteoglycan core protein. We now report size- and polymer-specific effects of diverse cationic peptides on endothelial cell cytoskeletal rearrangement and transmonolayer permeability. Our results indicate that cell surface HSGAGs are actively involved in barrier regulation and directly mediate, in part, cationic peptide-induced signaling that leads to increases in endothelial permeability and cytoskeletal reorganization. These data further suggest that the syndecan family of heparan sulfate proteoglycans participate in polycation-induced signaling and highlights a novel role for the glycocalyx.

12.2 Results

12.2.1 Polycationic peptides increase endothelial permeability

We examined the role of the polycationic peptides PA and polylysine (PL) on endothelial permeability as measured by TEER. Both PA (90 kDa) and PL (84 kDa) produced rapid decreases in TEER as demonstrated in **Figure 12.1**, with maximal permeability occurring at a concentration of 50 $\mu\text{g/ml}$. By comparison, dextran 70, a neutral polymer of similar size (70 kDa), did not affect TEER values at concentrations of 10, 50, and 100 $\mu\text{g/ml}$ (data not shown).

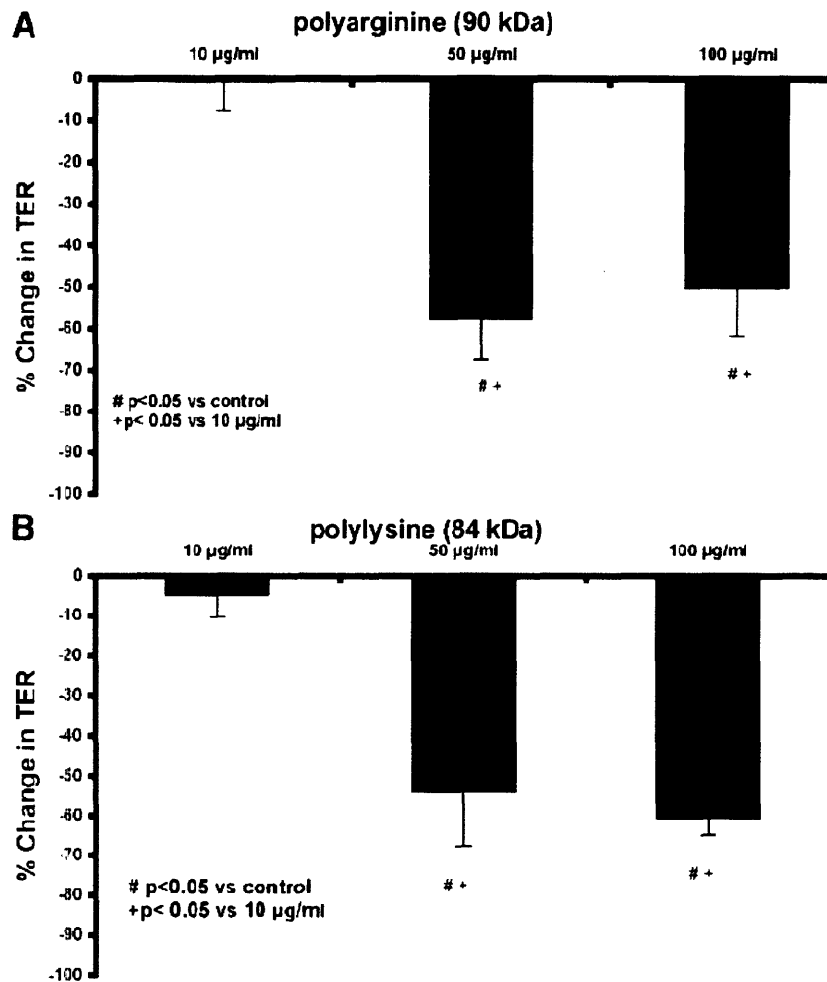


Figure 12.1. Polycations induce monolayer dysfunction. A) Polyarginine (PA: 90 kDa) dose response on endothelial cell monolayer permeability. PA ≥ 50 $\mu\text{g/ml}$ provoked an “all-or-none” loss in barrier function. B) polylysine (PL: 83 kDa) dose response on increased endothelial cell monolayer permeability. PL ≥ 50 $\mu\text{g/ml}$ also provoked a maximal change in transendothelial electrical resistance (TER). Data are means \pm SD ($n = 5-8$). # denotes $p < 0.05$ vs. control; + denotes $p < 0.05$ vs. 10 $\mu\text{g/ml}$.

We next tested the effect of polycation size on endothelial barrier function and demonstrated the multivalent requirement of cationic peptides for this response. Monomers of L-arginine failed to alter TEER (**Figure 12.2A**), whereas PA at each size tested (11.8, 38, and 90 kDa) produced maximal reductions in TEER (**Figure 12.2A**). Consistent with these results, L-lysine monomers did not significantly alter TEER (**Figure 12.2B**), whereas larger polymers of lysine (32 and 84 kDa) both reduced TEER maximally (**Figure 12.2B**). The observation that monomers of L-arginine and L-lysine failed to increase endothelial permeability supports the notion that signal activation may require cross-linking of cell surface domains. Although the

polymers of arginine and lysine used in these studies were both polydispersed, the response to the smallest PA (11.8 kDa) differed dramatically from the response to the smallest PL (7.3 kDa). PA (11.8 kDa) induced maximal barrier dysfunction, whereas the 7.3-kDa PL polymer did not affect lung TEER (**Figure 12.2B**), suggesting specificity in the response evoked by interaction between the cationic peptide structure and the unknown binding site(s) on the endothelial surface.

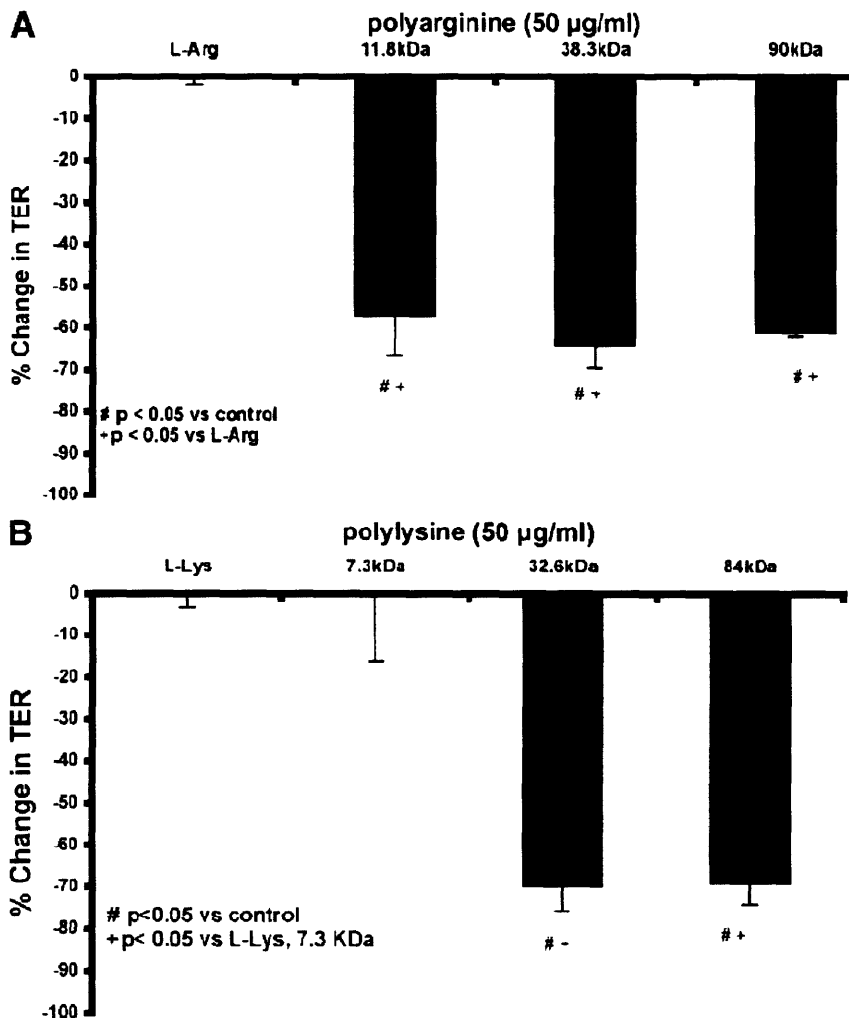


Figure 12.2. Polymers of cationic units are necessary for monolayer dysfunction. A) PA size response at 50 µg/ml on endothelial cell monolayer permeability. Monomers of L-arginine (L-Arg) had no effect on TER. All sizes of PA tested provoked maximal loss in TER. B) PL size response at 50 µg/ml on endothelial cell monolayer permeability. Monomers of L-lysine (L-Lys) and the 7.3-kDa polymer did not alter TER. PL at both 32 and 84 kDa caused maximal increase in permeability. Data are means ± SD ($n = 6-8$). # denotes $p < 0.05$ vs. control; + denotes $p < 0.05$ vs. monomers.

12.2.2 HSGAGs mediate PA-induced barrier dysfunction

We hypothesized that cationic peptides mediate cellular effects via interaction with anionic GAGs present on the endothelial surface composed primarily of HSGAGs and chondroitin sulfate-like GAGs. To examine the dependence of cationic peptide-induced decrease in TEER on endothelial GAGs, we selectively removed either HSGAGs or chondroitin sulfate GAGs via enzymatic cleavage using heparinase III and chondroitinase ABC, respectively. Removal of either heparan sulfates or chondroitin sulfates had no effect on baseline TEER; however, the removal of cell surface heparan sulfate with heparinase III significantly attenuated PA-induced permeability (~50%; **Figure 12.3**), whereas chondroitin sulfate removal did not alter PA-induced barrier dysfunction (**Figure 12.3**). We next quantified the amount of heparan sulfate removed by heparinase III pretreatment to link enzyme activity with the alterations in PA-induced barrier dysfunction. Heparinase III (15 mU/ml) pretreatment removed ~67% of the releasable heparan sulfate pool (**Table 12.1**). Given this close linkage between the amount of heparan sulfate removed and the magnitude of attenuation of PA-induced barrier dysfunction, these data suggest that heparan sulfate proteoglycans are key participants in cationic peptide-induced endothelial barrier dysfunction.

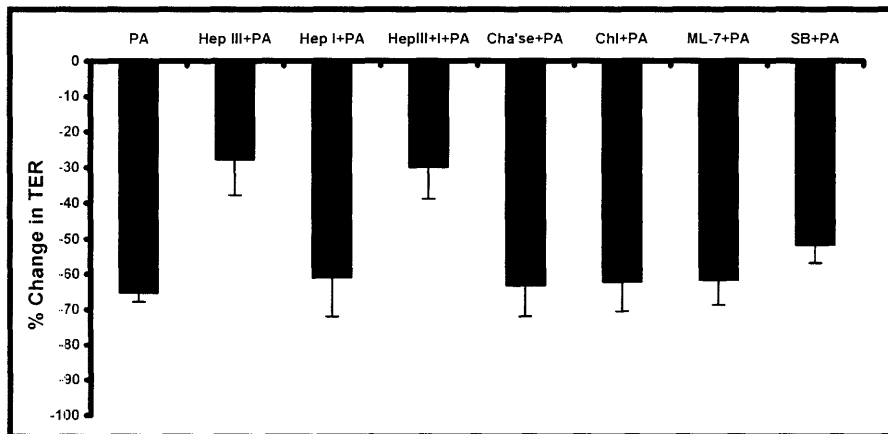


Figure 12.3. Alterations in cell surface GAGs affect polycation-induced permeability. PA (90 kDa, 50 μ g/ml) provokes an ~65% decrease in TER. Pretreatment with heparinase III (Hep III+PA) attenuated the PA-induced decrease in TER by 50%. Pretreatment with heparinase I (Hep I+PA) failed to alter the PA-mediated decrease in TER. The combination of heparinase I and heparinase III (Hep III+I+PA) had no effect beyond Hep III alone. Hep I and Hep III had no effect on baseline TER (not shown). Chondroitinase ABC lyase (Cha'se+PA) failed to alter PA-induced permeability. Cha'se had no effect on baseline TER (not shown). Chlorate treatment (Chi+PA) failed to alter PA-induced permeability. Both the myosin light chain kinase inhibitor 1-(5-iodonaphthalene-1-sulfonyl)-1H-hexahydro-1,4-diazepine HCl (ML-7: 20 μ M) and the p38 MAPK inhibitor SB-20358 (20 μ M) failed to alter the PA-induced barrier dysfunction. Data are means \pm SD ($n = 6-8$).

To exclude persistent HSGAGs not removed with heparinase III as a possible explanation for the remaining 50% of the PA-induced barrier dysfunction that was refractory to heparinase III, we pretreated monolayers with heparinase I alone and in combination with heparinase III, before PA stimulation. Heparinase III cleaves primarily between unsulfated or monosulfated saccharides within the GAG chain, whereas heparinase I generally cleaves at more highly sulfated saccharides [321]. Heparinase I alone had no effect on PA-induced barrier dysfunction, and the mix of heparinase I and III provided no additional attenuation of the PA response compared with heparinase III alone. Enzyme activity assays demonstrated that heparinase I released 40% of labeled heparan sulfate (**Table 12.1**). The combination of heparinases I and III had no effect on PA-induced TEER beyond that of heparinase III alone (**Figure 12.3**), and enzyme activity assays demonstrated no additional release when the enzymes were used in combination. We next examined the role of chondroitin sulfate-like GAGs by predigesting the cell surface with chondroitinase ABC lyase (2.5 mU/ml) before PA treatment. This dose of chondroitinase is severalfold higher than previously used [188] to remove endothelial cell surface chondroitin sulfate. Pretreatment of bovine lung microvascular endothelial cells (BLMVEC) with chondroitinase had no effect on PA-induced permeability (**Figure 12.3**), and enzyme activity assays demonstrated that chondroitin sulfate-like GAGs only accounted for 15% of cell surface-labeled GAG (**Table 12.1**).

Enzyme	Concentration mU/ml	% ³⁵ SO ₄ Released
Heparinase III	15	67
Heparinase I	15	40
Heparinase I + III	15 + 15	62
Chondroitinase	2.5	16

Table 12.1. Quantification of enzyme activity. ³⁵SO₄-releasable activity from bovine lung microvascular endothelial cells (BLMVEC) by glycosaminoglycan-degrading enzymes (see Experimental Procedures).

To correlate these enzyme results with HSGAG structure, we characterized the disaccharide composition of the HSGAGs from lung microvascular endothelial cells by capillary electrophoresis [227]. These studies demonstrated (**Table 12.2**) that 41% of the disaccharides

were monosulfated and 59% were unsulfated disaccharides. The predominance of monosulfated and unsulfated disaccharides directly correlates with the observed activity of heparinase III [321] and the observed attenuation of the PA-induced permeability response by heparinase III pretreatment.

Disaccharide	BLMVEC in MCDB-131	BLMVEC in SF-RPMI 1640	BLMVEC in SF-RPMI 1640 + chlorate, 50 mM
$\Delta U_{2S}H_{NS,6S}$	0	0	0
$\Delta U_{2S}H_{NS}$	0	0	0
$\Delta UH_{NS,6S}$	0	0	0
$\Delta U_{2S}H_{NAc,6S}$	0	0	0
ΔUH_{NS}	0.83	0.63	0.25
$\Delta U_{2S}H_{NAc}$	12.91	14.46	5.56
$\Delta UH_{NAc,6S}$	27.77	26.23	11.27
ΔUH_{NAc}	57.87	58.31	82.73

Table 12.2. Heparan sulfate disaccharide composition. Heparan sulfate from BLMVEC was digested completely, and disaccharides were identified by capillary electrophoresis. Disaccharide composition was measured in cells cultured in standard culture medium (MCDB-131), in sulfate-free RPMI 1640 (SF-RPMI 1640), and sulfate-free RPMI 1640 plus 50 mM sodium chlorate for 24 hours. U, uronic acid, H, glucosamine, 2S, 2-O-sulfate, 6S, 6-O-sulfate, NAc, N-acetyl, NS, N-sulfate.

12.2.3 HSGAG sulfation level does not affect PA-induced permeability

To investigate the structural requirements of HSGAGs in mediating PA-induced signaling, we pretreated monolayers for 24 h with sodium chlorate in sulfate-free RPMI 1640, which reduces endothelial HSGAGs by 65% (**Table 12.2**) and chondroitin sulfation by 90% [188]. Chlorate treatment failed to alter either baseline TEER or PA-induced barrier dysfunction (**Figure 12.3**), suggesting that simple charge interaction alone is not solely responsible for mediating PA binding and associated signal activation but requires an additional specific structural characteristic of the repeating disaccharide units.

12.2.4 Anti-syndecan and anti-heparan sulfate antibody cross-linking and endothelial barrier function

The size-dependent effect of polycations on barrier dysfunction suggests that peptide-mediated cross-linking of heparan sulfate chains may be a necessary step for activating pathways

that result in increased endothelial permeability. We attempted to cross-link heparan sulfate chains using polyvalent antibodies (IgM class), raised against lung fibroblast heparan sulfates, with and without isotype-specific secondary antibodies while simultaneously measuring TEER. The rationale of these studies was to determine whether other mechanisms of heparan sulfate cross-linking would also elicit barrier dysfunction. Antibodies to syndecan-1, syndecan-4, and heparan sulfate were added to endothelial monolayers after establishing stable baseline electrical resistance as described above. Dilutions for each antibody was as follows: anti-syndecan-1 (N-18) 1:50; antisyndecan-4 (N-19) 1:50; anti-heparan sulfate 1:50. Isotype-specific secondary antibodies were used at 1:50, 1:40, and 1:50 dilutions, respectively.

Neither anti-heparan sulfate antibodies alone nor the addition of a secondary antibody to promote a lattice formation influenced barrier function (data not shown). In addition, cross-linking of the syndecan core protein, the primary heparan sulfate proteoglycans on endothelial cells, with anti-syndecan antibodies, both with and without isotype-specific secondary antibodies (to promote extended cross-linking), failed to alter barrier function (data not shown). These observations suggest that cross-linking per se is insufficient to activate the appropriate pathways that lead to increases in permeability and suggest that there are specific structural requirements for both the cationic peptide and the heparan sulfates to activate permeability-related signaling pathways.

12.2.5 PA induces syndecan-1 and syndecan-4 clustering and actin stress fiber formation

Alterations in cytoskeletal organization within vascular endothelial cells are well recognized as central mechanisms determining barrier regulation [97]. Actin stress fiber formation and altered cell function can be induced by antibody-mediated clustering of cell surface syndecan [385]. Therefore, to correlate functional changes in endothelial monolayer permeability with structural changes that account for increased permeability, we examined syndecan-1 and syndecan-4 localization and actin organization in response to PA challenge. In control endothelial cells, syndecan-1 distribution was limited to the cell periphery (**Figure 12.4A**), and cells demonstrated the typical peripheral actin band with a few centrally located stress fibers (**Figure 12.4B**). Treatment of endothelial monolayers with PA (90 kDa, 50 μ g/ml) caused a significant change in syndecan-1 distribution, from a continuous peripheral pattern to a

punctuate pattern consistent with clustering (**Figure 12.4C**), and altered the polymerized actin cytoskeleton from a peripheral distribution to predominately cytoplasmic stress fibers (**Figure 12.4D**). These changes in syndecan-1 and actin were associated with gap formation between adjacent endothelial cells (**Figure 12.4D**, arrows), consistent with the associated increase in monolayer permeability reflected by TEER.

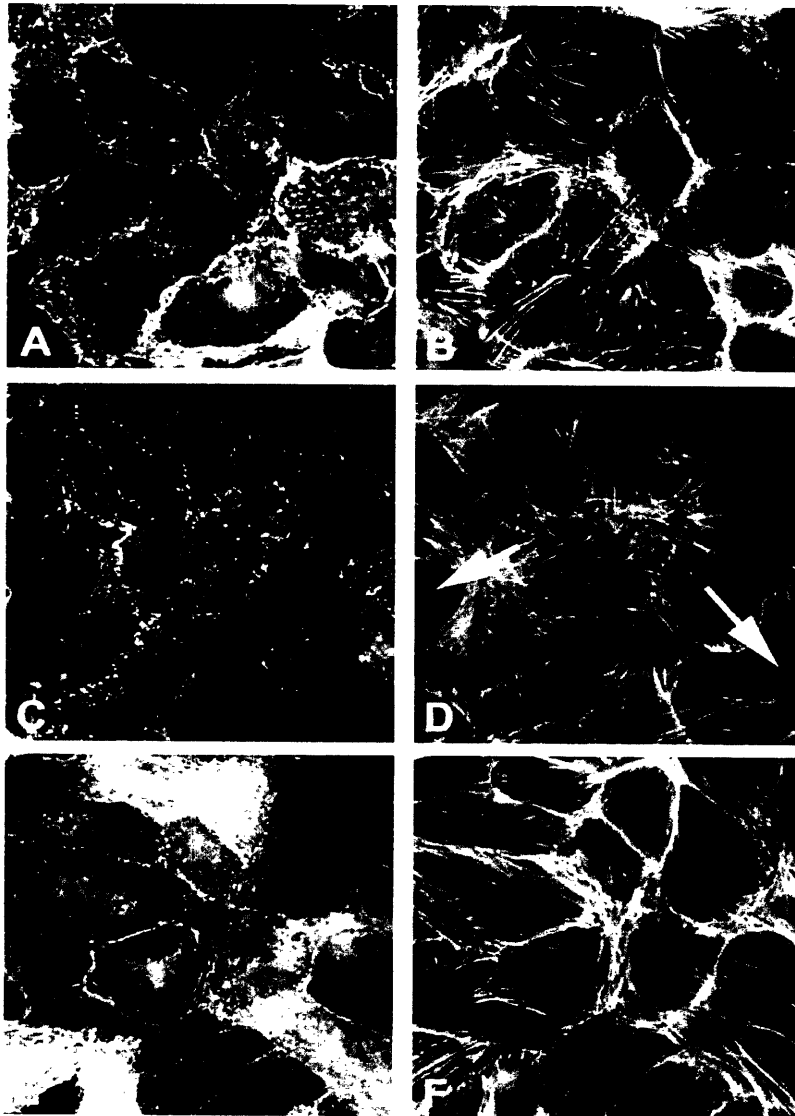


Figure 12.4. Heparinase III treatment attenuates PA-induced peripheral syndecan-1 clustering.

A) Immunofluorescence images of syndecan-1 showing peripheral staining pattern in control cells. B) Control cell actin staining showing cortical actin and some stress fiber. C) PA (90 kDa, 50 µg/ml, 30-minute incubation) induced syndecan-1 clustering around periphery and caused loss of cortical actin with concurrent actin stress fiber formation (D) that is associated with intercellular gap formation (arrows). E) Heparinase III pretreatment (15 mU/ml for 1.5 h) attenuated PA effects on syndecan-1 localization and prevented loss of cortical actin and also prevented intracellular gap formation (F). Heparinase treatment alone had no effect on syndecan-1 or localization (not shown).

Under basal conditions, syndecan-4 staining localized to the cell periphery, as did actin, specifically at areas of cell-cell contact; there was also significant perinuclear staining (**Figures 12.5A and C**). After PA treatment, syndecan-4 was notably absent from cell-cell contacts and

demonstrated reduced staining in the perinuclear region but demonstrated enhanced localization in a linear pattern throughout the cytoplasm (**Figure 12.5B**), suggestive of colocalization with actin (**Figure 12.5D**) and/or microfilaments. Thus both syndecan-1 and syndecan-4 demonstrated significant changes in localization after PA stimulation, and these changes occurred in association with dramatic actin stress fiber formation.

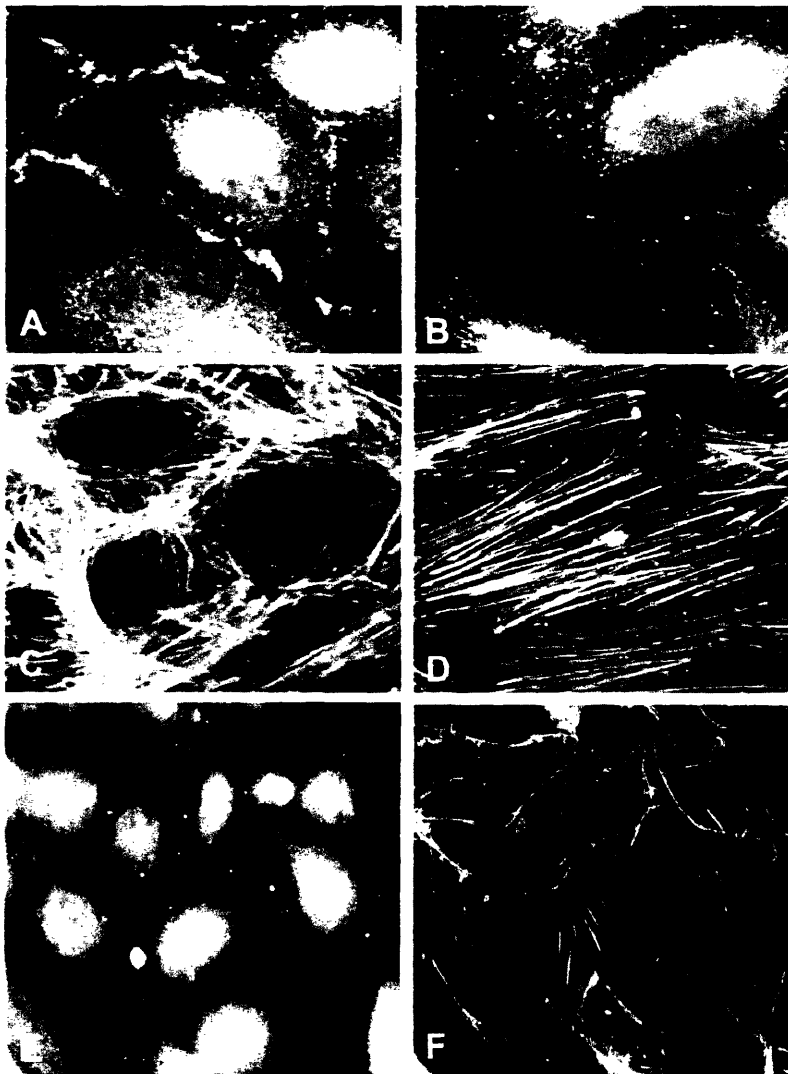


Figure 12.5. Heparinase III attenuates PA-induced peripheral syndecan-4 loss and stress fiber formation.

A) Control cell syndecan-4 staining shows a dense peripheral staining pattern. B) PA (90 kDa, 50 $\mu\text{g}/\text{ml}$, 30-min incubation) causes loss of peripheral syndecan-4 and localization of syndecan-4, suggestive of actin or microtubule/microfilament association. C) Control cells display dense cortical actin. D) PA treated cells display dense stress fibers. E) Hep III pretreatment (15 mU/ml, 1.5 h) partially attenuated PA-induced loss of peripheral syndecan-4 and attenuated actin stress fiber formation (F).

12.2.6 Heparinase III pretreatment abolishes PA-induced actin cytoskeletal reorganization and syndecan localization

To confirm that HSGAGs were directly involved in mediating syndecan clustering and actin reorganization, cell surface heparan sulfates were removed with heparinase III before treatment with PA. Immunofluorescent studies revealed that removal of cell surface heparan sulfates completely abolished PA-induced actin reorganization, syndecan-1 clustering, and interendothelial gap formation (**Figures 12.4E and F**), whereas heparinase III treatment alone had no effect on actin or syndecan-1 localization (data not shown). Heparinase III pretreatment also attenuated PA-induced syndecan-4 clustering and actin reorganization (**Figures 12.5E and F**).

12.2.7 Signaling pathways involved in cationic peptide-mediated barrier dysfunction

Increases in endothelial cell stress fibers implicates an activation of the endothelial cell contractile apparatus. We examined the role of two major signaling pathways known to contribute to endothelial cell stress fiber formation, MLCK, and p38 MAPK [141] [144] on cationic peptide-mediated endothelial permeability. To examine the role of MLCK on myosin light chain phosphorylation, we first assessed the levels of myosin light chain phosphorylation after a PA challenge and found that PA did not increase the level of phosphorylation of myosin light chain (data not shown). Consistent with these results, 1-(5-iodonaphthalene-1-sulfonyl)-1H-hexahydro-1,4-diazepine HCl (ML-7), a specific MLCK inhibitor, was used at a concentration (20 μ M) that has been shown to completely inhibit MLCK phosphorylation in response to numerous agonists [490] and failed to alter PA-induced barrier dysfunction as assessed by TEER (**Figure 12.3**), suggesting that PA acts through MLCK-independent pathways to modulate cytoskeletal organization and barrier function. We have also previously reported a p38 MAPK pathway [144, 362] leading to marked stress fiber not associated with myosin light chain phosphorylation. To assess this signaling pathway, we tested SB-20358, a p38 MAPK inhibitor, which failed to affect the PA response on TEER (**Figure 12.3**). The concentration of SB-20358 used (20 μ M) has been shown to significantly inhibit p38 MAPK [325]. These results suggest a

novel mechanism of stress fiber formation that does not require an increase in either MLCK or p38 MAPK activity.

12.3 Discussion

In this study, we demonstrate that endothelial HSGAGs mediate cationic peptide-induced signaling that leads to endothelial cytoskeletal rearrangement and barrier dysfunction. This cationic peptide-mediated loss in barrier function was associated with syndecan-1 and syndecan-4 clustering and actin stress fiber formation; removal of cell surface HSGAGs attenuated these responses. Together, these observations suggest that syndecan heparan sulfates serve as an endothelial cell surface binding domain for cationic peptides and initiate stimulus/coupling responses that signal via the actin cytoskeleton to increase endothelial permeability. However, it is likely that there are additional participants involved in this complex signaling pathway that lead to changes in endothelial barrier function. These data provide the first account in identifying an endothelial-surface binding domain for inflammatory cationic peptides and provide mechanistic insight for the recent observations of Gautum et al. [146], who demonstrated that the neutrophil-derived cationic peptide, HBP, is responsible for the increase in vascular permeability produced by endothelial cell interaction with activated neutrophils.

Like HBP/CAP37, PA and PL are highly cationic molecules that have been utilized as models of neutrophil- and eosinophil-derived cationic peptides [327, 429]. PL promotes edema formation when injected intradermally [327] and increases lung epithelial permeability when instilled into the intra-alveolar space [429]. The mechanism(s) responsible for these effects was unknown, and the direct effects of cationic peptides on endothelial and epithelial cells could not be separated from secondary paracrine mediators, such as mast cell degranulation or macrophage activation. Polycation-induced permeability was postulated to occur through charge-mediated binding to anionic sites on the cell surface, presumably sulfated proteoglycans [327]. The cellular effects of polycations are size dependent [327], suggesting that cationic peptides cross-link cell surface domains, and the greater the number of cross-linked "receptors" the greater the intensity of signal amplification. Our data support this concept, since monomers of L-arginine and L-lysine

failed to alter endothelial barrier properties, whereas larger polymers induced maximal signal activation and greater changes in permeability.

Our results with the small polycation polymers require specific comment as the 11.8-kDa polymer of arginine induced maximal barrier dysfunction, whereas the smallest lysine polymer (7.3 kDa) did not alter endothelial permeability. Because the cationic peptides used in this study were all polydispersed, we expected similar results for these two peptides. The difference between the size response of PA (11.8 kDa) and PL (7.3 kDa) suggests there is structural specificity of the putative binding domain for these basic amino acid residues. The lack of effect of sodium chlorate on PA-induced barrier dysfunction further suggests that the interaction of PA with its receptor involves more complex stereoselectivity as opposed to simple charge interaction.

The specificity for arginine-mediated binding to heparan sulfate has been reported by Liu and colleagues [275], who demonstrated that the binding of tissue factor pathway inhibitor-2/matrix-associated serine protease inhibitor to heparan sulfate and dermatan sulfate occurred selectively through arginine-mediated interaction. Likewise, Michel and colleagues [301] demonstrated that serum albumin reduces capillary permeability via arginine-mediated interaction with the endothelial cell surface, whereas modification of lysine residues had no effect on the ability of albumin to modulate permeability; similar results were obtained when modified albumins were tested on the permeability of cultured endothelial cells [384]. Last, Vepa et al. [489] demonstrated that PA was more potent in activating endothelial cell phospholipase D compared with PL. Thus our data are consistent with a number of reports demonstrating that whereas arginine and lysine residues carry the same electrical charge, other structural characteristics allow endothelial proteins and HSGAGs to discriminate between these residues.

A specific focus of this work was to characterize the endothelial receptor for inflammatory cationic peptides with endothelial HSGAGs as likely candidates. Endothelial cells express three HSGAGs, including perlecan, syndecan, and glypican. Of the three, only the syndecans are known to influence cytoskeletal organization, cell-cell adhesion, and motility [528]. Given that these processes are associated with changes in vascular permeability [97], syndecans were the most likely candidate molecule in our search for a cationic peptide receptor. To establish that syndecans participate in cationic peptide-induced signaling, we examined syndecan localization after stimulation with PA and found PA induced 1) actin stress fiber

formation, 2) syndecan-1 to cluster around the cell periphery, and 3) syndecan-4 to distribute in a centralized linear pattern, suggestive of localization with actin or microfilaments and/or microtubules. Because antibody-mediated cross-linking of syndecan has been associated with syndecan clustering and subsequent stress fiber formation [420], we hypothesize that cationic peptides cross-link heparan sulfates to promote similar changes in syndecan localization and actin organization. Syndecan-1 clustering precedes and likely mediates actin reorganization in response to PA as removal of heparan sulfates by heparinase III completely abolished both syndecan clustering and actin stress fiber formation while reducing the barrier disruption of PA by 50%. This suggests that other cell surface domains may be involved and/or other signaling pathways are activated that affect permeability independent of actin reorganization. Removal of chondroitin sulfate-like GAGs with chondroitinase did not effect PA-mediated permeability changes.

We offer three possible explanations regarding the complex relationship between the enzyme activity data (**Table 12.1**), the compositional analysis (**Table 12.2**), and the effects of enzyme pretreatment (**Figure 12.3**) on PA-mediated barrier disruption. Briefly, heparinase III released 67% of labeled heparan sulfates and reduced PA-induced barrier dysfunction by 50%. Thus there is a close correlation between the amount of heparan sulfate released and the attenuation of the effects of PA on TEER. Heparinase I, however, released 40% of labeled heparan sulfates but had no effect on attenuating PA-induced barrier dysfunction. The simplest explanation for this observation is that the heparan sulfates released by heparinase I were not carried on syndecans but, perhaps, carried by glypican or perlecan and, therefore, not involved in barrier regulation. An alternative explanation is that the additional 27% of the heparan sulfates released by heparinase III (compared with heparinase I) surpassed a crucial cell surface GAG content that is required to participate in cross-linking or activation of intracellular signals that are associated with barrier regulation. Last, heparan sulfates can have similar global composition but possess markedly different focal sequences, referred to as "fine structure". These differences in heparan sulfate focal sequence have been shown to differentially alter endothelial responses to fibroblast growth factor-mediated signaling [31]. Thus the heparan sulfates removed by heparinase I may have had focal sequences that did not participate in barrier regulation.

HSGAG-mediated signaling has been well documented as numerous growth factors, including the fibroblast growth factor family and vascular endothelial growth factor-165 [57,

182] as well as matrix elements [80, 190], require HSGAGs as coligands for maximal receptor activation. Langford and colleagues [253] also demonstrated that both the number and position of heparan sulfates on the syndecan core protein can influence heparan-mediated signaling. Last, the fine structure of the heparan sulfates also influences heparan-mediated signaling and cell behavior [416]. Thus through undetermined mechanisms, the heparan sulfates can modulate syndecan-induced signal activation and subsequent cell function.

Our data suggest that PA-induced cross-linking of syndecan heparan sulfates activates signaling pathways associated with syndecan clustering and actin cytoskeletal reorganization. The mechanism(s) responsible for clustering remains largely unknown. Polycations, like PA and PL, activate endothelial cell phospholipase D apparently through a protein kinase C (PKC)-dependent mechanism [489] such that activation of PKC may be an initial event. The signaling pathways leading to actin reorganization via syndecan-1 likely include Src family of kinases, cortactin, tubulin, and microfilament-regulated processes, whereas syndecan-4-mediated actin organization involves PKC- and phosphatidylinositol 4,5-bisphosphate-dependent processes [528]. It is well known that endothelial cell actin reorganization and permeability is strongly influenced by endothelial-specific MLCK activity [142]; in general, alterations in endothelial permeability occur via activation of MLCK-dependent or p38 MAPK pathways [97, 321]. We examined the activity of MLCK in response to PA treatment and found no increase in myosin light chain phosphorylation, and ML-7, a specific inhibitor of MLCK, had no effect on PA-induced barrier dysfunction. We also tested the p38 MAPK inhibitor, SB-203580, and found that it had no effect on PA- or PL-mediated permeability. These observations suggest that heparan sulfate-directed signaling may act through novel mechanism(s) to induce contractile activity and cytoskeletal rearrangement. Currently, we are exploring this exciting possibility.

In summary, we have identified HSGAGs as an endothelial receptor for cationic peptides and have found that signals activated via HSGAG cross-linking result in cytoskeletal reorganization and subsequent barrier dysfunction. Syndecan-1 and syndecan-4 heparan sulfates appear to be mediators for these events, although we cannot exclude a role for other accessory participants. These data identify another important step in understanding mechanism(s) involved in PMN-induced inflammation and associated changes in vascular permeability and highlight a proinflammatory role for specific components of the glycocalyx.

12.4 Significance

The ability of HSGAGs to influence cellular behaviors is often associated with their capacity to bind to growth factors and support or inhibit their activities. GAGs on the cell surface are known to be important mediators of microvascular permeability. This study sought to develop an *in vitro* model system for microvascular permeability, define the critical GAGs, and explore how they may mediate the cellular response leading to increased permeability. A model system was developed by which the polycations PA and PL were added to BLMVECs, and the TEER was measured. The polycations tested reduced TEER in BLMVECs efficaciously and reproducibly. Only PA was used, however, for the subsequent experiments. To explore the importance of various GAGs, cells were treated with heparinases and chondroitinases prior to PA treatment. Only the heparinases reduced the magnitude of TEER reduction induced by PA, demonstrating that HSGAGs are the key mediator. Furthermore, the effects of heparinase III were greater than heparinase I, consistent with the predominantly mono- and un-sulfated disaccharides found on the cell surface of BLMVEC. In order to understand how HSGAGs could mediate BLMVEC monolayer dysfunction, immunohistochemical studies were performed, and provided evidence of syndecan-1 and -4 clustering, as well as actin stress fiber formation, providing a putative mechanism by which PA leads to structural alterations and corresponding reductions in TEER. These results demonstrate that HSGAGs and associated heparan sulfate proteoglycans are key mediators of polycation-mediated monolayer dysfunction leading to cytoskeletal reorganization in the model system developed. Furthermore, the results of this study provide important insight into how cationic proteins derived from neutrophils during an acute inflammatory response can lead to the microvascular permeability associated with inflammation.

12.5 Experimental Procedures

Cell culture and reagents. BLMVEC were obtained from American Type Culture Collection (Rockville, MD) and Vec Technologies (Rensselaer, NY) and cultured in DMEM and MCDB-131, respectively, and supplemented with 10% fetal calf serum. Cells were used from *passages 6-10*. All reagents were from Sigma Chemical (St. Louis, MO) unless otherwise stated. Heparinase I and heparinase III were purchased from Sigma Chemical and Seikagaku America (Falmouth, MA). Polyclonal antibodies to syndecan-1 and syndecan-4 were purchased from Santa Cruz Biotechnology (Santa Cruz, CA). Monoclonal antibody (BB4) to syndecan-1 was purchased from Serotec (Raleigh, NC), and isotype-specific secondary antibodies were from Jackson ImmunoResearch (West Grove, PA). Anti-heparan sulfate antibody was from Seikagaku America.

Measurement of transendothelial electrical resistance. Endothelial cells were grown to confluence in polycarbonate wells containing evaporated gold microelectrodes (surface area 10^{-3} cm²) in series with a larger gold counter electrode (surface area 1 cm²) connected to a phase-sensitive locked-in amplifier, as we and others have previously described [143, 148]. Measurements of TEER were performed using an electrical cell-substrate impedance sensor (Applied BioPhysics, Troy, NY). Briefly, current was applied across the electrodes by a 4,000-Hz alternate current voltage source with an amplitude of 1 V in series with a 1-M Ω resistor to approximate a constant current source (\sim 1 mA). The in-phase and out-of-phase voltages between the electrodes were monitored in real time with the lock-in amplifier and subsequently converted to scalar measurements of transendothelial impedance, of which resistance was the primary focus. TEER was monitored for at least 30 min to establish a baseline resistance that, for BLMVEC, was typically $6-10 \times 10^3 \Omega$. Each monolayer served as its own control, and percent change in TEER for groups was pooled and expressed as means \pm SE.

GAG analysis. To quantify the amount of GAG chain removed from the cell surface by enzymatic treatment, we measured the release of ³⁵SO₄-labeled heparan and chondroitin sulfate and remaining cell-associated radioactivity. Briefly, endothelial cells were cultured in 12-well plates and labeled for 60 h with 30 μ Ci/ml ³⁵SO₄ in sulfate-free medium and were then washed

three times with PBS. The cells were then incubated for an additional 24 h in complete medium; before enzyme assay, cells were washed three times with serum-free medium. Enzyme solutions were placed onto confluent monolayers of BLMVEC, and aliquots of medium were collected over a 3-h period and counted. Cells were then lysed overnight with 0.1 N NaOH, and total cell-bound radioactivity was counted. All enzyme assays were done in triplicate. The amount of radioactivity released by each enzyme was expressed as the percentage of total cell counts.

Heparan sulfate disaccharide analysis was performed as previously described [227]. Briefly, endothelial cells were digested with a mixture of heparinase I, II, and III with fragments separated by capillary electrophoresis. Disaccharides were identified by comparison against comigration of known standards.

Immunofluorescence microscopy. Confluent monolayers of human lung microvascular endothelial cells were cultured on glass coverslips and treated with PA (90 kDa, 50 µg/ml) for 30 min and 1 h. Human lung microvascular endothelial cells were chosen for these parallel studies because commercially available anti-syndecan antibodies do not cross-react with bovine syndecans. Cells were fixed with 3.7% paraformaldehyde, permeabilized with 0.25% Triton X-100, and incubated with Texas red-phalloidin (Molecular Probes, Portland, OR) to visualize filamentous actin. Syndecan was localized by incubating monolayers with anti-syndecan-1 and anti-syndecan-4 antibodies followed by anti-IgGFITC-labeled secondary antibody. Cell monolayers were then examined by fluorescence microscopy (Nikon Eclipse TE-200 inverted microscope).

Statistics. For all TEER measurements, each monolayer served as its own control, and percentage change from baseline was determined. Data from each group were pooled and analyzed by one-way ANOVA, and groups were compared with a Student-Neuman-Keuls test using Sigma Stat (SPSS, Chicago, IL). Data are presented as percent change in TEER ± SE.

Chapter 13. Characterization of chemisorbed hyaluronic acid directly immobilized on solid substrates

This report was previously published in *Journal of Biomedical Materials Research Part B: Applied Biomaterials*. See reference [455] for details. All figures in this chapter were adapted from the original publication.

13.0 Summary

HA has a number of potential biomedical applications in drug delivery and tissue engineering. For these applications, a prerequisite is to understand the characteristic of HA films directly immobilized to solid substrates. Here, we demonstrate that high molecular weight HA can be directly immobilized onto hydrophilic substrates without any chemical manipulation, allowing for the formation of an ultrathin chemisorbed layer. HA is stabilized on these surfaces through hydrogen bonding between the hydrophilic moieties in HA [such as carboxylic acid (-COOH) or hydroxyl (-OH) groups] with silanol (-SiOH), carboxylic acid or hydroxyl groups on the hydrophilic substrates. Despite the water solubility, the chemisorbed HA layer remained stable on glass or silicon oxide substrates for at least 7 days in phosphate-buffered saline. Furthermore, HA immobilized on silicon and other dioxide surfaces in much higher quantities than other polysaccharides including dextran sulfate, heparin, heparin sulfate, chondroitin sulfate, dermatan sulfate, and alginic acid. This behavior is related to the molecular entanglement and intrinsic stiffness of HA as a result of strong internal and external hydrogen bonding as well as high molecular weight. These results demonstrate that HA can be used to coat surfaces through direct immobilization.

13.1 Introduction

Recently, polysaccharide coatings have attracted much attention in biomaterials research due to their ability to reduce fouling of surfaces by biological species [85, 174, 276, 311-313, 352, 353, 376, 500, 515]. Although the mechanism of protein or cell resistance is not completely

understood, conformation and dehydration of polysaccharides through interactions with water, as well as charge interactions are believed to be important [312]. A variety of polysaccharides have been explored for use as potential low-fouling surface modifiers. These include dextrans [352, 353, 376, 500], carboxymethylated dextrans [85, 174, 276], and other carboxylated polysaccharides such as alginic acid and HA [311, 313, 515]. Of these polysaccharides, HA has received much attention due to its unique properties. HA is a linear polysaccharide composed of repeating disaccharide units of *N*-acetyl-D-glucosamine linked to D-glucuronic acid, and unlike other GAGs, HA is not sulfated. As a component of the extracellular matrix, HA plays an important role in lubrication, water sorption, water retention, and a number of cellular functions such as attachment, migration, and proliferation [54, 340]. HA is therefore an attractive building block for new biocompatible and biodegradable polymers that have applications in drug delivery, tissue engineering, and viscosupplementation [1, 17, 364, 373].

The formation of a stable HA coating has potential biomedical applications ranging from bioactive surfaces to the formation of multilayer polyelectrolyte films [28, 277, 308]. To generate HA-coated surfaces, various immobilization techniques have been employed ranging from covalent attachment [67, 294, 311, 452], layer-by-layer deposition [374, 466], and binding with natural ligands such as p32 [437]. These strategies, however, involve potentially complicated synthetic approaches that require the use of chemicals, UV light, or cumbersome procedures to prepare additional binding layers, limiting their potential as a general route to HA surface immobilization.

Here, we demonstrate the formation of a stable, chemisorbed HA layer on hydrophilic surfaces, such as glass and silicon oxides, and characterize it using X-ray photoelectron microscopy (XPS), ellipsometry, and atomic force microscopy (AFM). In addition, we examined the underlying mechanism by studying the HA layer formation at various pH conditions and with washing procedures. Evidence suggests that the HA is stabilized on the surface through hydrogen bonding between the hydrophilic moieties in HA, such as carboxylic acid (-COOH) or hydroxyl (-OH) groups with silanol (-SiOH), carboxylic acid or hydroxyl groups on the hydrophilic substrates. The chemisorbed HA layer remains stable in PBS for at least 7 days without losing its resistant properties. HA is therefore an important biological molecule that can be directly immobilized on substrates with high efficiency and stability.

13.2 Results and Discussion

13.2.1 Detection of a chemisorbed HA layer

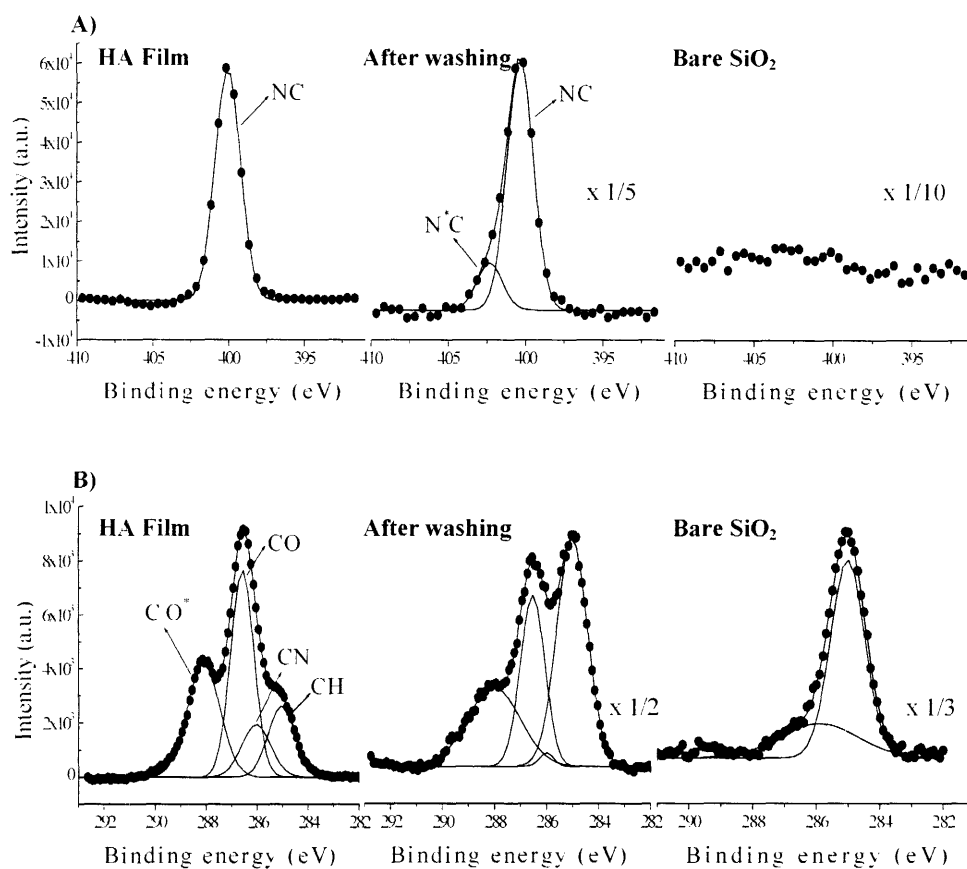


Figure 13.1. XPS Spectra of HA surfaces. High-resolution XPS spectra for (A) nitrogen (N 1s) and (B) carbon (C 1s) peaks in HA recorded for as-spun, washed, and bare silicon oxide substrates. For carbon peaks of an as-spun and a washed film, the spectra were deconvoluted with four Gaussian peaks that are assigned at each oxidized state. For convenience, the peak for the strongly oxidized carbon (CO*) was not deconvoluted in detail. All films were prepared and characterized on the silicon oxide substrate to take advantage of the flat surface.

The presence of a chemisorbed HA layer on silicon dioxide substrates or glass was verified by analyzing the elemental composition (carbon, oxygen, nitrogen, and silicon) of the surfaces using XPS. In particular, the detection of nitrogen in the XPS spectra was strong evidence to support the presence of a residual HA layer (**Figure 13.1**) because nitrogen is found in HA but not the substrate. As expected, no nitrogen was detected on the bare silicon oxide. The

intensity at 400.1 eV (N 1s) decreased to about 25% of its original intensity after washing with PBS, though the peak remained, indicating a residual layer of HA (**Figure 13.1A**). A new XPS peak was also detected at 402.3 eV (15.5%) after washing, suggesting a modified oxidation state of nitrogen, denoted N^{*}C. We hypothesize that the new peak originates from the partial protonation or hydrogen bonding of nitrogen to silanol groups (-SiOH) on the surface. The persistence of the nitrogen peak and the emergence of a new oxidized state (N^{*}C) generated after washing are consistent with a residual layer on the surface formed by chemical interactions between the layer and the substrate.

The carbon peak (C 1s) of an as-spun film contains four peaks that are located at 285.0 (16.1%), 286.1 (12.7%), 286.6 (40.0%), and 288.1 (31.2%), consistent with previous reports (**Figure 13.1B**) [438]. The amount of unfunctionalized hydrocarbon (285 eV) was higher than expected (7.1%) [438], which may be attributed to carbon adsorption from the air. In order of increasing binding energies these peaks represent the hydrocarbon environment (HC), carbon singly bound to nitrogen (CN), carbon singly bound to oxygen (CO), strongly oxidized carbons (CO^{*}) including carbon doubly bound to oxygen and a combined peak representing both amide and carboxylate ion carbon atoms (CON and COO) [438]. In contrast to the as-spun coatings, the relative intensities were substantially changed after washing with the peak locations slightly shifted. Two factors potentially responsible for this behavior are the increased portion of unfunctionalized hydrocarbon from the substrate, and the surface interactions between HA and the substrate. Based on the modified oxidation state of nitrogen in the XPS spectra and hydrophilic moieties in HA, some strong interactions, such as hydrogen bonding, may play an important role in the formation of the chemisorbed layer. In a separate experiment, the HA film was completely washed away on hydrophobic substrates such as untreated polystyrene (data not shown), which indicates that other hydrophobic interactions could be ruled out in examining the origin of the chemisorbed layer.

To analyze the thickness of the HA film, we used ellipsometry, AFM, and XPS measurements at two different angles. At a 90° take-off angle (long penetration depth), silicon peaks were not seen for an as-spun sample (i.e., thick HA film on a glass), as opposed to bare silicon oxide and washed film controls. On the other hand, silicon peaks were nearly absent on the washed film when a 30° take-off angle was used (short penetration depth; **Figure 13.2**). This indicates that the residual film was extremely thin, less than 5-10 nm depending on the element

and electron selected, the thickness ranging within the penetration depth, and the substrate surface is nearly fully covered with the chemisorbed layer. The presence of the chemisorbed layer was further confirmed by ellipsometry and AFM measurements. The ellipsometry results indicated the initial thickness of the HA film was about 330 nm, which decreased drastically to about 3 nm after washing and then remained at the same value. Furthermore, the roughness of a residual layer (2.1 nm) is between that of the substrate (1.8 nm) and the as-spun film (2.3 nm), which also supports the presence of a residual layer (**Figure 13.3**).

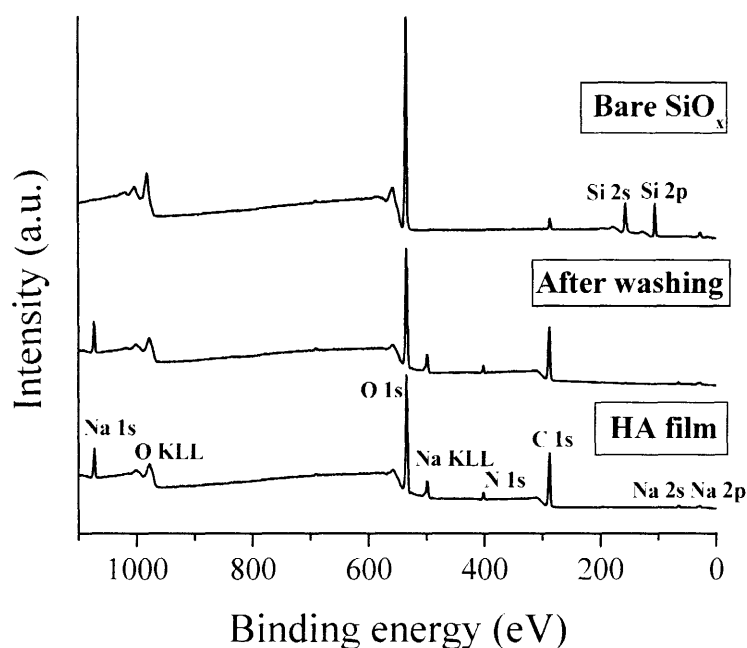


Figure 13.2. The wide scans of XPS spectra for as-spun, washed, and bare silicon oxide substrates. The results indicate that the substrate surface is nearly fully covered with the chemisorbed layer.

To further explore the potential mechanism of adhesion, we exposed silicon oxide surfaces to three different pH values of 2, 7, and 11 to test the effects of surface charge and hydrophobicity on the formation of a HA coating (see the experimental protocol). At acidic conditions (pH = 2), the hydroxyl groups present on the surface are protonated (OH_2^+) such that the adsorption of HA should be enhanced due to negative charge of HA. In contrast, because the surface is negatively charged (O^-), the adsorption would be reduced at basic conditions (pH = 11). At pH 11, the atomic mass percentage of nitrogen on the surface was 0.33% whereas it

increased to 3.61% when exposed to pH 2 (Table 13.1). These results indicate that HA is more likely to adsorb to positively charged surfaces than negatively charged surfaces. Interestingly, neutral surfaces (pH = 7) were also effective in adhering HA (3.34%), which also supports the presence of hydrogen bonding between HA and the hydroxyl groups.

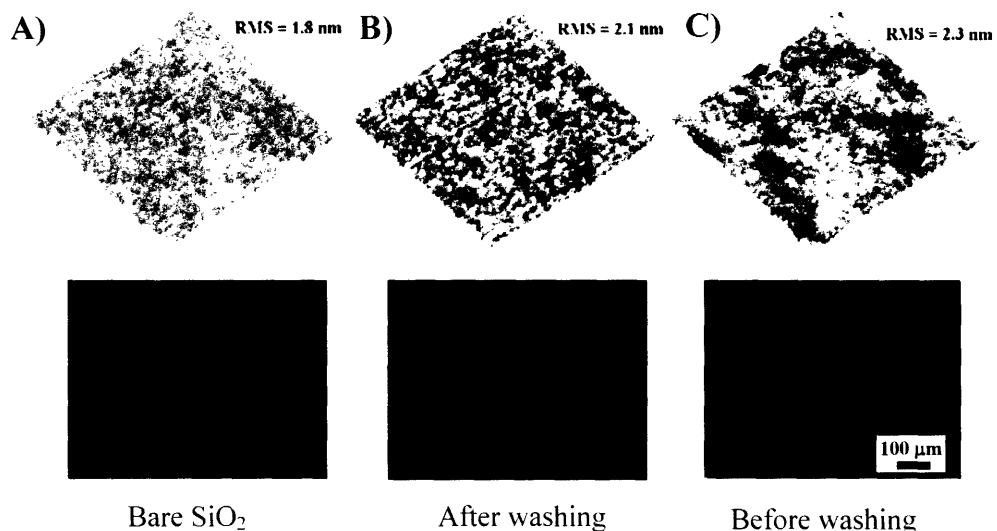


Figure 13.3. AFM images of HA surfaces. AFM images of surface roughness and the corresponding fluorescent images for FN adsorption for (A) a bare silicon oxide substrate, (B) a HA surface after thorough washing, and (C) an as-coated HA film. Note that the roughness of the film after washing locates between those of the other two surfaces, supporting the presence of a chemisorbed layer. The height scale is 5 nm and the scan size is $1 \times 1 \mu\text{m}^2$. The fluorescent images reveal that the surface is fully covered with HA even after extensive washing.

We next explored whether the current approach is ubiquitous in immobilizing polymers having hydrophilic moieties on hydrophilic substrates. A previous study reported that carboxyl (-COOH) groups were confined onto hydrophilic surfaces with additional thermal polymerization [439]. Poly(ethylene glycol)s, however, detach from the substrates upon hydration despite having hydrophilic moieties (-OH). We hypothesize that two factors are responsible for the formation of a chemisorbed HA layer. First, hydrogen bonding should be strong enough to endure the polymer swelling stress at the interface upon exposure to water. Second, the chemisorbed layer should have a dense molecular structure such as entanglement to prevent penetration of water molecules. Thus, sufficiently strong hydrogen bonding is required to prevent the adsorbed layer from peeling off from the surface. In this regard, the HA film should have

enough contact time with the surface to build a robust interface. As indicated by XPS, the amount of nitrogen adsorbed onto the surface was lower when the sample was washed within 30 min after spin coating (0.69%; **Table 13.1**) and significantly increased to 2.74% when the sample was dried overnight prior to washing. This indicates that the duration of exposure and sample drying may be important in the adsorption of the HA onto the surfaces.

Sample	Atomic Conc. %			
	C	N	O	Si
Exposure to pH 2	57.6	3.6	34.0	4.8
Exposure to pH 7	52.2	3.3	38.3	6.2
Exposure to pH 11	14.6	0.3	58.0	27.1
No washing + drying	49.2	2.7	38.8	9.3
Washing after 30 min + drying	11.7	0.7	64.6	23.0
Bare silicon dioxide	4.2	0	65.4	30.4

Table 13.1. Atomic Mass Percentage of Carbon, Nitrogen, Oxygen, and Silicon Elements for HA Films Formed under Various Conditions. Errors are within 5%.

With respect to the density of the molecular structure, HA is a highly hydrated polyanion, which forms network between domains in solutions [159, 240]. In addition, the polymer shows intrinsic stiffness due to hydrogen bonds between adjacent saccharides. HA immobilized on silicon and other dioxide surfaces in much higher quantities than other polysaccharides including dextran sulfate, heparin, HS, CS, DS, and alginic acid (**Table 13.2**) based on the highest nitrogen composition (3.75%) and the lowest oxygen-to-carbon ratio (0.64%). This behavior could be attributed to either differences between the molecular structures of various polysaccharides or their lower molecular weights compared to HA.

Sample	N	O	C	O : C
Untreated	0.00	92.4	7.6	12.2
HA	3.8	37.5	58.7	0.6
Heparin	0.2	89.4	10.4	8.6
HS	0.1	91.1	8.8	10.4
CS A	0.5	88.8	10.7	8.3
CS C	0.1	90.5	9.4	9.6
DS	0.4	89.0	10.6	8.4

Table 13.2. Atomic Mass Percentage of GAG Surfaces and Control Surfaces. XPS was performed on GAG surfaces formed on silicon dioxide after washing. Untreated surfaces are silicon dioxide only. Numbers for nitrogen, oxygen, and carbon refer to atomic mass percentage. Oxygen:Carbon is the atomic mass percentage of oxygen divided that by carbon. Errors are within 5%.

13.2.2 Protein resistance, degradability, and stability of a chemisorbed HA layer

To test the effectiveness of the HA surfaces for protein resistance, HA-modified surfaces were exposed to fluorescein isothiocyanate-labeled bovine serum albumin (FITC-BSA), fluorescein isothiocyanate-labeled goat anti-rabbit immunoglobulin G (FITC-IgG), and fibronectin (FN). The adhesion of FITC-BSA (0.46%), FITC-IgG (7.81%), and FN (6.22%) was significantly reduced ($p < 0.001$) on HA-coated surfaces compared to glass controls (100%) as measured by fluorescence intensity. Typical examples of the fluorescent images for a bare silicon oxide, a HA surface after thorough washing, and an as-coated HA film are shown in **Figure 13.3** when FN is applied to the surface with subsequent antibody staining (see the experimental protocol). As seen from the figure, HA is uniformly attached to the surface even after extensive washing. We also tested protein resistance of various other polysaccharide surfaces on glass using FN (**Figure 13.4**). Surfaces formed with other polysaccharides resisted the adsorption of FN significantly more than glass controls ($p < 0.05$). Despite this, most other polysaccharide surfaces were still significantly less resistant to FN absorption than HA coatings ($p < 0.05$).

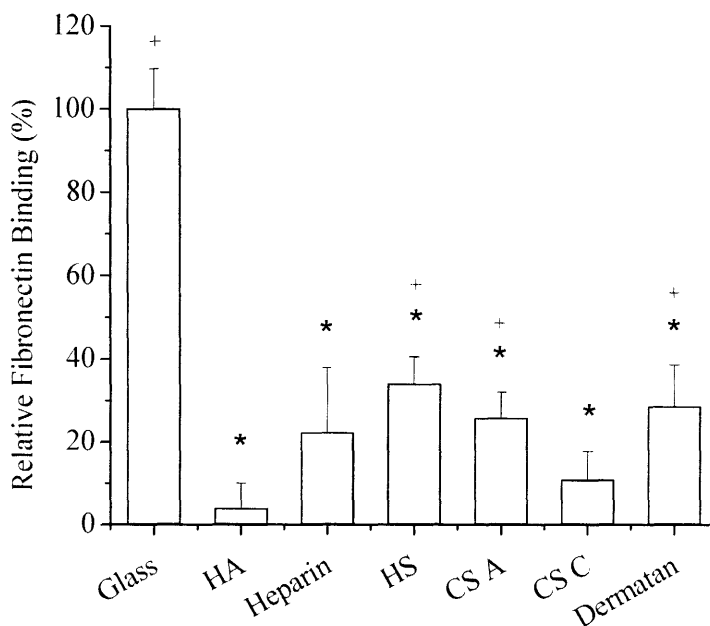


Figure 13.4. FN adsorption onto GAG surfaces measured by quantifying the fluorescence intensity. The results are normalized to glass (defined as 100) as the positive control and no protein (defined as 0). Data is presented as a percentage of the difference between untreated and glass. * denotes $p < 0.05$ compared to glass. + denotes $p < 0.05$ compared to HA.

Although HA is biodegradable in nature, the possibility of degradation can presumably be ruled out herein because oxidants such as $\text{HO}\cdot$ and $\text{HOCl}/\text{ClO}\cdot$ are believed to be important in the degradation of HA. The generation of reactive oxygen species is mediated by metal-ion catalysis ($\text{HO}\cdot$) *in vitro* [175, 305] or myeloperoxidase catalyzed reaction of H_2O_2 with Cl^- ($\text{HOCl}/\text{ClO}\cdot$) *in vivo*. To investigate long-term stability, XPS was performed on the aged samples, which revealed persistent nitrogen peaks even after a week in PBS solution. However, the uniform distribution of HA is difficult to measure by means of XPS. We therefore used fluorescent staining of the samples as a function of time to obtain a global assessment of HA adsorption. The chemisorbed HA layer was also stable for at least 7 days as determined by the analysis of fluorescent images (**Figure 13.5**). The presence of the HA surface greatly reduced the adsorption of FN (> 92%), even after the surface was exposed to PBS for 7 days prior to exposure FN adsorption and staining. These results indicate that at least in the case of silicon dioxide, the formation of a chemisorbed layer of HA is stable for at least 1 week.

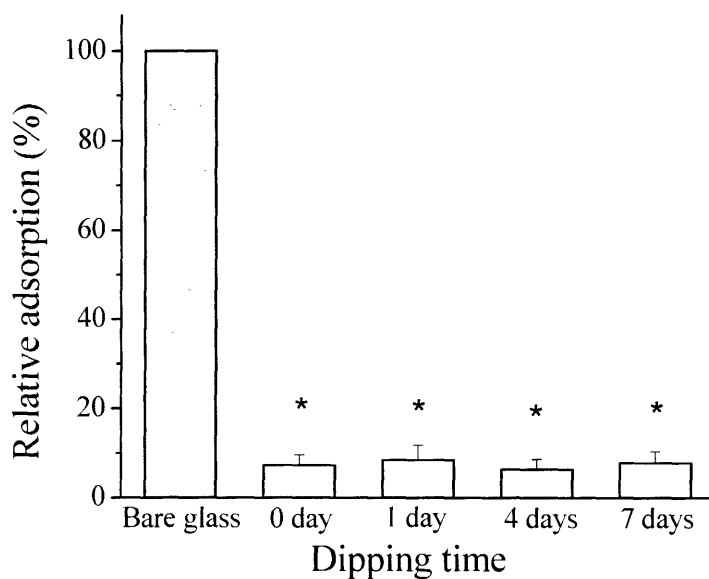


Figure 13.5. HA surfaces are stable for at least 7 days. The stability of the HA surface was examined by the quantitative analysis of protein adsorption as a function of exposure times to PBS prior to exposure and subsequent staining to FN. Note that the surface is stable and greatly reduces protein adsorption more than 92% even after exposure to PBS for up to 7 days. No contrast enhancement was made throughout the analysis. * denotes $p < 0.05$ compared to bare glass.

13.3 Significance

Despite its water solubility and hydrophilic nature, HA can be directly immobilized onto glass and silicon oxide substrates because of hydrogen bonding and high molecular weight. An ultrathin HA layer of about 3 nm is left behind even after extensive washing with PBS or water. The presence of this layer was verified with XPS, ellipsometry, and AFM measurements. Fluorescent staining and XPS showed that the resulting surfaces remain stable for at least 7 days. Thus, our approach could be a general route to the immobilization of HA and open a new way to attach other bioactive molecules having hydrophilic moieties to solid substrates.

13.4 Experimental Procedures

Materials. HA (lot no. 904572, $M_n = 2.1$ MDa by light scattering) was kindly supplied by Genzyme Inc. (Boston, MA). Silicon dioxide wafers (1 μm of SiO_2 on Si) were purchased from International Wafer Service (Portola Valley, CA) and used without further treatment. Heparin and HS were from Celsus Laboratories (Columbus, OH). CS A, CS C, DS, FITC-BSA, FITC-IgG, FN, and anti-FN antibody were purchased from Sigma (St. Louis, MO). Glass slides were treated with O_2 plasma for 1 min to generate -OH groups as well as to clean the surfaces unless otherwise indicated.

Surface characterization. Fluorescent optical images were obtained using an inverted microscope (Axiovert 200, Zeiss). XPS spectra were recorded using a Kratos AXIS Ultra spectrometer. Spectra were obtained with a monochromatic Al K_{α} X-ray source (1486.6 eV). Pass energy was 160 eV for survey spectra and 10 eV for high-resolution spectra. All spectra were calibrated with reference to the unfunctionalized aliphatic carbon at a binding energy of 285.0 eV. Spectra were recorded with similar settings (number of sweeps, integration times, etc.) from sample to sample to enable comparisons to be made. The analysis of the XPS spectra was performed on the basis of 90° unless otherwise indicated. Atomic force micrographs were obtained with tapping mode on a NanoScope III Dimension (Veeco Instruments, Rochester, NY) in air. The scan rate was 0.5 Hz and 256 lines were scanned per sample. Tapping mode tips, NSC15 - 300 kHz, were obtained from MikroMasch (Portland, OR). Data were processed using Nanoscope III 4.31r6 software (Veeco Instruments Inc.). The thickness of the chemisorbed HA layer was measured with a Gaertner L116A ellipsometer (Gaertner Scientific Corp., Skokie, IL) with a 632.8 nm He-Ne laser. A refractive index of 1.46 was used for all HA films, and a three-phase model was used to calculate thicknesses.

Construction and stability of a chemisorbed layer and testing protein adsorption. A few drops of HA solution (5 mg/mL in distilled water) were placed on the surface and spin coated (Model CB 15, Headway Research, Inc.) at 1000 rpm for 10 s. The samples were stored overnight at room temperature to allow the solvent to evaporate. To examine the effect of washing, some

samples were washed several times within 30 min of spin coating and then dried with a mild nitrogen stream. To examine the effect of pH, the silicon oxide surfaces were exposed for several hours to the solutions of pH 2, 7, and 11, respectively, leading to different oxidization states. HA films were prepared on those surfaces using the same procedure described above. In addition to HA, thin films of the other polysaccharides were prepared in the same manner.

To measure the immobilization of HA, heparin, HS, CS A, CS C, and DS films, we performed fluorescent staining for adhesion of various proteins on the coated surfaces. FITC-BSA (50 $\mu\text{g}/\text{mL}$), IgG (50 $\mu\text{g}/\text{mL}$), and FN (20 $\mu\text{g}/\text{mL}$) were dissolved in PBS solution (pH = 7.4; 10 mM sodium phosphate buffer, 2.7 mM KCl, and 137 mM NaCl). To measure FN adsorption, the surfaces were stained with anti-FN antibody for 45 min, followed by a 1 h incubation with the FITC-IgG antibody. A few drops of the protein solution were evenly distributed onto the HA surfaces. After storing at room temperature for 30 min, the surfaces were rinsed with PBS solution and water and then blown dry in a stream of nitrogen. To analyze stability, HA surfaces were placed in a PBS bath at various times and stored at room temperature for up to 7 days. The PBS solution was changed daily to prevent readsorption of dissociated HA onto the surface. The stability was subsequently analyzed by testing for FN adsorption. The slides were then examined under a fluorescent microscope under a UV light exposure of 2 s. Blank glass slides with or without FN staining were used as positive and negative controls respectively. Fluorescent images were analyzed quantitatively using Scion Image and the statistical analysis was performed using one-sided ANOVA tests with $p < 0.05$ to distinguish between statistical significance.

Chapter 14. Immobilized glycosaminoglycans regulate cancer cell activity

14.0 Summary

GAGs are complex sugars found in the ECM and on the cell surface, which regulate important processes including wound healing and cancer. Breakdown of the ECM, including the GAG component, is a critical step in cancer invasion and metastasis. The basement membrane (BM), prior to invasion, inhibits the growth and progression of tumors. We therefore sought to create artificial basement membrane-like surfaces by direct deposition of GAGs, and to subsequently determine their utility in regulate cancer cell activity. Stable surfaces could be produced with all 10 GAGs examined. Furthermore, the surfaces each exhibited unique abilities to affect B16-F10 murine melanoma cell adhesion, growth, and metastasis. The most effective surfaces, those that promoted cell adhesion, but inhibited proliferation and metastasis, were formed with heparin and hepIII-treated heparan sulfate. GAG surfaces can therefore effectively regulate cancer cell activity and can be selected to achieve desired responses for specific applications.

14.1 Introduction

Cancer invasion, angiogenesis, and metastasis are dependent on the controlled degradation and reformation of the ECM, including the BM [211, 272]. HSGAGs are the most abundant polysaccharide component of the BM, and are tethered to the protein components of the BM, including collagen IV and FN [29, 102, 211, 468]. The various elements are self-assembled into complex structural networks, which compartmentalize tissues and regulate cell behavior, after they are produced by and secreted from cells [430, 520]. The invasive process

specifically involves enzymes secreted to degrade the BM, enabling tumor and cellular entry into deeper tissues and ultimately, to the blood stream [102].

The BM serves a fundamental role in cancer, as penetration of the BM by the growing tumor defines it as invasive. As a result, the interactions between the cancer and the components of the BM and the ECM are critical in regulating cancer progression. Intact BMs, for example, resist tumor growth, and their digestion modulates cellular activity [371, 496]. Cleaving heparan sulfate proteoglycans can specifically promote cellular activities including cell migration and can alter responsiveness to extracellular cues [496]. Heparanase, which is expressed by human tumors, digests HSGAGs in the ECM [135, 242, 496]. Digestion of HSGAGs by heparanase promotes invasion, angiogenesis, and metastasis, and can even increase mortality [157]. In addition to HSGAGs, other GAGs also regulate cancer growth and progression. HA can promote invasion, angiogenesis and metastasis. Furthermore, HA is found in higher quantities in the pericellular space surrounding metastatic cells than around primary tumors which have not metastasized [231]. CS interacts with collagen IV in the BM, and can regulate the invasive process in melanomas through CD44 [239]. Additionally, both CS and DS are found in the BM surrounding cancer cells in quantities that increase as the cancer progresses [137].

GAGs in the ECM and those on the cell surface are well characterized as important modulators of tumor cell activity [38, 274, 427]. Cancer cell activity can be controlled by the addition or digestion of GAGs [274, 496]. While recreating the protein component of the BM inhibits tumor growth and progression [371], the ability to define cancer cell activity with artificial BMs formed from the GAG component, however, has not been examined. In this study, we created a BM-like surface by immobilizing GAGs, and sought to identify the best GAGs to control melanoma cell adhesion, growth and migration. An idealized GAG surface would bind cells but prevent proliferation and migration. Various GAGs were successfully immobilized and found to elicit unique sets of cell functions, which were distinct from GAGs free in the ECM. These studies identified that surfaces produced with heparin and hepIII-digested HS allowing the most optimal combination of adhesion, growth and migration.

14.2 Results and Discussion

14.2.1 GAGs can be immobilized to form stable chemisorbed surfaces

The deposition of polysaccharides to form adhered surfaces has received attention for their ability to reduce medical device thrombogenicity [179, 248, 401], to prevent biomaterial fouling [294, 312, 455], to inhibit bacterial and mammalian cell adhesion [311], and to reduce urologic stone formation [179, 230]. The heterogeneity of GAGs [77] suggests that a multitude of other medically important roles are possible. GAGs in the ECM and on the cell surface regulate cancer growth and progression [38, 274, 427, 496]. Components of the BM can additionally inhibit tumor cell proliferation and metastasis [371]. We therefore hypothesized that GAG surfaces, serving to recreate the BM, could serve as potent modulators of cancer cell activity. By employing a wide range of GAGs, surfaces with optimized properties could be selected.

The formation of GAG-coated surfaces can be achieved by a various methods, including covalent attachment, photoimmobilization, layer-by-layer deposition, and binding via natural ligands [67, 294, 311, 374, 437, 466]. Producing stable surfaces, however, often involves expensive and hazardous agents [294, 311]. Stable chemisorbed layers can be formed with HA and other GAGs in a single step through direct deposition. This simple and inexpensive technique forms stable surfaces through hydrogen bond formation [455]. Direct deposition therefore offers the ability to screen several GAGs for a variety of outputs at low cost, and as a result, was the technique selected for this study.

A limited number of commercially available GAGs with distinct physiochemical and biological properties exist. These are HA, CS A, CS C, DS, heparin and HS. Heparin is a highly sulfated HSGAG, predominantly at the 2-*O*, 6-*O*, and *N*-positions, and HS is undersulfated, with a greater percentage of unsulfated glucuronic acids [77]. We first sought to expand the number of GAGs that could be explored. For this purpose, we digested heparin and HS with hepI and hepIII. Digestion of HSGAGs with heparinases not only reduces their molecular weight, but also alters their biological effect [30, 104, 274]. Heparin and HS were digested with hepI or hepIII with the extent of digestion measured and confirmed by UV spectroscopy at 232 nm. The degree

of enzymatic cleavage confirmed to be sufficient to change the biological function compared to undigested HSGAG [30].

We first confirmed that stable, chemisorbed surfaces could be produced with all GAGs. Chemisorbed GAG surfaces were produced with HA, CS A, CS C, and DS, heparin (a highly sulfated HSGAG), heparin pretreated with either hepl or hepIII, HS (an undersulfated HSGAG), and HS pretreated with either hepl or hepIII on silicon dioxide substrates. The formation of surfaces with all GAGs was confirmed by measuring contact angle of water (**Figure 14.1**), XPS, and ellipsometry. A lower contact angle is representative of a more hydrophilic surface relative to the underlying substrate and is indicative of surface modification. We observed that the contact angles for HA ($p < 8 \times 10^{-6}$), CS A ($p < 0.0003$), CS C ($p < 0.0005$), DS ($p < 0.03$), heparin ($p < 0.003$), hepl digested heparin ($p < 4 \times 10^{-6}$), hepIII digested heparin ($p < 0.05$), HS ($p < 0.002$), hepl digested HS ($p < 0.0007$), and hepIII digested HS ($p < 0.0005$), were distinct from untreated silicon dioxide. The changes in contact angle confirm the presence of a surface modification.

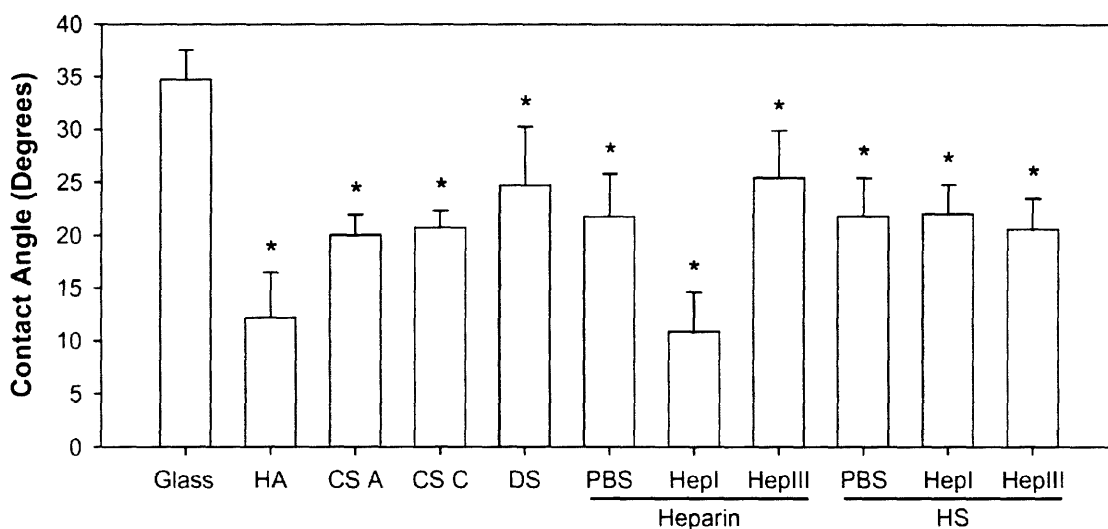


Figure 14.1. GAGs can be immobilized to create surfaces. Contact angles for water on various GAG surfaces were measured. Left and right contact angles were averaged and data is presented in degrees. * denotes $p < 0.05$ for a GAG surface compared to silicon dioxide (untreated).

The differences between the contact angles could be indicative of either the degree of surface modification or the inherent differences in the hydrophilicity of the GAGs tested. In order to further clarify this phenomenon, and to confirm the presence of GAGs in the surface,

XPS was performed. The silicon dioxide substrate does not have nitrogen. The hexosamine component of all GAG disaccharides, however, does contribute nitrogen. Therefore, detectable nitrogen in surfaces would confirm successful GAG deposition and the atomic mass percentages would allow for quantities of GAGs immobilized to be grossly quantified. These data indicated that although other GAGs had not chemisorbed onto surfaces at the same levels as HA, they did form layers that could be used to examine their role in influencing cell behavior. The ability to form GAG surfaces on the hydrophilic silicon dioxide substrate was also examined by ellipsometry to measure surface thickness, which again verified the successful formation of GAG surfaces (data not shown). HA surfaces were thickest as judged by ellipsometry. This result was confirmed by atomic force microscopy (data not shown). HA has an intrinsic stiffness due to intramolecular hydrogen bonds, forming an entangled network between various domains [159]. The increased thickness of HA surfaces could have resulted from the increased length of the polysaccharide chain, the reduced negative charge per disaccharide, or the intrinsic differences between the molecular structures of HA and other GAGs.

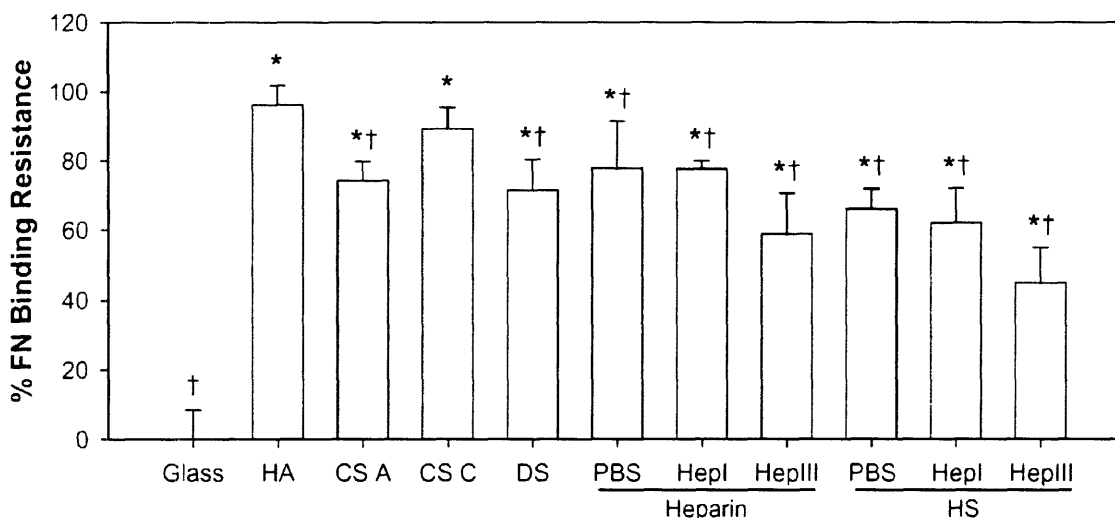


Figure 14.2. GAG surfaces inhibit protein adhesion. FN adsorption onto GAG surfaces was measured by quantifying the fluorescence intensity. The resistance of FN binding was determined by normalizing the intensity results to glass (defined as 0) and no FN treatment (defined as 100). Data is presented as the percent reduction in bound FN compared to glass, which readily binds FN. * denotes $p < 0.05$ compared to glass, and † denotes $p < 0.05$ compared to HA.

Using similar analyses, all GAGs were found to form surfaces on glass, and HA, heparin, HS, and DS formed surfaces on polystyrene. We next sought to confirm that GAG deposition was widespread across substrates. HA adhered to substrates prevents the binding of negatively

charged proteins over the entirety of the surface [455]. The ability of GAG surfaces to prevent protein binding was therefore investigated. The amount of FN (**Figure 14.2**) and bovine serum albumin (data not shown) that bound to GAG surfaces was compared to substrate only (no protein resistance; the negative control) and surfaces with no FN or BSA added (maximal protein resistance; the positive control). HA inhibited $96.2 \pm 5.5\%$ of FN binding ($p < 2 \times 10^{-7}$), which was not significantly different from the positive control ($p > 0.99$). CS A ($74.3 \pm 5.5\%$; $p < 9 \times 10^{-7}$), CS C ($89.2 \pm 6.1\%$; $p < 2 \times 10^{-7}$), DS ($71.5 \pm 8.8\%$; $p < 2 \times 10^{-6}$), heparin ($77.8 \pm 13.6\%$; $p < 2 \times 10^{-5}$), hepI digested heparin ($77.6 \pm 2.3\%$; $p < 2 \times 10^{-5}$), hepIII digested heparin ($58.9 \pm 11.7\%$; $p < 4 \times 10^{-5}$), HS ($66.0 \pm 5.8\%$; $p < 2 \times 10^{-6}$), hepI digested HS ($62.1 \pm 9.9\%$; $p < 7 \times 10^{-6}$), and hepIII digested HS ($45.1 \pm 9.9\%$; $p < 7 \times 10^{-5}$), each produced surfaces that significantly inhibited FN binding. All surfaces therefore resisted protein binding consistent with widespread surface formation [455]. FN resistance additionally confirmed surface stability for at least 4 days (data not shown). Similar results were observed with BSA binding.

Digestion of HSGAGs altered the ability of surfaces to resist protein adhesion compared to undigested HSGAGs. Surfaces formed with hepIII digested heparin ($p < 0.02$) and with hepIII digested HS ($p < 0.009$) allowed for significantly more protein binding than heparin and HS respectively, while treatment of either heparin or HS with hepI ($p > 0.27$) did not alter the protein adhesive properties. Interestingly, hepIII digested heparin yielded a surface that had similar protein binding properties as HS ($p > 0.70$). The properties of digested HSGAGs may therefore be different from those of undigested HSGAGs, offering four additional surfaces that can be used to examine the effects on cell function.

14.2.2 GAG surfaces regulate cell adhesive, proliferative, and migratory properties

After validating that the 10 GAGs could form surfaces, we next examined how they would affect cancer cells. We reasoned that GAG surfaces, if effective at regulating cancer cells, would be most likely to have value for skin cancers and ovarian cancer. After the surgical excision of skin cancers, by Mohs procedure for example, recurrence can occur from subclinical spread of cancer cells [20, 78]. In ovarian cancer, instrumenting the tumor can seed the abdomen with neoplastic cells [279, 375, 471]. The ability of GAG surfaces to affect cancer cells was therefore examined on B16-F10 murine melanoma cells. For anti-cancer purposes, we reasoned

that an idealized surface would promote cell adhesion, but inhibit cell growth and metastasis. As such, if applied post-surgically, cancer cells would adhere to the surface but not proliferate or seed locally.

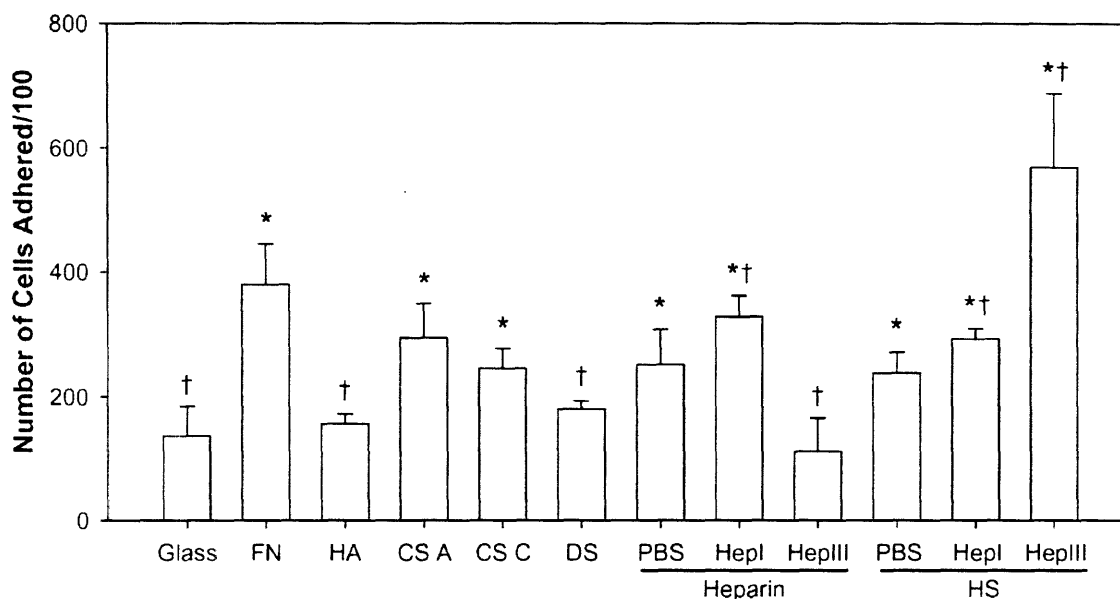


Figure 14.3. GAG surfaces modulate cell adhesion. B16-F10 cells were added to GAG surfaces formed on glass. The percentage of cells adhered after 2 hours was determined by measuring whole cell count. * denotes $p < 0.05$ compared to glass. † denotes $p < 0.05$ compared to FN.

Surfaces were formed on glass with each GAG, B16-F10 cells were deposited, and the number of cells adhered was determined after two hours. $11.1 \pm 2.9\%$ of cells adhered to glass alone. Cells adhered to all GAG surfaces with varying degrees of efficiency (**Figure 14.3**). HA, DS and hepIII-digested heparin surfaces resisted cell adhesion similar to glass alone ($p > 0.16$). CS C, heparin, and HS surfaces promoted more cell adhesion than glass alone ($p < 0.03$), but less than FN-treated glass ($p < 0.03$). CS A, hepI-digested heparin, and hepI-digested HS surfaces promoted similar cellular adhesion as FN-treated glass ($p > 0.07$), significantly more than glass ($p < 0.008$). HepIII-digested HS surfaces notably *promoted* cell adhesion more than FN-treated glass ($p < 0.05$), with $46.1 \pm 9.7\%$ of cells adhering.

The effects of GAG surfaces on cell proliferation were next examined. On glass, cell number increased $643.6 \pm 23.0\%$ over 96 hours. FN-treated glass only yielded a $293.8 \pm 42.9\%$ increase in whole cell number. The various GAG surfaces also influenced cell proliferation

(Figure 14.4). When normalized to the number of cells adhered, surfaces formed with CS C ($761.8 \pm 108.8\%$), DS ($256.0 \pm 18.4\%$), hepl-digested heparin ($197.2 \pm 14.1\%$), heplIII-digested heparin ($272.2 \pm 16.4\%$), HS ($344.2 \pm 19.2\%$) promoted cell proliferation over 96 hours. Surfaces formed with HA ($-67.1 \pm 5.1\%$), CS A ($-43.4 \pm 2.5\%$), heparin ($-69.1 \pm 5.2\%$), hepl-digested HS ($-62.2 \pm 4.2\%$), and heplIII-digested HS ($-58.5 \pm 12.2\%$) however, *reduced* whole cell number.

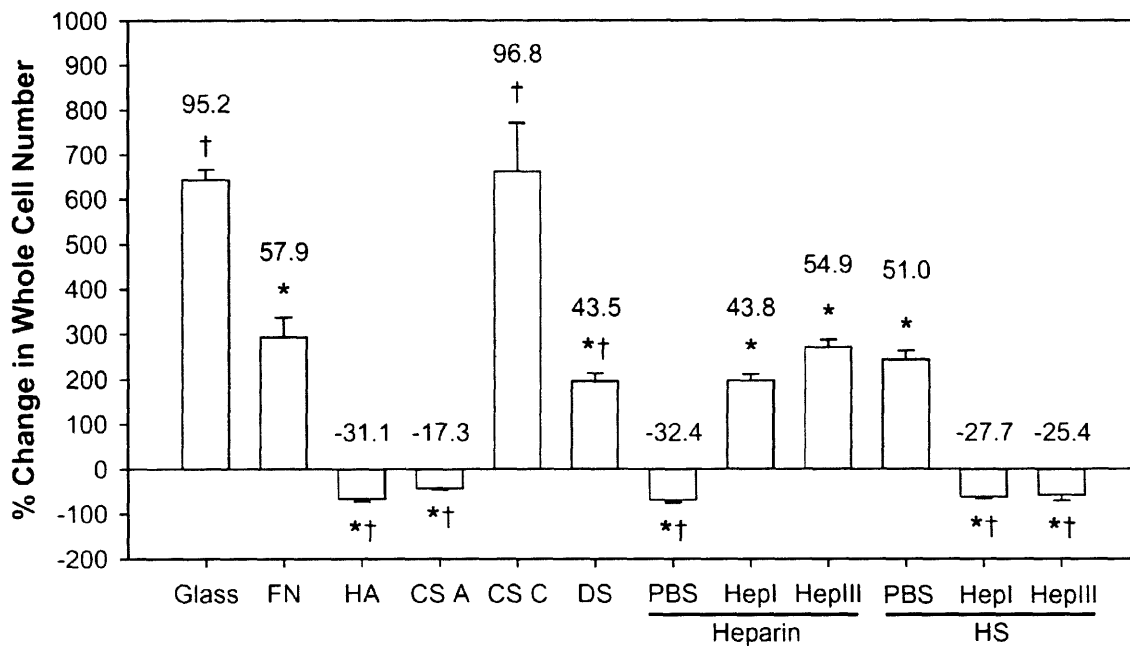


Figure 14.4. GAG surfaces regulate proliferation. GAG surfaces were created on glass. B16-F10 cells were added to surfaces, and whole cell number was determined at 2, 24, 48, 72, and 96 hours by measuring whole cell count. Data is presented as percent change in whole cell number after 96 hours compared to the number of cells adhered at 2 hours. Numbers illustrate the average percent growth per day. * denotes $p < 0.05$ compared to glass. † denotes $p < 0.05$ compared to FN.

Finally, we explored the effects on metastasis. FAK and CD44 expression were used as an *in vitro* surrogate for metastasis as their expression is associated with migration and metastasis [198, 231, 239, 433, 447]. The expression of these markers was modulated by GAG surfaces (Figure 14.5). DS and heplIII digested HS surfaces yielded cells with the highest expression of FAK and CD44. Intermediate levels of signaling was observed with FN, HA, CS C, hepl-digested heparin, heplIII-digested heparin, and HS-digested hepl surfaces. Cells added to untreated, CS A, heparin, and HS surfaces exhibited the most restricted distributions of FAK and

CD44. Cellular expression of β_1 -integrin, which has been associated with local adhesion to a surface [23], and for f-actin, which is associated with changes in cell-cell contacts [98, 130], were not altered by various GAG surfaces (data not shown), verifying that the observed expression changes were marker-specific.

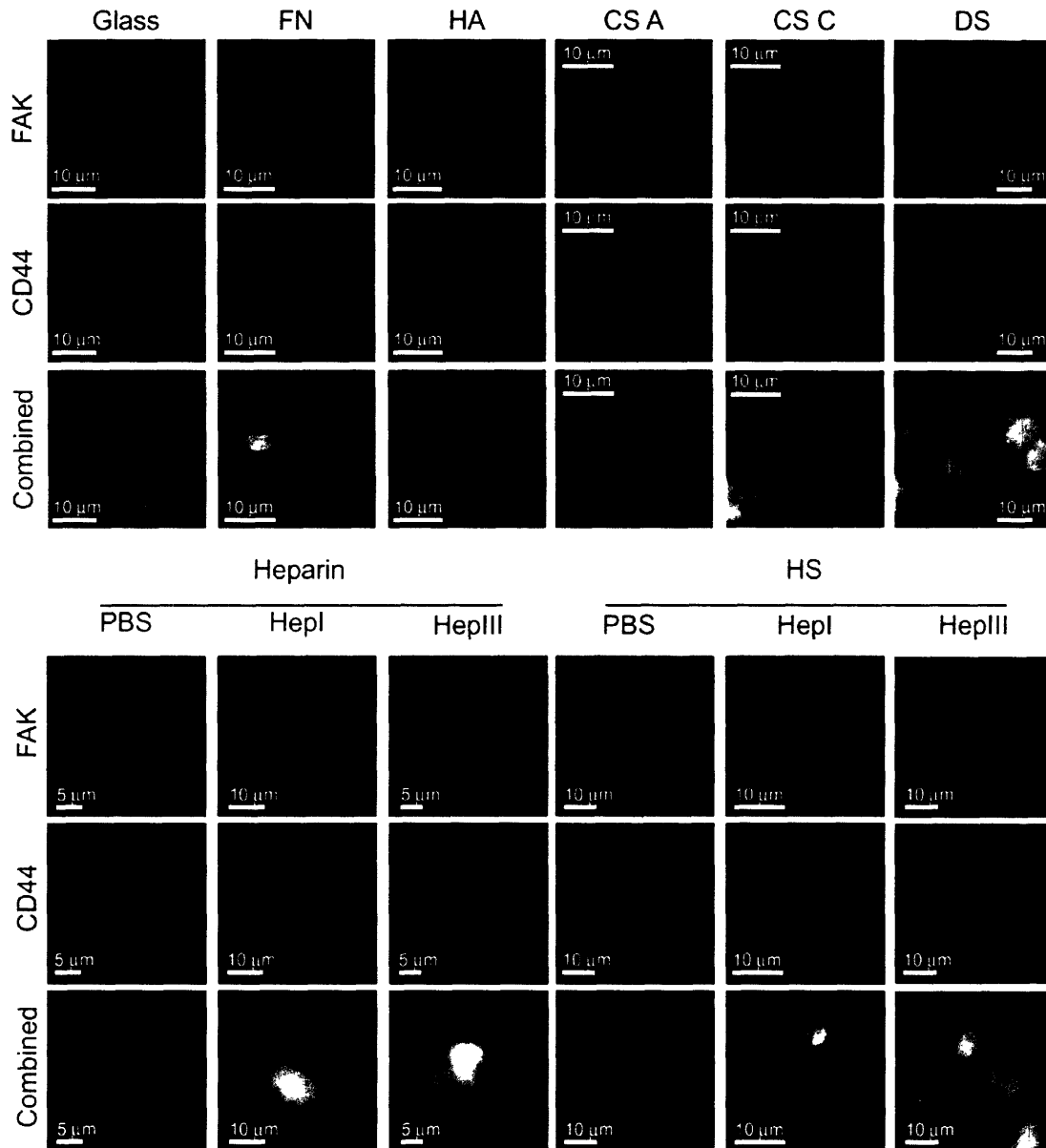


Figure 14.5. GAG surfaces alter FAK and CD44 expression. B16-F10 cells were immobilized on GAG surfaces. Cells were fixed after 24 hours. Immunohistochemistry was performed for FAK (green) and CD44 (red) using appropriate antibodies, as well as for cell nuclei (blue) using DAPI. The “combined” row represents an overlay of immunohistochemical results for all three markers.

14.2.3 GAG surfaces elicit biological effects that are distinct from those of GAGs free in the ECM

To confirm that the cellular effects observed were not merely a function of adding GAGs to cells, but rather, that GAG surfaces exhibit novel functionality, the ability of GAGs free in media to alter proliferation was investigated. B16-F10 cells were treated with GAGs at concentrations between 500 ng/ml and 500 μ g/ml. These concentrations were sufficient to provide similar and greater quantities of GAG than was found on the surfaces, based on calculations using surface thickness and average disaccharide volume for various GAGs.

At the concentrations examined, HA ($p > 0.26$), heparin ($p > 0.14$), and hepI-digested heparin ($p > 0.26$), did not alter cell proliferation (**Figure 14.6A**). CS C ($p < 0.03$), DS ($p < 0.002$), hepIII-digested heparin ($p < 0.006$), HS ($p < 0.006$), hepI-digested HS ($p < 0.005$), and hepIII-digested HS ($p < 0.002$) surfaces inhibited B16-F10 cell growth in dose dependent manners. CS A, however, supported cell growth, yielding a final whole cell number $154.1 \pm 16.5\%$ ($p < 0.002$) of that of untreated cells. To confirm that the proliferative response to immobilized GAGs was distinct from free GAGs, the percent proliferation after 72 hours compared to untreated cells was determined, and the results for immobilized (bound) GAGs were divided by that of free GAGs (**Figure 14.6B**). A result of ~ 1.0 indicates a similar response to a given GAG presented in different manners. Only hepIII-digest HS (1.1) had a ratio near 1.0, while all others were greater than 1.2 or less than 0.7, demonstrating a distinct response pattern. The cellular effects observed with GAG surfaces are therefore novel and cannot be recapitulated by GAGs free in solution.

Hydrogen bonds are formed between the GAG and the substrate when GAGs are chemisorbed to produce surfaces [455]. As a result, both the mobility of the GAGs and the potential conformations the GAGs can assume are likely reduced. The appropriate three-dimensional structures and spatial orientations of GAGs are important for functional interactions with proteins [319, 392]. It is therefore reasonable that the ability of GAGs to alter cell function is changed when they are immobilized to produce surfaces.

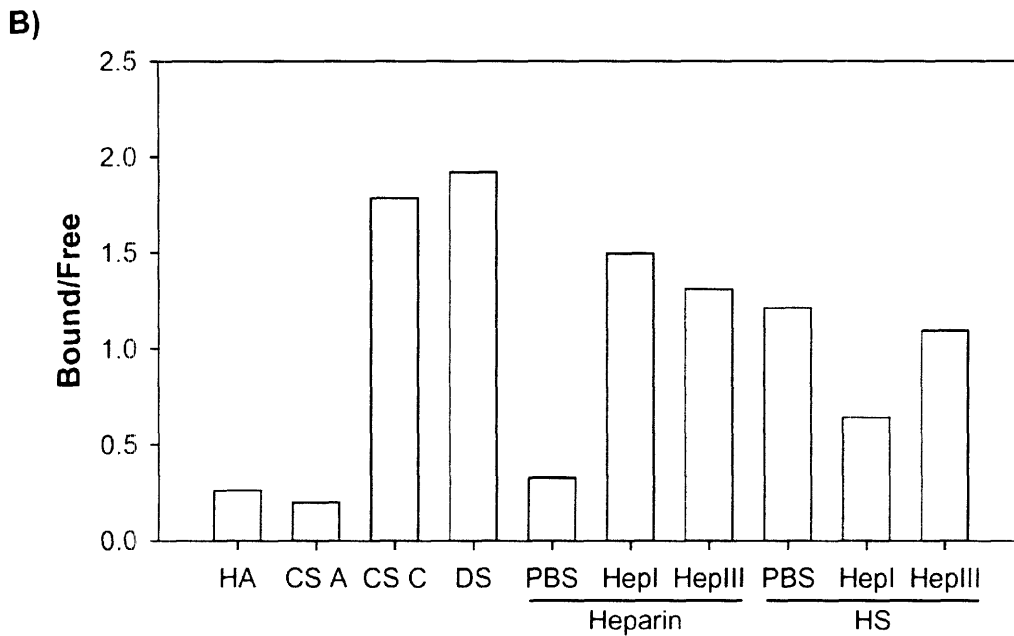
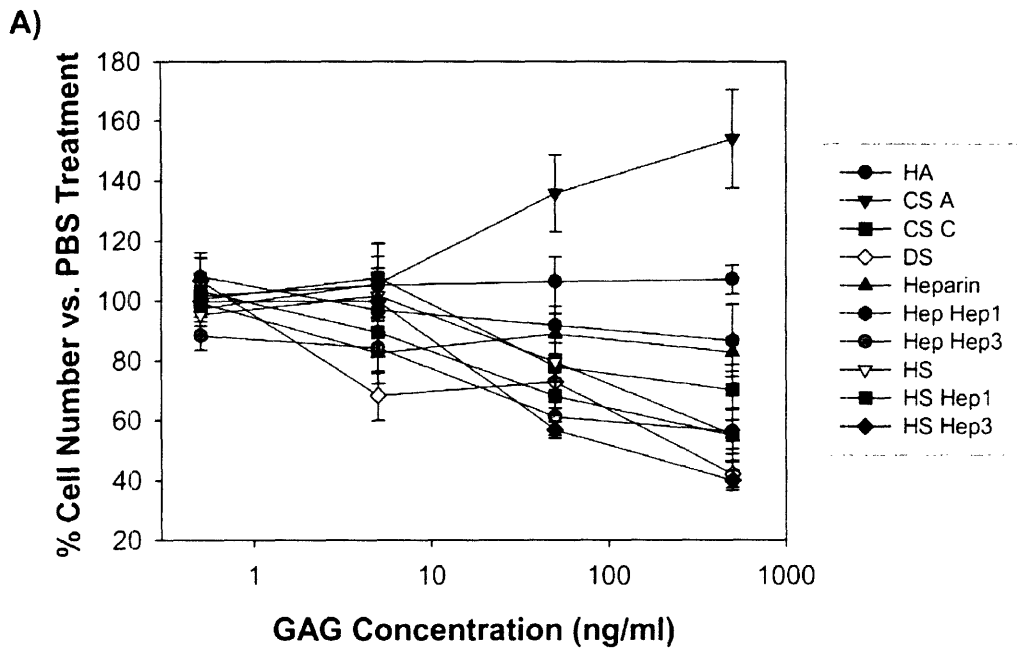


Figure 14.6. Immobilized GAGs regulate proliferation distinct from free GAGs. A) B16-F10 cells were treated with GAGs, and whole cell number was determined after 72 hours. Data was normalized as the percent of cells in GAG treated conditions compared to the PBS treated condition. B) The effect of immobilized (bound) GAGs on B16-F10 cell proliferation was compared to the effect of free GAGs. Whole cell number of B16-F10 cells added to surfaces was determined after 72 hours, and normalized as the percent of cells in GAG treated conditions compared to the PBS treated condition. Percent change for cells on a given immobilized GAG was divided by the percent change for cells exposed to the same free GAG. Data is presented as bound/free. A result of 1.0 denotes that cells responded the same to immobilized and free GAGs.

14.2.4 Selected GAG surfaces have potent anti-cancer activities

The goal of this study was to explore the ability of GAG surfaces to regulate cancer cells and to identify GAGs that produced surfaces with optimal properties. Ideally, such a surface would promote cell adhesion, but inhibit cell growth and metastasis. The specific responses of the various GAG surfaces are summarized in **Table 14.1**. Unfortunately, no single surface was the best at promoting cell adhesion, inhibiting proliferation and preventing metastasis. Nonetheless, two GAG surfaces, hepIII digested HS and heparin, had interesting and promising properties.

GAGs		Cell Adhesion	Cell Proliferation	FAK/CD44 Expression
HA		+	-	++
Heparin	PBS	++	-	+
	HepI	++	+	++
	HepIII	+	+	++
HS	PBS	++	+	+
	HepI	++	-	++
	HepIII	+++	-	+++
CS A		++	-	+
CS C		++	++	++
DS		+	+	+++

Table 14.1. GAG surfaces regulate B16-F10 cell activities in distinct manners. Each of the biological measures was stratified into three levels of responses. Cell adhesion and FAK/CD44 expression are described as low (+), middle (++), or high (+++). Proliferation is described as inhibited (-), promoted (+), or strongly promoted (++)

Other hand, elicited only moderate cell adhesion, but the greatest growth inhibitory effect, reducing whole cell number by $69.1 \pm 5.2\%$, and perhaps the most restricted expression pattern of FAK and CD44. Each of these surfaces has strong properties suggesting potential utility.

Of note, the data presented also serves to screen the various GAG surfaces for other potential applications. To prevent biomaterial fouling, low protein binding, cell adhesion, and cell growth would be preferred, for example [311, 312]. These properties are offered by HA surfaces. For a potential bioreactor system to remove metastatic cells from the blood or other bodily fluids but still enable study, ideal properties would be strong cell adhesion and cell growth, a combination of properties that could be achieved with CS C surfaces.

HepIII digested HS surfaces best promoted cell adhesion and prevented proliferation. Whole cell number was reduced by $58.5 \pm 12.2\%$ compared to the number of cells adhered over four days. B16-F10 cells added to hepIII digested HS surfaces, however, exhibited high levels of FAK and CD44 expression, suggesting that migratory and metastatic activity would not be inhibited, and perhaps promoted [198, 231, 239, 433, 447]. Heparin, on the

This study demonstrates that GAG surfaces have potential therapeutic value for cancer. Whether the effects remain constant between cancer types is not clear, and warrants additional investigation. Furthermore, future work to understand the specific mechanism by which GAG surfaces confer their effects is necessary to design idealized surfaces. This study provides a framework in which the cellular response to specific GAG surfaces can be efficiently examined, allowing exploration of other GAGs and additional cell lines.

14.3 Significance

GAGs are important regulators of physiological and pathological functions, including normal development, wound healing, and cancer progression. These complex sugars, found in the ECM and on the cell surface, are an important component of the BM. The BM, in addition to other ECM components, plays an important role in preventing the invasion, progression, and metastasis of cancer. GAGs were chemisorbed to substrates to produce a BM-like environment to determine if GAG surfaces would be an effective way to regulate cancer cell activities. All of the 10 GAGs examined formed stable surfaces using a common, simple, and inexpensive method. Furthermore, each of the GAGs regulated the ability of B16-F10 murine melanoma cells to adhere, grow and metastasize. The goal of these studies was to specifically identify GAGs that could be used therapeutically for cancer, which would most likely have applications in skin cancers and ovarian cancers, where subclinical growth and tumor instrumentation are common causes for relapses. Ideal surfaces would promote adhesion but inhibit growth and metastasis. Two such surfaces were identified. Heparin potently inhibited growth and metastasis with moderate adhesion, while hepIII digested HS induced strong adhesion and inhibited growth, but did not prevent metastatic activity. These results demonstrate that GAG surfaces can be used to regulate cancer cell activity. Furthermore, heparin and hepIII digested HS surfaces may have potential therapeutic value to reduce recurrences after surgical treatment for skin and ovarian cancers.

14.4 Experimental Procedures

Proteins and Reagents. HA (lot # 904572, $M_n = 2.1$ MDa, by light scattering) was generously provided by Genzyme, Inc. (Boston, MA). Silicon dioxide wafers ($1\ \mu\text{m SiO}_2$ on Si) were from International Wafer Service (Portola Valley, CA). Heparin and HS were from Celsus Laboratories (Columbus, OH). CS A, CS C, and DS were from (Sigma, St. Louis, MO). FBS was from Hyclone (Logan, UT). L-glutamine, penicillin/streptomycin, and PBS were from GibcoBRL (Gaithersburg, MD). FITC-labeled BSA, FN, rabbit anti-FN, and goat anti-rabbit-FITC were from Sigma.

Production and Characterization of GAG surfaces. Glass slides were treated with O_2 plasma for one minute to clean the surfaces and to generate OH groups. Silicon dioxide wafers were not treated prior to use. Chemisorbed layers of various GAGs on solid substrates were generated as described [455]. Briefly, a few drops of 5 mg/ml solutions of various GAGs in distilled water were placed on silicon dioxide, glass, or polystyrene substrates, and the films were coated by spin coating at 1000 rpm for 10 seconds. Surfaces were created with HA, CS A, CS C, DS, heparin, HS, and heparin as well as HS pretreated with hepl or heplIII [30]. For surfaces produced with digested HSGAGs, heparin and HS at 5 mg/ml were treated with hepl or heplIII for 30 minutes and boiled for 30 minutes [30]. Partial digestion was confirmed by UV spectroscopy at 232 nm [31]. Once the films were cast, solvent was evaporated overnight.

Analysis of all GAG surface was performed after washing. To confirm GAG deposition, XPS spectra were obtained using a Kratos AXIS Ultra spectrometer, with a monochromatic Al K_{α} X-ray source (1486.6 eV). Pass energy was 160 eV for survey spectra and 10 eV for high-resolution spectra. Spectra were calibrated with respect to the unfunctionalized aliphatic carbon with a binding energy of 285.0 eV. Identical settings were used for all samples to allow for comparisons to be made. Analysis was performed at 90° .

The chemical and physical properties were examined by determining the contact angle of water as well as the thickness of the GAG layer. The thicknesses of the adsorbed GAG layers were assessed with a Gaertner L116A ellipsometer with a 632.8 nm He-Ne laser (Gaertner Scientific Corp., Skokie, IL). Thickness was calculated with a three-phase model.

The ability of various GAG surfaces to promote or resist protein binding was performed as described using FITC-BSA and FN [455]. FN adsorption was examined for GAG surfaces stored in PBS for 1, 2, 3, and 4 days. Stability was assessed by determining whether the percent of protein bound remained consistent over time.

B16-F10 proliferation assay with free GAGs. B16-F10 cells (American Type Culture Collection, Manassas, VA) were maintained and used for proliferation assays as described [32]. Briefly B16-F10 cells were diluted to 5×10^4 cells/ml and added to 24-well plates. After serum-starvation for 24 hours, cells were treated with 500 ng/ml, 5 μ g/ml, 50 μ g/ml, and 500 μ g/ml of GAGs. Control cells were treated with an equivalent volume (10 μ l) PBS. Partial digestion was performed as described [30, 31]. Whole cell numbers were determined by electronic cell counter after 72 hours. Cells were washed twice with PBS and treated with 500 μ l/well trypsin for 5 minutes. Cell counts were performed on 400 μ l from each well. Average whole cell counts for experimental conditions were normalized as the percentage of control cells present at the experimental endpoint.

Cell adhesion and proliferation on immobilized GAGs. B16-F10 cells were grown until confluence in 75 cm² flasks. Each flask was washed with 20 ml PBS, and treated with 3 ml trypsin-EDTA at 37°C for 3-5 minutes, until cells detached. Cells were centrifuged for 3 minutes at 195 x g. The supernatant was aspirated and the cells were resuspended in 10 ml media. Cell density was measured by electronic cell counter, and the suspension was diluted to 1×10^6 cells/ml in FBS-deficient media. Surfaces on silicon dioxide were placed on 100 mm dishes, washed twice and incubated for 2 hours under UV light in PBS supplemented with 100 μ g/ml penicillin and 100 U/ml streptomycin. Sufficient cell suspension to create a fluid film across the entirety of the GAG surface (130 μ l) was added to each GAG surface. To measure effects on cell adhesion, cells were incubated on surfaces for 2 hours and washed with PBS. The adhered cells were quantified by electronic cell counter after treatment with 1 ml trypsin-EDTA sufficient to detach the cells. To measure effects on cell proliferation, cells were added and allowed to grow for 2 hours as described. After 2 hours, plates containing surfaces were washed, supplemented with 10 ml FBS-deficient media, and incubated for an additional 22, 46, 70, or 94 hours at 37°C. Cells were counted by electronic cell counter after trypsin treatment.

Immunohistochemistry. B16-F10 cells were added to GAG or control surfaces as described. Surfaces were washed twice with PBS after 2 hours to remove cells that did not adhere. Cells were grown on surfaces for an additional 22 hours, washed with PBS, and fixed for 10 minutes in 3.7% formalin. Cells were treated with 0.1% triton X-100 for 5 minutes and preincubated in 1% bovine serum albumin in PBS for 30 minutes.

Rabbit anti-FAK (Upstate Group, Charlottesville, VA) and rat anti-CD44 (United States Biological, Swampscott, MA) were added to cells at a 1:100 dilution and incubated for 4 hours. Cells were subsequently treated with Texas red-labeled goat anti-rat secondary antibody (Molecular Probes, Eugene, OR) and FITC-labeled chicken anti-goat secondary antibody (Molecular Probes) and incubated for 1 hour. Cells were then treated with DAPI (Molecular Probes) for 5 minutes at room temperature. Alternatively, goat polyclonal antibodies to β_1 integrin (Santa Cruz Biotechnology, Santa Cruz, CA) were added at a 1:100 dilution and incubated 4 hours. FITC-labeled chicken anti-goat secondary antibody (Molecular Probes) and Texas red-labeled phalloidin (Molecular Probes) were added and incubated for 1 hour. DAPI was then added for 5 minutes at room temperature.

Staining was then visualized by fluorescence microscopy. Controls of no antibody, primary antibody only, and secondary antibody only were performed. For both staining sets, fluorescent optical images were obtained using an inverted microscope (Axiovert 200, Zeiss) and acquired with Openlab 3.1.5 software. Images were processed using Adobe Illustrator 10.0.

Statistical analysis. Results are expressed as mean \pm standard deviation. The Student's *t* test was used for statistical analysis. A *p* value of < 0.05 was considered statistically significant.

Chapter 15. Conclusions and future work

Developing techniques to understand the effects of GAGs on cells is of growing importance as biochemical and analytical tools to probe GAG structure and function progressively emerge. The results of the research described in this thesis shed important insight into the biological activities of GAGs, the mechanisms by which GAGs can regulate cell function, and the importance of GAGs in various diseases. Furthermore, the methods developed and described can help to further explore the cellular effects of GAGs on proteins, cells, and diseases.

In order to explore the functions of GAGs, HSGAG-FGF2 interactions were first examined as a model system. Studies exploring the utility of dFGF2 in stroke validated that this engineered protein could be used to promote functional recovery of stroke. Further work, however, is necessary to determine its potential to become a new treatment for this important condition. Cell surface HSGAGs were also characterized as important modulators of FGF2. Specifically, the presence or absence of specific structural moieties within the cell surface HSGAG can determine a cell's responsiveness to FGF2. This finding was confirmed for other members of the FGF protein family. Furthermore, these effects were validated in other cell systems, including cancer growth and metastasis, where they can similarly influence the activity of other protein families. Of importance, these findings elucidated that specific HSGAG moieties can independently influence primary tumor growth and metastasis. The potential for specific cell derived HSGAGs to control aspects of cancer growth and progression warrants further investigation.

The ability of other GAGs to influence FGFs as well as VEGFs was subsequently examined. Highly sulfated HSGAGs and CS/DS GAGs were found to regulate FGF1, FGF2, FGF7, VEGF-A, VEGF-C, and VEGF-D. Additionally, these GAGs could regulate cellular activity in a pool of growth factors. Specifically, heparin and highly sulfated DS elicited opposing responses from mixtures of FGF7 and VEGF-A, suggesting that GAGs could be used to define the behavior of cells when they are exposed to combinations of growth factors.

The effects of FGFs in the colonic epithelium were additionally investigated. FGFs were found to elicit cellular responses in cells not expressing the corresponding FGFRs. Syndecan-1 served to shuttle FGFs to the nucleus where they could induce cellular responses. Based on

these results, syndecan-1 was investigated as a potential modulator of inflammatory bowel disease, and was found to have a protective effect against chemically induced colitis. Future work is necessary to further establish syndecan-1 as a protective agent in inflammatory bowel disease, and to determine its therapeutic potential.

Attempts to explore intracellular GAGs led to the discovery that forming conjugates between heparin and a class of polymers, poly(β -amino ester)s, can promote heparin internalization by endocytosis. Poly(β -amino ester)-heparin conjugates are taken up preferentially by cancer cells, likely as a function of their faster endocytic rate. Upon internalization, conjugates induce apoptotic cell death, with maximal effects observed in melanoma cells. In cells where conjugates do not promote cell death, such as in Burkitt's lymphoma cells, where they promote cell growth, they can be used to probe cell function, and have been used to determine that cell surface HSGAGs are important modulators of Burkitt's lymphoma proliferation that can be targeted to inhibit cell growth. Application of poly(β -amino ester)-heparin conjugates to tumors *in vivo* demonstrates that they are not only effective at preventing tumor growth, but also they do not have detectable toxicity. These findings demonstrate that internalized heparin is a potential new anti-cancer agent that warrants further investigation. Furthermore, endocytic rate is an important feature of cancer cells distinguishing them from non-transformed cells, which can be harnessed by drug delivery systems and anti-cancer agents to enable targeted delivery of chemotherapeutics. Future work will be necessary to further validate the anti-cancer effects of poly(β -amino ester)-heparin conjugates, to confirm the low toxicity associated with their use, and to determine their value as a potential therapeutic.

Finally, studies that aimed to broaden the scope of GAG biology revealed that HSGAGs are important mediators of inflammation-induced vascular permeability, and that GAG surfaces are an effective means to influence cancer cell activity. Inflammatory peptides were found to promote endothelial monolayer dysfunction through cell surface syndecan clustering and stress fiber formation. This finding can serve as the basis for future studies probing the specific cellular pathways by which inflammatory peptides induce vascular permeability. GAGs could be immobilized on substrates forming surfaces with stability provided by hydrogen bonds. GAG surfaces elicited cellular activities in cancer cells distinct from GAGs free in the ECM. Furthermore, by developing a library of GAG surfaces, those with desired properties can be

selected. Future work is necessary to identify and develop optimal GAG surfaces in order to determine their potential in various biological applications.

Taken together, the results presented demonstrate several mechanisms by which GAGs can regulate cell function. The model systems in which the studies were performed were relevant to various pathologies, suggesting that these results may be of importance in developing new treatments for disease. Further understanding of the roles of GAGs in these and other systems, as well as the use of the new technologies described, may prove important in gaining a deeper understanding of several human pathologies, potentially leading to new treatments.

Abbreviations

A5	Polymer composed of diacrylate “A” and amine “5”
AFM	Atomic force microscopy
AJ	Adherens junction
AT-III	Antithrombin III
BAEC	Bovine aortic endothelial cell
BL	Burkitt’s lymphoma
BLMVEC	Bovine lung microvascular endothelial cell
BM	Basement membrane
BSA	Bovine serum albumin
CPM	Counts per minute
CS	Chondroitin sulfate
DAPI	4'-6-Diamidino-2-phenylindole
ddDS	Doubly chemically oversulfated dermatan sulfate fraction DT
dFGF2	Dimeric fibroblast growth factor 2
DFMO	Difluoromethylornithine
DG	Dentate gyrus of the hippocampus
diDS	Chemically oversulfated dermatan sulfate fraction DT
DMEM	Dulbecco’s modified Eagle medium
DS	Dermatan sulfate
DS DT	Dermatan sulfate fraction DT
DSS	Dextran sodium sulfate
DTT	Dithiothreitol
EBV	Epstein-Barr virus
EC	Endothelial cell
ECM	Extracellular matrix
Erk	Extracellular signal regulated kinase
FBS	Fetal bovine serum
FGF	Fibroblast growth factor
FGFR	Fibroblast growth factor receptor
FITC	Fluorescein isothiocyanate
FITC-BSA	Fluorescein isothiocyanate -labeled bovine serum albumin
FITC-IgG	Fluorescein isothiocyanate -labeled goat anti-rabbit immunoglobulin G
FN	Fibronectin
Fz	Frizzled
GAG	Glycosaminoglycan
GPI	Glycosylphosphatidylinositol
HA	Hyaluronic acid
HBP	Heparin-binding protein
HBSS	Hank’s buffered saline solution
Hep	Heparinase
HRP	Horseradish peroxidase
HS	Heparan sulfate
HSGAG	Heparin/heparan sulfate-like glycosaminoglycan
HSPG	Heparan sulfate proteoglycan

IBD	Inflammatory bowel disease
Ig	Immunoglobulin
IL-3	Interleukin-3
LDH	Lactic acid dehydrogenase
LMP	Latent membrane protein
LMWH	Low molecular weight heparin
MCA	Middle cerebral artery
MEM	Minimal essential medium alpha
MI	Mitogenic index
MLCK	Myosin light chain kinase
NBT-II	Nara bladder tumor No. 2
ODC	Ornithine decarboxylase
PA	Polyarginine
PAE	Poly(β -amino ester)
PBS	Phosphate buffered saline
PDZ	PSD95/DLG/ZO-1
PEI	Poly(ethylene imine)
PG	Proteoglycan
PI	Proliferative index
PI3K	Phosphoinositol 3-kinase
PKC	Protein kinase C
PL	Polylysine
PMA	Phorbol 12-myristate 13-acetate
PMN	Polymorphonuclear leukocyte
RT	reverse transcriptase
SMC	Smooth muscle cell
SVC	Subventricular zone
TCF/LEF	T cell factor/lymphoid enhancer factor
TEER	Transendothelial electrical resistances
TER	Transepithelial resistance
TGF	Transforming growth factor
TM	Ammonium tetrathiomolybdate
TJ	Tight junction
UDS	Unfractionated DS
VEGF	Vascular endothelial growth factor
VEGFR	Vascular endothelial growth factor receptor
XPS	X-ray photoelectron microscopy
ZO-1	Zona occludens-1

References

1. Abantangelo, G., and Weigel, P. (2000). *New frontiers in medical science: redefining hyaluron.* (Amsterdam: Elsevier).
2. Achen, M.G., Jeltsch, M., Kukk, E., Makinen, T., Vitali, A., Wilks, A.F., Alitalo, K., and Stackner, S.A. (1998). Vascular endothelial growth factor D (VEGF-D) is a ligand for the tyrosine kinases VEGF receptor 2 (Flk1) and VEGF receptor 3 (Flt4). *Proc Natl Acad Sci U S A* *95*, 548-553.
3. Adams, D.H., and Shaw, S. (1994). Leucocyte-endothelial interactions and regulation of leucocyte migration. *Lancet* *343*, 831-836.
4. Akinc, A., Lynn, D.M., Anderson, D.G., and Langer, R. (2003). Parallel synthesis and biophysical characterization of a degradable polymer library for gene delivery. *J Am Chem Soc* *125*, 5316-5323.
5. Alexander, C.M., Reichsman, F., Hinkes, M.T., Lincecum, J., Becker, K.A., Cumberledge, S., and Bernfield, M. (2000). Syndecan-1 is required for Wnt-1-induced mammary tumorigenesis in mice. *Nat Genet* *25*, 329-332.
6. Allen, B.L., Filla, M.S., and Rapraeger, A.C. (2001). Role of heparan sulfate as a tissue-specific regulator of FGF-4 and FGF receptor recognition. *J Cell Biol* *155*, 845-858.
7. Anderson, D.G., Lynn, D.M., and Langer, R. (2003). Semi-automated synthesis and screening of a large library of degradable cationic polymers for gene delivery. *Angew Chem Int Ed* *42*, 3153-3158.
8. Anderson, D.G., Peng, W., Akinc, A., Hossain, N., Kohn, A., Padera, R., Langer, R., and Sawicki, J.A. (2004). A polymer library approach to suicide gene therapy for cancer. *Proc Natl Acad Sci U S A* *101*, 16028-16033.
9. Anderson, J.M., Van Itallie, C.M., Peterson, M.D., Stevenson, B.R., Carew, E.A., and Mooseker, M.S. (1989). ZO-1 mRNA and protein expression during tight junction assembly in Caco-2 cells. *J Cell Biol* *109*, 1047-1056.
10. Anderson, W.F. (1998). Human gene therapy. *Nature* *392*, 25-30.
11. Antman, E.M., and Handin, R. (1998). Low-molecular-weight heparins: an intriguing new twist with profound implications. *Circulation* *98*, 287-289.
12. Arfors, K.E., Lundberg, C., Lindbom, L., Lundberg, K., Beatty, P.G., and Harlan, J.M. (1987). A monoclonal antibody to the membrane glycoprotein complex CD18 inhibits polymorphonuclear leukocyte accumulation and plasma leakage in vivo. *Blood* *69*, 338-340.
13. Arnott, S., Mitra, A.K., and Raghunathan, S. (1983). Hyaluronic acid double helix. *J Mol Biol* *169*, 861-872.
14. Ashikaga, T., Strada, S.J., Thompson, W.J. (1997). Altered expression of cyclic nucleotide phosphodiesterase isozymes during culture of aortic endothelial cells. *Biochem Pharmacol* *54*, 1071-1079.
15. Ay, I., Sugimori, H., and Finklestein, S.P. (2001). Intravenous basic fibroblast growth factor (bFGF) decreases DNA fragmentation and prevents downregulation of Bcl-2 expression in the ischemic brain following middle cerebral artery occlusion in rats. *Brain Res Mol Brain Res* *87*, 71-80.
16. Baird, A. (1994). Fibroblast growth factors: activities and significance of non-neurotrophin neurotrophic growth factors. *Curr Opin Neurobiol* *4*, 78-86.

17. Balazs, E.A., and Denlinger, J.L. (1989). Clinical uses of hyaluronan: the biology of hyaluronan. In *Clinical uses of hyaluronan: the biology of hyaluronan*, D. Evered and J. Welan, eds. (New York: Wiley), pp. 265-280.
18. Ballinger, M.D., Shyamala, V., Forrest, L.D., Deuter-Reinhard, M., Doyle, L.V., Wang, J.X., Panganiban-Lustan, L., Stratton, J.R., Apell, G., Winter, J.A., Doyle, M.V., Rosenberg, S., and Kavanaugh, W.M. (1999). Semirational design of a potent, artificial agonist of fibroblast growth factor receptors. *Nat Biotechnol* *17*, 1199-1204.
19. Bame, K.J., Venkatesan, I., Dehdashti, J., McFarlane, J., and Burfeind, R. (2002). Characterization of a novel intracellular heparanase that has a FERM domain. *Biochem J* *364*, 265-274.
20. Batra, R.S., and Kelley, L.C. (2002). Predictors of extensive subclinical spread in nonmelanoma skin cancer treated with Mohs micrographic surgery. *Arch Dermatol* *138*, 1043-1051.
21. Bayatti, N., and Engele, J. (2001). Cyclic AMP modulates the response of central nervous system glia to fibroblast growth factor-2 by redirecting signalling pathways. *J Neurochem* *78*, 972-980.
22. Bazill, G.W., and Dexter, T.M. (1990). Role of endocytosis in the action of ether lipids on WEHI-3B, HL60, and FDCP-mix A4 cells. *Cancer Res* *50*, 7505-7512.
23. Beauvais, D.M., and Rapraeger, A.C. (2003). Syndecan-1-mediated cell spreading requires signaling by α 5 β 3 integrins in human breast carcinoma cells. *Exp Cell Res* *286*, 219-232.
24. Beauvais, D.M., and Rapraeger, A.C. (2004). Syndecans in tumor cell adhesion and signaling. *Reprod Biol Endocrinol* *2*, 3-14.
25. Beck, P.L., and Podolsky, D.K. (1999). Growth factors in inflammatory bowel disease. *Inflamm Bowel Dis* *5*, 44-60.
26. Belting, M., Havsmark, B., Jonsson, M., Persson, S., and Fransson, L.A. (1996). Heparan sulphate/heparin glycosaminoglycans with strong affinity for the growth-promoter spermine have high antiproliferative activity. *Glycobiology* *6*, 121-129.
27. Belting, M., Borsig, L., Fuster, M.M., Brown, J.R., Persson, L., Fransson, L.A., and Esko, J.D. (2002). Tumor attenuation by combined heparan sulfate and polyamine depletion. *Proc Natl Acad Sci U S A* *99*, 371-376.
28. Bernard, B.A., Newton, S.A., and Olden, K. (1983). Effect of size and location of the oligosaccharide chain on protease degradation of bovine pancreatic ribonuclease. *J Biol Chem* *258*, 12198-12202.
29. Bernfield, M., Gotte, M., Park, P.W., Reizes, O., Fitzgerald, M.L., Lincecum, J., and Zako, M. (1999). Functions of cell surface heparan sulfate proteoglycans. *Annu Rev Biochem* *68*, 729-777.
30. Berry, D., Kwan, C.P., Shriver, Z., Venkataraman, G., and Sasisekharan, R. (2001). Distinct heparan sulfate glycosaminoglycans are responsible for mediating Fibroblast Growth Factor-2 biological activity through different Fibroblast Growth Factor Receptors. *Faseb J* *15*, 1422-1424.
31. Berry, D., Shriver, Z., Natke, B., Kwan, C.P., Venkataraman, G., and Sasisekharan, R. (2003). Heparan sulphate glycosaminoglycans derived from endothelial cells and smooth muscle cells differentially modulate fibroblast growth factor-2 biological activity through fibroblast growth factor receptor-1. *Biochem J* *373*, 241-249.

32. Berry, D., Lynn, D.M., Sasisekharan, R., and Langer, R. (2004). Poly(beta-amino ester)s promote cellular uptake of heparin and cancer cell death. *Chem Biol* *11*, 487-498.
33. Berry, D., Shriver, Z., Venkataraman, G., and Sasisekharan, R. (2004). Quantitative assessment of FGF regulation by cell surface heparan sulfates. *Biochem Biophys Res Commun* *314*, 994-1000.
34. Berry, D., Jenniskens, G., Dull, R., and Sasisekharan, R. (2003). Functional activity of cell-surface heparan-sulfate glycosaminoglycan is dependent on focal sequence.
35. Berryman, D.E., and Bensadoun, A. (1995). Heparan sulfate proteoglycans are primarily responsible for the maintenance of enzyme activity, binding, and degradation of lipoprotein lipase in Chinese hamster ovary cells. *J Biol Chem* *270*, 24525-24531.
36. Billottet, C., Janji, B., Thiery, J.P., and Jouanneau, J. (2002). Rapid tumor development and potent vascularization are independent events in carcinoma producing FGF-1 or FGF-2. *Oncogene* *21*, 8128-8139.
37. Bjornsson, S. (1998). Quantitation of proteoglycans as glycosaminoglycans in biological fluids using an Alican blue dot analysis. *Anal Biochem* *256*, 229-237.
38. Blackhall, F.H., Merry, C.L., Davies, E.J., and Jayson, G.C. (2001). Heparan sulfate proteoglycans and cancer. *Br J Cancer* *85*, 1094-1098.
39. Blumberg, R.S., and Strober, W. (2001). Prospects for research in inflammatory bowel disease. *Jama* *285*, 643-647.
40. Boehm, T., Folkman, J., Browder, T., and O'Reilly, M.S. (1997). Antiangiogenic therapy of experimental cancer does not induce acquired drug resistance. *Nature* *390*, 404-407.
41. Bogousslavsky, J., Victor, S.J., Salinas, E.O., Pallay, A., Donnan, G.A., Fieschi, C., Kaste, M., Orgogozo, J.M., Chamorro, A., and Desmet, A. (2002). Fibrinogen (trafermin) in acute stroke: results of the European-Australian phase II/III safety and efficacy trial. *Cerebrovasc Dis* *14*, 239-251.
42. Bonneh-Barkay, D., Shlissel, M., Berman, B., Shaoul, E., Admon, A., Vlodavsky, I., Carey, D.J., Asundi, V.K., Reich-Slotky, R., and Ron, D. (1997). Identification of glypican as a dual modulator of the biological activity of fibroblast growth factors. *J Biol Chem* *272*, 12415-12421.
43. Borregaard, N., and Cowland, J.B. (1997). Granules of the human neutrophilic polymorphonuclear leukocyte. *Blood* *89*, 3503-3521.
44. Borsig, L., Wong, R., Feramisco, J., Nadeau, D.R., Varki, N.M., and Varki, A. (2001). Heparin and cancer revisited: mechanistic connections involving platelets, P-selectin, carcinoma mucins, and tumor metastasis. *Proc Natl Acad Sci U S A* *98*, 3352-3357.
45. Bossennec, V., Petitou, M., and Perly, B. (1990). ¹H-n.m.r. investigation of naturally occurring and chemically oversulphated dermatan sulphates. Identification of minor monosaccharide residues. *Biochem J* *267*, 625-630.
46. Bottaro, D.P. (2002). The role of extracellular matrix heparan sulfate glycosaminoglycan in the activation of growth factor signaling pathways. *Ann N Y Acad Sci* *961*, 158.
47. Bourin, M.C., Lundgren-Akerlund, E., and Lindahl, U. (1990). Isolation and characterization of the glycosaminoglycan component of rabbit thrombomodulin proteoglycan. *J Biol Chem* *265*, 15424-15431.
48. Bourin, M.C., and Lindahl, U. (1993). Glycosaminoglycans and the regulation of blood coagulation. *Biochem J* *289* (Pt 2), 313-330.

49. Bousvaros, A., Zurkowski, D., Fishman, S.J., Keough, K., Law, T., Sun, C., and Leichtner, A.M. (1997). Serum basic fibroblast growth factor in pediatric Crohn's disease. Implications for wound healing. *Dig Dis Sci* *42*, 378-386.
50. Brauchle, M., Madlener, M., Wagner, A.D., Angermeyer, K., Lauer, U., Hofschneider, P.H., Gregor, M., and Werner, S. (1996). Keratinocyte growth factor is highly overexpressed in inflammatory bowel disease. *Am J Pathol* *149*, 521-529.
51. Brazeau, G.A., Attia, S., Poxon, S., and Hughes, J.A. (1998). In vitro myotoxicity of selected cationic macromolecules used in non-viral gene delivery. *Pharm Res* *15*, 680-684.
52. Brodsky, R.A., Mukhina, G.L., Li, S., Nelson, K.L., Chiurazzi, P.L., Buckley, J.T., and Borowitz, M.J. (2000). Improved detection and characterization of paroxysmal nocturnal hemoglobinuria using fluorescent aerolysin. *Am J Clin Pathol* *114*, 459-466.
53. Bryckaert, M., Guillonnet, X., Hecquet, C., Perani, P., Courtois, Y., and Mascarelli, F. (2000). Regulation of proliferation-survival decisions is controlled by FGF1 secretion in retinal pigmented epithelial cells. *Oncogene* *19*, 4917-4929.
54. Bulpitt, P., and Aeschlimann, D. (1999). New strategy for chemical modification of hyaluronic acid: preparation of functionalized derivatives and their use in the formation of novel biocompatible hydrogels. *J Biomed Mater Res* *47*, 152-169.
55. Byrne, F.R., Farrell, C.L., Aranda, R., Rex, K.L., Scully, S., Brown, H.L., Flores, S.A., Gu, L.H., Danilenko, D.M., Lacey, D.L., Ziegler, T.R., and Senaldi, G. (2002). rHuKGF ameliorates symptoms in DSS and CD4(+)/CD45RB(Hi) T cell transfer mouse models of inflammatory bowel disease. *Am J Physiol Gastrointest Liver Physiol* *282*, G690-701.
56. Cadigan, K.M., and Nusse, R. (1997). Wnt signaling: a common theme in animal development. *Genes Dev* *11*, 3286-3305.
57. Capila, I., and Linhardt, R.J. (2002). Heparin-protein interactions. *Angew Chem Int Ed Engl* *41*, 391-412.
58. Cardin, A.D., and Weintraub, H.J. (1989). Molecular modeling of protein-glycosaminoglycan interactions. *Arteriosclerosis* *9*, 21-32.
59. Carey, D.J., Stahl, R.C., Cizmeci-Smith, G., and Asundi, V.K. (1994). Syndecan-1 expressed in Schwann cells causes morphological transformation and cytoskeletal reorganization and associates with actin during cell spreading. *J Cell Biol* *124*, 161-170.
60. Carey, D.J. (1997). Syndecans: multifunctional cell-surface co-receptors. *Biochem J* *327 (Pt 1)*, 1-16.
61. Casu, B., and Lindahl, U. (2001). Structure and biological interactions of heparin and heparan sulfate. *Adv Carbohydr Chem Biochem* *57*, 159-206.
62. Casu, B., Guerrini, M., Naggi, A., Perez, M., Torri, G., Ribatti, D., Carminati, P., Giannini, G., Penco, S., Pisano, C., Belleri, M., Rusnati, M., and Presta, M. (2002). Short heparin sequences spaced by glycol-split uronate residues are antagonists of fibroblast growth factor 2 and angiogenesis inhibitors. *Biochemistry* *41*, 10519-10528.
63. Chang, Z., Meyer, K., Rapraeger, A.C., and Friedl, A. (2000). Differential ability of heparan sulfate proteoglycans to assemble the fibroblast growth factor receptor complex in situ. *FASEB J* *14*, 137-144.
64. Chaouchi, N., Arvanitakis, L., Auffredou, M.T., Blanchard, D.A., Vazquez, A., and Sharma, S. (1995). Characterization of transforming growth factor-beta 1 induced apoptosis in normal human B cells and lymphoma B cell lines. *Oncogene* *11*, 1615-1622.

65. Chauhan-Patel, R., and Spruce, A.E. (1998). Differential regulation of potassium currents by FGF-1 and FGF-2 in embryonic *Xenopus laevis* myocytes. *J Physiol* 512 (Pt 1), 109-118.
66. Chellaiah, A.T., McEwen, D.G., Werner, S., Xu, J., and Ornitz, D.M. (1994). Fibroblast growth factor receptor (FGFR) 3. Alternative splicing in immunoglobulin-like domain III creates a receptor highly specific for acidic FGF/FGF-1. *J Biol Chem* 269, 11620-11627.
67. Chen, G., Ito, Y., Imanishi, Y., Magnani, A., Lamponi, S., and Barbucci, R. (1997). Photoimmobilization of sulfated hyaluronic acid for antithrombogenicity. *Bioconjug Chem* 8, 730-734.
68. Chen, Y., Chou, K., Fuchs, E., Havran, W.L., and Boismenu, R. (2002). Protection of the intestinal mucosa by intraepithelial gamma delta T cells. *Proc Natl Acad Sci U S A* 99, 14338-14343.
69. Cheng, C.W., Smith, S.K., and Charnock-Jones, D.S. (2003). Wnt-1 signaling inhibits human umbilical vein endothelial cell proliferation and alters cell morphology. *Exp Cell Res* 291, 415-425.
70. Choubey, D., and Gutterman, J.U. (1997). Inhibition of E2F-4/DP-1-stimulated transcription by p202. *Oncogene* 15, 291-301.
71. Chu, C.L., Buczek-Thomas, J.A., and Nugent, M.A. (2004). Heparan sulphate proteoglycans modulate fibroblast growth factor-2 binding through a lipid raft-mediated mechanism. *Biochem J* 379, 331-341.
72. Chua, C.C., Rahimi, N., Forsten-Williams, K., and Nugent, M.A. (2004). Heparan sulfate proteoglycans function as receptors for fibroblast growth factor-2 activation of extracellular signal-regulated kinases 1 and 2. *Circ Res* 94, 316-323.
73. Ciruna, B., and Rossant, J. (2001). FGF signaling regulates mesoderm cell fate specification and morphogenetic movement at the primitive streak. *Dev Cell* 1, 37-49.
74. Citores, L., Wesche, J., Kolpakova, E., and Olsnes, S. (1999). Uptake and intracellular transport of acidic fibroblast growth factor: evidence for free and cytoskeleton-anchored fibroblast growth factor receptors. *Mol Biol Cell* 10, 3835-3848.
75. Clasper, S., Vekemans, S., Fiore, M., Plebanski, M., Wordsworth, P., David, G., and Jackson, D.G. (1999). Inducible expression of the cell surface heparan sulfate proteoglycan syndecan-2 (fibroglycan) on human activated macrophages can regulate fibroblast growth factor action. *J Biol Chem* 274, 24113-24123.
76. Cobel-Geard, R.J., and Hassouna, H.I. (1983). Interaction of protamine sulfate with thrombin. *Am J Hematol* 14, 227-233.
77. Conrad, H.E. (1998). *Heparin-Binding Proteins* (San Diego: Academic Press).
78. Cook, J., and Zitelli, J.A. (1998). Mohs micrographic surgery: a cost analysis. *J Am Acad Dermatol* 39, 698-703.
79. Cosgrove, R.H., Zacharski, L.R., Racine, E., and Andersen, J.C. (2002). Improved cancer mortality with low-molecular-weight heparin treatment: a review of the evidence. *Semin Thromb Hemost* 28, 79-87.
80. Couchman, J.R., and Woods, A. (1999). Syndecan-4 and integrins: combinatorial signaling in cell adhesion. *J Cell Sci* 112 (Pt 20), 3415-3420.
81. Couchman, J.R. (2003). Syndecans: proteoglycan regulators of cell-surface microdomains? *Nat Rev Mol Cell Biol* 4, 926-937.
82. Cronauer, M.V., Hittmair, A., Eder, I.E., Hobisch, A., Culig, Z., Ramoner, R., Zhang, J., Bartsch, G., Reissigl, A., Radmayr, C., Thurnher, M., and Klocker, H. (1997). Basic

- fibroblast growth factor levels in cancer cells and in sera of patients suffering from proliferative disorders of the prostate. *Prostate* 31, 223-233.
83. Crystal, R.G. (1995). Transfer of genes to humans: early lessons and obstacles to success. *Science* 270, 404-410.
 84. Curry, F.E., and Michel, C.C. (1980). A fiber matrix model of capillary permeability. *Microvasc Res* 20, 96-99.
 85. Dai, L., Zientek, P., St. Johns, H., Pasic, P., Chatelier, R., and Griesser, H.J. (1996). Surface modification of polymeric biomaterials. In *Surface modification of polymer biomaterials*, B. Rastner and D. Castner, eds. (New York: Plenum Press), p. 147.
 86. David, G. (1993). Integral membrane heparan sulfate proteoglycans. *Faseb J* 7, 1023-1030.
 87. Davis, J.C., Venkataraman, D., Shriver, Z., Raj, P.A., and Sasisekharan, R. (1999). Oligomeric self-association of basic fibroblast growth factor in the absence of heparin-like glycosaminoglycans. *Biochemistry Journal* 341, 613-620.
 88. Day, R.M., Mitchell, T.J., Knight, S.C., and Forbes, A. (2003). Regulation of epithelial syndecan-1 expression by inflammatory cytokines. *Cytokine* 21, 224-233.
 89. Deguchi, Y., Okutsu, H., Okura, T., Yamada, S., Kimura, R., Yuge, T., Furukawa, A., Morimoto, K., Tachikawa, M., Ohtsuki, S., Hosoya, K., and Terasaki, T. (2002). Internalization of basic fibroblast growth factor at the mouse blood-brain barrier involves a heparan sulfate proteoglycan. *J Neurochem* 83, 381-389.
 90. Delehedde, M., Lyon, M., Sergeant, N., Rahmoune, H., and Fernig, D.G. (2001). Proteoglycans: pericellular and cell surface multireceptors that integrate external stimuli in the mammary gland. *J Mammary Gland Biol Neoplasia* 6, 253-273.
 91. Di Sabatino, A., Ciccocioppo, R., Armellini, E., Morera, R., Ricevuti, L., Cazzola, P., Fulle, I., and Corazza, G.R. (2004). Serum bFGF and VEGF correlate respectively with bowel wall thickness and intramural blood flow in Crohn's disease. *Inflamm Bowel Dis* 10, 573-577.
 92. DiGabriele, A.D., Lax, I., Chen, D.I., Svahn, C.M., Jaye, M., Schlessinger, J., and Hendrickson, W.A. (1998). Structure of a heparin-linked biologically active dimer of fibroblast growth factor. *Nature* 393, 812-817.
 93. Dignass, A.U., Tsunekawa, S., and Podolsky, D.K. (1994). Fibroblast growth factors modulate intestinal epithelial cell growth and migration. *Gastroenterology* 106, 1254-1262.
 94. Dorkin, T.J., Robinson, M.C., Marsh, C., Bjartell, A., Neal, D.E., and Leung, H.Y. (1999). FGF8 over-expression in prostate cancer is associated with decreased patient survival and persists in androgen independent disease. *Oncogene* 18, 2755-2761.
 95. Dorkin, T.J., Robinson, M.C., Marsh, C., Neal, D.E., and Leung, H.Y. (1999). aFGF immunoreactivity in prostate cancer and its co-localization with bFGF and FGF8. *J Pathol* 189, 564-569.
 96. Dudas, J., Ramadori, G., Knittel, T., Neubauer, K., Raddatz, D., Egedy, K., and Kovalszky, I. (2000). Effect of heparin and liver heparan sulphate on interaction of HepG2-derived transcription factors and their cis-acting elements: altered potential of hepatocellular carcinoma heparan sulphate. *Biochem J* 350 Pt 1, 245-251.
 97. Dudek, S.M., and Garcia, J.G. (2001). Cytoskeletal regulation of pulmonary vascular permeability. *J Appl Physiol* 91, 1487-1500.

98. Dull, R.O., Dinavahi, R., Schwartz, L., Humphries, D.E., Berry, D., Sasisekharan, R., and Garcia, J.G. (2003). Lung endothelial heparan sulfates mediate cationic peptide-induced barrier dysfunction: a new role for the glycocalyx. *Am J Physiol Lung Cell Mol Physiol* 285, L986-995.
99. Dull, R.O., Dinavahi, R., Schwartz, L., Humphries, D.E., Berry, D., Sasisekharan, R., and Garcia, J.G.N. (2003). Lung endothelial heparan sulfates mediate cationic peptide-Induced barrier dysfunction: a new role for the glycocalyx. *Am J Physiol Lung Cell Mol Physiol*.
100. Duteil, S., Gariel, P., Girault, S., Mallet, A., Feve, C., and Siret, L. (1999). Identification of heparin oligosaccharides by direct coupling of capillary electrophoresis/ionspray-mass spectrometry. *Rapid Commun Mass Spectrom* 13, 1889-1898.
101. Edelman, E.R., Adams, D.H., Karnovsky, M.J. (1990). Effect of controlled adventitial heparin delivery on smooth muscle cell proliferation following endothelial injury. *Proc Natl Acad Sci U S A* 87, 3773-3777.
102. Edovitsky, E., Elkin, M., Zcharia, E., Peretz, T., and Vlodaysky, I. (2004). Heparanase gene silencing, tumor invasiveness, angiogenesis, and metastasis. *J Natl Cancer Inst* 96, 1219-1230.
103. el-Hariry, I., Pagnatelli, M., and Lemoine, N. (1997). Fibroblast growth factor 1 and fibroblast growth factor 2 immunoreactivity in gastrointestinal tumours. *J Pathol* 181, 39-45.
104. Ernst, S., Langer, R., Cooney, C.L., and Sasisekharan, R. (1995). Enzymatic degradation of glycosaminoglycans. *Crit Rev in Biochem Mol Biol* 30, 387-444.
105. Ernst, S., Venkataraman, G., Winkler, S., Godavarti, R., Langer, R., Cooney, C.L., and Sasisekharan, R. (1996). Expression in *Escherichia coli*, purification and characterization of heparinase I from *Flavobacterium heparinum*. *Biochem J* 315 (Pt 2), 589-597.
106. Ernst, S., *et al* (1996). Expression in *Escherichia coli*, purification and characterization of heparinase I from *Flavobacterium heparinum*. *Biochemical Journal* 315, 589-597.
107. Eroglu, A., Toner, M., and Toth, T.L. (2002). Beneficial effect of microinjected trehalose on the cryosurvival of human oocytes. *Fertil Steril* 77, 152-158.
108. Esko, J.D., and Lindahl, U. (2001). Molecular diversity of heparan sulfate. *J Clin Invest* 108, 169-173.
109. Esko, J.D., and Selleck, S.B. (2002). Order out of chaos: assembly of ligand binding sites in heparan sulfate. *Annu Rev Biochem* 71, 435-471.
110. Ettenson, D.S., Koo, E.W.Y., Januzzi, J.L., and Edelman, E.R. (2000). Endothelial heparan sulfate is necessary but not sufficient for control of vascular smooth muscle cell growth. *J Cell Physiol* 184, 93-100.
111. Faham, S., Hileman, R.E., Fromm, J.R., Linhardt, R.J., and Rees, D.C. (1996). Heparin structure and interactions with basic fibroblast growth factor. *Science* 271, 1116-1120.
112. Faham, S., Hileman, R.E., Fromm, J.R., Lindhart, R.J., and Rees, D.C. (1996). Heparin structure and interactions with basic fibroblast growth factor. *Science* 271, 1116-1120.
113. Fairbrother, W.J., Champe, M.A., Christinger, H.W., Keyt, B.A., and Starovasnik, M.A. (1998). Solution structure of the heparin-binding domain of vascular endothelial growth factor. *Structure* 6, 637-648.
114. Fannon, M., and Nugent, M.A. (1996). Basic fibroblast growth factor binds its receptors, is internalized, and stimulates DNA synthesis in Balb/c3T3 cells in the absence of heparan sulfate. *J Biol Chem* 271, 17949-17956.

115. Fannon, M., Forsten, K.E., and Nugent, M.A. (2000). Potentiation and inhibition of bFGF binding to heparin: a model for regulation of cellular response. *Biochemistry* 39, 1434-1445.
116. Fannon, M., Forsten-Williams, K., Dowd, C.J., Freedman, D.A., Folkman, J., and Nugent, M.A. (2003). Binding inhibition of angiogenic factors by heparan sulfate proteoglycans in aqueous humor: potential mechanism for maintenance of an avascular environment. *Faseb J* 17, 902-904.
117. Farquhar, M.G., and Palade, G.E. (1963). Junctional complexes in various epithelia. *J Cell Biol* 17, 375-412.
118. Feng, S., Wang, F., Matsubara, A., Kan, M., and McKeehan, W.L. (1997). Fibroblast growth factor receptor 2 limits and receptor 1 accelerates tumorigenicity of prostate epithelial cells. *Cancer Res* 57, 5369-5378.
119. Fernig, D.G., and Gallagher, J.T. (1994). Fibroblast growth factors and their receptors: an information network controlling tissue growth, morphogenesis and repair. *Prog Growth Factor Res* 5, 353-377.
120. Ferrara, N., Gerber, H.P., and LeCouter, J. (2003). The biology of VEGF and its receptors. *Nat Med* 9, 669-676.
121. Fialka, I., Steinlein, P., Ahorn, H., Bock, G., Burbelo, P.D., Haberfellner, M., Lottspeich, F., Paiha, K., Pasquali, C., and Huber, L.A. (1999). Identification of syntenin as a protein of the apical early endocytic compartment in Madin-Darby canine kidney cells. *J Biol Chem* 274, 26233-26239.
122. Fidler, I.J., and Kripke, M.L. (1977). Metastasis results from preexisting variant cells within a malignant tumor. *Science* 197, 893-895.
123. Filmus, J., and Selleck, S.B. (2001). Glypicans: proteoglycans with a surprise. *J Clin Invest* 108, 497-501.
124. Finch, P.W., Rubin, J.S., Miki, T., Ron, D., and Aaronson, S.A. (1989). Human KGF is FGF-related with properties of a paracrine effector of epithelial cell growth. *Science* 245, 752-755.
125. Finch, P.W., Pricolo, V., Wu, A., and Finkelstein, S.D. (1996). Increased expression of keratinocyte growth factor messenger RNA associated with inflammatory bowel disease. *Gastroenterology* 110, 441-451.
126. Finch, P.W., and Cheng, A.L. (1999). Analysis of the cellular basis of keratinocyte growth factor overexpression in inflammatory bowel disease. *Gut* 45, 848-855.
127. Fisher, M., Meadows, M.E., Do, T., Weise, J., Trubetsky, V., Charette, M., and Finklestein, S.P. (1995). Delayed treatment with intravenous basic fibroblast growth factor reduces infarct size following permanent focal cerebral ischemia in rats. *J Cereb Blood Flow Metab* 15, 953-959.
128. Fitzgerald, M.L., Wang, Z., Park, P.W., Murphy, G., and Bernfield, M. (2000). Shedding of syndecan-1 and -4 ectodomains is regulated by multiple signaling pathways and mediated by a TIMP-3-sensitive metalloproteinase. *J Cell Biol* 148, 811-824.
129. Fitzgerald, M.L., Wang, Z., Park, P.W., Murphy, G., and Bernfield, M. (2000). Shedding of syndecan-1 and -4 ectodomains is regulated by multiple signaling pathways and mediated by a TIMP-3-sensitive metalloproteinase. *J Cell Biol* 148, 811-824.
130. Florian, J.A., Kosky, J.R., Ainslie, K., Pang, Z., Dull, R.O., and Tarbell, J.M. (2003). Heparan sulfate proteoglycan is a mechanosensor on endothelial cells. *Circ Res* 93, e136-142.

131. Folkman, J., Langer, R., Linhardt, R.J., Haudenschild, C., and Taylor, S. (1983). Angiogenesis inhibition and tumor regression caused by heparin or a heparin fragment in the presence of cortisone. *Science* 221, 719-725.
132. Folkman, J., Szabo, S., Stovroff, M., McNeil, P., Li, W., and Shing, Y. (1991). Duodenal ulcer. Discovery of a new mechanism and development of angiogenic therapy that accelerates healing. *Ann Surg* 214, 414-425; discussion 426-417.
133. Folkman, J. (2001). Angiogenesis-dependent diseases. *Semin Oncol* 28, 536-542.
134. Forsten, K.E., Courant, N.A., and Nugent, M.A. (1997). Endothelial proteoglycans inhibit bFGF binding and mitogenesis. *J Cell Physiol* 172, 209-220.
135. Friedmann, Y., Vlodaysky, I., Aingorn, H., Aviv, A., Peretz, T., Pecker, I., and Pappo, O. (2000). Expression of heparanase in normal, dysplastic, and neoplastic human colonic mucosa and stroma. Evidence for its role in colonic tumorigenesis. *Am J Pathol* 157, 1167-1175.
136. Fujiwara, Y., and Kaji, T. (1999). Possible mechanism for lead inhibition of vascular endothelial cell proliferation: a lower response to basic fibroblast growth factor through inhibition of heparan sulfate synthesis. *Toxicology* 133, 147-157.
137. Fukatsu, T., Sobue, M., Nagasaka, T., Ohiwa, N., Fukata, S., Nakashima, N., and Takeuchi, J. (1988). Immunohistochemical localization of chondroitin sulphate and dermatan sulphate proteoglycans in tumour tissues. *Br J Cancer* 57, 74-78.
138. Gallagher, J.T., Turnbull, J.E., and Lyon, M. (1992). Patterns of sulphation in heparan sulphate: polymorphism based on a common structural theme. *Int J Biochem* 24, 553-560.
139. Gallagher, J.T., Turnbull, J.E., and Lyon, M. (1992). Heparan sulphate proteoglycans: molecular organisation of membrane-associated species and an approach to polysaccharide sequence analysis. *Adv Exp Med Biol* 313, 49-57.
140. Gallagher, J.T. (1997). Structure-activity relationship of heparan sulphate. *Biochem Soc Trans* 25, 1206-1209.
141. Garcia, J.G., Davis, H.W., and Patterson, C.E. (1995). Regulation of endothelial cell gap formation and barrier dysfunction: role of myosin light chain phosphorylation. *J Cell Physiol* 163, 510-522.
142. Garcia, J.G., Lazar, V., Gilbert-McClain, L.I., Gallagher, P.J., and Verin, A.D. (1997). Myosin light chain kinase in endothelium: molecular cloning and regulation. *Am J Respir Cell Mol Biol* 16, 489-494.
143. Garcia, J.G., Schaphorst, K.L., Shi, S., Verin, A.D., Hart, C.M., Callahan, K.S., and Patterson, C.E. (1997). Mechanisms of ionomycin-induced endothelial cell barrier dysfunction. *Am J Physiol* 273, L172-184.
144. Garcia, J.G., Wang, P., Schaphorst, K.L., Becker, P.M., Borbiev, T., Liu, F., Birukova, A., Jacobs, K., Bogatcheva, N., and Verin, A.D. (2002). Critical involvement of p38 MAP kinase in pertussis toxin-induced cytoskeletal reorganization and lung permeability. *Faseb J* 16, 1064-1076.
145. Gardiner, K.R., Anderson, N.H., Rowlands, B.J., and Barbul, A. (1995). Colitis and colonic mucosal barrier dysfunction. *Gut* 37, 530-535.
146. Gautam, N., Olofsson, A.M., Herwald, H., Iversen, L.F., Lundgren-Akerlund, E., Hedqvist, P., Arfors, K.E., Flodgaard, H., and Lindbom, L. (2001). Heparin-binding protein (HBP/CAP37): a missing link in neutrophil-evoked alteration of vascular permeability. *Nat Med* 7, 1123-1127.

147. Gavioli, R., Frisan, T., Vertuani, S., Bornkamm, G.W., and Masucci, M.G. (2001). c-myc overexpression activates alternative pathways for intracellular proteolysis in lymphoma cells. *Nat Cell Biol* 3, 283-288.
148. Giaever, I., and Keese, C.R. (1993). A morphological biosensor for mammalian cells. *Nature* 366, 591-592.
149. Gimbrone, M.A. (1995). Vascular endothelium in health and disease. In *Molecular Cardiovascular Medicine*. E. Haber, ed. (Scientific American Medicine), pp. 49-61.
150. Giraux, J.L., Matou, S., Bros, A., Tapon-Brethaudiere, J., Letourneur, D., Fischer, A.M. (1998). Modulation of human endothelial cell proliferation and migration by fucoidan and heparin. *Eur J Cell Biol* 77, 352-359.
151. Giri, D., Ropiquet, F., and Ittmann, M. (1999). Alterations in expression of basic fibroblast growth factor (FGF) 2 and its receptor FGFR-1 in human prostate cancer. *Clin Cancer Res* 5, 1063-1071.
152. Giri, D., Ropiquet, F., and Ittmann, M. (1999). FGF9 is an autocrine and paracrine prostatic growth factor expressed by prostatic stromal cells. *J Cell Physiol* 180, 53-60.
153. Givol, D., and Yayon, A. (1992). Complexity of FGF receptors: genetic basis for structural diversity and functional specificity. *Faseb J* 6, 3362-3369.
154. Godavarti, R., Cooney, C.L., Langer, R., and Sasisekharan, R. (1996). Heparinase I from *Flavobacterium heparinum*. Identification of a critical histidine residue essential for catalysis as probed by chemical modification and site-directed mutagenesis. *Biochemistry* 35, 6846-6852.
155. Godavarti, R., Davis, M., Venkataraman, G., Cooney, C., Langer, R., and Sasisekharan, R. (1996). Heparinase III from *Flavobacterium heparinum*: cloning and recombinant expression in *Escherichia coli*. *Biochem Biophys Res Commun* 225, 751-758.
156. Godavarti, R., and Sasisekharan, R. (1998). Heparinase I from *Flavobacterium heparinum*. Role of positive charge in enzymatic activity. *J Biol Chem* 273, 248-255.
157. Goldshmidt, O., Zcharia, E., Abramovitch, R., Metzger, S., Aingorn, H., Friedmann, Y., Schirrmacher, V., Mitrani, E., and Vlodavsky, I. (2002). Cell surface expression and secretion of heparanase markedly promote tumor angiogenesis and metastasis. *Proc Natl Acad Sci U S A* 99, 10031-10036.
158. Graeven, U., Rodeck, U., Karpinski, S., Jost, M., Philippou, S., and Schmiegel, W. (2001). Modulation of angiogenesis and tumorigenicity of human melanocytic cells by vascular endothelial growth factor and basic fibroblast growth factor. *Cancer Res* 61, 7282-7290.
159. Gribbon, P., Heng, B.C., and Hardingham, T.E. (1999). The molecular basis of the solution properties of hyaluronan investigated by confocal fluorescence recovery after photobleaching. *Biophys J* 77, 2210-2216.
160. Grootjans, J.J., Zimmermann, P., Reekmans, G., Smets, A., Degeest, G., Durr, J., and David, G. (1997). Syntenin, a PDZ protein that binds syndecan cytoplasmic domains. *Proc Natl Acad Sci U S A* 94, 13683-13688.
161. Gross, J.L., Morrison, R.S., Eidsvoog, K., Herblin, W.F., Kornblith, P.L., and Dexter, D.L. (1990). Basic fibroblast growth factor: a potential autocrine regulator of human glioma cell growth. *J Neurosci Res* 27, 689-696.
162. Guerrini, M., Agulles, T., Bisio, A., Hricovini, M., Lay, L., Naggi, A., Poletti, L., Sturiale, L., Torri, G., and Casu, B. (2002). Minimal heparin/heparan sulfate sequences for binding to fibroblast growth factor-1. *Biochem Biophys Res Commun* 292, 222-230.

163. Guimond, S., Maccarana, M., Olwin, B.B., Lindahl, U., and Rapraeger, A.C. (1993). Activating and inhibitory heparin sequences for FGF-2 (basic FGF). Distinct requirements for FGF-1, FGF-2 and FGF-4. *J Biol Chem* 268, 23906-23914.
164. Guimond, S.E., Turnbull, J.E (1999). Fibroblast growth factor receptor signalling is dictated by specific heparan sulfate saccharides. *Current Biology* 9, 1343-1346.
165. Gumbiner, B.M. (1996). Cell adhesion: the molecular basis of tissue architecture and morphogenesis. *Cell* 84, 345-357.
166. Habuchi, H., Suzuki, S., Saito, T., Tamura, T., Harada, T., Yoshida, K., and Kimata, K. (1992). Structure of a heparan sulphate oligosaccharide that binds to basic fibroblast growth factor. *Biochem J* 285 (Pt 3), 805-813.
167. Hahnenberger, R., Jakobson, A.M., Ansari, A., Wehler, T., Svahn, C.M., and Lindahl, U. (1993). Low-sulphated oligosaccharides derived from heparan sulphate inhibit normal angiogenesis. *Glycobiology* 3, 567-573.
168. Halaban, R. (1999). Melanoma cell autonomous growth: the Rb/E2F pathway. *Cancer Metastasis Rev* 18, 333-343.
169. Han, D.S., Li, F., Holt, L., Connolly, K., Hubert, M., Miceli, R., Okoye, Z., Santiago, G., Windle, K., Wong, E., and Sartor, R.B. (2000). Keratinocyte growth factor-2 (FGF-10) promotes healing of experimental small intestinal ulceration in rats. *Am J Physiol Gastrointest Liver Physiol* 279, G1011-G1022.
170. Han, R.O., Ettenson, D.S., Koo, E.W., and Edelman, E.R. (1997). Heparin/heparan sulfate chelation inhibits control of vascular repair by tissue-engineering endothelial cells. *Am J Physiol* 273, H2586-2595.
171. Han, X., Fink, M.P., and Delude, R.L. (2003). Proinflammatory cytokines cause NO*-dependent and -independent changes in expression and localization of tight junction proteins in intestinal epithelial cells. *Shock* 19, 229-237.
172. Hanahan, D., and Weinberg, R.A. (2000). The hallmarks of cancer. *Cell* 100, 57-70.
173. Hansen, C.A., Schroering, A.G., Carey, D.J., and Robishaw, J.D. (1994). Localization of a heterotrimeric G protein gamma subunit to focal adhesions and associated stress fibers. *J Cell Biol* 126, 811-819.
174. Hartley, P.G., McArthur, S.L., McLean, K.M., and Griesser, H.J. (2002). Physicochemical properties of polysaccharide coatings based on graded multilayer assemblies. *Langmuir* 18, 2383-2394.
175. Hawkins, C.L., and Davies, M.J. (1998). Degradation of hyaluronic acid, poly- and monosaccharides, and model compounds by hypochlorite: evidence for radical intermediates and fragmentation. *Free Radic Biol Med* 24, 1396-1410.
176. He, J., and Baum, L.G. (2003). Presentation of galectin-1 by extracellular matrix triggers T cell death. *J Biol Chem*.
177. Hermiston, M.L., and Gordon, J.I. (1995). Inflammatory bowel disease and adenomas in mice expressing a dominant negative N-cadherin. *Science* 270, 1203-1207.
178. Herr, A.B., Ornitz, D.M., Sasisekharan, R., Venkataraman, G., and Waksman, G. (1997). Heparin-induced self-association of fibroblast growth factor-2. Evidence for two oligomerization processes. *J Biol Chem* 272, 16382-16389.
179. Hildebrandt, P. (2002). Glycosaminoglycans--all round talents in coating technology. *Biomed Tech (Berl)* 47 Suppl 1 Pt 1, 476-478.

180. Ho, C.L., Sheu, L.F., and Li, C.Y. (2002). Immunohistochemical expression of basic fibroblast growth factor, vascular endothelial growth factor, and their receptors in stage IV non-Hodgkin lymphoma. *Appl Immunohistochem Mol Morphol* 10, 316-321.
181. Hopkins, A.M., Walsh, S.V., Verkade, P., Boquet, P., and Nusrat, A. (2003). Constitutive activation of Rho proteins by CNF-I influences tight junction structure and epithelial barrier function. *J Cell Sci* 116, 725-742.
182. Horowitz, A., Tkachenko, E., and Simons, M. (2002). Fibroblast growth factor-specific modulation of cellular response by syndecan-4. *J Cell Biol* 157, 715-725.
183. Hsia, E., Richardson, T.P., and Nugent, M.A. (2003). Nuclear localization of basic fibroblast growth factor is mediated by heparan sulfate proteoglycans through protein kinase C signaling. *J Cell Biochem* 88, 1214-1225.
184. Hu, X., Adamson, R.H., Liu, B., Curry, F.E., and Weinbaum, S. (2000). Starling forces that oppose filtration after tissue oncotic pressure is increased. *Am J Physiol Heart Circ Physiol* 279, H1724-1736.
185. Huhtala, M.T., Pentikainen, O.T., and Johnson, M.S. (1999). A dimeric ternary complex of FGFR [correction of FGFR1], heparin and FGF-I leads to an 'electrostatic sandwich' model for heparin binding. *Structure Fold Des* 7, 699-709.
186. Hulett, M.D., Freeman, C., Hamdorf, B.J., Baker, R.T., Harris, M.J., and Parish, C.R. (1999). Cloning of mammalian heparanase, an important enzyme in tumor invasion and metastasis. *Nat Med* 5, 803-809.
187. Hull, M.A., Cullen, D.J., Hudson, N., and Hawkey, C.J. (1995). Basic fibroblast growth factor treatment for non-steroidal anti-inflammatory drug associated gastric ulceration. *Gut* 37, 610-612.
188. Humphries, D.E., Lee, S.L., Fanburg, B.L., and Silbert, J.E. (1986). Effects of hypoxia and hyperoxia on proteoglycan production by bovine pulmonary artery endothelial cells. *J Cell Physiol* 126, 249-253.
189. Humphries, D.E., Wong, G.W., Friend, D.S., Gurish, M.F., Qiu, W.T., Huang, C., Sharpe, A.H., and Stevens, R.L. (1999). Heparin is essential for the storage of specific granule proteases in mast cells. *Nature* 400, 769-772.
190. Iba, K., Albrechtsen, R., Gilpin, B., Frohlich, C., Loechel, F., Zolkiewska, A., Ishiguro, K., Kojima, T., Liu, W., Langford, J.K., Sanderson, R.D., Brakebusch, C., Fassler, R., and Wewer, U.M. (2000). The cysteine-rich domain of human ADAM 12 supports cell adhesion through syndecans and triggers signaling events that lead to beta1 integrin-dependent cell spreading. *J Cell Biol* 149, 1143-1156.
191. Ibrahimi, O.A., Eliseenkova, A.V., Plotnikov, A.N., Yu, K., Ornitz, D.M., and Mohammadi, M. (2001). Structural basis for fibroblast growth factor receptor 2 activation in Apert syndrome. *Proc Natl Acad Sci U S A* 98, 7182-7187.
192. Inman, G.J., and Allday, M.J. (2000). Apoptosis induced by TGF-beta 1 in Burkitt's lymphoma cells is caspase 8 dependent but is death receptor independent. *J Immunol* 165, 2500-2510.
193. Inman, G.J., Binne, U.K., Parker, G.A., Farrell, P.J., and Allday, M.J. (2001). Activators of the Epstein-Barr virus lytic program concomitantly induce apoptosis, but lytic gene expression protects from cell death. *J Virol* 75, 2400-2410.
194. Iozzo, R.V., and Murdoch, A.D. (1996). Proteoglycans of the extracellular environment: clues from the gene and protein side offer novel perspectives in molecular diversity and function. *Faseb J* 10, 598-614.

195. Iozzo, R.V. (1998). Matrix proteoglycans: from molecular design to cellular function. *Annu Rev Biochem* *67*, 609-652.
196. Iozzo, R.V., and San Antonio, J.D. (2001). Heparan sulfate proteoglycans: heavy hitters in the angiogenesis arena. *Journal of Clinical Investigation* *108*, 349-355.
197. Ishihara, M. (1994). Structural requirements in heparin for binding and activation of FGF-1 and FGF-4 are different from that for FGF-2. *Glycobiology* *4*, 817-824.
198. Itano, N., Sawai, T., Atsumi, F., Miyaishi, O., Taniguchi, S., Kannagi, R., Hamaguchi, M., and Kimata, K. (2004). Selective expression and functional characteristics of three mammalian hyaluronan synthases in oncogenic malignant transformation. *J Biol Chem* *279*, 18679-18687.
199. Izzard, C.S., Radinsky, R., and Culp, L.A. (1986). Substratum contacts and cytoskeletal reorganization of BALB/c 3T3 cells on a cell-binding fragment and heparin-binding fragments of plasma fibronectin. *Exp Cell Res* *165*, 320-336.
200. Jacks, T., and Weinberg, R.A. (2002). Taking the study of cancer cell survival to a new dimension. *Cell* *111*, 923-925.
201. Jackson, M.W., Roberts, J.S., Heckford, S.E., Ricciardelli, C., Stahl, J., Choong, C., Horsfall, D.J., and Tilley, W.D. (2002). A potential autocrine role for vascular endothelial growth factor in prostate cancer. *Cancer Res* *62*, 854-859.
202. Jackson, R.L., Busch, S.J., and Cardin, A.D. (1991). Glycosaminoglycans: molecular properties, protein interactions, and role in physiological processes. *Physiol Rev* *71*, 481-539.
203. Jameson, J., Ugarte, K., Chen, N., Yachi, P., Fuchs, E., Boismenu, R., and Havran, W.L. (2002). A role for skin gammadelta T cells in wound repair. *Science* *296*, 747-749.
204. Jandik, K.A., Gu, K., and Linhardt, R.J. (1994). Action pattern of polysaccharide lyases on glycosaminoglycans. *Glycobiology* *4*, 289-296.
205. Jeffers, M., McDonald, W.F., Chillakuru, R.A., Yang, M., Nakase, H., Deegler, L.L., Sylander, E.D., Rittman, R., Bendele, A., Sartor, R.B., and Lichenstein, H.S. (2002). A novel human fibroblast growth factor treats experimental intestinal inflammation. *Gastroenterology* *123*, 1151-1162.
206. Jemal, A., Murray, T., Ward, E., Samuels, A., Tiwari, R.C., Ghafoor, A., Feuer, E.J., and Thun, M.J. (2005). Cancer statistics, 2005. *CA Cancer J Clin* *55*, 10-30.
207. Jin, L., Abrahams, J.P., Skinner, R., Petitou, M., Pike, R.N., and Carrell, R.W. (1997). The anticoagulant activation of antithrombin by heparin. *Proceedings of the National Academy of Sciences USA* *94*, 14683-14688.
208. Jones, T.A., and Schallert, T. (1994). Use-dependent growth of pyramidal neurons after neocortical damage. *J Neurosci* *14*, 2140-2152.
209. Joukov, V., Pajusola, K., Kaipainen, A., Chilov, D., Lahtinen, I., Kukk, E., Saksela, O., Kalkkinen, N., and Alitalo, K. (1996). A novel vascular endothelial growth factor, VEGF-C, is a ligand for the Flt4 (VEGFR-3) and KDR (VEGFR-2) receptor tyrosine kinases. *Embo J* *15*, 290-298.
210. Kabanov, A.V., and Kabanov, V.A. (1995). DNA complexes with polycations for the delivery of genetic material into cells. *Bioconjug Chem* *6*, 7-20.
211. Kalluri, R. (2003). Basement membranes: structure, assembly and role in tumour angiogenesis. *Nat Rev Cancer* *3*, 422-433.
212. Kamp, P., Strathmann, A., and Ragg, H. (2001). Heparin cofactor II, antithrombin-beta and their complexes with thrombin in human tissues. *Thromb Res* *101*, 483-491.

213. Kan, M., Wu, X., Wang, F., and McKeegan, W.L. (1999). Specificity for fibroblast growth factors determined by heparan sulfate in a binary complex with the receptor kinase. *J Biol Chem* 274, 15947-15952.
214. Kan, M., Wang, F., Xu, J., Crabb, J.W., Hou, J., and McKeegan, W.L. (1993). An essential heparin-binding domain in the fibroblast growth factor receptor kinase. *Science* 259, 1918-1921.
215. Kanai, M., Rosenberg, I., and Podolsky, D.K. (1997). Cytokine regulation of fibroblast growth factor receptor 3 IIIb in intestinal epithelial cells. *Am J Physiol* 272, G885-G893.
216. Kanazawa, S., Tsunoda, T., Onuma, E., Majima, T., Kagiya, M., and Kikuchi, K. (2001). VEGF, basic-FGF, and TGF-beta in Crohn's disease and ulcerative colitis: a novel mechanism of chronic intestinal inflammation. *Am J Gastroenterol* 96, 822-828.
217. Kannan, K., Sharpless, N.E., Xu, J., O'Hagan, R.C., Bosenberg, M., and Chin, L. (2003). Components of the Rb pathway are critical targets of UV mutagenesis in a murine melanoma model. *Proc Natl Acad Sci U S A* 100, 1221-1225.
218. Kaslovsky, R.A., Horgan, M.J., Lum, H., McCandless, B.K., Gilboa, N., Wright, S.D., and Malik, A.B. (1990). Pulmonary edema induced by phagocytosing neutrophils. Protective effect of monoclonal antibody against phagocyte CD18 integrin. *Circ Res* 67, 795-802.
219. Kato, M., Wang, H., Kainulainen, V., Fitzgerald, M.L., Ledbetter, S., Ornitz, D.M., and Bernfield, M. (1998). Physiological degradation converts the soluble syndecan-1 ectodomain from an inhibitor to a potent activator of FGF-2. *Nat Med* 4, 691-697.
220. Katoh, M. (2001). Differential regulation of WNT2 and WNT2B expression in human cancer. *Int J Mol Med* 8, 657-660.
221. Katoh, M. (2002). Regulation of WNT3 and WNT3A mRNAs in human cancer cell lines NT2, MCF-7, and MKN45. *Int J Oncol* 20, 373-377.
222. Kawakami, N., Kashiwagi, S., Kitahara, T., Yamashita, T., and Ito, H. (1995). Effect of local administration of basic fibroblast growth factor against neuronal damage caused by transient intracerebral mass lesion in rats. *Brain Res* 697, 104-111.
223. Kawamata, T., Alexis, N.E., Dietrich, W.D., and Finklestein, S.P. (1996). Intracisternal basic fibroblast growth factor (bFGF) enhances behavioral recovery following focal cerebral infarction in the rat. *J Cereb Blood Flow Metab* 16, 542-547.
224. Kawamata, T., Dietrich, W.D., Schallert, T., Gotts, J.E., Cocke, R.R., Benowitz, L.I., and Finklestein, S.P. (1997). Intracisternal basic fibroblast growth factor enhances functional recovery and up-regulates the expression of a molecular marker of neuronal sprouting. *Proc Natl Acad Sci U S A* 94, 8179-8184.
225. Kawamata, T., Ren, J., Cha, J.H., and Finklestein, S.P. (1999). Intracisternal antisense oligonucleotide to growth associated protein-43 blocks the recovery-promoting effects of basic fibroblast growth factor after focal stroke. *Exp Neurol* 158, 89-96.
226. Kawashima, H., Atarashi, K., Hirose, M., Hirose, J., Yamada, S., Sugahara, K., and Miyasaka, M. (2002). Oversulfated chondroitin/dermatan sulfates containing GlcAbeta1/IdoAalpha1-3GalNAc(4,6-O-disulfate) interact with L- and P-selectin and chemokines. *J Biol Chem* 277, 12921-12930.
227. Keiser, N., Venkataraman, G., Shriver, Z., and Sasisekharan, R. (2001). Direct isolation and sequencing of specific protein-binding glycosaminoglycans. *Nat Med* 7, 123-128.

228. Keuren, J.F., Wielders, S.J., Willems, G.M., Morra, M., Cahalan, L., Cahalan, P., and Lindhout, T. (2003). Thrombogenicity of polysaccharide-coated surfaces. *Biomaterials* 24, 1917-1924.
229. Khan, M.Y., Jaikaria, N.S., Frenz, D.A., Villanueva, G., and Newman, S.A. (1988). Structural changes in the NH₂-terminal domain of fibronectin upon interaction with heparin. Relationship to matrix-driven translocation. *J Biol Chem* 263, 11314-11318.
230. Khan, S.R., and Kok, D.J. (2004). Modulators of urinary stone formation. *Front Biosci* 9, 1450-1482.
231. Kim, H.R., Wheeler, M.A., Wilson, C.M., Iida, J., Eng, D., Simpson, M.A., McCarthy, J.B., and Bullard, K.M. (2004). Hyaluronan facilitates invasion of colon carcinoma cells in vitro via interaction with CD44. *Cancer Res* 64, 4569-4576.
232. Kitagawa, H., Tanaka, Y., Yamada, S., Seno, N., Haslam, S.M., Morris, H.R., Dell, A., and Sugahara, K. (1997). A novel pentasaccharide sequence GlcA(3-sulfate)(beta 1-3)GalNAc(4-sulfate)(beta 1-4)(Fuc alpha 1-3)GlcA(beta 1-3)GalNAc(4-sulfate) in the oligosaccharides isolated from king crab cartilage chondroitin sulfate K and its differential susceptibility to chondroitinases and hyaluronidase. *Biochemistry* 36, 3998-4008.
233. Klagsbrun, M., and Edelman, E.R. (1989). Biological and biochemical properties of fibroblast growth factors. Implications for the pathogenesis of atherosclerosis. *Arteriosclerosis* 9, 269-278.
234. Klagsbrun, M., and Baird, A. (1991). A dual receptor system is required for basic fibroblast growth factor activity. *Cell* 67, 229-231.
235. Klein, E., Klein, G., Nadkarni, J.S., Nadkarni, J.J., Wigzell, H., and Clifford, P. (1968). Surface IgM-kappa specificity on a Burkitt lymphoma cell in vivo and in derived culture lines. *Cancer Res* 28, 1300-1310.
236. Klein, G. (1981). The role of gene dosage and genetic transpositions in carcinogenesis. *Nature* 294, 313-318.
237. Klein, G. (1983). Specific chromosomal translocations and the genesis of B-cell-derived tumors in mice and men. *Cell* 32, 311-315.
238. Klein, M.D., Drongowski, R.A., Linhardt, R.J., and Langer, R.S. (1982). A colorimetric assay for chemical heparin in plasma. *Anal Biochem* 124, 59-64.
239. Knutson, J.R., Iida, J., Fields, G.B., and McCarthy, J.B. (1996). CD44/chondroitin sulfate proteoglycan and alpha 2 beta 1 integrin mediate human melanoma cell migration on type IV collagen and invasion of basement membranes. *Mol Biol Cell* 7, 383-396.
240. Kobayashi, Y., Okamoto, A., and Nishinari, K. (1994). Viscoelasticity of hyaluronic-acid with different molecular-weights. *Biorheology* 31, 234-244.
241. Koketsu, N., Berlove, D.J., Moskowitz, M.A., Kowall, N.W., Caday, C.G., and Finklestein, S.P. (1994). Pretreatment with intraventricular basic fibroblast growth factor decreases infarct size following focal cerebral ischemia in rats. *Ann Neurol* 35, 451-457.
242. Koliopanos, A., Friess, H., Kleeff, J., Shi, X., Liao, Q., Pecker, I., Vlodysky, I., Zimmermann, A., and Buchler, M.W. (2001). Heparanase expression in primary and metastatic pancreatic cancer. *Cancer Res* 61, 4655-4659.
243. Kolset, S.O., Prydz, K., and Pejler, G. (2004). Intracellular proteoglycans. *Biochem J* 379, 217-227.

244. Konduri, S., Lakka, S.S., Tasiou, A., Yanamandra, N., Gondi, C.S., Dinh, D.H., Olivero, W.C., Gujrati, M., and Rao, J.S. (2001). Elevated levels of cathepsin B in human glioblastoma cell lines. *Int J Oncol* 19, 519-524.
245. Kresse, H., and Schonherr, E. (2001). Proteoglycans of the extracellular matrix and growth control. *J Cell Physiol* 189, 266-274.
246. Kreuger, J., Salmivirta, M., Sturiale, L., Giminez-Gallego, G., and Lindhahl, U. (2001). Sequence analysis of heparan sulfate epitopes with graded affinities for fibroblast growth factors 1 and 2. *J Biol Chem* 276, 30744-30752.
247. Kreuger, J., Matsumoto, T., Vanwildemeersch, M., Sasaki, T., Timpl, R., Claesson-Welsh, L., Spillmann, D., and Lindahl, U. (2002). Role of heparan sulfate domain organization in endostatin inhibition of endothelial cell function. *Embo J* 21, 6303-6311.
248. Krpski, W.C., Bass, A., Kelly, A.B., Marzec, U.M., Hanson, S.R., and Harker, L.A. (1990). Heparin-resistant thrombus formation by endovascular stents in baboons. Interruption by a synthetic antithrombin. *Circulation* 82, 570-577.
249. Kubo, H., Cao, R., Brakenhielm, E., Makinen, T., Cao, Y., and Alitalo, K. (2002). Blockade of vascular endothelial growth factor receptor-3 signaling inhibits fibroblast growth factor-2-induced lymphangiogenesis in mouse cornea. *Proc Natl Acad Sci U S A* 99, 8868-8873.
250. Kwan, C.-P., Venkataraman, G., Shriver, Z., Raman, R., Liu, D., Qi, Y., Varticovski, L., and Sasisekharan, R. (2001). Probing Fibroblast Growth Factor Dimerization and Role of Heparin-Like Glycosaminoglycans in Modulating Dimerization and Signaling. *J Biol Chem* 276, 23421-23429.
251. Laird, A.D., Vajkoczy, P., Shawver, L.K., Thurnher, A., Liang, C., Mohammadi, M., Schlessinger, J., Ullrich, A., Hubbard, S.R., Blake, R.A., Fong, T.A., Strawn, L.M., Sun, L., Tang, C., Hawtin, R., Tang, F., Shenoy, N., Hirth, K.P., McMahon, G., and Cherrington (2000). SU6668 is a potent antiangiogenic and antitumor agent that induces regression of established tumors. *Cancer Res* 60, 4152-4160.
252. Landriscina, M., Bagala, C., Mandinova, A., Soldi, R., Micucci, I., Bellum, S., Prudovsky, I., and Maciag, T. (2001). Copper induces the assembly of a multiprotein aggregate implicated in the release of fibroblast growth factor 1 in response to stress. *J Biol Chem* 276, 25549-25557.
253. Langford, J.K., Stanley, M.J., Cao, D., and Sanderson, R.D. (1998). Multiple heparan sulfate chains are required for optimal syndecan-1 function. *J Biol Chem* 273, 29965-29971.
254. Lappi, D.A., Ying, W., Barthelemy, I., Martineau, D., Prieto, I., Benatti, L., Soria, M., and Baird, A. (1994). Expression and activities of a recombinant basic fibroblast growth factor-saporin fusion protein. *J Biol Chem* 269, 12552-12558.
255. Larrain, J., Alvarez, J., Hassell, J.R., and Brandan, E. (1997). Expression of perlecan, a proteoglycan that binds myogenic inhibitory basic fibroblast growth factor, is down regulated during skeletal muscle differentiation. *Exp Cell Res* 234, 405-412.
256. Laterre, P.F., Wittebole, X., and Dhainaut, J.F. (2003). Anticoagulant therapy in acute lung injury. *Crit Care Med* 31, S329-336.
257. Laurent, T.C., and Fraser, J.R. (1992). Hyaluronan. *Faseb J* 6, 2397-2404.
258. Ledley, F.D. (1995). Nonviral gene therapy: the promise of genes as pharmaceutical products. *Hum Gene Ther* 6, 1129-1144.

259. Lehr, H.A., Bittinger, F., and Kirkpatrick, C.J. (2000). Microcirculatory dysfunction in sepsis: a pathogenetic basis for therapy? *J Pathol* *190*, 373-386.
260. Leung, H.Y., Dickson, C., Robson, C.N., and Neal, D.E. (1996). Over-expression of fibroblast growth factor-8 in human prostate cancer. *Oncogene* *12*, 1833-1835.
261. Ley, K. (2001). Pathways and bottlenecks in the web of inflammatory adhesion molecules and chemoattractants. *Immunol Res* *24*, 87-95.
262. Li, Q., Park, P.W., Wilson, C.L., and Parks, W.C. (2002). Matrilysin shedding of syndecan-1 regulates chemokine mobilization and transepithelial efflux of neutrophils in acute lung injury. *Cell* *111*, 635-646.
263. Liaw, P.C., Becker, D.L., Stafford, A.R., Fredenburgh, J.C., and Weitz, J.I. (2001). Molecular basis for the susceptibility of fibrin-bound thrombin to inactivation by heparin cofactor ii in the presence of dermatan sulfate but not heparin. *J Biol Chem* *276*, 20959-20965.
264. Lim, Y., Kim, S.M., Lee, Y., Lee, W., Yang, T., Lee, M., Suh, H., and Park, J. (2001). Cationic hyperbranched poly(amino ester): a novel class of DNA condensing molecule with cationic surface, biodegradable three-dimensional structure, and tertiary amine groups in the interior. *J Am Chem Soc* *123*, 2460-2461.
265. Lim, Y.B., Han, S.O., Kong, H.U., Lee, Y., Park, J.S., Jeong, B., and Kim, S.W. (2000). Biodegradable polyester, poly[alpha-(4-aminobutyl)-L-glycolic acid], as a non-toxic gene carrier. *Pharm Res* *17*, 811-816.
266. Lim, Y.B., Kim, S.M., Suh, H., and Park, J.S. (2002). Biodegradable, endosome disruptive, and cationic network-type polymer as a highly efficient and nontoxic gene delivery carrier. *Bioconjug Chem* *13*, 952-957.
267. Lin, L.L., Wartmann, M., Lin, A.Y., Knopf, J.L., Seth, A., and Davis R.J. (1993). cPLA2 is phosphorylated and activated by MAP kinase. *Cell* *72*, 269-278.
268. Lin, X., Buff, E.M., Perrimon, N., and Michelson, A.M. (1999). Heparan sulfate proteoglycans are essential for FGF receptor signaling during *Drosophila* embryonic development. *Development* *126*, 3715-3723.
269. Lindahl, U. (1990). Biosynthesis of heparin. *Biochem Soc Trans* *18*, 803-805.
270. Linhardt, R.J., Galliher, P.M., and Cooney, C.L. (1986). Polysaccharide lyases. *Appl Biochem Biotechnol* *12*, 135-176.
271. Linhardt, R.J. (2004). Heparin-induced cancer cell death. *Chem Biol* *11*, 420-422.
272. Liotta, L.A., and Kohn, E.C. (2001). The microenvironment of the tumour-host interface. *Nature* *411*, 375-379.
273. Little, S.R., Lynn, D.M., Ge, Q., Anderson, D.G., Puram, S.V., Chen, J., Eisen, H.N., and Langer, R. (2004). Poly-beta amino ester-containing microparticles enhance the activity of nonviral genetic vaccines. *Proc Natl Acad Sci U S A* *101*, 9534-9539.
274. Liu, D., Shriver, Z., Venkataraman, G., El Shabrawi, Y., and Sasisekharan, R. (2002). Tumor cell surface heparan sulfate as cryptic promoters or inhibitors of tumor growth and metastasis. *Proc Natl Acad Sci U S A* *99*, 568-573.
275. Liu, Y., Stack, S.M., Lakka, S.S., Khan, A.J., Woodley, D.T., Rao, J.S., and Rao, C.N. (1999). Matrix localization of tissue factor pathway inhibitor-2/matrix-associated serine protease inhibitor (TFPI-2/MSPI) involves arginine-mediated ionic interactions with heparin and dermatan sulfate: heparin accelerates the activity of TFPI-2/MSPI toward plasmin. *Arch Biochem Biophys* *370*, 112-118.

276. Lofas, S., and Johnsson, B. (1990). A novel hydrogel matrix on gold surfaces in surface-plasmon resonance sensors for fast and efficient covalent immobilization of ligands. *J Chem Soc Chem Commun*, 1526-1528.
277. Lohmander, L.S., De Luca, S., Nilsson, B., Hascall, V.C., Caputo, C.B., Kimura, J.H., and Heinegard, D. (1980). Oligosaccharides on proteoglycans from the swarm rat chondrosarcoma. *J Biol Chem* 255, 6084-6091.
278. Lortat-Jacob, H., and Grimaud, J.A. (1991). Interferon-gamma C-terminal function: new working hypothesis. Heparan sulfate and heparin, new targets for IFN-gamma, protect, relax the cytokine and regulate its activity. *Cell Mol Biol* 37, 253-260.
279. Lundholm, K., Hulten, L., Engaras, B., Nordgren, S., and Svaninger, G. (1994). [Laparoscopy is not suitable in malignant tumors. Risk of neoplasm seeding by instrument]. *Lakartidningen* 91, 4262-4265.
280. Lundin, L., Larsson, H., Kreuger, J., Kanda, S., Lindahl, U., Salmivirta, M., and Claesson-Welsh, L. (2000). Selectively desulfated heparin inhibits fibroblast growth factor-induced mitogenicity and angiogenesis. *J Biol Chem* 275, 24653-24660.
281. Luo, D., Woodrow-Mumford, K., Belcheva, N., and Saltzman, W.M. (1999). Controlled DNA delivery systems. *Pharm Res* 16, 1300-1308.
282. Luo, D., and Saltzman, W.M. (2000). Synthetic DNA delivery systems. *Nat Biotechnol* 18, 33-37.
283. Luo, D., Han, E., Belcheva, N., and Saltzman, W.M. (2004). A self-assembled, modular DNA delivery system mediated by silica nanoparticles. *J Control Release* 95, 333-341.
284. Lush, C.W., and Kvietys, P.R. (2000). Microvascular dysfunction in sepsis. *Microcirculation* 7, 83-101.
285. Lynn, D.M., and Langer, R. (2000). Degradable Poly(β -amino esters): Synthesis, Characterization, and Self-assembly with plasmid DNA. *J. Am. Chem. Soc* 122, 10761-10768.
286. Lynn, D.M., Anderson, D.G., Putnam, D., and Langer, R. (2001). Accelerated Discovery of Synthetic Transfection Vectors: Parallel Synthesis and Screening of a Degradable Polymer Library. *J. Am. Chem. Soc.* 123, 8155-8156.
287. Lyon, M., Rushton, G., and Gallagher, J.T. (1997). The interaction of the transforming growth factor-betas with heparin/heparan sulfate is isoform-specific. *J Biol Chem* 272, 18000-18006.
288. Ma, J., Qiu, J., Hirt, L., Dalkara, T., and Moskowitz, M.A. (2001). Synergistic protective effect of caspase inhibitors and bFGF against brain injury induced by transient focal ischaemia. *Br J Pharmacol* 133, 345-350.
289. Maccarana, M., Casu, B., and Lindahl, U. (1993). Minimal sequence in heparin/heparan sulfate required for binding of basic fibroblast growth factor. *J Biol Chem* 268, 23898-23905.
290. Maheu, E., Ayral, X., and Dougados, M. (2002). A hyaluronan preparation (500-730 kDa) in the treatment of osteoarthritis: a review of clinical trials with Hyalgan. *Int J Clin Pract* 56, 804-813.
291. Maimone, M.M., and Tollefsen, D.M. (1991). Structure of a dermatan sulfate hexasaccharide that binds to heparin cofactor II with high affinity. *J Biol Chem* 266, 14830.
292. Majack, R.A., and Clowes, A.W. (1984). Inhibition of vascular smooth muscle cell migration by heparin-like glycosaminoglycans. *Journal of Cell Physiol* 138, 253-256.

293. Marshall, J.C. (2003). Such stuff as dreams are made on: mediator-directed therapy in sepsis. *Nat Rev Drug Discov* 2, 391-405.
294. Mason, M., Vercruyssen, K.P., Kirker, K.R., Frisch, R., Marecak, D.M., Prestwich, G.D., and Pitt, W.G. (2000). Attachment of hyaluronic acid to polypropylene, polystyrene, and polytetrafluoroethylene. *Biomaterials* 21, 31-36.
295. Matter, K., and Balda, M.S. (2003). Signalling to and from tight junctions. *Nat Rev Mol Cell Biol* 4, 225-236.
296. McQuade, K.J., and Rapraeger, A.C. (2003). Syndecan-1 transmembrane and extracellular domains have unique and distinct roles in cell spreading. *J Biol Chem*.
297. Menger, M.D., and Vollmar, B. (2000). Role of microcirculation in transplantation. *Microcirculation* 7, 291-306.
298. Merry, C.L., Lyon, M., Deakin, J.A., Hopwood, J.J., and Gallagher, J.T. (1999). Highly sensitive sequencing of the sulfated domains of heparan sulfate. *J Biol Chem* 274, 18455-18462.
299. Mertens, G., Van der Schueren, B., van den Berghe, H., and David, G. (1996). Heparan sulfate expression in polarized epithelial cells: the apical sorting of glypican (GPI-anchored proteoglycan) is inversely related to its heparan sulfate content. *J Cell Biol* 132, 487-497.
300. Miceli, R., Hubert, M., Santiago, G., Yao, D.L., Coleman, T.A., Huddleston, K.A., and Connolly, K. (1999). Efficacy of keratinocyte growth factor-2 in dextran sulfate sodium-induced murine colitis. *J Pharmacol Exp Ther* 290, 464-471.
301. Michel, C.C., Phillips, M.E., and Turner, M.R. (1985). The effects of native and modified bovine serum albumin on the permeability of frog mesenteric capillaries. *J Physiol* 360, 333-346.
302. Michelacci, Y.M., and Dietrich, C.P. (1976). Chondroitinase C from *Flavobacterium heparinum*. *J Biol Chem* 251, 1154-1158.
303. Michelacci, Y.M., Horton, D.S., and Poblacion, C.A. (1987). Isolation and characterization of an induced chondroitinase ABC from *Flavobacterium heparinum*. *Biochim Biophys Acta* 923, 291-301.
304. Millane, R.P., Mitra, A.K., and Arnott, S. (1983). Chondroitin 4-sulfate: comparison of the structures of the potassium and sodium salts. *J Mol Biol* 169, 903-920.
305. Miller, R.A., and Britigan, B.E. (1995). The formation and biologic significance of phagocyte-derived oxidants. *J Investig Med* 43, 39-49.
306. Miranti, C.K., and Brugge, J.S. (2002). Sensing the environment: a historical perspective on integrin signal transduction. *Nat Cell Biol* 4, E83-90.
307. Mitra, A.K., Arnott, S., Atkins, E.D., and Isaac, D.H. (1983). Dermatan sulfate: molecular conformations and interactions in the condensed state. *J Mol Biol* 169, 873-901.
308. Miyake, K., Underhill, C.B., Lesley, J., and Kincade, P.W. (1990). Hyaluronate can function as a cell adhesion molecule and CD44 participates in hyaluronate recognition. *J Exp Med* 172, 69-75.
309. Mochizuki, Y., Tsuda, S., Kanetake, H., and Kanda, S. (2002). Negative regulation of urokinase-type plasminogen activator production through FGF-2-mediated activation of phosphoinositide 3-kinase. *Oncogene* 21, 7027-7033.

310. Montesano, R., Vassalli, J.D., Baird, A., Guillemin, R., and Orci, L. (1986). Basic fibroblast growth factor induces angiogenesis in vitro. *Proc Natl Acad Sci U S A* 83, 7297-7301.
311. Morra, M., and Cassineli, C. (1999). Non-fouling properties of polysaccharide-coated surfaces. *J Biomater Sci Polym Ed* 10, 1107-1124.
312. Morra, M. (2000). On the molecular basis of fouling resistance. *J Biomater Sci Polym Ed* 11, 547-569.
313. Morra, M., Cassineli, C., Pavesop, A., and Renier, D. (2003). Atomic force microscopy evaluation of aqueous interfaces of immobilized hyaluron. *J Colloid Interface Sci* 259, 236-243.
314. Morris, T.A., Marsh, J.J., Konopka, R., Pedersen, C.A., and Chiles, P.G. (2000). Anti-thrombotic efficacies of enoxaparin, dalteparin, and unfractionated heparin in venous thrombo-embolism. *Thromb Res* 100, 185-194.
315. Morrison, J.A., Klingelhutz, A.J., and Raab-Traub, N. (2003). Epstein-Barr virus latent membrane protein 2A activates beta-catenin signaling in epithelial cells. *J Virol* 77, 12276-12284.
316. Morrison, J.A., Gulley, M.L., Pathmanathan, R., and Raab-Traub, N. (2004). Differential signaling pathways are activated in the Epstein-Barr virus-associated malignancies nasopharyngeal carcinoma and Hodgkin lymphoma. *Cancer Res* 64, 5251-5260.
317. Moy, F.J., Safran, M., Seddon, A.P., Kitchen, D., Bohlen, P., Aviezer, D., Yayon, A., and Powers, R. (1997). Properly oriented heparin-decasaccharide-induced dimers are the biologically active form of basic fibroblast growth factor. *Biochemistry* 36, 4782-4791.
318. Mulligan, R.C. (1993). The basic science of gene therapy. *Science* 260, 926-932.
319. Mulloy, B., and Forster, M.J. (2000). Conformation and dynamics of heparin and heparan sulfate. *Glycobiology* 10, 1147-1156.
320. Murphy-Ullrich, J.E., Westrick, L.G., Esko, J.D., and Mosher, D.F. (1988). Altered metabolism of thrombospondin by Chinese hamster ovary cells defective in glycosaminoglycan synthesis. *J Biol Chem* 263, 6400-6406.
321. Nader, H.B., Kobayashi, E.Y., Chavante, S.F., Tersariol, I.L., Castro, R.A., Shinjo, S.K., Naggi, A., Torri, G., Casu, B., and Dietrich, C.P. (1999). New insights on the specificity of heparin and heparan sulfate lyases from *Flavobacterium heparinum* revealed by the use of synthetic derivatives of K5 polysaccharide from *E. coli* and 2-O-desulfated heparin. *Glycoconj J* 16, 265-270.
322. Nakamoto, T., Chang, C.S., Li, A.K., and Chodak, G.W. (1992). Basic fibroblast growth factor in human prostate cancer cells. *Cancer Res* 52, 571-577.
323. Nanbo, A., Inoue, K., Adachi-Takasawa, K., and Takada, K. (2002). Epstein-Barr virus RNA confers resistance to interferon-alpha-induced apoptosis in Burkitt's lymphoma. *Embo J* 21, 954-965.
324. Naor, D., Sionov, R.V., and Ish-Shalom, D. (1997). CD44: structure, function, and association with the malignant process. *Adv Cancer Res* 71, 241-319.
325. Natarajan, V., Scribner, W.M., Morris, A.J., Roy, S., Vepa, S., Yang, J., Wadgaonkar, R., Reddy, S.P., Garcia, J.G., and Parinandi, N.L. (2001). Role of p38 MAP kinase in diperoxovanadate-induced phospholipase D activation in endothelial cells. *Am J Physiol Lung Cell Mol Physiol* 281, L435-449.
326. Natke, B., Venkataraman, G., Nugent, M.A., and Sasisekharan, R. (2000). Heparinase treatment of bovine smooth muscle cells inhibits fibroblast growth factor-2 binding to

- fibroblast growth factor receptor but not FGF-2 mediated cellular proliferation. *Angiogenesis* 3, 249-257.
327. Needham, L., Hellewell, P.G., Williams, T.J., and Gordon, J.L. (1988). Endothelial functional responses and increased vascular permeability induced by polycations. *Lab Invest* 59, 538-548.
 328. Nelson, S.R., deSouza, N.M., and Allison, D.J. (2000). Endovascular stents and stent-grafts: is heparin coating desirable? *Cardiovasc Intervent Radiol* 23, 252-255.
 329. Nelson, W.J., and Nusse, R. (2004). Convergence of Wnt, beta-catenin, and cadherin pathways. *Science* 303, 1483-1487.
 330. Nieduszynski, I.A., Huckerby, T.N., Dickenson, J.M., Brown, G.M., Tai, G.H., and Bayliss, M.T. (1990). Structural aspects of skeletal keratan sulphates. *Biochem Soc Trans* 18, 792-793.
 331. Nugent, M.A., and Edelman, E.R. (1992). Kinetics of basic fibroblast growth factor binding to its receptor and heparan sulfate proteoglycan: a mechanism for cooperativity. *Biochemistry* 31, 8876-8883.
 332. Nugent, M.A., Karnovsky, M.J., and Edelman, E.R. (1993). Vascular cell-derived heparan sulfate shows coupled inhibition of basic fibroblast growth factor binding and mitogenesis in vascular smooth muscle cells. *Circ Res* 73, 1051-1060.
 333. Nugent, M.A., Nugent, H.M., Iozzo, R.V., Sanchack, K., and Edelman, E.R. (2000). Perlecan is required to inhibit thrombosis after deep vascular injury and contributes to endothelial cell-mediated inhibition of intimal hyperplasia. *Proc Natl Acad Sci U S A* 97, 6722-6727.
 334. Numa, F., Hirabayashi, K., Kawasaki, K., Sakaguchi, Y., Sugino, N., Suehiro, Y., Suminami, Y., Hirakawa, H., Umayahara, K., Nawata, S., Ogata, H., and Kato, H. (2002). Syndecan-1 expression in cancer of the uterine cervix: association with lymph node metastasis. *Int J Oncol* 20, 39-43.
 335. Nurcombe, V., Ford, M.D., Wildschut, J.A., and Bartlett, P.F. (1993). Developmental regulation of neural response to FGF-1 and FGF-2 by heparan sulfate proteoglycan. *Science* 260, 103-106.
 336. Nurcombe, V., Smart, C.E., Chipperfield, H., Cool, S.M., Boilly, B., and Hondermarck, H. (2000). *Journal of Biological Chemistry* 275, 30009-30018.
 337. Nusrat, A., Turner, J.R., and Madara, J.L. (2000). Molecular physiology and pathophysiology of tight junctions. IV. Regulation of tight junctions by extracellular stimuli: nutrients, cytokines, and immune cells. *Am J Physiol Gastrointest Liver Physiol* 279, G851-857.
 338. Oeben, M., Keller, R., Stuhlsatz, H.W., and Greiling, H. (1987). Constant and variable domains of different disaccharide structure in corneal keratan sulphate chains. *Biochem J* 248, 85-93.
 339. Oelschlager, C., Romisch, J., Staubitz, A., Stauss, H., Leithauser, B., Tillmanns, H., and Holschermann, H. (2002). Antithrombin III inhibits nuclear factor kappaB activation in human monocytes and vascular endothelial cells. *Blood* 99, 4015-4020.
 340. Oerther, S., Le Gall, H., Payan, E., Lapique, F., Presle, N., Hubert, P., Dexheimer, J., and Netter, P. (1999). Hyaluronate-alginate gel as a novel biomaterial: mechanical properties and formation mechanism. *Biotechnol Bioeng* 63, 206-215.
 341. Olofsson, A.M., Vestberg, M., Herwald, H., Rygaard, J., David, G., Arfors, K.E., Linde, V., Flodgaard, H., Dedio, J., Muller-Esterl, W., and Lundgren-Akerlund, E. (1999).

- Heparin-binding protein targeted to mitochondrial compartments protects endothelial cells from apoptosis. *J Clin Invest* 104, 885-894.
342. Omata, F., Birkenbach, M., Matsuzaki, S., Christ, A.D., and Blumberg, R.S. (2001). The expression of IL-12 p40 and its homologue, Epstein-Barr virus-induced gene 3, in inflammatory bowel disease. *Inflamm Bowel Dis* 7, 215-220.
343. Ong, S.H., Guy, G.R., Hadari, Y.R., Laks, S., Gotoh, N., Schlessinger, J., and Lax, I. (2000). FRS2 proteins recruit intracellular signaling pathways by binding to diverse targets on fibroblast growth factor and nerve growth factor receptors. *Mol Cell Biol* 20, 979-989.
344. Ong, S.H., Hadari, Y.R., Gotoh, N., Guy, G.R., Schlessinger, J., and Lax, I. (2001). Stimulation of phosphatidylinositol 3-kinase by fibroblast growth factor receptors is mediated by coordinated recruitment of multiple docking proteins. *Proc Natl Acad Sci U S A* 98, 6074-6079.
345. O'Reilly, M.S., Boehm, T., Shing, Y., Fukai, N., Vasios, G., Lane, W.S., Flynn, E., Birkhead, J.R., Olsen, B.R., and Folkman, J. (1997). Endostatin: an endogenous inhibitor of angiogenesis and tumor growth. *Cell* 88, 277-285.
346. Ornitz, D.M., Yayon, A., Flanagan, J.G., Svahn, C.M., Levi, E., and Leder, P. (1992). Heparin is required for cell-free binding of basic fibroblast growth factor to a soluble receptor and for mitogenesis in whole cells. *Mol Cell Biol* 12, 240-247.
347. Ornitz, D.M., Herr, A.B., Nilsson, M., Westman, J., Svahn, C.M., and Waksman, G. (1995). FGF binding and FGF receptor activation by synthetic heparan-derived di- and trisaccharides. *Science* 268, 432-436.
348. Ornitz, D.M., Xu, J., Colvin, J.S., McEwen, D.G., MacArthur, C.A., Coulier, F., Gao, G., and Goldfarb, M. (1996). Receptor specificity of the fibroblast growth factor family. *J Biol Chem* 271, 15292-15297.
349. Ornitz, D.M., and Itoh, N. (2001). Fibroblast growth factors. *Genome Biol* 2, REVIEWS3005.
350. Ornitz, D.M., Herr, A.B., Nilsson, M., Westman, J., Svahn, C.M., and Waksman, G. (1995). FGF binding and FGF receptor activation by synthetic heparan-derived di- and trisaccharides. *Science* 268, 432-436.
351. Ornitz, D.M., Xu, J., Colvin, J.S., McEwen, D.G., MacArthur, C.A., Coulier, F., Gao, G., and Goldfarb, M. (1996). Receptor specificity of the fibroblast growth factor family. *J Biol Chem* 271, 15292-15297.
352. Osterberg, E., Bergstrom, K., Holmberg, K., Riggs, J.A., Vanalstine, J.M., Schuman, T.P., Burns, N.L., and Harris, J.M. (1993). Comparison of polysaccharide and poly(ethylene glycol) coatings for reduction of protein adsorption on polystyrene surfaces. *Colloids Surf A* 77, 159-169.
353. Osterberg, E., Bergstrom, K., Holmberg, K., Schuman, T.P., Riggs, J.A., Burns, N.L., Van Alstine, J.M., and Harris, J.M. (1995). Protein-rejecting ability of surface-bound dextran in end-on and side-on configurations: comparison to PEG. *J Biomed Mater Res* 29, 741-747.
354. Ostrovsky, O., Berman, B., Gallagher, J., Mulloy, B., Fernig, D.G., Delehedde, M., and Ron, D. (2002). Differential effects of heparin saccharides on the formation of specific fibroblast growth factor (FGF) and FGF receptor complexes. *J Biol Chem* 277, 2444-2453.

355. Ostrovsky, O., Berman, B., Gallagher, J., Mulloy, B., Fernig, D.G., Delehedde, M., and Ron, D. (2001). Differential effects of heparin saccharides on the formation of specific fibroblast growth factor (FGF) and FGF receptor complexes. *J Biol Chem* 277, 2444-2453.
356. Ozen, M., Giri, D., Ropiquet, F., Mansukhani, A., and Ittmann, M. (2001). Role of fibroblast growth factor receptor signaling in prostate cancer cell survival. *J Natl Cancer Inst* 93, 1783-1790.
357. Paavonen, K., Puolakkainen, P., Jussila, L., Jahkola, T., and Alitalo, K. (2000). Vascular endothelial growth factor receptor-3 in lymphangiogenesis in wound healing. *Am J Pathol* 156, 1499-1504.
358. Padera, R., Venkataraman, G., Berry, D., Godvarti, R., and Sasisekharan, R. (1999). FGF-2/fibroblast growth factor receptor/heparin-like glycosaminoglycan interactions: a compensation model for FGF-2 signaling. *Faseb J* 13, 1677-1687.
359. Panyam, J., Zhou, W.Z., Prabha, S., Sahoo, S.K., and Labhasetwar, V. (2002). Rapid endo-lysosomal escape of poly(DL-lactide-co-glycolide) nanoparticles: implications for drug and gene delivery. *Faseb J* 16, 1217-1226.
360. Park, P.W., Pier, G.B., Hinkes, M.T., and Bernfield, M. (2001). Exploitation of syndecan-1 shedding by *Pseudomonas aeruginosa* enhances virulence. *Nature* 411, 98-102.
361. Park, Y., Yu, G., Gunay, N.S., and Linhardt, R.J. (1999). Purification and characterization of heparan sulfate proteoglycan from bovine brain. *Biochem J* 344, 723-730.
362. Patterson, C.E., Stasek, J.E., Schaphorst, K.L., Davis, H.W., and Garcia, J.G. (1995). Mechanisms of pertussis toxin-induced barrier dysfunction in bovine pulmonary artery endothelial cell monolayers. *Am J Physiol* 268, L926-934.
363. Pedersen, L.C., Tsuchida, K., Kitagawa, H., Sugahara, K., Darden, T.A., and Negishi, M. (2000). Heparan/chondroitin sulfate biosynthesis. Structure and mechanism of human glucuronyltransferase I. *J Biol Chem* 275, 34580-34585.
364. Pei, M., Solchaga, L.A., Seidel, J., Zeng, L., Vunjak-Novakovic, G., Caplan, A.I., and Freed, L.E. (2002). Bioreactors mediate the effectiveness of tissue engineering scaffolds. *Faseb J* 16, 1691-1694.
365. Pellegrini, L., Burke, D.F., von Delft, F., Mulloy, B., and Blundell, T.L. (2000). Crystal structure of fibroblast growth factor receptor ectodomain bound to ligand and heparin. *Nature* 407, 1029-1034.
366. Penc, S.F., Pomahac, B., Winkler, T., Dorschner, R.A., Eriksson, E., Herndon, M., and Gallo, R.L. (1998). Dermatan sulfate released after injury is a potent promoter of fibroblast growth factor-2 function. *J Biol Chem* 273, 28116-28121.
367. Pereira, H.A., Shafer, W.M., Pohl, J., Martin, L.E., and Spitznagel, J.K. (1990). CAP37, a human neutrophil-derived chemotactic factor with monocyte specific activity. *J Clin Invest* 85, 1468-1476.
368. Pereira, H.A., Erdem, I., Pohl, J., and Spitznagel, J.K. (1993). Synthetic bactericidal peptide based on CAP37: a 37-kDa human neutrophil granule-associated cationic antimicrobial protein chemotactic for monocytes. *Proc Natl Acad Sci U S A* 90, 4733-4737.
369. Perez-Moreno, M., Jamora, C., and Fuchs, E. (2003). Sticky business: orchestrating cellular signals at adherens junctions. *Cell* 112, 535-548.

370. Perrimon, N., and Bernfield, M. (2000). Specificities of heparan sulphate proteoglycans in developmental processes. *Nature* *404*, 725-728.
371. Petersen, O.W., Ronnov-Jessen, L., Howlett, A.R., and Bissell, M.J. (1992). Interaction with basement membrane serves to rapidly distinguish growth and differentiation pattern of normal and malignant human breast epithelial cells. *Proc Natl Acad Sci U S A* *89*, 9064-9068.
372. Petitou, M., Herault, J.P., Bernat, A., Driguez, P.A., Duchaussoy, P., Lormeau, J.C., and Herbert, J.M. (1999). Synthesis of thrombin-inhibiting heparin mimetics without side effects. *Nature* *398*, 417-422.
373. Piacquadio, D., Jarcho, M., and Goltz, R. (1997). Evaluation of hylan b gel as a soft-tissue augmentation implant material. *J Am Acad Dermatol* *36*, 544-549.
374. Picart, C., Lavalle, P., Hubert, P., Cuisineier, F.J.G., Decher, G., Schaff, P., and Voegel, J.C. (2001). Buildup mechanism for poly(L-lysine)/hyaluronic acid films onto a solid surface. *Langmuir* *17*, 7414-7424.
375. Picone, O., Aucouturier, J.S., Louboutin, A., Coscas, Y., and Camus, E. (2003). Abdominal wall metastasis of a cervical adenocarcinoma at the laparoscopic trocar insertion site after ovarian transposition: case report and review of the literature. *Gynecol Oncol* *90*, 446-449.
376. Piehler, J., Brecht, A., Hehl, K., and Gauglity, G. (1999). Protein interactions in covalently attached dextran layers. *Colloids Surf B* *13*, 325-336.
377. Piepkorn, M.W., and Daynes, R.A. (1983). Heparin effect on DNA synthesis in a murine fibrosarcoma cell line: influence of anionic density. *J Natl Cancer Inst* *71*, 615-618.
378. Plotnikov, A.N., Schlessinger, J., Hubbard, S.R., and Mohammadi, M. (1999). Structural basis of FGF receptor dimerization and activation. *Cell* *98*, 641-650.
379. Plotnikov, A.N., Hubbard, S.R., Schlessinger, J., and Mohammadi, M. (2000). Crystal structures of two FGF-FGFR complexes reveal the determinants of ligand-receptor specificity. *Cell* *101*, 413-424.
380. Podolsky, D.K. (2002). Inflammatory bowel disease. *N Engl J Med* *347*, 417-429.
381. Polnaszek, N., Kwabi-Addo, B., Peterson, L.E., Ozen, M., Greenberg, N.M., Ortega, S., Basilico, C., and Ittmann, M. (2003). Fibroblast growth factor 2 promotes tumor progression in an autochthonous mouse model of prostate cancer. *Cancer Res* *63*, 5754-5760.
382. Poste, G., and Fidler, I.J. (1980). The pathogenesis of cancer metastasis. *Nature* *283*, 139-146.
383. Powell, A.K., Fernig, D.G., and Turnbull, J.E. (2002). Fibroblast growth factor receptors 1 and 2 interact differently with heparin/heparan sulfate. *J Biol Chem* *277*, 28554-28563.
384. Powers, M.R., Blumenstock, F.A., Cooper, J.A., and Malik, A.B. (1989). Role of albumin arginyl sites in albumin-induced reduction of endothelial hydraulic conductivity. *J Cell Physiol* *141*, 558-564.
385. Pries, A.R., Secomb, T.W., and Gaegtgens, P. (2000). The endothelial surface layer. *Pflugers Arch* *440*, 653-666.
386. Pupa, S.M., Menard, S., Forti, S., and Tagliabue, E. (2002). New insights into the role of extracellular matrix during tumor onset and progression. *J Cell Physiol* *192*, 259-267.
387. Putnam, D., Gentry, C.A., Pack, D.W., and Langer, R. (2001). Polymer-based gene delivery with low cytotoxicity by a unique balance of side-chain termini. *Proc Natl Acad Sci U S A* *98*, 1200-1205.

388. Pye, D.A., Vives, R.R., Turnbull, J.E., Hyde, P., and Gallagher, J.T. (1998). Heparan sulfate oligosaccharides require 6-O-sulfation for promotion of basic fibroblast growth factor mitogenic activity. *J Biol Chem* *273*, 22936-22942.
389. Pye, D.A., Vives, R.R., Hyde, P., and Gallagher, J.T. (2000). Regulation of FGF-1 mitogenic activity by heparan sulfate oligosaccharides is dependent on specific structural features: differential requirements for the modulation of FGF-1 and FGF-2. *Glycobiology* *10*, 1183-1192.
390. Qi, J.H., Matsumoto, T., Huang, K., Olausson, K., Christofferson, R., and Claesson-Welsh, L. (1999). Phosphoinositide 3 kinase is critical for survival, mitogenesis and migration but not for differentiation of endothelial cells. *Angiogenesis* *3*, 371-380.
391. Qiang, Y.W., Endo, Y., Rubin, J.S., and Rudikoff, S. (2003). Wnt signaling in B-cell neoplasia. *Oncogene* *22*, 1536-1545.
392. Raman, R., Venkataraman, G., Ernst, S., Sasisekharan, V., and Sasisekharan, R. (2003). Structural specificity of heparin binding in the fibroblast growth factor family of proteins. *Proc Natl Acad Sci U S A* *100*, 2357-2362.
393. Ramaswamy, S., Ross, K.N., Lander, E.S., and Golub, T.R. (2003). A molecular signature of metastasis in primary solid tumors. *Nat Genet* *33*, 49-54.
394. Rao, D.S., Hyun, T.S., Kumar, P.D., Mizukami, I.F., Rubin, M.A., Lucas, P.C., Sanda, M.G., and Ross, T.S. (2002). Huntingtin-interacting protein 1 is overexpressed in prostate and colon cancer and is critical for cellular survival. *J Clin Invest* *110*, 351-360.
395. Rapraeger, A.C., Kruffka, A., and Olwin, B.B. (1991). Requirement of heparin sulfate for bFGF-mediated fibroblast growth and myoblast differentiation. *Science* *252*, 1705-1708.
396. Rapraeger, A.C. (1993). The coordinated regulation of heparan sulfate, syndecans and cell behavior. *Curr Opin Cell Biol* *5*, 844-853.
397. Rapraeger, A.C. (1995). In the clutches of proteoglycans: how does heparan sulfate regulate FGF binding? *Chem Biol* *2*, 645-649.
398. Ren, J.M., and Finklestein, S.P. (1997). Time window of infarct reduction by intravenous basic fibroblast growth factor in focal cerebral ischemia. *Eur J Pharmacol* *327*, 11-16.
399. Rhomberg, A.J., Ernst, S., Sasisekharan, R., and Biemann, K. (1998). Mass spectrometric and capillary electrophoretic investigation of the enzymatic degradation of heparin-like glycosaminoglycans. *Proc Natl Acad Sci USA* *95*, 4176-4181.
400. Robinson, C.J., and Stringer, S.E. (2001). The splice variants of vascular endothelial growth factor (VEGF) and their receptors. *J Cell Sci* *114*, 853-865.
401. Robinson, K.A., Roubin, G.S., Siegel, R.J., Black, A.J., Apkarian, R.P., and King, S.B., 3rd (1988). Intra-arterial stenting in the atherosclerotic rabbit. *Circulation* *78*, 646-653.
402. Roghani, M., Mansukhani, A., Dell'Era, P., Bellosa, P., Basilico, C., Rifkin, D.B., and Moscatelli, D. (1994). Heparin increases the affinity of basic fibroblast growth factor for its receptor but is not required for binding. *J Biol Chem* *269*, 3976-3984.
403. Ropiquet, F., Giri, D., Lamb, D.J., and Ittmann, M. (1999). FGF7 and FGF2 are increased in benign prostatic hyperplasia and are associated with increased proliferation. *J Urol* *162*, 595-599.
404. Ropiquet, F., Giri, D., Kwabi-Addo, B., Mansukhani, A., and Ittmann, M. (2000). Increased expression of fibroblast growth factor 6 in human prostatic intraepithelial neoplasia and prostate cancer. *Cancer Res* *60*, 4245-4250.
405. Ropiquet, F., Giri, D., Kwabi-Addo, B., Schmidt, K., and Ittmann, M. (2000). FGF-10 is expressed at low levels in the human prostate. *Prostate* *44*, 334-338.

406. Rops, A.L., van der Vlag, J., Lensen, J.F., Wijnhoven, T.J., van den Heuvel, L.P., van Kuppevelt, T.H., and Berden, J.H. (2004). Heparan sulfate proteoglycans in glomerular inflammation. *Kidney Int* 65, 768-785.
407. Rosini, P., Bonaccorsi, L., Baldi, E., Chiasserini, C., Forti, G., De Chiara, G., Lucibello, M., Mongiat, M., Iozzo, R.V., Garaci, E., Cozzolino, F., and Torcia, M.G. (2002). Androgen receptor expression induces FGF2, FGF-binding protein production, and FGF2 release in prostate carcinoma cells: role of FGF2 in growth, survival, and androgen receptor down-modulation. *Prostate* 53, 310-321.
408. Roskelley, C.D., Srebrow, A., and Bissell, M.J. (1995). A hierarchy of ECM-mediated signalling regulates tissue-specific gene expression. *Curr Opin Cell Biol* 7, 736-747.
409. Ross, R. (1993). The pathogenesis of atherosclerosis: a perspective for the 1990s. *Nature* 362, 801-809.
410. Ross, T.S., and Gilliland, D.G. (1999). Transforming properties of the Huntingtin interacting protein 1/ platelet-derived growth factor beta receptor fusion protein. *J Biol Chem* 274, 22328-22336.
411. Rostand, K.S., and Esko, J.D. (1997). Microbial adherence to and invasion through proteoglycans. *Infect Immun* 65, 1-8.
412. Ruf, I.K., Rhyne, P.W., Yang, H., Borza, C.M., Hutt-Fletcher, L.M., Cleveland, J.L., and Sample, J.T. (1999). Epstein-barr virus regulates c-MYC, apoptosis, and tumorigenicity in Burkitt lymphoma. *Mol Cell Biol* 19, 1651-1660.
413. Ruf, I.K., Rhyne, P.W., Yang, H., Borza, C.M., Hutt-Fletcher, L.M., Cleveland, J.L., and Sample, J.T. (2001). EBV regulates c-MYC, apoptosis, and tumorigenicity in Burkitt's lymphoma. *Curr Top Microbiol Immunol* 258, 153-160.
414. Saksela, O., Moscatelli, D., Sommer, A., and Rifkin, DB. (1988). Endothelial cell-derived heparan sulfate binds basic fibroblast growth factor and protects it from proteolytic degradation. *J Cell Biol* 107, 743-751.
415. Sandborn, W.J., Sands, B.E., Wolf, D.C., Valentine, J.F., Safdi, M., Katz, S., Isaacs, K.L., Wruble, L.D., Katz, J., Present, D.H., Loftus, E.V., Jr., Graeme-Cook, F., Odenheimer, D.J., and Hanauer, S.B. (2003). Repifermin (keratinocyte growth factor-2) for the treatment of active ulcerative colitis: a randomized, double-blind, placebo-controlled, dose-escalation trial. *Aliment Pharmacol Ther* 17, 1355-1364.
416. Sanderson, R.D., Turnbull, J.E., Gallagher, J.T., and Lander, A.D. (1994). Fine structure of heparan sulfate regulates syndecan-1 function and cell behavior. *J Biol Chem* 269, 13100-13106.
417. Sanderson, R.D. (2001). Heparan sulfate proteoglycans in invasion and metastasis. *Semin Cell Dev Biol* 12, 89-98.
418. Sandset, P.M., Bendz, B., and Hansen, J.B. (2000). Physiological function of tissue factor pathway inhibitor and interaction with heparins. *Haemostasis* 30 Suppl 2, 48-56.
419. Sannes, P.L., Khosla, J., Li, C.M., and Pagan, I. (1998). Sulfation of extracellular matrices modifies growth factor effects on type II cells on laminin substrata. *Am J Physiol* 275, L701-708.
420. Saoncella, S., Echtermeyer, F., Denhez, F., Nowlen, J.K., Mosher, D.F., Robinson, S.D., Hynes, R.O., and Goetinck, P.F. (1999). Syndecan-4 signals cooperatively with integrins in a Rho-dependent manner in the assembly of focal adhesions and actin stress fibers. *Proc Natl Acad Sci U S A* 96, 2805-2810.

421. Sasaki, T., Larsson, H., Kreuger, J., Salmivirta, M., Claesson-Welsh, L., Lindahl, U., Hohenester, E., and Timpl, R. (1999). Structural basis and potential role of heparin/heparan sulfate binding to the angiogenesis inhibitor endostatin. *Embo J* 18, 6240-6248.
422. Sasisekharan, R., Bulmer, M., Moremen, K.W., Cooney, C.L., and Langer, R. (1993). Cloning and expression of heparinase I gene from *Flavobacterium heparinum*. *Proc Natl Acad Sci U S A* 90, 3660-3664.
423. Sasisekharan, R., Moses, M.A., Nugent, M.A., Cooney, C.L., and Langer, R. (1994). Heparinase inhibits neovascularization. *Proc Natl Acad Sci USA* 91, 1524-1528.
424. Sasisekharan, R., Leckband, D., Godavarti, R., Venkataraman, G., Cooney, C.L., and Langer, R. (1995). Heparinase I from *Flavobacterium heparinum*: the role of the cysteine residue in catalysis as probed by chemical modification and site-directed mutagenesis. *Biochemistry* 34, 14441-14448.
425. Sasisekharan, R., Venkataraman, G., Godavarti, R., Ernst, S., Cooney, C.L., and Langer, R. (1996). Heparinase I from *Flavobacterium heparinum*. Mapping and characterization of the heparin binding domain. *J Biol Chem* 271, 3124-3131.
426. Sasisekharan, R., and Venkataraman, G. (2000). Heparin and heparan sulfate: biosynthesis, structure and function. *Curr Opin Chem Biol* 4, 626-631.
427. Sasisekharan, R., Shriver, Z., Venkataraman, G., and Narayanasami, U. (2002). Roles of heparan-sulphate glycosaminoglycans in cancer. *Nat Rev Cancer* 2, 521-528.
428. Sato, N., Shimada, M., Nakajima, H., Oda, H., and Kimura, S. (1994). Cloning and expression in *Escherichia coli* of the gene encoding the *Proteus vulgaris* chondroitin ABC lyase. *Appl Microbiol Biotechnol* 41, 39-46.
429. Saumon, G., Soler, P., and Martet, G. (1995). Effect of polycations on barrier and transport properties of alveolar epithelium in situ. *Am J Physiol* 269, L185-194.
430. Schittny, J.C., and Yurchenco, P.D. (1989). Basement membranes: molecular organization and function in development and disease. *Curr Opin Cell Biol* 1, 983-988.
431. Schlessinger, J., Plotnikov, A.N., Ibrahimi, O.A., Eliseenkova, A.V., Yeh, B.K., Yayon, A., Linhardt, R.J., and Mohammadi, M. (2000). Crystal structure of a ternary FGF-FGFR-heparin complex reveals a dual role for heparin in FGFR binding and dimerization. *Mol Cell* 6, 743-750.
432. Schmidtchen, A., Frick, I.M., and Bjorck, L. (2001). Dermatan sulphate is released by proteinases of common pathogenic bacteria and inactivates antibacterial alpha-defensin. *Mol Microbiol* 39, 708-713.
433. Schneider, G.B., Kurago, Z., Zaharias, R., Gruman, L.M., Schaller, M.D., and Hendrix, M.J. (2002). Elevated focal adhesion kinase expression facilitates oral tumor cell invasion. *Cancer* 95, 2508-2515.
434. Scholle, F., Bendt, K.M., and Raab-Traub, N. (2000). Epstein-Barr virus LMP2A transforms epithelial cells, inhibits cell differentiation, and activates Akt. *J Virol* 74, 10681-10689.
435. Schonherr, E., and Hausser, H.J. (2000). Extracellular matrix and cytokines: a functional unit. *Dev Immunol* 7, 89-101.
436. Sebestyen, A., Totth, A., Mihalik, R., Szakacs, O., Paku, S., and Kopper, L. (2000). Syndecan-1-dependent homotypic cell adhesion in HT58 lymphoma cells. *Tumour Biol* 21, 349-357.

437. Sengupta, K., Schilling, J., Marx, S., Markus, F., and Sackmann, E. (2003). Supported membrane coupled ultra-thin layer of hyaluronic acid: viscoelastic properties of a tissue-surface mimetic system. *Biophysical J* 84, 381a.
438. Shard, A.G., Davies, M.C., Tendler, J.J.B., Benedetti, L., Purbrick, M.D., Paul, A., and Beamson, G. (1997). X-ray photoelectron spectroscopy and time-of-flight SIMS investigations of hyaluronic acid derivatives. *Langmuir* 13, 2080-2014.
439. Shibasaki, Y., Seki, A., and Teishi, N. (1995). Thermoanalytical study on anchoring effects of long-chain diynoic acids in thermal polymerization. *Thermochimica Acta* 253, 103-110.
440. Shriver, Z., Hu, Y., Pojasek, K., and Sasisekharan, R. (1998). Heparinase II from *Flavobacterium heparinum*. Role of cysteine in enzymatic activity as probed by chemical modification and site-directed mutagenesis. *J Biol Chem* 273, 22904-22912.
441. Shriver, Z., Hu, Y., and Sasisekharan, R. (1998). Heparinase II from *Flavobacterium heparinum*. Role of histidine residues in enzymatic activity as probed by chemical modification and site-directed mutagenesis. *J Biol Chem* 273, 10160-10167.
442. Shriver, Z., Liu, D., Hu, Y., and Sasisekharan, R. (1999). Biochemical investigations and mapping of the calcium-binding sites of heparinase I from *Flavobacterium heparinum*. *J Biol Chem* 274, 4082-4088.
443. Shriver, Z., Sundaram, M., Venkataraman, G., Fareed, J., Linhardt, R., Biemann, K., and Sasisekharan, R. (2000). Cleavage of the antithrombin III binding site in heparin by heparinases and its implication in the generation of low molecular weight heparin. *Proc Natl Acad Sci U S A* 97, 10365-10370.
444. Shriver, Z., Liu, D., and Sasisekharan, R. (2002). Emerging views of heparan sulfate glycosaminoglycan structure/activity relationships modulating dynamic biological functions. *Trends Cardiovasc Med* 12, 71-77.
445. Sleeman, M., Fraser, J., McDonald, M., Yuan, S., White, D., Grandison, P., Kumble, K., Watson, J.D., and Murison, J.G. (2001). Identification of a new fibroblast growth factor receptor, FGFR5. *Gene* 271, 171-182.
446. Smetsers, T.F., van de Westerlo, E.M., ten Dam, G.B., Clarijs, R., Versteeg, E.M., van Geloof, W.L., Veerkamp, J.H., van Muijen, G.N., and van Kuppevelt, T.H. (2003). Localization and characterization of melanoma-associated glycosaminoglycans: differential expression of chondroitin and heparan sulfate epitopes in melanoma. *Cancer Res* 63, 2965-2970.
447. Sood, A.K., Coffin, J.E., Schneider, G.B., Fletcher, M.S., DeYoung, B.R., Gruman, L.M., Gershenson, D.M., Schaller, M.D., and Hendrix, M.J. (2004). Biological significance of focal adhesion kinase in ovarian cancer: role in migration and invasion. *Am J Pathol* 165, 1087-1095.
448. Sperinde, G.V., and Nugent, M.A. (2000). Mechanisms of fibroblast growth factor 2 intracellular processing: a kinetic analysis of the role of heparan sulfate proteoglycans. *Biochemistry* 39, 3788-3796.
449. Spivak-Kroizman, T., Lemmon, M.A., Dikic, I., Ladbury, J.E., Pinchasi, D., Huang, J., Jaye, M., Crumley, G., Schlessinger, J., and Lax, I. (1994). Heparin-induced oligomerization of FGF molecules is responsible for FGF receptor dimerization, activation, and cell proliferation. *Cell* 79, 1015-1024.

450. Stacker, S.A., Caesar, C., Baldwin, M.E., Thornton, G.E., Williams, R.A., Prevo, R., Jackson, D.G., Nishikawa, S., Kubo, H., and Achen, M.G. (2001). VEGF-D promotes the metastatic spread of tumor cells via the lymphatics. *Nat Med* 7, 186-191.
451. Stauber, D.J., DiGabriele, A.D., and Hendrickson, W.A. (2000). Structural interactions of fibroblast growth factor receptor with its ligands. *Proc Natl Acad Sci USA* 97, 49-54.
452. Stile, R.A., Barber, T.A., Castner, D.G., and Healy, K.E. (2002). Sequential robust design methodology and X-ray photoelectron spectroscopy to analyze the grafting of hyaluronic acid to glass substrates. *J Biomed Mater Res* 61, 391-398.
453. Strowski, M.Z., Cramer, T., Schafer, G., Juttner, S., Walduck, A., Schipani, E., Kemmner, W., Wessler, S., Wunder, C., Weber, M., Meyer, T.F., Wiedenmann, B., Jons, T., Naumann, M., and Hocker, M. (2003). Helicobacter pylori stimulates host vascular endothelial growth factor-A (vegf-A) gene expression via MEK/ERK-dependent activation of Sp1 and Sp3. *Faseb J*.
454. Sugahara, K., and Kitagawa, H. (2002). Heparin and heparan sulfate biosynthesis. *IUBMB Life* 54, 163-175.
455. Suh, K.Y., Yang, J.M., Khademhosseini, A., Berry, D., Tran, T.N., Park, H., and Langer, R. (2005). Characterization of chemisorbed hyaluronic acid directly immobilized on solid substrates. *J Biomed Mater Res B Appl Biomater* 72, 292-298.
456. Summerford, C., Bartlett, P.F., and Samulski, R.J. (1999). AlphaVbeta5 integrin: a co-receptor for adeno-associated virus type 2 infection. *Nat Med* 5, 78-82.
457. Sundaram, M., Qi, Y., Shriver, Z., Liu, D., Zhao, G., Venkataraman, G., Langer, R., and Sasisekharan, R. (2003). Rational design of low-molecular weight heparins with improved in vivo activity. *Proc Natl Acad Sci U S A* 100, 651-656.
458. Swanson, R.A., Morton, M.T., Tsao-Wu, G., Savalos, R.A., Davidson, C., and Sharp, F.R. (1990). A semiautomated method for measuring brain infarct volume. *J Cereb Blood Flow Metab* 10, 290-293.
459. Szabo, S., Folkman, J., Vattay, P., Morales, R.E., Pinkus, G.S., and Kato, K. (1994). Accelerated healing of duodenal ulcers by oral administration of a mutein of basic fibroblast growth factor in rats. *Gastroenterology* 106, 1106-1111.
460. Tanaka, Y., Adams, D.H., Hubscher, S., Hirano, H., Siebenlist, U., and Shaw, S. (1993). T-cell adhesion induced by proteoglycan-immobilized cytokine MIP-1 beta. *Nature* 361, 79-82.
461. Tapon-Brethaudiere, J., Drouet, B., Matou, S., Mourao, P.A., Bros, A., Letourneur, D., and Fischer, A.M. (2000). Modulation of vascular human endothelial and rat smooth muscle cell growth by a fucosylated chondroitin sulfate from echinoderm. *Thromb Haemost* 84, 332-337.
462. Teien, A.N., and Lie, M. (1975). Heparin assay in plasma: a comparison of five clotting methods. *Thromb Res* 7, 777-788.
463. Teien, A.N., Lie, M., and Abildgaard, U. (1976). Assay of heparin in plasma using a chromogenic substrate for activated factor X. *Thromb Res* 8, 413-416.
464. Teien, A.N., and Lie, M. (1977). Evaluation of an amidolytic heparin assay method: increased sensitivity by adding purified antithrombin III. *Thromb Res* 10, 399-410.
465. Teoh, K.H., Young, E., Bradley, C.A., and Hirsh, J. (1993). Heparin binding proteins. Contribution to heparin rebound after cardiopulmonary bypass. *Circulation* 88, II420-425.

466. Thierry, B., Winnik, F.M., Merhi, Y., and Tabrizian, M. (2003). Nanocoatings onto arteries via layer-by-layer deposition: toward the in vivo repair of damaged blood vessels. *J Am Chem Soc* *125*, 7494-7495.
467. Thodeti, C.K., Albrechtsen, R., Grauslund, M., Asmar, M., Larsson, C., Takada, Y., Mercurio, A.M., Couchman, J.R., and Wewer, U.M. (2003). ADAM12/syndecan-4 signaling promotes beta 1 integrin-dependent cell spreading through protein kinase Calpha and RhoA. *J Biol Chem* *278*, 9576-9584.
468. Timpl, R. (1996). Macromolecular organization of basement membranes. *Curr Opin Cell Biol* *8*, 618-624.
469. Tkachenko, E., and Simons, M. (2002). Clustering induces redistribution of syndecan-4 core protein into raft membrane domains. *J Biol Chem* *277*, 19946-19951.
470. Tkachenko, E., Lutgens, E., Stan, R.V., and Simons, M. (2004). Fibroblast growth factor 2 endocytosis in endothelial cells proceed via syndecan-4-dependent activation of Rac1 and a Cdc42-dependent macropinocytic pathway. *J Cell Sci* *117*, 3189-3199.
471. Toki, N., Tsukamoto, N., Kaku, T., Toh, N., Saito, T., Kamura, T., Matsukuma, K., and Nakano, H. (1991). Microscopic ovarian metastasis of the uterine cervical cancer. *Gynecol Oncol* *41*, 46-51.
472. Torcia, M., Lucibello, M., De Chiara, G., Labardi, D., Nencioni, L., Bonini, P., Garaci, E., and Cozzolino, F. (1999). Interferon-alpha-induced inhibition of B16 melanoma cell proliferation: interference with the bFGF autocrine growth circuit. *Biochem Biophys Res Commun* *262*, 838-844.
473. Travis, A.J., Merdiushev, T., Vargas, L.A., Jones, B.H., Purdon, M.A., Nipper, R.W., Galatioto, J., Moss, S.B., Hunnicutt, G.R., and Kopf, G.S. (2001). Expression and localization of caveolin-1, and the presence of membrane rafts, in mouse and Guinea pig spermatozoa. *Dev Biol* *240*, 599-610.
474. Trowbridge, J.M., and Gallo, R.L. (2002). Dermatan sulfate: new functions from an old glycosaminoglycan. *Glycobiology* *12*, 117R-125R.
475. Trowbridge, J.M., Rudisill, J.A., Ron, D., and Gallo, R.L. (2002). Dermatan sulfate binds and potentiates activity of keratinocyte growth factor (FGF-7). *J Biol Chem* *277*, 42815-42820.
476. Tumova, S., Woods, A., and Couchman, J.R. (2000). Heparan sulfate proteoglycans on the cell surface: versatile coordinators of cellular functions. *Int J Biochem and Cell Biol* *32*, 269-288.
477. Turnbull, J.E., Fernig, D.G., Ke, Y., Wilkinson, M.C., and Gallagher, J.T. (1992). Identification of the basic fibroblast growth factor binding sequence in fibroblast heparan sulfate. *J Biol Chem* *267*, 10337-10341.
478. Turnbull, J.E., Hopwood, J.J., and Gallagher, J.T. (1999). A strategy for rapid sequencing of heparan sulfate and heparin saccharides. *Proc Natl Acad Sci U S A* *96*, 2698-2703.
479. Tyagi, M., Rusnati, M., Presta, M., and Giacca, M. (2001). Internalization of HIV-1 tat requires cell surface heparan sulfate proteoglycans. *J Biol Chem* *276*, 3254-3261.
480. Unger, E.F., Goncalves, L., Epstein, S.E., Chew, E.Y., Trapnell, C.B., Cannon, R.O.r., and Quyyumi, A.A. (2000). Effects of a single intracoronary injection of basic fibroblast growth factor in stable angina pectoris. *Am J Cardiol* *85*, 1414-1419.
481. van de Westerlo, E.M., Smetsers, T.F., Dennissen, M.A., Linhardt, R.J., Veerkamp, J.H., van Muijen, G.N., and van Kuppevelt, T.H. (2002). Human single chain antibodies

- against heparin: selection, characterization, and effect on coagulation. *Blood* 99, 2427-2433.
482. van Kuppevelt, T.H., Dennissen, M.A., van Venrooij, W.J., Hoet, R.M., and Veerkamp, J.H. (1998). Generation and application of type-specific anti-heparan sulfate antibodies using phage display technology. Further evidence for heparan sulfate heterogeneity in the kidney. *J Biol Chem* 273, 12960-12966.
483. Varki, A. (1993). Biological roles of oligosaccharides: all of the theories are correct. *Glycobiology* 3, 97-130.
484. Varner, J.A., and Cheresh, D.A. (1996). Integrins and cancer. *Curr Opin Cell Biol* 8, 724-730.
485. Veikkola, T., Karkkainen, M., Claesson-Welsh, L., and Alitalo, K. (2000). Regulation of angiogenesis via vascular endothelial growth factor receptors. *Cancer Res* 60, 203-212.
486. Venkataraman, G., Sasisekharan, V., Herr, A.B., Ornitz, D.M., Waksman, G., Cooney, C.L., Langer, R., and Sasisekharan, R. (1996). Preferential self-association of basic fibroblast growth factor is stabilized by heparin during receptor dimerization and activation. *Proc Natl Acad Sci U S A* 93, 845-850.
487. Venkataraman, G., Shriver, Z., Davis, J.C., and Sasisekharan, R. (1999). Fibroblast growth factors 1 and 2 are distinct in oligomerization in the presence of heparin-like glycosaminoglycans. *Proc Natl Acad Sci USA* 96, 1892-1897.
488. Venkataraman, G., Shriver, Z., Raman, R., and Sasisekharan, R. (1999). Sequencing Complex Polysaccharides. *Science* 286, 537-542.
489. Vepa, S., Scribner, W.M., and Natarajan, V. (1997). Activation of endothelial cell phospholipase D by polycations. *Am J Physiol* 272, L608-613.
490. Verin, A.D., Birukova, A., Wang, P., Liu, F., Becker, P., Birukov, K., and Garcia, J.G. (2001). Microtubule disassembly increases endothelial cell barrier dysfunction: role of MLC phosphorylation. *Am J Physiol Lung Cell Mol Physiol* 281, L565-574.
491. Vernon, R.B., and Sage, E.H. (1995). Between molecules and morphology. Extracellular matrix and creation of vascular form. *Am J Pathol* 147, 873-883.
492. Vlodavsky, I., Korner, G., Ishai-Michaeli, R., Bashkin, P., Bar-Shavit, R., and Fuks, Z. (1990). Extracellular matrix-resident growth factors and enzymes: possible involvement in tumor metastasis and angiogenesis. *Cancer Metastasis Rev* 9, 203-226.
493. Vlodavsky, I., Miao, H.Q., Medalion, B., Danagher, P., and Ron, D. (1996). Involvement of heparan sulfate and related molecules in sequestration and growth promoting activity of fibroblast growth factor. *Cancer Metastasis Rev* 15, 177-186.
494. Vlodavsky, I., Friedmann, Y., Elkin, M., Aingorn, H., Atzmon, R., Ishai-Michaeli, R., Bitan, M., Pappo, O., Peretz, T., Michal, I., Spector, L., and Pecker, I. (1999). Mammalian heparanase: gene cloning, expression and function in tumor progression and metastasis. *Nat Med* 5, 793-802.
495. Vlodavsky, I., and Friedmann, Y. (2001). Molecular properties and involvement of heparanase in cancer metastasis and angiogenesis. *J Clin Invest* 108, 341-347.
496. Vlodavsky, I., Goldshmidt, O., Zcharia, E., Atzmon, R., Rangini-Guatta, Z., Elkin, M., Peretz, T., and Friedmann, Y. (2002). Mammalian heparanase: involvement in cancer metastasis, angiogenesis and normal development. *Semin Cancer Biol* 12, 121-129.
497. Wada, K., Sugimori, H., Bhide, P.G., Moskowitz, M.A., and Finklestein, S.P. (2003). Effect of basic fibroblast growth factor treatment on brain progenitor cells after permanent focal ischemia in rats. *Stroke* 34, 2722-2728.

498. Wakisaka, N., Murono, S., Yoshizaki, T., Furukawa, M., and Pagano, J.S. (2002). Epstein-barr virus latent membrane protein 1 induces and causes release of fibroblast growth factor-2. *Cancer Res* 62, 6337-6344.
499. Walenga, J.M., Jeske, W.P., Bara, L., Samama, M.M., and Fareed, J. (1997). Biochemical and pharmacologic rationale for the development of a synthetic heparin pentasaccharide. *Thromb Res* 86, 1-36.
500. Wang, D., Liu, S., Trummer, B.J., Deng, C., and Wang, A. (2002). Carbohydrate microarrays for the recognition of cross-reactive molecular markers of microbes and host cells. *Nat Biotechnol* 20, 275-281.
501. Wang, H., Toida, T., Kim, Y.S., Capila, I., Hilemna, R.E., Bernfield, M., and Linhardt, R.J. (1997). Glycosaminoglycans can induce fibroblast growth factor-2 mitogenicity without significant growth factor binding. *Biochem Biophys Res Commun* 235, 369-373.
502. Wang, L., Malsch, R., and Harenberg, J. (1997). Heparins, low-molecular-weight heparins, and other glycosaminoglycans analyzed by agarose gel electrophoresis and azure A-silver staining. *Semin Thromb Hemost* 23, 11-16.
503. Wen, W., Moses, M.A., Wiederschain, D., Arbiser, J.L., and Folkman, J. (1999). The generation of endostatin is mediated by elastase. *Cancer Res* 59, 6052-6056.
504. Wong, P., and Burgess, W.H. (1998). FGF2-Heparin co-crystal complex-assisted design of mutants FGF1 and FGF7 with predictable heparin affinities. *J Biol Chem* 273, 18617-18622.
505. Woods, A., Couchman, J.R., Johansson, S., and Hook, M. (1986). Adhesion and cytoskeletal organisation of fibroblasts in response to fibronectin fragments. *Embo J* 5, 665-670.
506. Wu, W., Shu, X., Hovsepyan, H., Mosteller, R.D., and Broek, D. (2003). VEGF receptor expression and signaling in human bladder tumors. *Oncogene* 22, 3361-3370.
507. Xin, L., Xu, R., Zhang, Q., Li, T.P., and Gan, R.B. (2000). Kringle 1 of human hepatocyte growth factor inhibits bovine aortic endothelial cell proliferation stimulated by basic fibroblast growth factor and causes cell apoptosis. *Biochem Biophys Res Commun* 277, 186-190.
508. Yamada, S., Yoshida, K., Sugiura, M., Sugahara, K., Khoo, K.H., Morris, H.R., and Dell, A. (1993). Structural studies on the bacterial lyase-resistant tetrasaccharides derived from the antithrombin III-binding site of porcine intestinal heparin. *J Biol Chem* 268, 4780-4787.
509. Yamagata, M., Kimata, K., Oike, Y., Tani, K., Maeda, N., Yoshida, K., Shimomura, Y., Yoneda, M., and Suzuki, S. (1987). A monoclonal antibody that specifically recognizes a glucuronic acid 2-sulfate-containing determinant in intact chondroitin sulfate chain. *J Biol Chem* 262, 4146-4152.
510. Yan, G., Fukabori, Y., McBride, G., Nikolaropolous, S., and McKeehan, W.L. (1993). Exon switching and activation of stromal and embryonic fibroblast growth factor (FGF)-FGF receptor genes in prostate epithelial cells accompany stromal independence and malignancy. *Mol Cell Biol* 13, 4513-4522.
511. Yayon, A., Klagsbrun, M., Esko, J.D., Leder, P., and Ornitz, D.M. (1991). Cell surface, heparin-like molecules are required for binding of basic fibroblast growth factor to its high affinity receptor. *Cell* 64, 841-848.

512. Ye, S., Luo, Y., Lu, W., Jones, R.B., Linhardt, R.J., Capila, I., Toida, T., Kan, M., Pelletier, H., and McKeehan, W.L. (2001). Structural basis of interaction of FGF-1, FGF-2, and FGF-7 with different heparan sulfate motifs. *Biochemistry* *40*, 14429-14439.
513. Yeaman, C., Grindstaff, K.K., and Nelson, W.J. (1999). New perspectives on mechanisms involved in generating epithelial cell polarity. *Physiol Rev* *79*, 73-98.
514. Yeh, B.K., Igarashi, M., Eliseenkova, A.V., Plotnikov, A.N., Sher, I., Ron, D., Aaronson, S.A., and Mohammadi, M. (2003). Structural basis by which alternative splicing confers specificity in fibroblast growth factor receptors. *Proc Natl Acad Sci U S A* *100*, 2266-2271.
515. Yoshioka, T., Tsuru, K., Hayakawa, S., and Osaka, A. (2003). Preparation of alginic acid layers on stainless-steel substrates for biomedical applications. *Biomaterials* *24*, 2889-2894.
516. Youakim, A., and Ahdieh, M. (1999). Interferon-gamma decreases barrier function in T84 cells by reducing ZO-1 levels and disrupting apical actin. *Am J Physiol* *276*, G1279-G1288.
517. Yuge, T., Furukawa, A., Nakamura, K., Nagashima, Y., Shinozaki, K., Nakamura, T., and Kimura, R. (1997). Metabolism of the intravenously administered recombinant human basic fibroblast growth factor, trafermin, in liver and kidney: degradation implicated in its selective localization to the fenestrated type microvasculatures. *Biol Pharm Bull* *20*, 786-793.
518. Yun, M.S., Kim, S.E., Jeon, S.H., Lee, J.S., and Choi, K.Y. (2004). Both ERK and Wnt/ β -catenin pathways are involved in Wnt3a-induced proliferation. *J Cell Sci*.
519. Yung, S., Woods, A., Chan, T.M., Davies, M., Williams, J.D., and Couchman, J.R. (2001). Syndecan-4 up-regulation in proliferative renal disease is related to microfilament organization. *Faseb J* *15*, 1631-1633.
520. Yurchenco, P.D., and Schittny, J.C. (1990). Molecular architecture of basement membranes. *Faseb J* *4*, 1577-1590.
521. Zacharski, L.R., Henderson, W.G., Rickles, F.R., Forman, W.B., Cornell, C.J., Jr., Forcier, R.J., Harrower, H.W., and Johnson, R.O. (1979). Rationale and experimental design for the VA Cooperative Study of Anticoagulation (Warfarin) in the Treatment of Cancer. *Cancer* *44*, 732-741.
522. Zacharski, L.R., Henderson, W.G., Rickles, F.R., Forman, W.B., Cornell, C.J., Jr., Forcier, R.J., Edwards, R., Headley, E., Kim, S.H., O'Donnell, J.R., O'Dell, R., Tornyo, K., and Kwaan, H.C. (1981). Effect of warfarin on survival in small cell carcinoma of the lung. Veterans Administration Study No. 75. *Jama* *245*, 831-835.
523. Zacharski, L.R., and Ornstein, D.L. (1998). Heparin and cancer. *Thromb Haemost* *80*, 10-23.
524. Zauner, W., Brunner, S., Buschle, M., Ogris, M., and Wagner, E. (1999). Differential behaviour of lipid based and polycation based gene transfer systems in transfecting primary human fibroblasts: a potential role of polylysine in nuclear transport. *Biochim Biophys Acta* *1428*, 57-67.
525. Zeeh, J.M., Procaccino, F., Hoffmann, P., Aukerman, S.L., McRoberts, J.A., Soltani, S., Pierce, G.F., Lakshmanan, J., Lacey, D., and Eysselein, V.E. (1996). Keratinocyte growth factor ameliorates mucosal injury in an experimental model of colitis in rats. *Gastroenterology* *110*, 1077-1083.

526. Zhang, Z., Coomans, C., and G., D. (2001). Membrane heparan sulfate proteoglycan-supported FGF2-FGFR1 signaling: evidence in support of the "cooperative end structures" model. *J Biol Chem* 276, 41921-41929.
527. Zhou, F.Y., Owens, R.T., Hermonen, J., Jalkanen, M., and Hook, M. (1997). Is the sensitivity of cells for FGF-1 and FGF-2 regulated by cell surface heparan sulfate proteoglycans? *Eur J Cell Biol* 73, 166-174.
528. Zimmermann, P., and David, G. (1999). The syndecans, turners of transmembrane signaling. *FASEB J* 13, S91-S100.
529. Zimmermann, P., and David, G. (1999). The syndecans, tuners of transmembrane signaling. *Faseb J* 13 *Suppl*, S91-S100.
530. Zimmermann, P., Tomatis, D., Rosas, M., Grootjans, J., Leenaerts, I., Degeest, G., Reekmans, G., Coomans, C., and David, G. (2001). Characterization of syntenin, a syndecan-binding PDZ protein, as a component of cell adhesion sites and microfilaments. *Mol Biol Cell* 12, 339-350.



Room 14-0551
77 Massachusetts Avenue
Cambridge, MA 02139
Ph: 617.253.5668 Fax: 617.253.1690
Email: docs@mit.edu
<http://libraries.mit.edu/docs>

DISCLAIMER OF QUALITY

Due to the condition of the original material, there are unavoidable flaws in this reproduction. We have made every effort possible to provide you with the best copy available. If you are dissatisfied with this product and find it unusable, please contact Document Services as soon as possible.

Thank you.

Some pages in the original document contain color pictures or graphics that will not scan or reproduce well.